PEOPLE'S DEMOCRATIC REPUBLIC OF ALGERIA MINISTRY OF HIGHER EDUCATION AND SCIENTIFIC RESEARCH

IBN KHALDOUN UNIVERSITY OF TIARET

FACULTY OF APPLIED SCIENCES

ELECTRICAL ENGINEERING DEPARTMENT

THESIS

Presented by:

MIMOUNI Amina

Thesis submitted in fulfillment of the requirements for:

Degree of DOCTORATE (L.M.D) in Renewable Energies

Surveillance and Diagnosis of Power Converters in Photovoltaic System

Presented on

under board of examiners composed of

President	HASSAINE Said	Pr	U. Tiaret
Supervisor	LARIBI Souad	MCA	U. Tiaret
Co-Supervisor	SEBAA Morsli	Pr	U. Tiaret
Examiner	MIHOUB Youcef	MCA	U. Tiaret
Examiner	MERADI Samir	MCA	U. Algiers
Examiner	GUENTRI Hocine	MCA	U. Mila
Invited	ALLAOUI Tayeb	Pr	U. Tiaret

2023/2024

Acknowledgements

Praise be to Allah, for enlightening our path to knowledge and granting us the good will, patience and courage for the completion of this work.

I would like to express my sincere gratitude to my supervisor Dr. Souad LARIBI, a lecturer at the University of Tiaret, for the continuous support of my PhD study and related research, for her patience and motivation. Providing me invaluable assistance during the entire research and writing process of this thesis. Additionally, I extend my appreciation to my thesis co-supervisor, Pr. Morsli SEBAA a professor at the University of Tiaret for his, continuous encouragement, and guidance. A special thanks to Pr. Tayeb ALLAOUI, a Professor at the University of Tiaret and the head lab of L2GEGI for his comments and help on my research work.

I extend my sincere acknowledgement to Pr. Grzegorz Iwanski, a Professor at Warsaw University of Technology, for his invaluable collaboration and support throughout the process of researching and writing of this thesis.

I am deeply grateful to Mr. HASSAINE Said, Professor at the University of Tiaret, for graciously accepting the honor of chairing the jury. Additionally, I extend my sincere appreciation to the esteemed members of the jury: MIHOUB Youcef a lecturer at Ibn Khaldoun University. GUENTRI HOUCINE a lecturer at the University of Mila, and MERADI Samir a lecturer at National School of Advanced Technologies of Algiers for their valuable contributions to the evaluation of this work.

I express my gratitude to all who have contributed to the completion of this thesis in different roles. Your support, whether it was through offering encouragement, providing assistance, or guiding along the way, has been invaluable and greatly appreciated.

Dedication

This Thesis is dedicated to:

My parents

My family

My cherished ones, whose unwavering support has been my strength

Abstract: The integration of PV systems into the electrical grid relies heavily on the efficient operation of power converters. Serving as the essential link between PV panels and the grid. However, the reliability and performance of grid-connected PV systems are often challenged by various faults that can occur within the power converters. These faults, including open circuit faults. Addressing these faults is imperative to maintain the stability and efficiency of the PV system within the grid context. Consequently, the development of robust surveillance and diagnosis techniques for power converters is of paramount importance. By effectively identifying and mitigating faults. For the diagnosis of boost converters, an innovative method utilizing inductor current analysis is proposed. Through extensive results, it is demonstrated that this approach offers rapid and accurate detection of open circuit fault. In the case of inverters, the thesis introduces a technique based on symmetrical components analysis for classifying various fault scenarios that may arise. Different results validate the efficacy of this approach, particularly in detecting faults at different current levels, thereby enhancing the system's resilience to potential malfunctions. Moreover, to mitigate the adverse effects of faults on the overall system operation, a strategy involving the implementation fault tolerant control of boost converter and three phase current limitation is proposed. This proactive measure serves to minimize the impact of faults, safeguarding the stability of the PV system.

Key words: Grid connected PV system, Open circuit fault, Power converters, Fault diagnosis

ملخص : ***يعتمد دمج الأنظمة الكهروضوئية في الشبكة الكهربائية بشكل كبير على التشغيل الفعال لمحولات الطاقة. بمثابة الرابط الأساسي بين الألواح الكهروضوئية والشبكة. ومع ذلك، غالبًا ما تواجه هذه المحولات تحديات بسبب الأعطال المختلفة التي يمكن أن تحدث داخل محولات . وتشمل هذه الأعطال أعطال الدائرة المفتوحة التي تحدث على مستوى المفاتيح الألكترونية. تعد معالجة هذه الأخطاء أمرًا ضروريًا للحفاظ على استقرار وكفاءة النظام الكهروضوئي ضمن سياق الشبكة. وبالتالي، فإن تطوير تقنيات المراقبة والتشخيص القوية لمحولات الطاقة له أهمية قصوى. من خلال تحديد الأخطاء وتخفيفها بشكل فعال. لتشخيص محولات التيار المستمر/مستمر، تم اقتراح طريقة مبتكرة تسخدم تحليل تيار المحث. ومن خلال النتائج الشاملة، ثبت أن هذا النهج يوفر اكتشافًا سريعًا ودقيقًا لأعطال الدائرة المفتوحة. في حالة العاكسات، تقدم الأطروحة تقنية رائدة تعتمد على تحليل المكونات المتماثلة لتصنيف سيناريوهات الأعطال المختلفة التي قد تنشأ. وتؤكد نتائج المحاكاة فعالية هذا النهج، لا سيما في اكتشاف الأخطاء عند قيم تيارات مختلفة، وبالتالي تعزيز مرونة النظام في مواجهة الأعطال المحتملة. علاوة على ذلك، للتخفيف من الآثار الضارة للأخطاء على تشغيل النظام بشكل عام، تم اقتراح استراتيجية تتضمن التحكم في تحمل الأخطاء في التنفيذ لمحول التيار مستمر/مستمر وتقييد التيار ثلاثي الطور. يعمل هذا الإجراء الاستباقي على تقليل تأثير الأخطاء، والحفاظ على استقرار وطول عمر النظام الكهروضوئي.***

الكلمات المفتاحية : نظام الكهروضوئي متصل بالشبكة، عيب الدائرة المفتوحة، محولات الطاقة، تشخيص الأعطال

Résumé: L'intégration des systèmes PV dans le réseau électrique repose largement sur le fonctionnement efficace des convertisseurs de puissance, qui servent de lien essentiel entre les panneaux PV et le réseau. Cependant, la fiabilité et les performances des systèmes PV connectés au réseau sont souvent mises à l'épreuve par divers défauts pouvant survenir dans les convertisseurs de puissance, y compris les défauts de circuit ouvert au niveau les interrupteurs de commutation. La résolution de ces défauts est impérative pour maintenir la stabilité et l'efficacité du système PV. En conséquence, le développement de techniques de surveillance et de diagnostic robustes pour les convertisseurs de puissance revêt une importance primordiale. Pour le diagnostic des convertisseurs DC-DC, une méthode innovante utilisant l'analyse du courant de l'inductance est proposée. Des résultats étendus démontrent que cette approche offre une détection rapide et précise des défauts de circuit ouvert. Dans le cas des onduleurs, la thèse présente une technique robuste basée sur l'analyse des composantes symétriques pour classifier divers scénarios de défauts pouvant survenir. Les différents résultats valident l'efficacité de cette approche, en particulier dans la détection de défauts à différents niveaux de courant, améliorant ainsi la résilience du système aux dysfonctionnements potentiels. De plus, pour atténuer les effets néfastes des défauts sur le fonctionnement global du système, une stratégie impliquant la mise en œuvre d'un contrôle tolérant aux défauts du convertisseur DC-DC et une limitation du courant triphasé est proposée. Cette mesure proactive vise à réduire au minimum l'impact des défauts, garantissant ainsi la stabilité du système.

Mots clés : Système PV connecté au réseau, Défaut de circuit ouvert, Convertisseurs statiques, Diagnostic et détection des défaut.

Table of contents

List of Figures

Chapter 01

Chapter 02

Chapter 03

Chapter 04

Chapter 05

List of Tables

Chapter 01

Chapter 02

Chapter 03

Chapter 04

Chapter 05

List of symbols

$y(t)$: Process output

$u(t)$: Process input

θ: the model parameter

$\hat{\theta}$: the estimated model parameter

r(t): the residual

x(k): system state

u(k): control input

y(k): measured output

$\hat{x}(k)$: estimates of the state

$\hat{y}(k)$: estimate of the output

L: The observer gain

$e(k)$: output error

b_j: Optional bias term of the j^{th} neuron

x_i: The input data

w: The weight vector vertical to the hyperplane

b: The bias

N: number of sampled points

τ: The time shift parameter

x(τ): The time-domain signal

g(t − τ) : The time window

I_{sc}: Short Circuit current

I_m: Maximum Current of the solar cell

V_m: Maximum Voltage of the solar cell

P_m: Maximum power of the solar cell

V_{oc}: Open circuit voltage

η: Efficiency

FF: Fill Factor

S: Surface of solar cells

N_s : Number of solar cells in series

N_p : Number of solar cells in parallel

I_{pv} : The photon current generated by the PV cell.

I_d : The reverse saturation current of the diode.

I_{sh} : The leakage current through R_{sh}.

q: The charge of an electron

V_{pv} : The cell output voltage.

a : The diode ideality constant

k : Boltzmann's constant

T : The cell temperature.

I_{ph} : The photon current generated by a PV cell

G: Absorbed irradiance

K_v : The open-circuit temperature coefficient.

V_t : The thermodynamic potential

L: inductor

F_{sw}: Switching frequency

D : Duty cycle

γV_{pv} : maximum power point voltage ripple factor

Δi_L: Estimated inductor ripple current

V_o: Desired output voltage

V_i: Typical input voltage

S_y (y=a,b,c): The switching function

V_{dc}: The DC supply voltage to the inverter

V_{ab}, V_{bc}, V_{ca} : The phase-phase voltages

v_a, v_b, v_c : The three-phase output voltages

A_r: Modulating signal

A_t : Triangular carrier signal

m_a : Modulation index

m_f : Frequency modulation index

f_r : Frequency of the control signal

f_t : Switching frequency

P_{PV}: the nominal power of PV modules

ω: the rotational frequency of the generated sine wave

ΔV_{dc} : the amplitude of voltage ripple

V_{LL}: a line-to-line grid voltage

i_a, i_b, i_c : Three phase currents

i_d, i_q : The dq-axis components corresponding to the inverter phase currents

v_{dq} : The dq-axis components corresponding to the grid phase voltage

$v_{refd\text{-}pwm}$,$v_{refq\text{-}pwm}$: inverter output phase voltage

List of abbreviations

GW: Gegawatt

PV: Photovoltaic

ROI: Return On Investment

TW: Terawatt

DC: Direct Current

AC: Alternative Current

SCF: Short Circuit Fault

OCF: Open Circuit Fault

PFTC: Passive Fault Tolerant Control

AFTC: Active Fault Tolerant Control

FDD: Fault Detection and Diagnosis

ML: Machine Learning

AI: Artificial Intelligence

ANN: Artificial Neural Network

SVM: Support Vector Machine

DFT: Discrete Fourier Transform

WT: wavelet transform

STFT: short-time Fourier transform

EMD: Empirical Mode Decomposition

HHT: Hilbert-Huang transform

FT: Fourier Transform

IMF: Intrinsic Mode Function

PCA: Principal Components Analysis

MF: Membership Functions

RE: Renewable Energy

RER: Renewable Energy Resources

EU: European Union

CO_2: Carbon Dioxide

MW: Megawatt

CSP: Concentrated Solar Power

SHC: Solar Heating and Cooling

CdTe: Cadmium Telluride

CIGS: Copper Indium Gallium Selenide

c-Si: crystalline Silicon

GPV : PV Generator

ESS: Energy storage systems

PWM: Pulse Width Modulation

IGBT: Insulated-Gate Bipolar Transistors

MOSFET:

VSI: Voltage Source Inverter

MPPT: Maximum Power Point Tracker

P&O: Perturb and Observe

PSO: Particle Swarm Optimization

GWO: Grey Wolf Optimization

SMC: Sliding Mode Control

PI: Proportional Integral

PLL: Phase Locked Loop

VOC: Voltage Oriented Control

FT: Fault Tolerant

LPF: Low Pass Filter

PCB: Printed Circuit Board

DAS: Data Acquisition System

ACD: AC Disconnects

General Introduction

In response to the declining availability of fossil fuels and the environmental concerns linked to their use, significant global efforts are underway to explore alternative energy sources. Fossil fuels, such as petroleum, coal, and natural gas, have long dominated the world's energy supply but come with substantial environmental drawbacks. Their combustion is a major contributor to greenhouse gas emissions, increasing climate change. In light of this, the shift towards renewable energies has gained momentum as a sustainable and environmentally friendly solution. The increasing global emphasis on renewable energy arises from its inherent sustainability and environmental benefits compared to fossil fuels. Renewable sources such as (wind, solar, biomass, hydroelectricity… etc) offer abundant, safe, and inexhaustible energy options. Governments worldwide are investing in renewable technologies to achieve sustainability goals and address environmental concerns like climate change. The projected rise in global electricity generation from renewables reflects a significant shift towards cleaner energy systems, supported by substantial investments [1].

At the end of 2021, global renewable generation capacity reached 3,064 Gigawatts (GW), with hydropower leading at 1,230 GW, closely followed by solar and wind energy at 849 GW each. The year saw a significant increase of 257 GW in renewable capacity, marking a growth rate of 9.1% compared to the previous year. This expansion was primarily driven by solar energy, which added 133 GW, and wind energy, which contributed 93 GW. These developments underscore the accelerating dominance of renewable energy in the global energy mix, propelled by declining costs, technological advancements, and supportive policies. This transition towards cleaner and more sustainable energy sources reflects a growing commitment to mitigate climate change and build a resilient energy infrastructure worldwide [2].

Among these alternatives, solar energy emerges as a promising option. By harnessing sunlight through the photovoltaic effect, solar photovoltaic (PV) energy offers a clean, sustainable, and pollution-free electricity source. In recent years, the PV system market has experienced significant expansion, driven by several factors including cost reductions, supportive governmental policies, and advancements in power electronics. This surge in demand underscores the growing viability of solar installations in terms of return on investment (ROI), positioning PV energy as a reliable and economically competitive solution for electricity generation. The widespread adoption of PV systems, particularly those integrated into distribution networks, highlights their pivotal role in the ongoing global transition towards sustainable energy sources. Notably, the global cumulative capacity of installed and commissioned PV increased by more than 25% last year thanks to post-Covid price hikes and geo-political strife. It reached about 1.2TW by the end of 2022 [3].

Problem Statement

Photovoltaic systems, while offering sustainable and renewable energy solutions, are susceptible to various types of failures stemming from external and internal operating conditions that can undermine system performance and profitability. These faults stem from diverse factors such as environmental conditions and component failures. Understanding the potential faults impacting PV systems is crucial, emphasizing their diverse origins ranging from environmental conditions to component failures. It underscores the critical importance of proactively addressing these faults to maintain the reliability and efficiency of PV installations. These failures encompass all components of PV systems, including PV modules, cabling, converters, and inverters. The various fault categories encountered on both the DC and AC sides of PV systems. Beginning with DC side faults, including earth faults, bridging faults, open circuit faults, and mismatch faults. Additionally, MPPT faults. Transitioning to the AC side, like grid outages, total blackouts, and inverter malfunctions.

Among the faults that can afflict PV systems, those affecting power components are of paramount importance due to their critical role in system operation. Power components such as DC-DC converters and inverters play a vital role in converting and managing electrical energy within the system. However, they are also susceptible to various faults that can compromise system performance and reliability, stemming from factors such as component aging and operational stresses. A statistical study across diverse sectors reveals that 38% of all faults in converters are attributed to power switching components, emphasizing the vulnerability of power semiconductors. Thermal stress emerges as the most influential factor affecting component and system reliability, accounting for 55% of failures [4]. Additionally, factors like humidity and mechanical vibrations are closely associated with power component failures. For instance, failures in these components pose significant risks, leading to energy loss and potential system downtime, highlighting the necessity for prompt resolution to ensure uninterrupted operation and optimal performance. Proactive measures are therefore imperative to mitigate the impact of such failures on PV system functionality.

Aims of the Thesis

The primary objective of this thesis is to devise a comprehensive methodology for the detection and localization of faults in power converters, particularly focusing on DC-DC converters and inverters, which are pivotal components within PV systems and profoundly influence their functionality and efficiency. These power converters are susceptible to various faults that can compromise the overall reliability and performance of the system, with power switching devices being particularly vulnerable. These faults, which can manifest as short circuit faults (SCF) or open circuit faults (OCF), have the potential to cause severe malfunctions within the system. Undetected faults pose a significant risk of damaging not only the power converter stage but also auxiliary circuits.

Rapid fault detection is essential in preventing faults from spreading to other components within a system. Therefore, in addressing this critical need, the thesis will focus on diagnosing Open Circuit Faults specifically in power switches. Through a comprehensive analysis of the distinct fault patterns and characteristics associated with OCF in switching devices, the thesis aims to develop robust fault detection algorithms and strategies. These methods will be designed to accurately identify and detect the location of OCF within power converters. Additionally, the thesis aims to integrate these diagnostic techniques into PV systems. This integration will facilitate proactive maintenance measures and help mitigate the adverse effects of faults on the operation of PV systems. Ultimately, by enabling timely fault detection and intervention, the thesis endeavors to enhance the reliability and resilience of PV systems, ensuring their continued optimal performance.

Main contributions

The main contributions of this thesis represent a comprehensive and multifaceted approach aimed at supporting the reliability and efficiency of grid-connected PV systems through a series of innovative fault detection and reconfiguration strategies. At the aim of these contributions lies the presentation of a robust fault detection method thoroughly designed to operate seamlessly across the diverse environmental and operational conditions typically encountered within PV systems. Utilizing algorithms, these proposed methods excel in swiftly and accurately identifying faults in power converters, thereby enabling timely interventions to prevent system downtime and reduce energy losses. Furthermore, the thesis expands its scope beyond fault detection to include proactive fault management and system reconfiguration strategies. In response to fault occurrences in either the inverter or DC-DC converter.

The research explores various methods to effectively manage and mitigate their impact on overall system performance. This involves developing control algorithms and reconfiguration techniques capable of adjusting system parameters and reallocating resources to maintain optimal operation despite the presence of faults. Additionally, the thesis advances in the field of rapid and robust fault detection, advocating for the integration of advanced algorithms to expedite maintenance actions and minimize system downtime. It also proposes fault-tolerant control strategies to maintain system functionality in the face of faults until maintenance can be carried out. Overall, these contributions aim to significantly enhance the reliability, efficiency, and longevity of PV systems by addressing the critical issue of fault detection and localization in power converters, particularly focusing on faults affecting switching devices.

Structure of the thesis

This thesis is structured into five cohesive chapters, each serving a specific purpose in advancing the understanding and application of fault diagnosis in PV systems.

Chapter 1: Sate of the Art of Fault Diagnosis

The chapter delves into essential terms and definitions pertinent to monitoring and fault diagnosis in systems. It offers a state of exploration of monitoring methods, categorizing fault diagnosis from traditional methods to advanced approaches, exploring diverse techniques for comprehensive fault analysis and system adaptability. the chapter equips readers with a comprehensive understanding of fault detection and diagnosis in industrial settings, facilitating informed decision-making in fault management, to ensure effective fault detection, system resilience, and improved operational efficiency in diverse system environments.

Chapter 2: State of the Art of PV Systems

The chapter provides an overview of global electricity production, emphasizing renewable sources, and discusses Algeria's solar potential within its ambitious renewable energy program. It explores generating electricity directly from solar irradiation, covering topics such as the PV effect, PV Generator design, and system architectures. These findings set the way for deeper exploration of advanced topics and PV applications in subsequent chapters, helping a comprehensive understanding of solar energy utilization and its role in sustainable electricity production.

Chapter 3: Modeling and Control of Grid-Connected PV Systems

In this chapter, we build upon the fundamental understanding established in the preceding section, delving deeper into the complexities surrounding the modeling and control of grid-connected PV systems. Here, we explore various mathematical models for PV arrays, power converters, and grid interfaces, essential for comprehending the dynamics and behavior of these systems. Additionally, the chapter examines control algorithms devised to maximize power generation from PV arrays while concurrently ensuring the stability and reliability of the grid to which they are connected. A notable focus lies on the pivotal role of the control strategies in optimizing overall system performance. By analyzing these aspects, the chapter aims to equip readers with the necessary knowledge to understand the modeling and controlling grid-connected PV systems.

Chapter 4: Diagnosis of DC-DC Converter Faults

In this chapter, we specifically focus on the family of non-isolated DC-DC static. Initially, we delve into the literature review aimed at identifying OCF in DC-DC converter, we then propose and examine fault detection method concerning the controllable switch of a boost converter. The fault detection algorithm is initially validated using MATLAB/Simulink. Numerous numerical simulations are conducted to demonstrate and validate the performance of these algorithms, the results showed promising results about the fault detection time, also the implementation of the fault-tolerant control strategy, like redundant component, efficient reconfiguration technique further minimize downtime, ensuring continuous operation and optimal performance despite faults.

Chapter 5: Diagnosis of Three-Phase Inverter Faults

This chapter delves into the topic of inverter fault diagnosis. It begins with an extensive literature review presenting diagnostic methods for detecting open-circuit faults in inverters, providing a comprehensive overview of the current state of art in this field. Subsequently, the chapter introduces the theoretical foundations of robust diagnosis algorithm developed for inverter fault diagnostics. This algorithm experiences rigorous testing and validation through a series of simulation tests to ensure their effectiveness and reliability. The chapter also delves into current limitation and overvoltage limitation strategies aimed at preventing component damage within PV systems. These strategies are essential for safeguarding system integrity and prolonging the lifespan of critical components.

Conclusion and Future Directions

The final conclusion summarizes the key findings of the thesis and reflects on their implications for the field of fault diagnosis in PV systems. It discusses potential avenues for future research, including the development of advanced diagnostic algorithms, the integration of fault diagnosis into new topologies dedicated for the PV applications. The chapter concludes with comprehensive remarks on the significance of fault diagnosis in enhancing the reliability and performance of grid-connected PV systems and underscores the importance of continued research and innovation in this area.

Chapter 1

State of art of diagnosis

1.1 Introduction

In a period of heightened global competition, industries are confronted with increasingly stringent demands, highlighting the imperative for a continuous availability of production tools. To address these challenges, both researchers and companies are progressively exploring methodologies centered around operational safety. The scope of fault diagnosis, traditionally confined to high-tech industries prioritizing reliability and security, has now expanded to encompass manufacturing sectors where the paramount concerns revolve around equipment availability and maintainability. Given the growing demand for reliability and safety in industrial systems. To achieve the outlined objectives of performance, safety, and availability in technical processes, diagnostic modules play a pivotal role in identifying deviations from the desired behavior and, under specific circumstances, reconfiguring the system's operation. The diagnostic process unfolds through three fundamental stages. Initially, the detection stage determines whether the involved process behaves or operates within the specified norms set by the engineer during system design. Subsequently, the second stage aims to characterize the fault by identifying specific features such as the time of occurrence, amplitude, and severity. The conclusive stage, building upon the preceding steps, involves deciding on the appropriate action for the system. This may involve maintaining the system in its current operating mode, reconfiguring its operation, or entirely shutting it down. In this chapter, following a review of various concepts and terminology specific to diagnostics, we will introduce diagnostics within the framework of a more comprehensive procedure referred to as diagnosis. The chapter concludes with an overview of various methods employed in industrial diagnostics.

1.2 Exploring Diagnostic Terminology and Fundamental Concepts

1.2.1 Terminology related to diagnosis

Prior to an in-depth exploration of diagnostic processes, it is imperative to establish a comprehensive understanding of the terminology employed. This part serves as a foundational guide, explaining key terms integral to fault detection and system analysis. By precisely defining these terms, this thesis aims to provide clarity and coherence in the subsequent discourse on diagnostic methodologies [5-10].

- Fault: A fault is an impermissible deviation of at least one characteristic parameter of the system in relation to normal operating conditions. A fault is the difference between the observed characteristic and the theoretical characteristic. In the absence of a fault, this deviation ideally zero.

- Failure: A failure defines a functional anomaly within a physical system, characterizes its inability to perform certain functions assigned to it.

- Break-Down: Breakdown is the inability of a device to perform its necessary function. It is clear that as soon as a failure occurs, characterized by the device ceasing to perform its function, the device will be declared to have failed. Consequently, a breakdown is always the result of a failure.

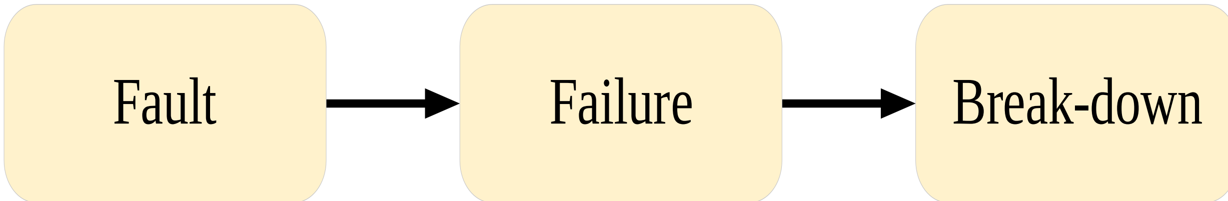

Figure 1. 1: Fault evolution [10].

- Malfunction: A malfunction denotes an irregularity or deviation from the expected and desired functioning of a system, occurring intermittently or periodically. It represents a temporary disruption in the system's performance without necessarily leading to a complete failure.

- Residual: Commonly known as a fault indicator or deviation variable, is a signal designed to indicate behavioral or functional anomalies. It is a quantity characterizing the difference produced by the comparison between the actual behavior and the nominal behavior of the system.

- Threshold: it is the limit value of the deviation of a residual, so that when it exceeds, a fault is declared as detected.

- Symptom: It is a change in an observable quantity compared with normal behavior.

- Operating Mode: A system typically operates in various modes, each serving a specific purpose. These modes include:

    - ✓ *Nominal Operating Mode:* This is the condition in which the equipment or system fulfills its intended mission under the specified operating conditions set by the manufacturer. It aligns with the requirements expected by both the manufacturer and the operator.

    - ✓ *Degraded Operating Mode:* This mode corresponds either to the partial fulfillment of the mission or the accomplishment of the mission with reduced performance. In other words, there is a degradation in the equipment or system, but it does not require a complete failure.

- Monitoring: Continuously in real-time, the process involves assessing the state of a physical system. This is achieved through the systematic recording of information, enabling the identification and signaling of any deviations or anomalies in the system's behavior.

- Supervision: This extends beyond more observation. It encompasses the proactive management of a physical system, including the implementation of predefined protocols. In the event of faults, supervision ensures appropriate actions are taken promptly to maintain the system's operational integrity.

1.2.2 Different structures of faults

A fault in a system indicates a deviation from normal operation. Faults come in different forms, with varying evolutions, natures, and types, highlighting the diverse ways in which a system's performance may be affected [9-11].

1.2.2.1 Evolution of the fault

- Sudden or Abrupt Fault: Characterized by a discontinuous temporal behavior, representing a sudden failure leading to total or partial malfunction [9-11].
- Gradual Fault: Exhibits a slow temporal behavior, making it challenging to detect, which develop gradually over time [9-11].
- Intermittent Fault: A special case of abrupt fault where the signal randomly returns to its nominal value. Often associated with false contacts and intermittent components failures [9-11].

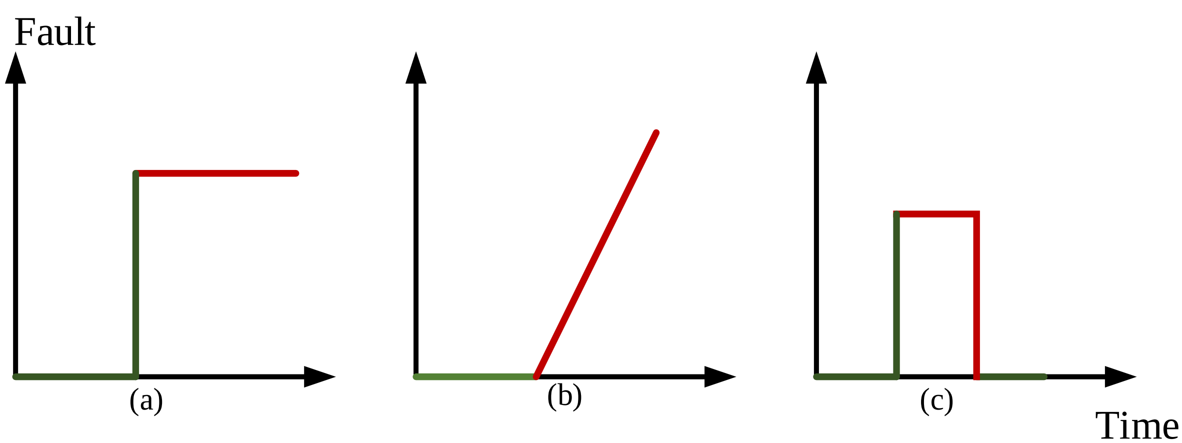

Figure 1. 2: Classification of fault based on time evolution: (a): Sudden fault, (b): Gradual fault, (c): Intermittent fault [9].

1.2.2.2 Nature of the fault

- Multiplicative Faults: These faults, affecting the dynamics of the process, are modeled as multiplicative faults. They correspond to parametric modifications of the model representing the system. Modeled by the multiplication of the system's input by a fault [9-11].

- Additive Faults: Additive faults are modeled as additive terms in the system's model. They influence the state of the system. Modeled by the addition of a variable to the system [9-11].

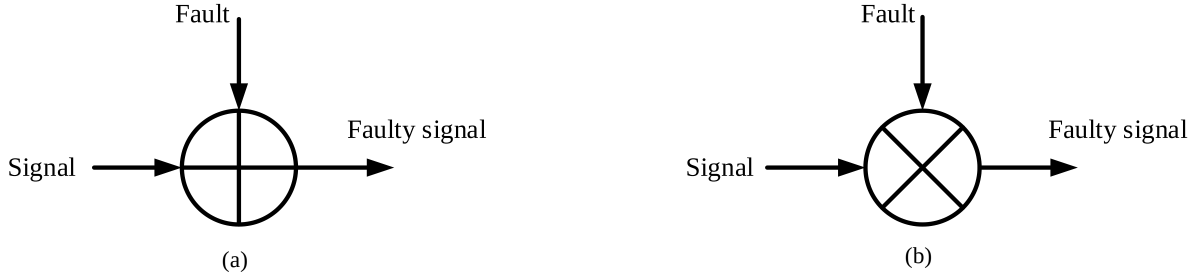

Figure 1. 3: Classification of faults based on the nature: (a): Additive fault, (b): Multiplicative fault [9].

1.2.2.3 Type of the fault

- Actuator Faults: refer to issues affecting the components responsible for initiating actions within a system. These actuators play a crucial role by translating control signals from the controller into various forms of output. When actuator faults occur, they introduce discrepancies between the intended commands and the actual output responses. There are two primary types of actuator faults: total loss of action and partial loss of action. In the case of a total loss, the actuator experiences a complete failure, making it unable to control the system. On the other hand, a partial loss of action involves the actuator still functioning but with a degraded performance, resulting in reduced action [5-6,11].

- Sensor Faults: Sensors serve to convert a physical quantity into a form that can be processed by computers. They typically act as the output interfaces of a system with the external environment. Thus, faults in the sensors are characterized by a discrepancy between the actual value of the quantity and its measurement. These faults will be added to the system outputs, representing a set of issues related to gathering information about the system's state [5-6,11].

- System Faults: Process faults are intrinsic to the system itself, leading to degradation of internal components through changes in parameters or structure. Structural Changes can result from modifications to the internal structure of the system. Also, parameter faults may involve alterations to internal parameters, impacting the overall behavior of the system [5-6,11].

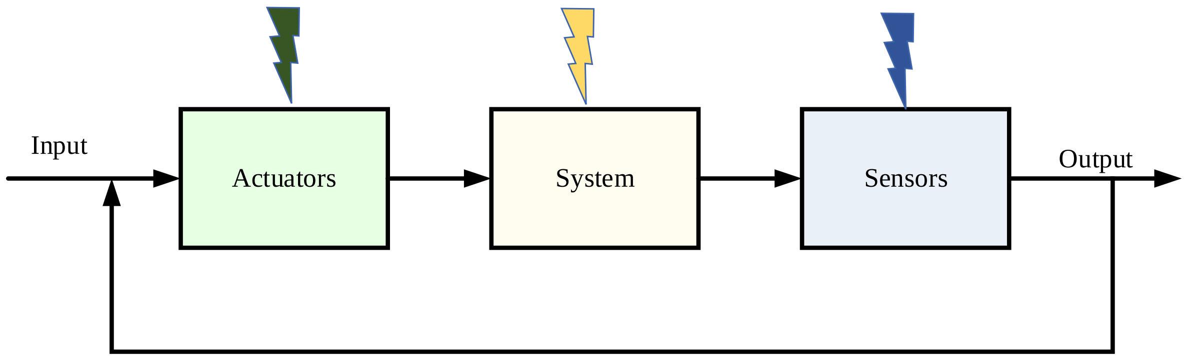

Figure 1. 4: Faults in Industrial system [11].

1.2.3 The fundamental stages of Fault Diagnosis

The pursuit of enhanced performance in production systems, coupled with increasingly stringent requirements for functionality, quality, cost, and safety, underscores the necessity for reliability. With a growing interest in the industrial sector, diagnostics have evolved into a distinct research theme. Within the literature, various definitions of diagnostics abound. Primarily centered on data extraction to determine potential causes of malfunctions, diagnostics identify the likely causes of failures through logical reasoning based on information gathered from inspection, control, or testing. Furthermore, they incorporate existing in-depth knowledge of the monitored system. For example, diagnostics encompass a collection of targeted observations (symptoms, findings, etc.), involving the explanation of their presence and tracing back to the root causes using knowledge about the considered system. Diagnostics is therefore a procedure consisting of detecting and locating a faulty component or element in a system. Detection refers to the diagnostician's ability to highlight the occurrence of one or more faults, and localization refers to the ability to further specify the nature of the occurred fault [12,13]

In this context, diagnosing an industrial system requires several stages summarized in Figure 1. 5 are detailed subsequently. Similarly, several stages can be introduced to establish diagnostics [10,13]:

- Data acquisition: This stage involves extracting necessary information from measurements and observations, using sensors or state estimators. The objective is to obtain characteristics associated with the normal and abnormal operations of the system.

- Fault detection: detection represents the initial level of diagnostics, where a decision is made regarding whether the system is functioning correctly or exhibiting a fault. The results of this phase trigger an alarm indicating a deviation from the healthy operating model.

- Fault localization: the aim is to locate the sub-system affected by the fault detected, which is responsible for the system failure. Locating the fault involves tracing back the symptoms to find all the faulty components.

- Fault identification: Identification is the determination of the type, magnitude and temporal behavior of the fault. It involves determining the element or elements causing the fault. Thereby providing a comprehensive explanation of the system's behavior in case of a malfunction.

- Decision Making: Once the malfunction is identified, the decision-making process comes into play to determine appropriate corrective actions. This may involve system shut down for maintenance, acceptance of degraded operation, or system reconfiguration.

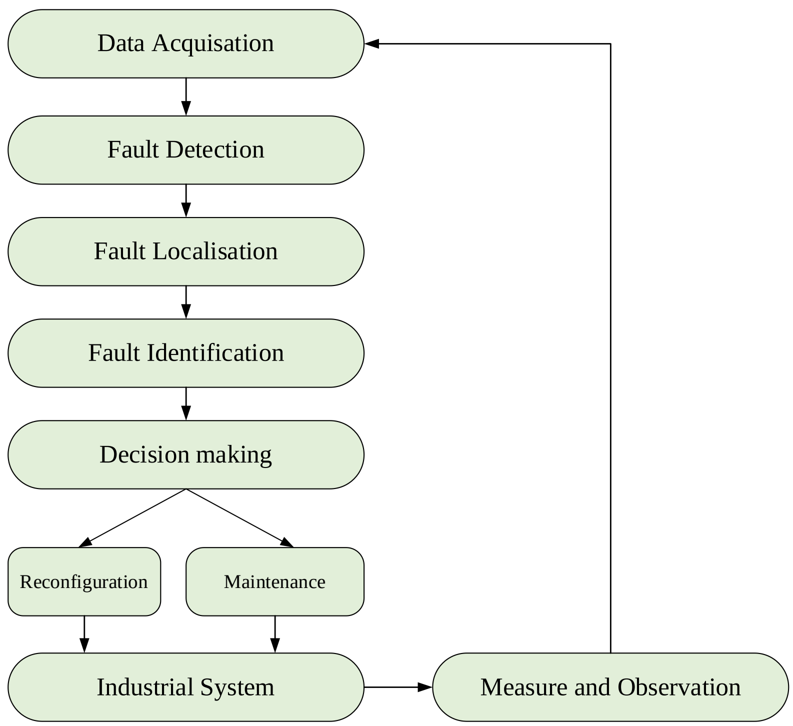

Figure 1. 5: Faut diagnosis steps in industrial system [12].

1.2.4 Requirements related to diagnostics

Effective diagnostics rely on specific foundational requirements. These criteria highlight the importance of a comprehensive understanding of potential faults and the need to strike a balance between completeness and precision in fault characterization. The outlined requirements ensure adaptability, reliability and continuous improvement, contributing to a robust diagnostic system [14,15].

- Rapid Diagnosis: The diagnostic tool must quickly detect and isolate faults upon their occurrence.

- Fault Discrimination: The tool should reliably differentiate between various types of faults.

- Identification of Multiple Faults: The tool must have the capability to identify multiple faults occurring simultaneously or within a short time frame.

- Robustness: The diagnostic tool must be robust in handling measurement noise and uncertainties in the system model.

- Implementation: Depending on the application, the diagnostic tool can be implemented either is integrated into the system it is monitoring. It operates using the system's resources and is directly connected to its processes, making it an inherent part of the system, or the diagnostic tool operates externally to the system. It's not an integral part of the system but functions independently.

- Adaptability: The tool should adapt to changes in the system, accommodating modifications, new parameters, or additional information obtained after installation.

1.2.5 Post diagnostic procedures

This step corresponds to the analysis of options available following the fault diagnosis and their implementation. Thus, after the detection and isolation of faults, it involves choosing between [14,15]:

- System Shutdown and Maintenance: is opted for in cases where the diagnosed fault demands prompt intervention. This course of action encompasses corrective maintenance to rectify the specific issue responsible for the fault or preventive maintenance aimed at mitigating potential future issues.

- System Operation with Revised Objectives: involves maintaining system functionality with altered goals instead of a complete shutdown. For instance, if a crucial component malfunctions, the system can transition from its standard operating mode to a degraded mode, ensuring the performance of essential functions.

- System Reconfiguration: Reconfiguring the system is a proactive strategy that involves restructuring the system's components or control mechanisms to adapt to the identified fault. This could include bypassing a faulty component, altering control algorithms, or redistributing tasks among functional components.

The choice among these options depends on factors such as the severity of the fault, safety considerations, the criticality of the system, and the impact on overall performance. Efficient post-diagnostic procedures are essential for minimizing disruptions, ensuring the system's reliability, and optimizing resource utilization. These procedures significantly contribute to the overall fault-tolerant design and operation of systems in various industries.

1.3 Fault tolerant control

A fault-tolerant system possesses the capability to maintain nominal objectives despite the occurrence of a fault and to adapt automatically to it. It aims to ensure system stability and/or acceptable degraded performance in the presence of faults. The traditional state feedback gain can be severely limited, leading to undesired behaviors or instability during a fault. To address these issues, new control laws have been developed specifically to sustain system performance and stability under faulty conditions. In industries like aerospace, avoiding these problems often involves relying on hardware redundancy with redundant actuators and sensors. However, this strategy is not only costly but also demands substantial maintenance. Analytically treated fault-tolerant control helps avoid such acquisition and maintenance expenses. The primary task of fault-tolerant control is to synthesize control laws with a structure that guarantees system stability and performance, not only when all control components are operational but also when sensors or actuators are faulty [16,17].

In the literature, control strategies are primarily divided into two groups of techniques: a passive approach (Passive Fault Tolerant Control, PFTC) and an active approach (Active Fault Tolerant Control, AFTC) [16-20]. Figure 1. 6 illustrates this classification.

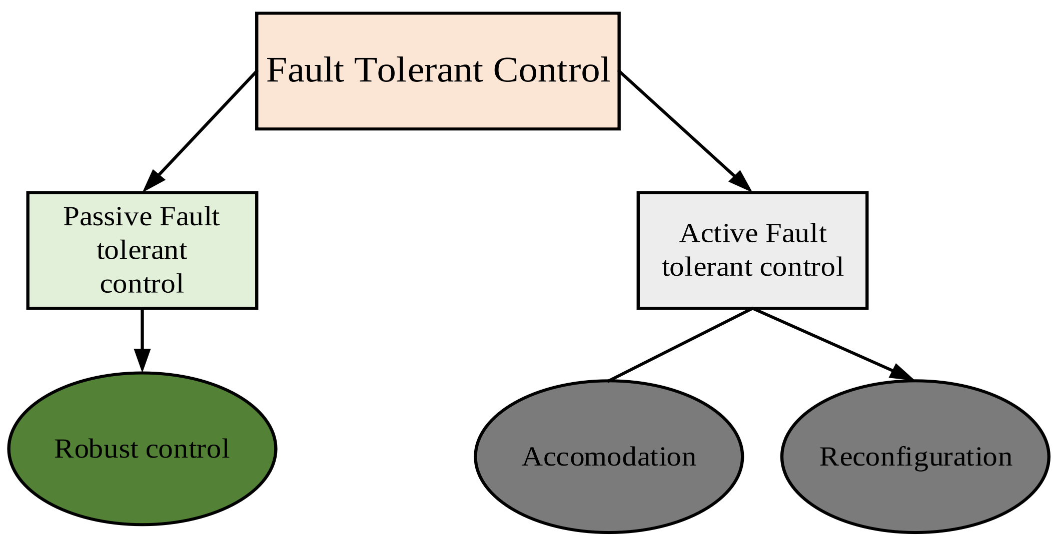

Figure 1. 6: Classification of Fault tolerant control [18].

1.3.1 Passive Fault tolerant control

Passive Fault-Tolerant Control (PFTC) involves approaches to control systems that are primarily based on robust control design techniques. The main goal of PFTC is to synthesize control laws that allow a system to continue functioning even in the presence of faults, without the need for immediate active intervention. The system is designed with redundancy and robustness to predefined faults, aiming to maintain acceptable performance levels during normal operation as well as in the presence of specific faulty modes.

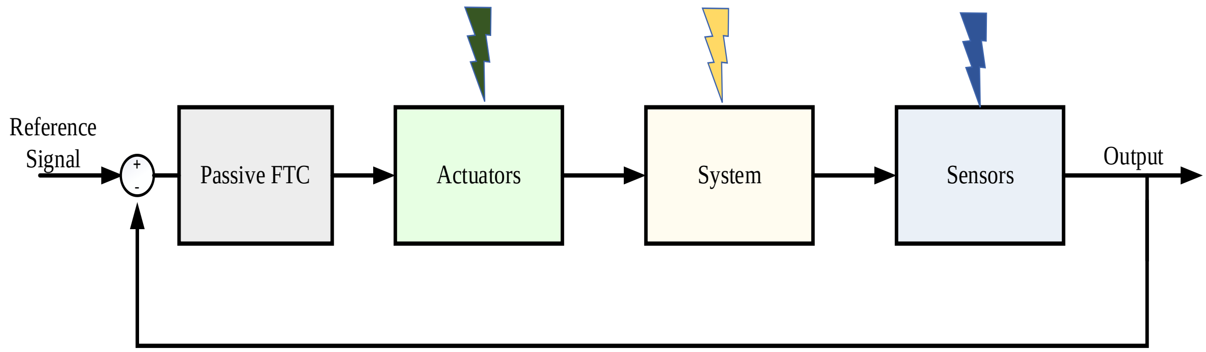

Figure 1. 7: Passive fault tolerant control scheme [18].

While passive methods are relatively simple to implement, they have limitations. Not all faults and their effects on the system can be completely known in advance, making passive approaches less flexible in handling a broad range of fault scenarios. The focus on stability often comes at the expense of optimal performance under all failure conditions.

1.3.2 Active Fault tolerant control

Active Fault-Tolerant Control (AFTC) stands out as a flexible and adaptive approach to addressing faults in dynamic systems. Unlike passive fault-tolerant control methods, AFTC actively incorporates a fault diagnosis block, which provides real-time information on fault detection, isolation, and identification. Comprising three main subsystems: reconfigurable controller, estimation scheme, and reconfiguration mechanism. AFTC enables dynamic adjustments to the control law during both nominal and faulty system conditions. This adaptability is crucial for preserving stability, security, and productivity in industrial processes, even in the presence of sensor and actuator faults. AFTC adopts two main strategies for handling faults: accommodation and reconfiguration. In the accommodation strategy, controller parameters are adapted to the dynamic properties of the faulty system while maintaining the same inputs and outputs as in the fault-free case. If accommodation is not feasible, the reconfiguration strategy involves the complete reconfiguration of the control loop, including the selection of new control configurations based on existing faults and the online design of a new control law [18-20].

Challenges faced by AFTC include addressing detection delays, false alarms, and undetected faults. The successful implementation of AFTC relies on an effective Fault Detection and Diagnosis (FDD) module, which plays a crucial role in providing accurate and timely fault information for activating the reconfiguration mechanism. AFTC is known for its superior performance compared to passive methods, as it can tolerate more severe faults and maintain higher performance levels in the face of system anomalies.

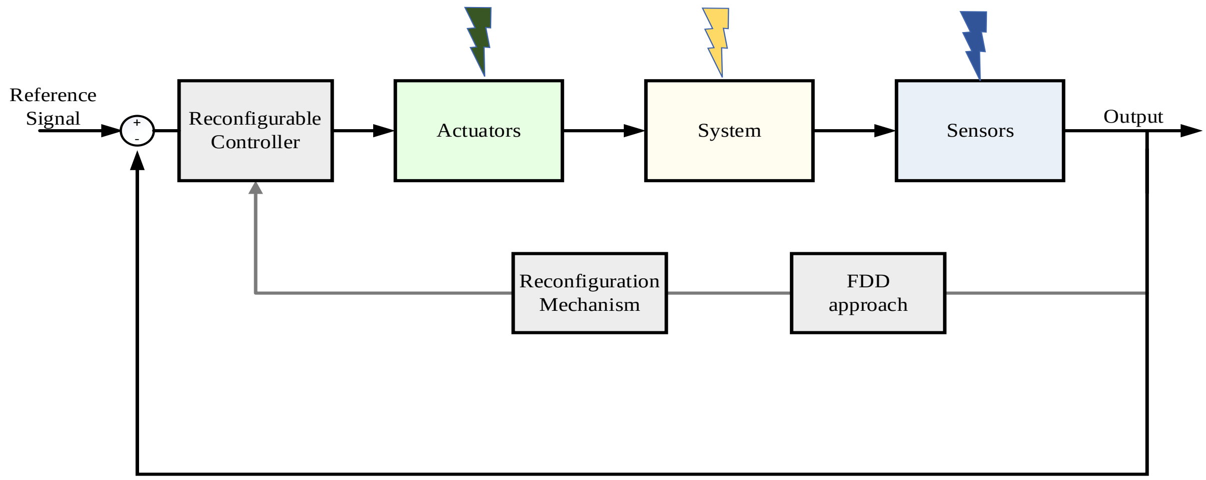

Figure 1. 8: Active fault tolerant control scheme [18].

1.4 Redundancy integration

In the landscape of system diagnostics, the integration of redundancy strategies plays a pivotal role in enhancing reliability. Redundancy as a general concept, aims to mitigate the impact of potential failures within a system. This multi-faceted approach involves the incorporation of backup elements, whether physical components or analytical relationships, to ensure continued functionality. The subsequent discussion will delve into two distinctive forms of redundancy: hardware redundancy and analytical redundancy [9,12,21].

1.4.1 Hardware Redundancy

The hardware redundancy method involves the integration of multiple actuators, a minimum of three sensors, multiple control systems, and software within a system. This configuration serves to validate information and identify degradation states through the analysis of measured signals. Widely applied in high-risk industries such as aviation and nuclear sectors, this method, despite being conceptually straightforward and effective, presents certain challenges.

Implemented without relying on knowledge of the monitored system's model, physical redundancy is characterized by its simplicity and emphasis on hardware elements. While ensuring the continuity of equipment functions, this approach encounters drawbacks, notably high sensor costs and constraints related to limited space during installation. The burdens associated with this method include increased weight, power consumption, volume, and expenses for both purchase and maintenance. These aspects impact factors such as weight augmentation and design complexity. Therefore, careful consideration is essential when opting for hardware redundancy, balancing its benefits in terms of system reliability with the associated drawbacks in terms of cost and practical implementation challenges [9,12,21].

1.4.2 Analytical Redundancy

Analytical redundancy is an approach in system diagnostics that leverages analytical relationships between measured variables during normal operation. These relationships, termed analytical redundancy relations, can originate from mathematical expressions of physical laws or result from statistical analyses of measurements. The primary purpose of analytical redundancy is to verify measurement consistency with the system model by generating fault indicator signals. If such relationships exist among measured variables, analytical redundancy allows the simultaneous use of measurement and model information. Despite requiring additional computations, this approach reduces the need for sensors compared to hardware redundancy. Analytical redundancy is particularly advantageous as it can detect faults affecting both the instrumentation chain and the controlled system, offering more comprehensive information than hardware redundancy. Additionally, it complements hardware redundancy by developing fault detection and isolation algorithms based on analytical input-output relationships between known variables, providing a robust diagnostic strategy [9,12,21].

1.5 State of art of diagnostic and classification

Fault diagnosis is a critical aspect of ensuring the reliable and efficient operation of complex systems across various industries. The classification of fault diagnosis approaches plays a pivotal role in understanding and addressing issues that may arise within these systems. As technology advances, diverse methodologies have emerged to detect, isolate, and rectify faults, contributing to the overall reliability and performance of systems. Many methods form the basis of diagnostic research, and the choice of one of these methods is linked to the knowledge one aims to acquire about the system, as well as the complexity of the system. In fact, three major families can be considered: model-based methods, data-based methods, knowledge-based methods and hybrid-based methods, as shown in Figure 1. 9[22-28]. The various search techniques for diagnostic methods operate on the principle of comparing the actual operation of the system to a reference illustrating its normal or abnormal operation. Exploring the fault diagnosis classifications provides a comprehensive understanding of the diverse strategies employed to maintain the integrity and functionality of complex systems.

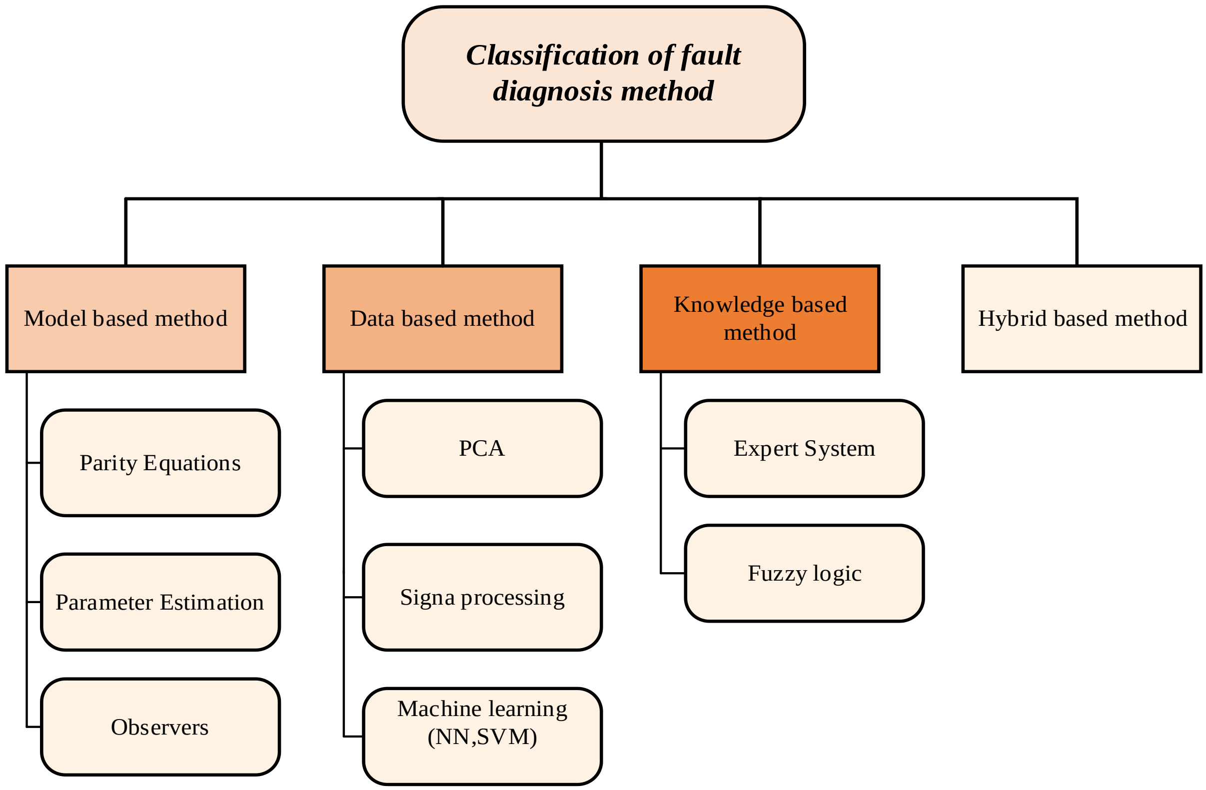

Figure 1. 9: Classification of fault diagnosis methods.

1.5.1 Model based methods

The operating principle of model-based fault detection methods is to compare the real behavior of the process with that of the nominal model of the fault-free process driven by the same input. Figure 1. 10 shows the schematic representation of a model-based fault detection mechanism. It consists of two main steps: residual generation and residual evaluation. The goal of residual generation is to produce a signal, called a residual signal, by comparing measurements with their estimates, and the purpose of residue evaluation is to check for the presence or absence of faults by analyzing the residual signal [26,28].

The generation of residuals characteristic of system operation is the fundamental problem of model-based diagnosis. A variety of methods for generating residuals exist in the literature [24,28]. Here we present some basic concepts, namely:

- Parity space approach.
- Parameter estimation-based approach.
- Observer-based approach.

All these methods are based on the use of a supposedly exact model of the system and generate residuals, which are the differences between the measured output signals and their estimate.

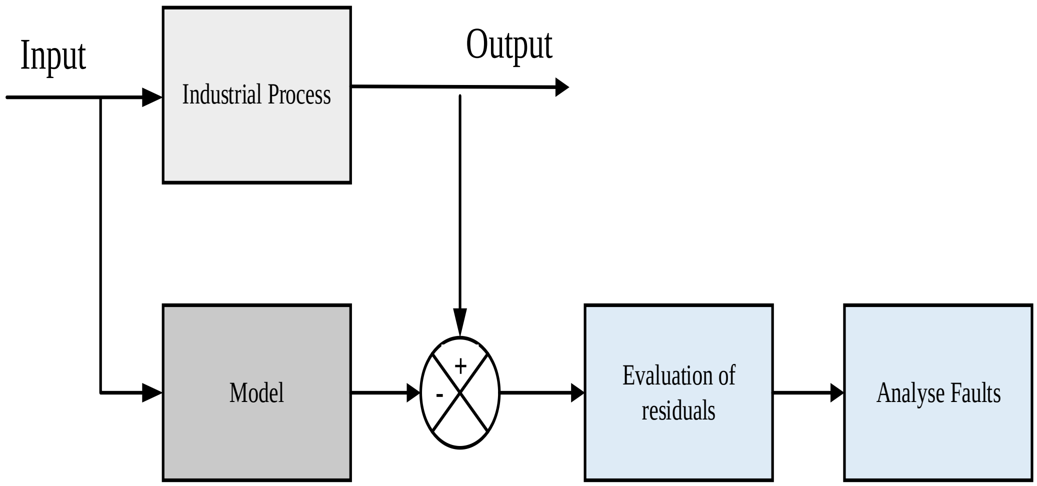

Figure 1. 10: Model based diagnosis approach scheme.

1.5.1.1 Parity space approach

This approach relies on generating signals to assess the consistency of measurements with their calculated values using a model (also referred to as measurement consistency or parity). In broad terms, the method involves verifying the algebraic closure of input-output relations in the model using real measurements. To achieve this, signals collected from the system are fed into input-output relations, and the signals thus created are utilized as residuals. This method was initially developed for static systems by Potter and Suman in 1977 [28,29]. The primary objective is to detect faults by identifying inconsistencies in these parity equations, revealed through a residual vector. The modification of system equations aims to decouple residuals from system states and different faults, enhancing diagnostic capabilities. Parity equations play a crucial role in fault detection, offering a systematic way to test the system's integrity and detect deviations from expected behavior [28-29].

1.5.1.2 Parameter estimation approach

The parameter estimation diagnosis method is a comprehensive approach designed for dynamic systems, specifically addressing faults linked to changes in model parameters. The process involves formulating equations that represent measurable input and output variables based on conservation equations. To simplify the estimation problem, model parameters are simplified, and variables are linearized in the equations. The core of the method lies in estimating model parameters and deriving physical parameters from these estimated model parameters. Fault detection is then executed by comparing changes in physical parameters to historical data, setting thresholds based on deviations from nominal values. Noteworthy is the requirement for persistent excitation of signals to ensure effective fault detection. Challenges include difficulty in determining physical parameters, The difficulty increases with more complex models. In summary, it's a systematic strategy for fault detection and isolation in dynamic systems [5,28,30].

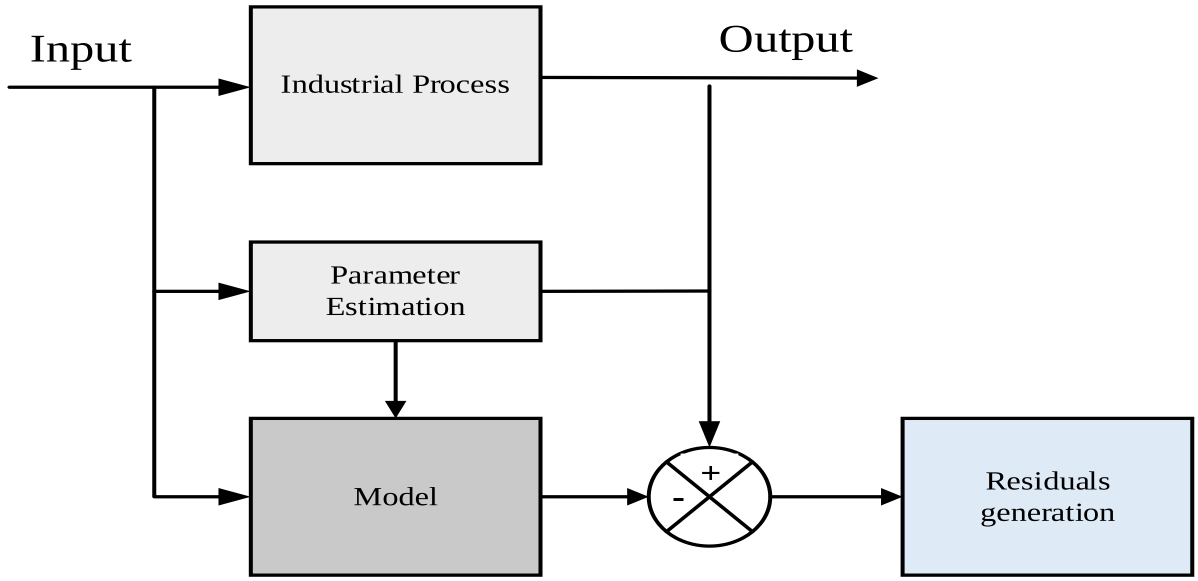

Figure 1. 11: Parameter estimation diagnosis method scheme [28].

The mathematical model of the process is given by the equation (1.1):

$$y(t) = f(u(t), \theta) \tag{1.1}$$

$y(t)$ is the output, $u(t)$ is the input, and θ represents the model parameters. The relationship g between the physical constants (p) and the model parameters (θ) is given in:

$$\theta = g(p) \tag{1.2}$$

$$\hat{\theta} = h(y(1), \ldots y(t), u(1), \ldots u(t)) \tag{1.3}$$

This equation involves estimating the model parameters ($\hat{\theta}$) based on the measurements of the system's inputs and outputs over time.

This (1.4) equation computes the residual or the difference between the true model parameters θ and their estimates $\hat{\theta}$. This residual is used in decision-making for fault detection.

$$r(t) = \theta(t) - \hat{\theta}(t) \tag{1.4}$$

1.5.1.3 Observer based approach

In the field of fault diagnosis, an observer-based approach involves the implementation of dynamic systems, known as observers, to estimate and track the behavior of a system's outputs and state variables. Unlike traditional observers used solely for state estimation, those employed in diagnosis serve a dual purpose: not only do they estimate the system's outputs, but they also play a crucial role in fault detection and isolation. By comparing the observer's output estimation with the actual measured outputs, the method generates residual that become apparent in the presence of faults or abnormalities. This observer-based diagnosis ensures robustness against uncertainties in the system model, disturbances, and measurement noise, while remaining sensitive to deviations caused by faults. The resulting residuals serve as reliable indicators for identifying and isolating faults within the system [28,30-31]. The block diagram of such a method is given in the following Figure 1. 12:

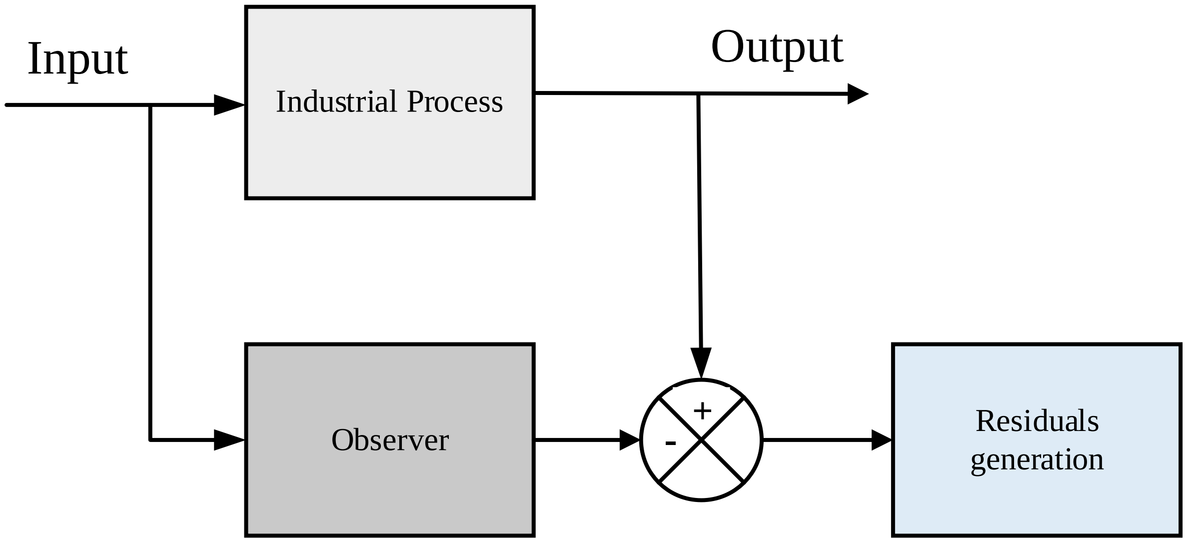

Figure 1. 12: Observer diagnosis approach scheme [31].

Several approaches have been proposed for fault detection, for example the classical Luenberger state observer. Luenberger Observer is detailed in the following equations:

Consider the following linear dynamic system which can be described by the state space model:

$$\begin{aligned} x(k+1) &= Ax(k) + Bu(k) \\ y(k) &= Cx(k) \end{aligned} \tag{1.5}$$

Where:

$x(k) \in R^n, u(k) \in R^m, y(k) \in R^p$ are the system state, control input, measured output respectively.

An observer-based fault detection filter is given in the following form:

$$\begin{aligned} \hat{x}(k+1) &= Ax(k) + Bu(k) + L(y(k) - C\hat{x}(k)) \\ \hat{y}(k) &= C\hat{x}(k) \end{aligned} \tag{1.6}$$

Where:

$\hat{x}(k)$ and $\hat{y}(k)$ are the estimates of the state and output, respectively. L is the observer gain to be designed and $e(k)$ is an output error.

$$\hat{x}(k+1) = (A - LC)\hat{x}(k) + Bu(k) + L(y(k)) \quad (1.7)$$

$$e(k) = y(k) - C\hat{x}(k) \quad (1.8)$$

$e(k)$ is the output residual.

In the threshold selection process, we determine a range acceptable for residuals. Residuals represent the differences between estimated and actual values in a system. If a residual surpasses this predetermined threshold, it indicates a significant deviation from the expected behavior, signaling a potential fault. The challenge in threshold setting lies in striking the right balance. If the threshold is set too high, there's a danger of overlooking faults. Conversely, a threshold set too low may lead to false alarms, falsely identifying normal system operation as a fault. Achieving an optimal balance is crucial for effective fault detection [21,31].

1.5.1.4 Advantages and Inconvenient of Model based methods

Model-based FDD proves advantageous when there is a comprehensive understanding of the system's behavior. Leveraging accurate mathematical models, it enables fast time detection of faults, also robust to false flags. This approach not only enhances the reliability of fault detection but also provides valuable insights into the root causes of issues. When applied in scenarios where a well-established understanding of system behavior exists, model-based FDD becomes a powerful tool for proactive maintenance [28,30-31].

However, challenges arise in situations where the system's behavior is highly when the complexity of models becomes difficult to manage in real-time. Accurately modeling nonlinear systems poses difficulties, and the handling of intricate models in dynamic industrial environments can be problematic [28,30-31].

1.5.2 Data based methods

In modern industrial systems, the increasing complexity and components necessitate advanced methods for effective condition monitoring and fault diagnosis. Among these, the data-driven diagnosis approach has emerged as a powerful paradigm, leveraging the wealth of information generated by sensors and systems during operation. Unlike traditional methods that rely heavily on expert knowledge and pre-defined models, the data-driven approach is characterized by its reliance on empirical observations and machine learning techniques. The deployment of this technology involves three fundamental steps: data collection, crucial for obtaining relevant information; data processing, where the importance of extracting features becomes apparent; and fault detection, diagnosis, and prediction [23,25,32].

1.5.2.1 Machine learning

Machine Learning (ML) is a subset of Artificial Intelligence (AI) that enables computers to perform tasks and make decisions based on data. It involves selecting essential features, choosing an appropriate ML architecture, and employing algorithms that can learn and enhance their performance over time as they are exposed to new data. The core of ML lies in the development of algorithms designed to improve and adapt through continuous exposure to new information. In the thesis, various methods will be explored for the supervised learning including but not limited to Artificial Neural Networks (ANNs), Support Vector Machines (SVM), and other relevant techniques (Random forests, etc.). However, the primary focus will be on brief investigation of ANN and SVM methodologies due to their significance and applicability in the diagnosis field [33,34].

1.5.2.1.1 Artificial Neural Network

Artificial Neural Networks are computational models that imitate the structure of the human brain. Comprising simple processing elements called "neurons", connected in a complex layer structure, ANNs approximate complex nonlinear functions with input, output, and hidden neurons. Their primary advantage over other tools lies in their capacity for learning and generalizing knowledge to unknown inputs. In the operation of a neural network, each neuron is connected to the neurons of the next layer through adaptable synaptic weights. The hierarchical structure of neural networks comprises layers, input, hidden, and output, each housing interconnected neurons. Neurons, similar to basic processing units, transmit signals within and between layers. The flow of signals from the input layer through the hidden layers to the output layer enables neural networks to process and transform input data into meaningful output [28,33-35].

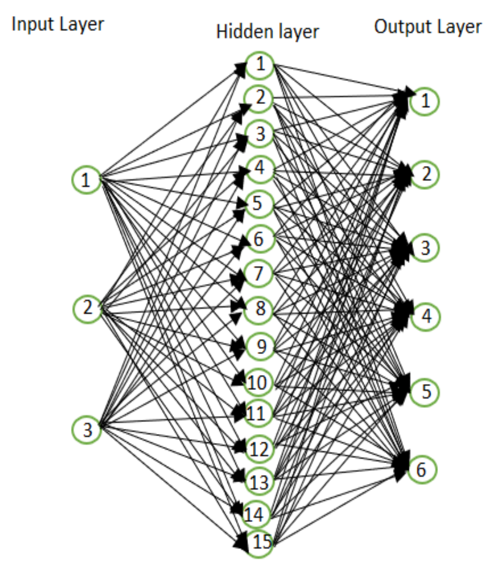

Figure 1. 13: Neural Network architecture with three layers [33].

Each neuron j in the hidden and output layers receives a signal from the neurons of the previous layer $v^T = [v_1, ..., v_r]$, scaled by the weight $w_j^T = [w_{1j}, ..., w_{rj}]$. The strength of connections between two linked neurons is represented in the weights, which are determined via the training process. The j^{th} neuron computes the following value:

$$s_j = w_j^T \cdot v + b_j \tag{1.9}$$

Where:

b_j : Optional bias term of the j^{th} neuron.

The input layer neuron uses a linear activation function and each input layer neuron j receives only one input signal x_j. The quantity s_j is passed through an activation function resulting in an output O_j. The most popular choice of the activation function is to use a sigmoid function which is given in the following equation:

$$O_j = \frac{1}{1+e^{-s_j}} \tag{1.10}$$

1.5.2.1.2 Support vector machine

Support Vector Machines (SVMs) are machine learning algorithms widely employed in classification tasks such as pattern recognition, portrait recognition, data analysis, and text classification. In the context of industrial system diagnosis. SVMs are utilized for machine fault detection and diagnosis by learning distinctive patterns from acquired signals, classifying these patterns based on fault occurrences in the machine. The key principle of SVMs involves finding the optimal hyperplane to separate data from different classes, maximizing the margin between them. SVMs can perform linear or nonlinear classifications, with nonlinear classifications being valuable when dealing with non-linearly separable data. In scenarios requiring multiclass classification, multiple SVM classifiers can collaboratively address the complexity. SVMs are applied in various industrial scenarios involving FDD, including fault classification, isolation, and prediction. For instance, SVMs can classify the type of fault based on features extracted from sensor data, isolate the location or source of the fault, and predict the occurrence or severity of a fault in a system or component [36-39].

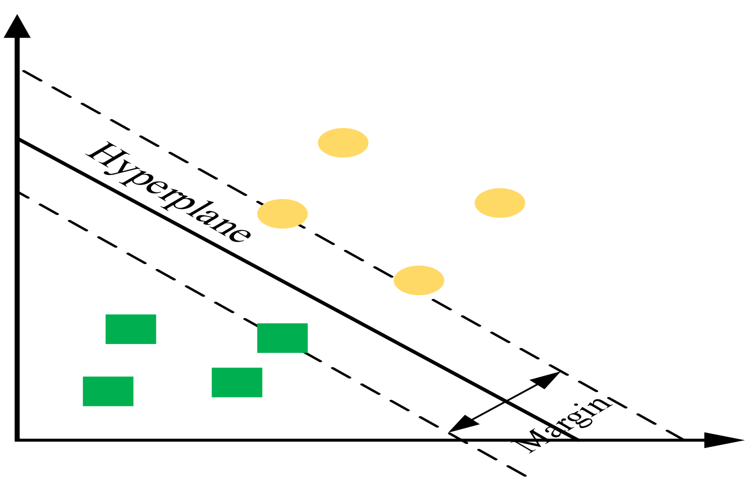

Figure 1. 14: Classification of support vector machine [37].

SVM's ability to handle large feature spaces and its nonlinear attributes make it suitable for machine fault detection. The SVM algorithm separates datasets into two classes using a hyperplane with maximum distance between support vectors in each class. Support vectors, representative data points, play a crucial role in defining the optimal hyperplane [36-39].

$$d(x) = wx_i + b \tag{1.11}$$

Where:

x_i is the input data, w is the weight vector vertical to the hyperplane, and b is the bias.

SVM attempts to separate the linearly separable data using a linear hyperplane equation. The parameters of the hyperplane are determined by minimizing the distance from the closest vectors, referred to as support vectors. The distance from a data point to the separating hyperplane is calculated based on the parameters w and b. In summary, SVMs, as ML algorithm, offer a robust and flexible approach to industrial system diagnosis, particularly in fault detection, classification, isolation, and prediction tasks. The underlying SVM theory, with its emphasis on structural risk minimization and the optimal separation of data, contributes to its effectiveness in handling complex industrial scenarios [36-39].

1.5.2.2 Signal processing

In the field of data processing techniques, feature extraction and feature selection stand out as pivotal components. Feature extraction involves the extraction of selective features from the original signal, effectively emphasizing variations among different operational conditions of the equipment. The primary methods for feature extraction encompass time-domain, frequency-domain, and time-frequency approaches, each chosen based on the derived characteristics' nature and physical relevance [40,41].

1.5.2.2.1 Time domain analysis

Time domain analysis, especially with the incorporation of statistical functions, is instrumental in establishing a baseline, detecting anomalies, recognizing fault patterns, and providing diagnostic information. This approach enhances the accuracy and reliability of fault detection and diagnosis in monitoring systems [40,41].

- Peak to peak amplitude: is the difference between the maximum positive and maximum negative values in a signal.

$$s_1 = x_{\max}(t) - x_{\min}(t) \tag{1.12}$$

- Mean amplitude: the average value of signal can be given in the following equation, where N is number of sampled points and x_i elements of x.

$$s_2 = \frac{1}{N}\sum_{i=1}^{N} x_i \tag{1.13}$$

- Root Mean Square amplitude: The square root of the average of the squared values of a set of numbers.

$$s_3 = \sqrt{\frac{1}{N}\sum_{i=1}^{N} x_i^{\,2}} \tag{1.14}$$

- Variance: A measure of deviation of signal from the mean value.

$$s_4 = \frac{\sum (x_i - s_2)^2}{N-1} \tag{1.15}$$

- Standard deviation: The square root of the variance is called the standard deviation of the signal x, and is expressed as:

$$s_5 = \sqrt{\frac{\sum (x_i - s_2)^2}{N-1}} \tag{1.16}$$

- Kurtosis: is utilized in vibration signal analysis to assess distribution shape, identify outliers, and recognize distinct fault signatures, providing sensitivity to deviations and aiding in early detection of issues.

$$s_6 = \frac{\sum_{i=1}^{N} (x_i - s_2)^4}{N s_5^{\,4}} \tag{1.17}$$

1.5.2.2.2 Frequency domain

Frequency domain analysis for diagnosis involves examining the distribution of signal energy across different frequency components, providing valuable insights into the distinctive patterns and abnormalities within a signal. This approach is widely applied in various fields, including machinery fault diagnosis, where specific frequency signatures help identify and address potential issues [40-44].

- Discrete Fourier transform

The Discrete Fourier Transform (DFT) is a mathematical technique that transforms a discrete signal from the time domain into its equivalent representation in the frequency domain, decomposing the signal into its individual sinusoidal components and providing insights into its frequency content.

$$X_{DFT}(k) = \sum_{n=0}^{N-1} x(n) e^{-j2\pi nk/N}, k = 0,1,......, N-1 \tag{1.18}$$

Here, k is the index, and N is the length of the signal.

- Frequency spectrum statistical features:

Frequency Spectrum Statistical Features involve extracting quantitative metrics from the frequency domain representation of a signal, offering insights into its spectral characteristics, which is vital for fault diagnosis.

1.5.2.2.3 Time-Frequency domain

Various techniques in time-frequency analysis have been developed and employed for fault diagnosis. Examples include the short-time Fourier transform (STFT), wavelet transform (WT), Hilbert-Huang transform (HHT), empirical mode decomposition (EMD), this part provides an introduction to signal processing in the time-frequency domain, offering explanations of several techniques used in this context [40-44].

- Short Fourier transform approach

Utilizing the Fourier Transform (FT) approach proves instrumental in extracting time-varying signal information within the frequency domain for condition monitoring, allowing for comparison with normal state characteristics. While the Fourier transform facilitates the analysis and diagnosis of signal states in the frequency domain, determining the exact time of frequency occurrence in the time domain remains a challenge. Based on the Fourier transform, the STFT method is presented to analyze the frequency information of a time-varying signal at a certain time interval or instant, The SFT for any signal x(t) is defined as:

$$SFT_x(t,\omega) = \int_{-\infty}^{+\infty} \left[x(\tau)g(t-\tau)\right] e^{-j\omega\tau} d\tau \tag{1.19}$$

Where:

τ is the time shift parameter, $x(\tau)$ is the time-domain signal, and $g(t - \tau)$ represent the time window.

- Wavelet transforms

The wavelet transform is an extension of the Fourier transform, which maps the original signal from the time domain to the time-frequency domain. The WT approach can be used to decompose the signal at multiple scales and obtain local features in the time-frequency domain through a series of wavelet basis functions and is one of the most important tools in the time-frequency analysis of non-stationary signals. Wavelet analysis finds applications in various fields, including fault diagnosis, image processing, and signal denoising, owing to its ability to capture dynamic signal characteristics. The mother wavelet ψ(t) can be expressed mathematically by the following equation

$$\psi_{s,\tau}(t) = \frac{1}{\sqrt{s}} \psi\left(\frac{t-\tau}{s}\right) \tag{1.20}$$

Where:

s represents the scaling parameter, τ is the transformation parameter, and t is the time. The original mother wavelet has s = 1 and $\tau = 0$.

The WT of the time domain vibration signal (x), $W_x(t)$ (s, τ) can be expressed using the following equation:

$$W_x(s,\tau) = \frac{1}{\sqrt{s}} \int x(t) \psi^*(\frac{t-\tau}{s}) dt \tag{1.21}$$

Where:

ψ^* represents the complex conjugate of $\psi(t)$ that is scaled and shifted using the s and τ parameters.

- Empirical mode decomposition

Empirical Mode Decomposition (EMD) is a powerful signal processing technique that can be employed for fault detection in various systems. EMD is particularly effective in analyzing non-stationary signals and has been successfully applied in condition monitoring and fault diagnosis. EMD decomposes a complex signal into a set of intrinsic mode functions (IMFs), which represent the signal's different frequency components. Each IMF reflects a specific oscillatory mode within the signal, providing a localized representation of signal variations.

1.5.2.3 Principal Components Analysis (PCA)

It is a widely used statistical tool for analyzing data collected from systems in operation to monitor their behavior. Principal Component Analysis (PCA) is a well-known numerical technique in the field of multivariate data analysis, specifically designed to reduce the dimensionality of the representation space of a system [28,45-46].

Given n observations (each observation has m observation variables), forming an n×m matrix, usually n is large. It is difficult to understand a complex matter described by a number of variables. If several key variables happened to reflect the main aspects, we only need to separate these variables for detailed analysis. PCA is such an analysis method. The central concept of PCA is to decrease the dimensionality of a dataset which has a variety of interrelated variables while remain the variation in it as much as possible. It constructs the so-called loading vectors consisted of a group of orthogonal vectors. These vectors are sorted by the value of variance. Taking into account a n × m training dataset (n observations and m observation variables) and stacking them into a matrix X, then the loading vectors are computed via the eigenvalue decomposition [24,42-44].

$$S = \frac{1}{n-1} X^T X = V \Lambda V^T \tag{1.22}$$

where $V \in R^{m \times m}$ is unitary matrix, and Λ is the main diagonal matrix which is sorted by the decreasing magnitude of the non-negative real eigenvalues along its main diagonal, (i.e. $\lambda_1 \geq \lambda_2$

... $\geq \lambda_m \geq 0$) and the rest elements of the main diagonal are zeroes. The column vectors in the matrix V are orthogonal, and the vectors in that matrix is named the loading vectors, λi is the i th characteristic value of the training dataset. T^2 statistic can be used to detect faults for multivariate process data. Assuming that $\Lambda=\Sigma^T \Sigma$, $\Sigma \in R^{n\times m}$, is invertible, the following PCA representation is utilized to calculated the T^2 statistic directly.

$$T^2 = x^T V(\Sigma^T \Sigma)^{-1} V^T x \quad (1.23)$$

The T^2 statistic for the lower-dimensional space is to be calculated as bellow:

$$T^2 = x^T P \Sigma_a^{-2} P^T x \quad (1.24)$$

Where P is consisted of a largest singular value, Σ_a contains first a row of Σ.

1.5.2.4 Advantages and Inconvenient

Data-driven diagnosis methods offer several advantages in industrial applications. Firstly, they excel at handling complex and dynamic systems. Secondly, data-driven approaches are adaptable and can evolve with changing conditions, making them well-suited for environments where system dynamics may vary over time [23,25,32].

While data-driven diagnosis methods offer powerful capabilities, they come with certain challenges. One notable drawback is the demand for substantial amounts of high-quality data for effective model training. Moreover, the reliance on historical data may limit the ability to predict entirely new or rare fault scenarios that have not been encountered in the past [23,25,32].

1.5.3 Knowledge based methods

Knowledge-based methods are employed when modeling a system becomes impractical due to cost, computational complexity, or data insufficiency. These methods are well-suited for systems with a limited number of inputs, outputs, and states or when specialized knowledge is essential. They fall into categories like expert systems, fuzzy logic approaches. While effective for small-scale systems with few operating modes, it's worth noting that developing rules based on the system's physical properties can be time-consuming, potentially impeding a comprehensive understanding of the system [22,24].

1.5.3.1 Fuzzy logic

Fault diagnosis using fuzzy logic, whether for fault detection or isolation, is generally based on Mamdani methods for fuzzy controllers or Takagi-Sugeno-Kang models for fuzzy models. A fuzzy controller can be presented in various ways, typically divided into three parts: fuzzification, representing the core of the controller with rules connecting inputs and outputs, and finally, inference and defuzzification, determining the real output value from fuzzy input sets [28,47-48].

- The fuzzification block which converts numerical values into linguistic values using membership functions (MFs), among the most used MFs are the triangular, gaussian and trapezoid. Fuzzification provides a series of fuzzy variables, joined by a vector, which will be introduced to the inference block.

- In the inference block, the values of the linguistic variables are linked by several rules that characterize the behavior of the system under different operating conditions.
- In the defuzzification block, the fuzzy values are converted back to real values that allows to infer the state of the system.

In the domain of diagnostics, fuzzy logic proves highly effective in translating quantitative knowledge, such as system residuals derived from measurements, into qualitative insights manifested as fault indications. This process unfolds through fuzzification, where precise data takes on fuzzy set representations to accommodate inherent uncertainties. Subsequently, the inference phase employs fuzzy rules to map these sets onto fault indications, imitating human-like reasoning. The final step, defuzzification, refines these fuzzy fault indications into precise and actionable diagnostic outputs, facilitating the transition from nuanced, uncertain data to decisively interpretable results. This methodological approach enables robust decision-making in complex diagnostic scenarios by embracing and managing the uncertainties present in real-world data [47-49].

1.5.3.2 System expert

Expert systems are tools designed to model the approach of experts in a specific domain, facilitating the formalization of their knowledge and providing a mechanism for its exploitation. When the knowledge representation mode is symbolic, the expert system approach is favored. In this context, a priori knowledge about the system is represented by a set of rules and facts (data manipulated by the rules), forming what is referred to as the knowledge base. This base is constructed with the assistance of formalization tools strongly linked to the application [24,50-51].

A knowledge base and an inference engine are discussed. The inference engine serves as the resolution organ, operating based on context-independent, resolution methods [24,50-51]. A typical resolution method involves the following steps:

- Selection of rules in the knowledge base based on established facts.
- Resolution of conflicts between the selected rules.
- Execution by specifying triggering conditions and consequences until the desired goal is achieved, such as diagnosis.

In diagnostic applications, this approach is well-suited for problems involving the manipulation of a significant amount of non-homogeneous data. It has been widely utilized in the diagnosis of static systems. However, for dynamic systems, this approach is less suitable for real-time problems and dynamic information management.

1.5.3.3 Advantages and Inconvenient

Knowledge-based diagnosis methods offer distinct advantages and drawbacks. On the positive side, these methods are particularly advantageous in situations where physical or mathematical modeling is resource-intensive, computationally complex, or when data availability is limited. They excel in applications involving systems with a modest number of inputs, outputs, and states, and are especially suitable when specialized knowledge is critical for accurate modeling. However, a notable drawback lies in the time and effort required to develop rules based on the system's physical properties. This can hinder a comprehensive understanding of the system, making knowledge-based methods less favorable in situations with novel or unforeseen faults that are not covered by existing rules [22,24].

1.5.4 Hybrid diagnosis methods

Individual FDD methods have their advantages and disadvantages and are thus more or less suitable for a given supervisory problem. There is no universal FDD method that outperforms all other methods under any requirements. Therefore, the motivation is to combine individual FDD methods in such a way that they complement each other. The overall objective of combining multiple FDD methods is to enhance the FDD system's effectiveness, in terms of a higher and more reliable decision and diagnosis accuracy. Hybrid FDD approaches combine two or more approaches. The combination of two or more FDD methods into a hybrid approach may be done in different ways. This integration aims to improve decision and diagnosis accuracy. Three main strategies for combining FDD methods are outlined: Serial Combination, Parallel Combination, and Mixed Combination [5,52-53].

- Serial Combination:

In the context of FDD, the serial combination strategy involves the sequential fusion of multiple FDD methods. This approach establishes a chain where the output of one FDD method becomes the input for the next in line. The significance of this method lies in its ability to enable the selection of the most suitable method for each transformation step in the FDD process. By doing so, it enhances the global efficiency of the system by reducing ambiguities and improving the final accuracy of the diagnosis. However, it is crucial to note that the success of this strategy relies on the compatibility between the input and output interfaces of successive methods [1,52-53].

- Parallel Combination:

The parallel combination strategy in FDD involves the simultaneous execution of multiple FDD methods independently. The outputs from these methods are then fused to create a more stable and reliable system. This strategy can be categorized into two subtypes: Information/Data Fusion and Decision Fusion. Information/Data Fusion focuses on combining outputs on the same transformation level, utilizing data or information fusion in measurement, feature, and symptom spaces. Decision Fusion, on the other hand, concentrates on enhancing fault diagnosis and class space by ensuring that each fused method provides novel and unique insights, categorized into utility-based or evidence-based methods [1,50-52].

- Mixed Combination:

The mixed combination strategy represents an integrated approach that combines aspects of both serial and parallel fusion strategies. By leveraging the strengths of each, this strategy aims to achieve comprehensive improvements in the FDD system's overall performance [5,52-53].

1.6 Conclusion

In this comprehensive chapter, we have covered the essential terms and definitions related to the monitoring and fault diagnosis of systems. The discourse extended to a state-of-the-art exploration of monitoring techniques tailored for industrial systems. We also explored the current techniques used for monitoring dynamic systems. We provided a brief but informative overview of monitoring methods. The previous sections discussed the different methods in process monitoring and fault diagnosis, which can be classified into four main groups. Notably model diagnosis-based methods which bring a profound understanding the mathematical models representing the normal behavior of a system. By comparing the predicted behavior from these models with observed data or measurements, deviations indicative of faults can be identified. This approach is especially effective when a comprehensive understanding of the system's dynamics is available, providing a formalized means of detecting and isolating faults based on deviations from expected norms. Conversely Data-based diagnosis methods rely on the analysis of empirical data to detect and identify faults within a system. These approaches involve statistical techniques, machine learning algorithms, or data-driven models that learn patterns and anomalies from historical or real-time data. By leveraging the information contained in the data, these methods can effectively identify deviations from normal system behavior and provide insights into potential faults or abnormalities. Knowledge-based diagnosis methods, on the other hand, utilize a system's prior knowledge, domain expertise, or explicit rules to diagnose faults. These methods involve establishing a set of rules or logical relationships that represent known cause-and-effect associations within the system. Hybrid diagnosis methods bring advantages by combining different techniques, offering comprehensive analysis, improved accuracy, and adaptability to dynamic systems. Their robustness, enhanced sensitivity.

Chapter 2

Overview of Photovoltaic Energy

2.1 Introduction

Renewable energy sources (Photovoltaic, wind, hydro, biomass, etc.) have seen increasing interest in recent decades as a result of the rise in energy demand on the one hand and the resource limitations associated with fossil fuel-based energy on the other. Alternative energy sources like solar power and wind power are incredibly promising for standalone and grid-connected applications. Among all Renewable Energy (RE) sources, solar energy is becoming increasingly common and competitive with conventional energy sources. This success is mainly due to technological developments in the PV energy system and the encouragement of government incentive programs. Global photovoltaic capacity has grown rapidly over the last decade. This rapid growth in total installed capacity is explained by the increased competitiveness of photovoltaic energy due to lower prices for PV system components, in particular PV modules, and the introduction of economic incentives or subsidies aimed at reducing the use of fossil fuels. In this chapter, we will discuss various aspects of PV systems. We begin with a brief reminder of the fundamental principle of the photovoltaic effect. We then present some statistics on the Algeria's production of PV energy. We then explore the construction of PV cells, detailing their effect and principle of operation, as well as the classification of PV systems, finally, the chapter closes with a summary conclusion.

2.2 Sustainable Horizons: Mapping the Global Terrain of Renewable Energy

The world is at a decisive turning point for the future of energy. Climate change, growing dependence on oil and other fossil fuels, increased imports, and rising energy costs have made developing countries exceptionally susceptible. These pressing challenges demand global and ambitious action. The renewable energy sector stands out for its ability to reduce greenhouse gas emissions and pollution, and to harness local and decentralized energy sources such as wind, solar, hydroelectric, and geothermal. These sources are unaffected by the volatility of fossil fuel markets and have the added advantage of stimulating technological development and economic growth. Undoubtedly, RE stands as the cornerstone for a sustainable future [54,55].

2.2.1 Navigating the Transition: Challenges and Opportunities in Shifting to Renewable Energy

Globally, the adoption of RE contributes to an impressive 11.04% reduction in overall carbon emissions. This reduction is achieved through optimizing the structure of energy sources and lowering the carbon emission coefficient. Regionally, Europe and Central Asia stand out with a substantial 10.13% reduction. In contrast, East Asia and the Pacific show a contrasting effect, contributing to a 4.12% increase in emissions, The results emphasize the continued importance of utilizing renewable energy, especially in developing or underdeveloped countries. Notably, some countries reduced carbon emissions by relying extensively on renewable energy rather than improving energy-use efficiency, the study concludes by suggesting policy implications for reducing CO_2 emissions in different countries [56]. In the presented graph in Figure2. 1, illustrating the global energy mix, a comprehensive snapshot of the distribution of energy sources worldwide is portrayed. The graph highlights the proportionate contributions of diverse sources such as fossil fuels, renewables energy [57].

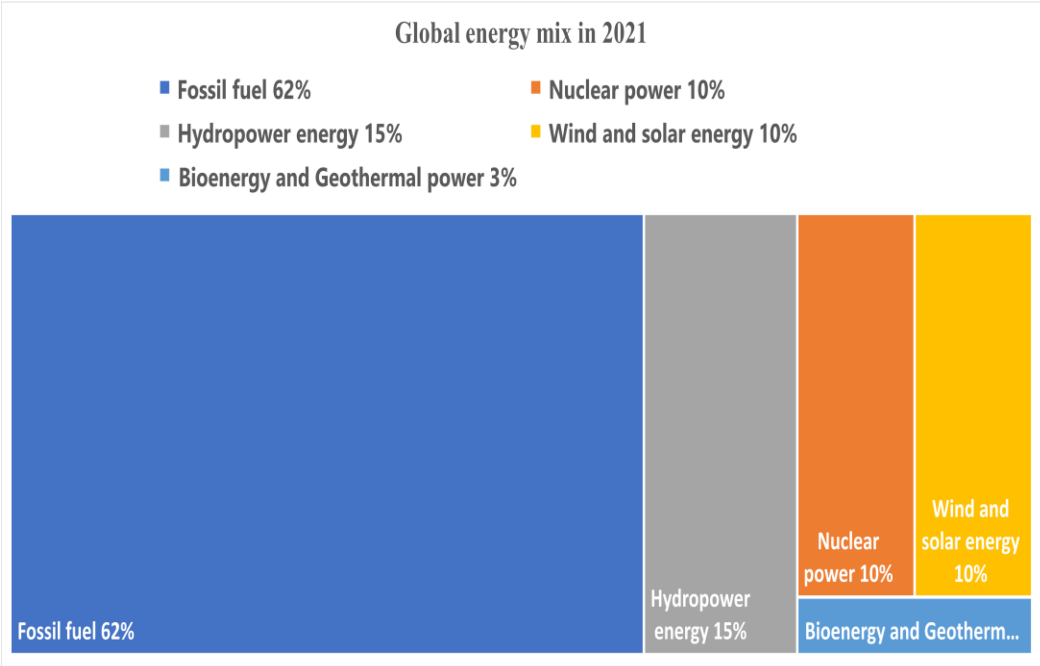

Figure 2. 1: Global energy mix in 2021 [57].

Figures 2. 2 and 2. 3 outline the remarkable growth of global Renewable Energy Resources (RER) despite the challenges of the COVID-19 pandemic. The linear increase in RER capacity, reaching 3,063.926 GW in 2021 from 1,443.923 GW in 2012, is evident in Figure 2. 2 Solar energy, especially photovoltaic type, shows rapid growth. The global surge in installed capacity for RER, showcased in Figure 2. 3, reflects a rapid increase across various regions, with Asia leading, followed by Europe, North America, South America, Eurasia, and Africa. Hydro energy dominates the installed capacity worldwide, while marine energy, concentrated in Asia and Europe, holds the smallest share. The Russian invasion of Ukraine has intensified the focus on securing energy sources, prompting accelerated transitions to RE, notably in the European Union (EU), seeking alternatives to Russian natural gas. Forecasts anticipate RER installed capacity exceeding 300 GW (8%), with solar photovoltaic reaching 190 GW (25% gain) and compensating for a 17% deficit in annual wind capacity. Despite notable cost increases in PV and Wind energy systems in 2021 and 2022 due to rising freight costs, raw materials, and manufacturing, the overall investment costs for PV and onshore wind farms have risen from 15% to 25%. However, the cost competitiveness of RER remains resilient, driven by historic record-breaking prices of fossil fuels and electricity globally, reaching six-fold increases in some European countries compared to the mean prices from 2016 to 2020 [54].

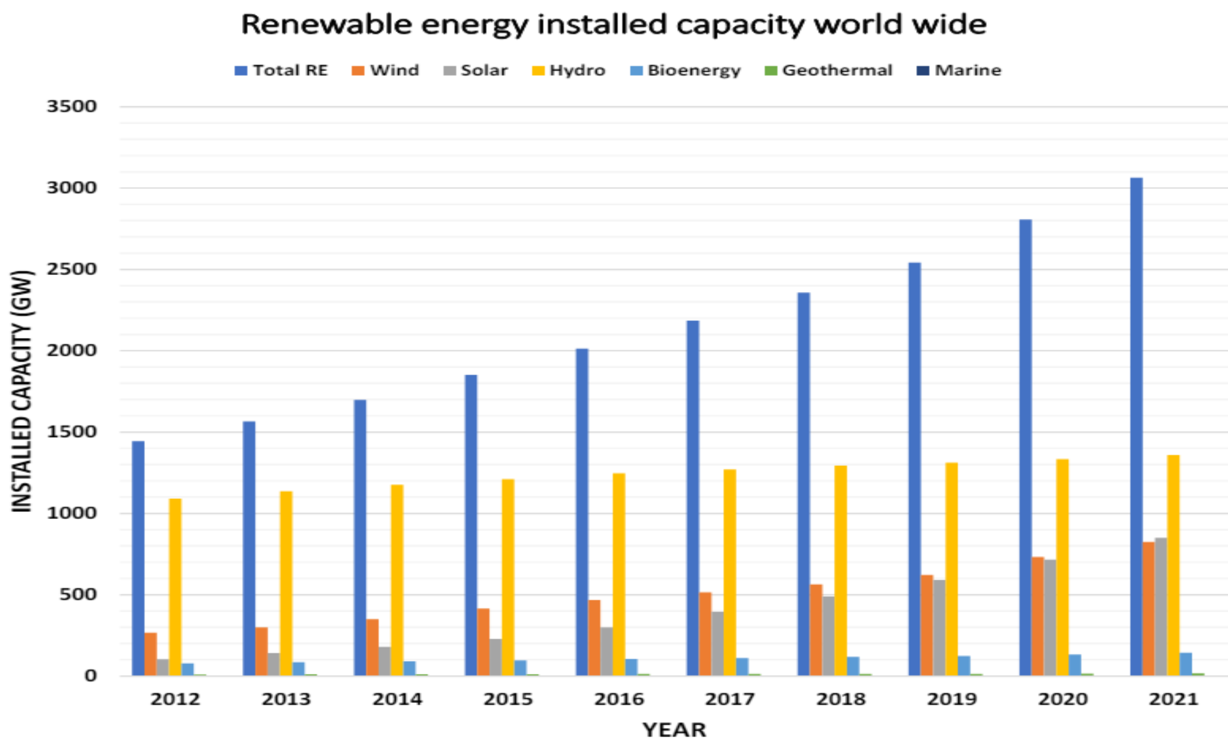

Figure 2. 2: RE installed capacity worldwide [54].

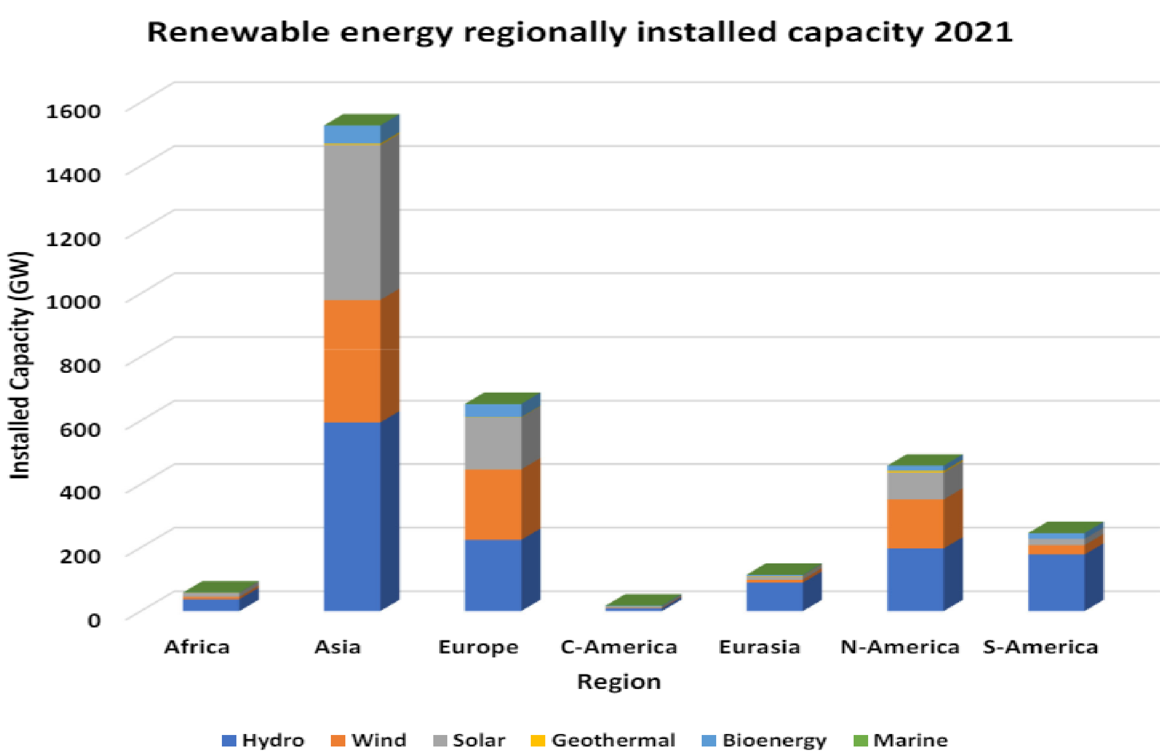

Figure 2. 3: RE regionally installed capacity 2021 [54].

The analysis highlights a fast-paced energy transition driven by falling costs of renewable technologies and policy innovations. It projects renewable energy's share to grow from 15% in 2015 to 63% by 2050, playing a crucial role in meeting climate objectives. However, a six-fold acceleration in renewables growth is needed compared to standard operations. Infrastructure planning, smart grids, and innovative financing models are crucial for successful energy transition. The shift towards renewable power, especially variable sources, requires systemic changes in the power sector, combining technology innovation with new market designs [54,58].

2.3 Renewable energy potential in Algeria

The current energy situation in Algeria is currently marked by a rising demand for energy, further amplified by significant population growth. This heightened energy demand is of particular concern, especially considering that nearly 99.47% of our electricity production still relies on fossil fuels, such as oil and gas. This heavy reliance on hydrocarbons not only carries substantial economic burdens but also substantially contributes to the emission of carbon dioxide CO_2. The escalating population growth, coupled with a consequent 7% increase in energy demand over the last decade, has led to a consistent elevation in our CO_2 emissions levels. Consequently, Algeria presently ranks as the third highest emitter of CO_2 on the African continent and holds a prominent position among developing nations in this regard. In 2014, our nation emitted 147 million metric tons of CO_2 and ranked 34^{th} globally in terms of fossil fuel emissions from gas flaring. Addressing these intricate challenges necessitates a determined shift towards renewable energy sources and substantial investment in energy efficient solutions. This approach is crucial to curbing our dependence on fossil fuels and mitigating the detrimental environmental consequences [59,60]. Figure 2. 4 depicts the percentage distribution of energy production in Algeria [61].

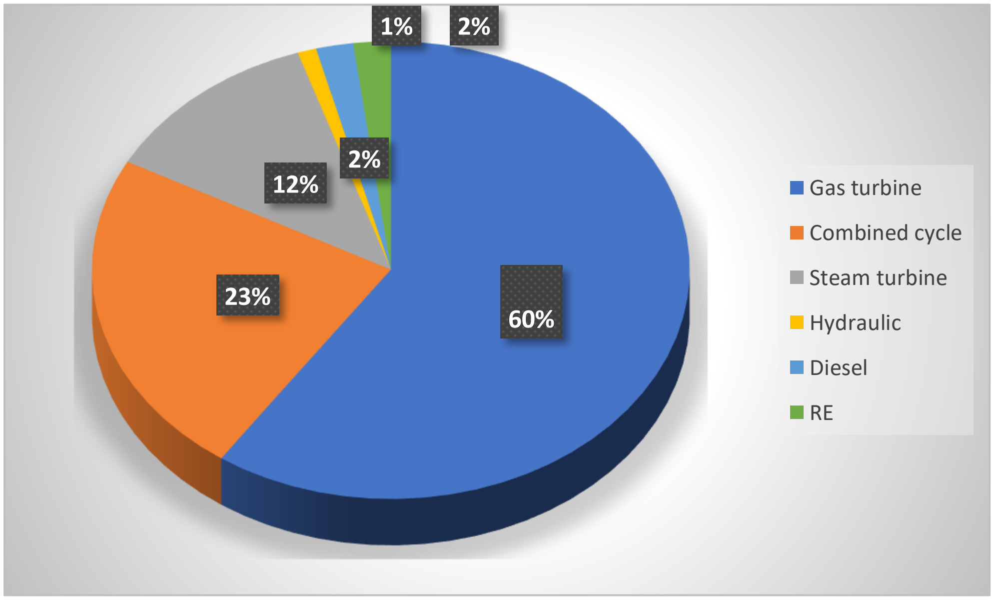

Figure 2. 4: Percentage distribution of energy production in Algeria [61].

2.3.1 National Programs of renewable energy in Algeria

Algeria has initiated a trajectory toward harnessing RE in order to provide comprehensive and sustainable problems of preserving fossil energy resources and solutions to the environmental challenges. This attempt is manifested through the launch of an ambitious program dedicated to the advancement of renewable energies [59].

This program, initially introduced by the government in February 2011, underwent revisions in May 2015 and was subsequently accorded national priority status in February 2016. Consequently, Algeria is embarking upon a transformative phase in energy sustainability by embracing a renewable energy initiative. This updated initiative strives to establish a renewable power capacity of approximately 22.000 MW by 2030, intended primarily for the national market, while also retaining the strategic objective of exportation. Achieving this will save a significant amount of natural gas, equal to eight times the gas used in 2014. Additionally, it could reduce CO_2 emissions by 348 million tons. The diagram 6 represents an array of renewable energy sources including photovoltaic and wind power, along with biomass, cogeneration, and geothermal energy [59]. Figure 2. 5 represents geographical position of Algeria in Africa [60].

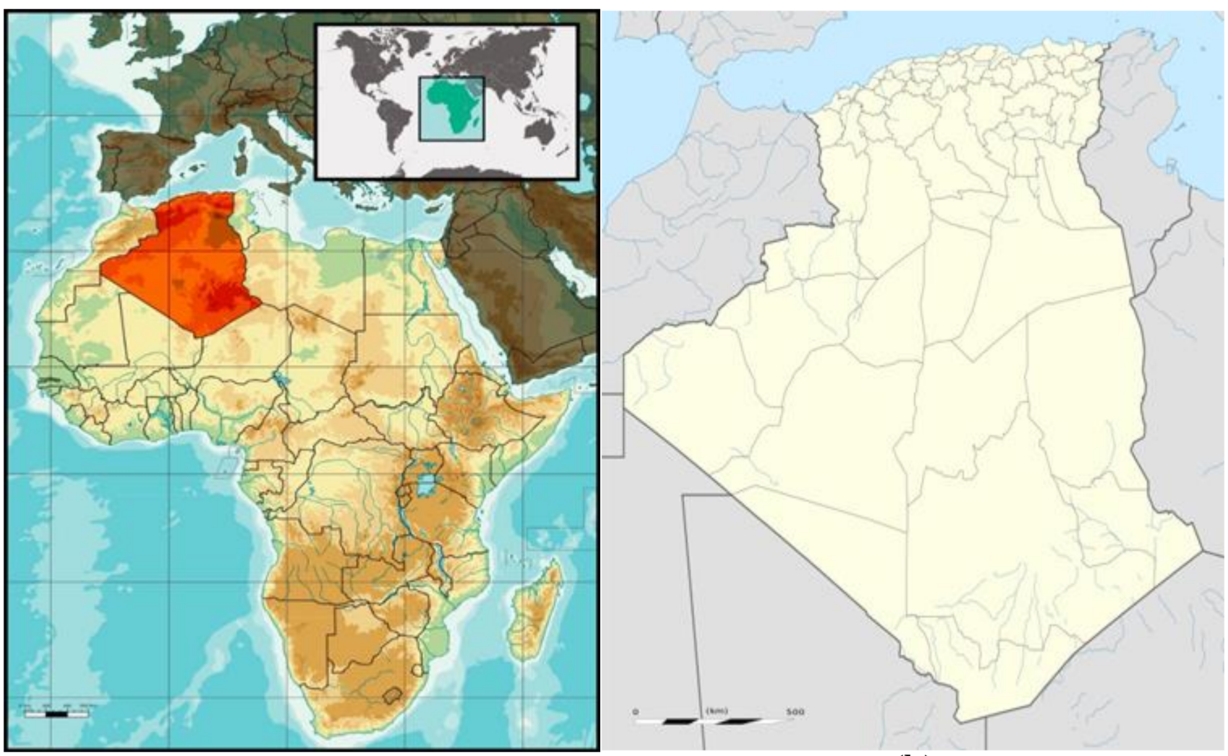

(a) (b)

Figure 2. 5: (a) Geographical position of Algeria in Africa. (b) Algeria’s map [62].

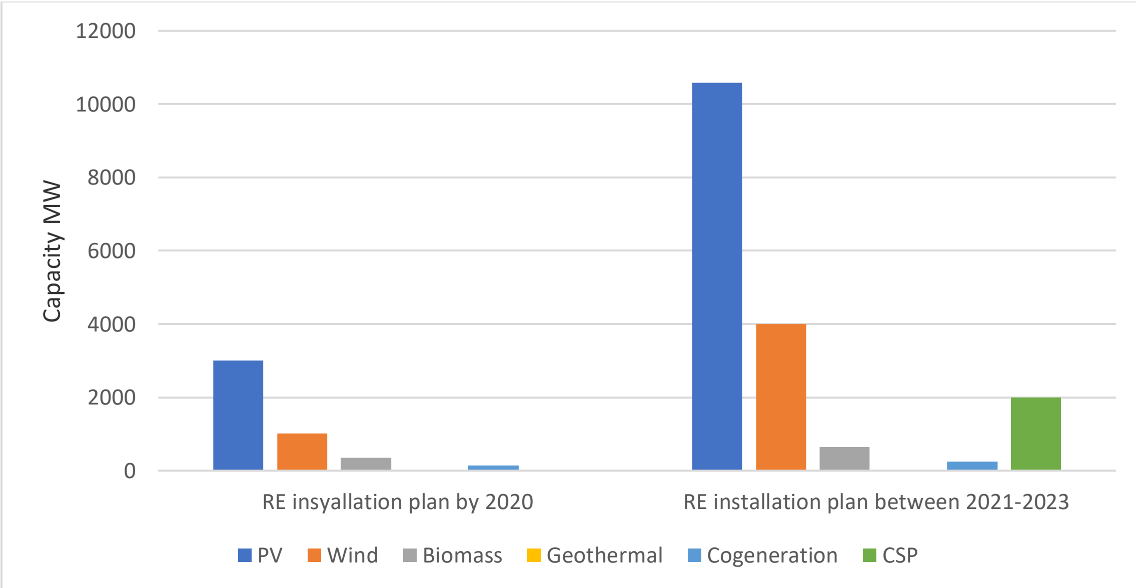

Figure 2. 6: Algeria RE projects.

The goals for RE are set in two time periods: 2015–20 and 2021–30. The aim is to encourage investment in various RE sources like solar, wind, geothermal, biomass, and more. By 2030, the plan is to generate a total of 22.000 megawatts (MW) of energy from RE. Out of this, 12.000 MW will be used within the country, and 10.000 MW will be exported. Table 2. 1 represents Projects currently underway and those planned for the future in Algeria [59].

Electric Power		
Type of RE	*1st Period (2015-20)*	*2nd Period (2021-30)*
PV	3000 MW	10575 MW
Wind	1010 MW	4000 MW
Biomass	360 MW	640 MW
Geothermal	5 MW	10 MW
Cogeneration	150 MW	250 MW
CSP	-	2000

Table 2. 1: Algeria RE current and future projects.

2.3.2 Solar energy potential energy in Algeria

Algeria's renewable energy potential is dominated by solar energy. Because of its geographical location, Algeria has one of the highest solar deposits in the world. The duration of sunshine over almost the entire country exceeds 2000 hours a year, and can reach 3000 hours on the High Plateaus and in the Sahara. The energy received daily on a horizontal surface is of the order of 5 kWh/m^2 over most of the country, nearly 1700 kWh/m^2/year in the north and 2650 kWh/m^2/year in the south [63]. Table 2. 2 represents sunshine and sun hours in Algeria.

	Coastal	*High plateaus*	*Sahara*
Surface (percentage)	4	10	86
Average duration of sunshine (h/ year)	2650	3000	3500
Received average energy (kWh/m^2/year)	1700	1900	2650

Table 2. 2: Sunshine and daylight hours in Algeria.

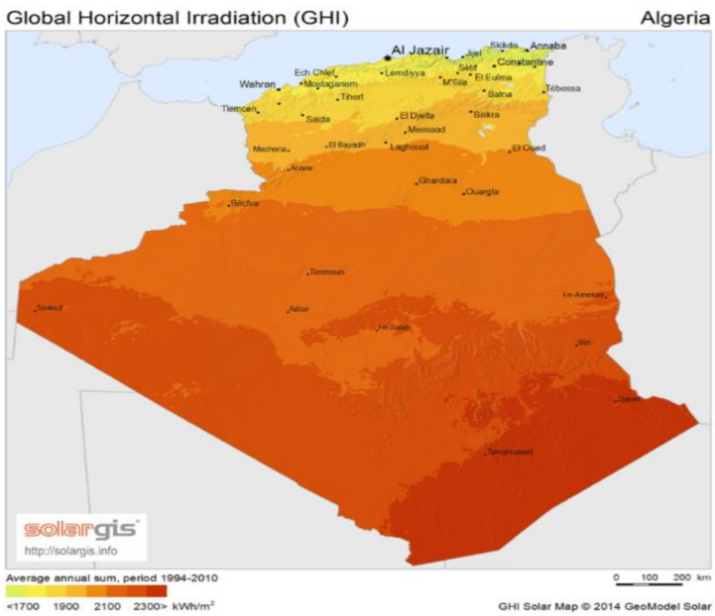

Figure 2. 7: Global horizontal irradiation map [64].

2.4 Solar's energy exploitation

Solar energy is currently exploited through two distinct approaches:

2.4.1 Solar thermal energy

Thermal conversion methods focus on capturing the heat energy inherent in sunlight. Concentrated Solar Power (CSP) systems use mirrors or lenses to concentrate sunlight onto a small area, generating intense heat. This heat is then utilized to produce steam, which drives the heat engine and generates electricity. CSP is particularly advantageous for large-scale, grid-connected power plants. On the other hand, Solar Heating and Cooling (SHC) technologies are designed to capture solar heat for direct use in heating applications, such as space heating or water heating. These systems often incorporate solar collectors to absorb and transfer heat to a fluid, which is then circulated for various heating purposes. Both CSP and SHC contribute to the efficient utilization of solar resources, providing solutions for electricity generation and direct heat applications [65,66].

2.4.2 Photovoltaic solar energy

Photovoltaic technology is centered around harnessing the light energy emitted by the sun and converting it directly into electricity. Solar panels, comprised of photovoltaic cells, composed mainly of silicon cells, these photovoltaic panels have the ability to convert photons into electrons. The efficiency and cost-effectiveness of PV technology have improved significantly over the years, making it a leading player in the solar energy landscape [65].

In this thesis, All the focus is for the analysis of the photovoltaic field, concentrating all the remaining parts of the thesis to a detailed study of the components, advances and applications of this technology.

(a) (b)

Figure 2. 8: (a) CSP. (b) PV solar energy [66].

2.5 Photovoltaic energy

Photovoltaic solar energy comes from the direct conversion of energy from photons in the sun's rays into electrical energy, using photovoltaic cells. Industrially, the materials most commonly used are silicon-based [67].

In the 19^{th} century, Edmond Becquerel, a French physicist, discovered the external photovoltaic effect by observing a current between two electrodes exposed to light. This discovery marked the beginning of the understanding of the transformation of light into electricity. In 1904, Albert Einstein further explains the theoretical framework foundation this photovoltaic phenomenon, providing a comprehensive understanding of the process. In 1916, the Polish chemist Jan Czochralski opened new possibilities by discovering the process of crystal growth, enabling the production of high-quality semiconductor monocrystals. Theoretical progress reached another milestone in 1949 when William B. Shockley established the theory of the PN junction, laying the theoretical foundations for modern solar cells. In 1954, Daryl Chapin, Calvin Fuller and Gerald Pearson put these theories into practice by developing the first silicon solar cell with an efficiency of 6%. A significant moment came on 17 March 1958, when the first use of photovoltaic energy in space was made by the American Vanguard satellite. Since then, research in this field has continued to progress rapidly, adopting new technologies to achieve ever-higher yields [67-69].

2.5.1 Photovoltaic solar cell

The PV cell is the smallest element of a photovoltaic system. It is composed of semi-conductor materials and directly transforms light energy into electrical energy. The operation of the PV cell is based on a physical phenomenon called the photovoltaic effect [70]. Figure 2. 9 shows a cross-section of a PV cell.

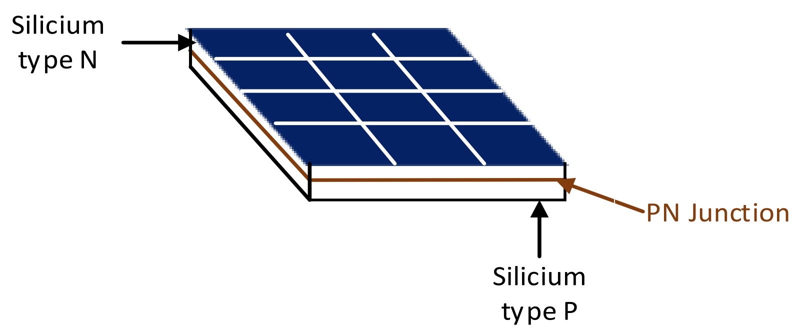

Figure 2. 9: Solar cell [70].

The PV effect is a crucial process wherein incident light energy is directly converted into electrical energy within a PV cell, primarily composed of semiconductor materials. Its structure is akin to that of a conventional diode, consisting of two distinct layers. The top layer, an N-doped region, is characterized by an excess of free electrons, while the P-type region possesses electron-deficient areas known as holes, forming a PN junction that establishes a potential barrier. When photons from incident light strike the solar cell's surface, they carry enough energy to elevate electrons in the semiconductor to higher energy states. In response, these excited electrons transition from the valence band to the conduction band, becoming mobile charge carriers. These liberated electrons, along with existing ones, move under the electric field toward the N-type region, while the holes shift towards the P-type region. This migration results in charge separation, with the N-type region acquiring a negative charge and the P-type region becoming positively charged. Consequently, this creates an electric current and a potential difference in the PV cell. The current and voltage generated by a PV cell depend on various parameters [68,71]. Figure 2. 10 represents the PV effect.

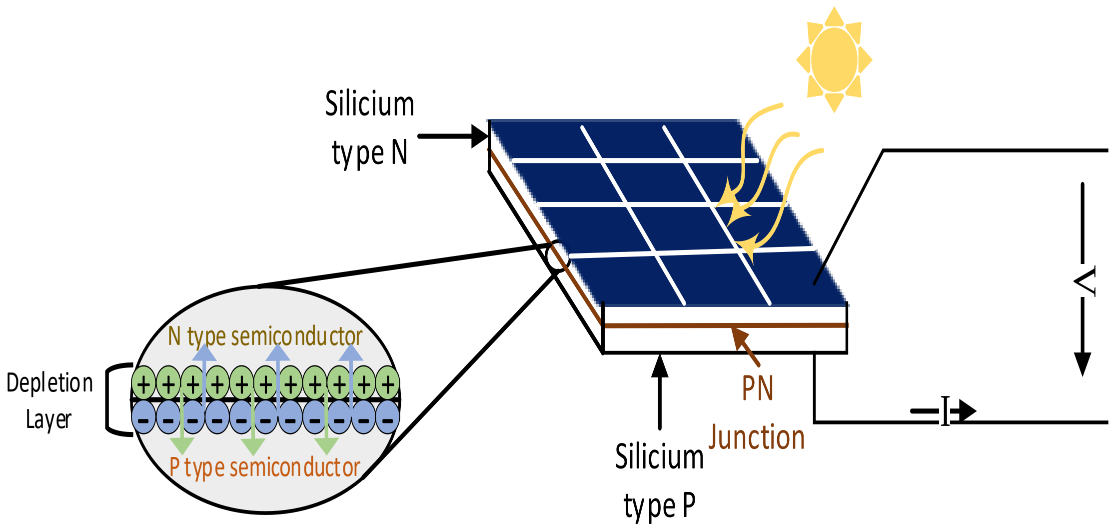

Figure 2. 10: PV effect [71].

2.5.2 Types of Solar cell Technologies

The evolution of solar cells spans three generations, each presenting unique characteristics and applications. The first generation, primarily composed of thick crystalline layers of silicon (mono-, poly-, and multicrystalline), marked the entry of solar cells into the market, leveraging processing information and raw materials from the microelectronics industry. Silicon-based PV cells, became widely adopted due to their relatively high efficiency. The second generation saw the emergence of thin film technologies, such as those based on CdTe, and copper (CIGS), designed as a lower-cost alternative to crystalline silicon cells. While these thin film cells offered improved mechanical properties suitable for flexible applications, there was a trade-off with reduced efficiency. In the current landscape, the third generation, often referred to as "emerging concepts," encompasses diverse approaches. The latest trends in silicon photovoltaic cell development focus on generating additional energy levels in the semiconductor's band structure, with a concentrated effort on third-generation solar cells [72-74]. Figure 2. 11 below shows the three main categories [72-74]:

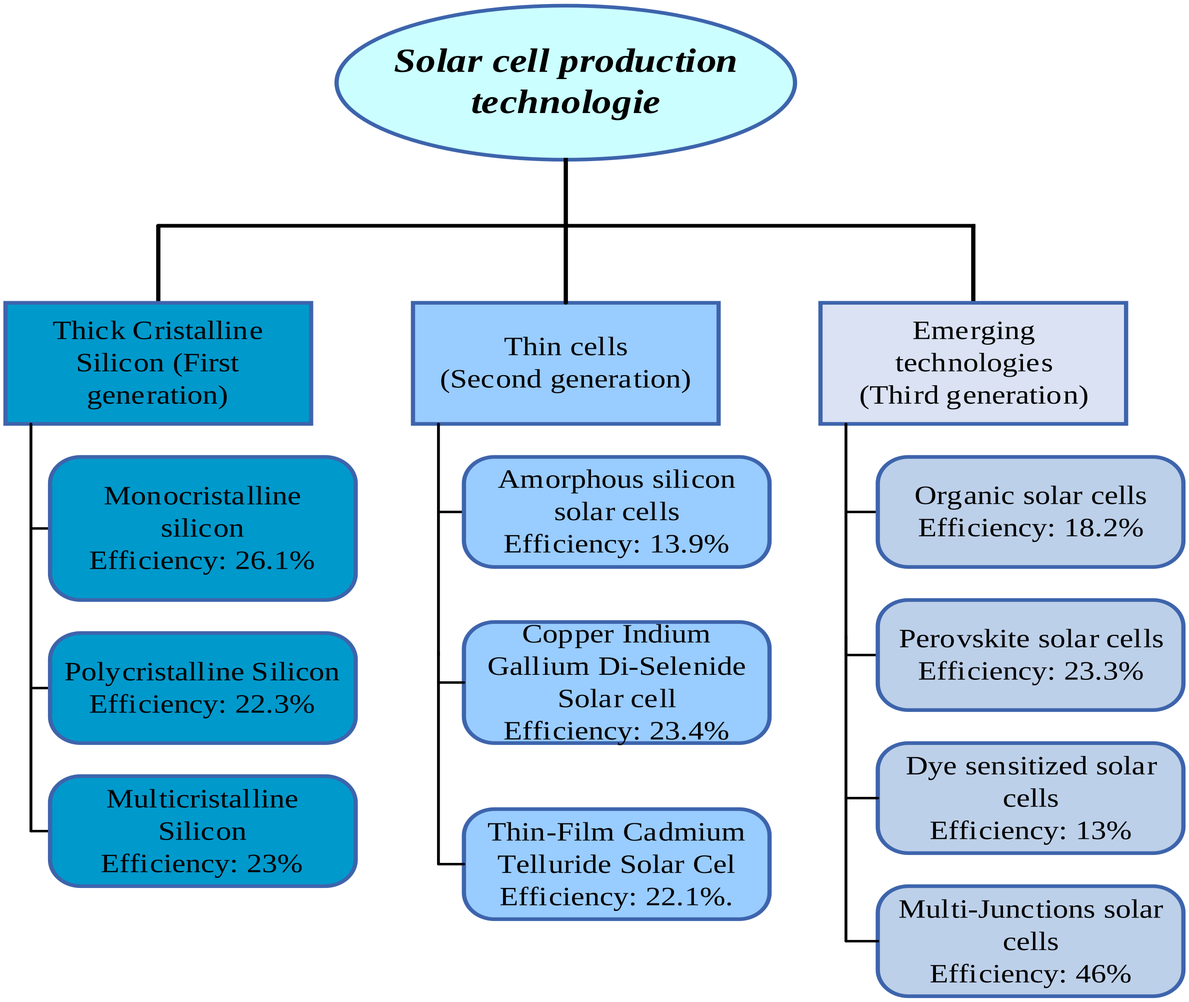

Figure 2. 11: Classification of solar cells.

2.5.2.1 First generation

Silicon solar cells, a cornerstone of the first-generation photovoltaic technology, have maintained their dominance despite the emergence of alternatives. Silicon's widespread use stems from its favorable bandgap energy of 1.17 eV and the abundance of high-quality material derived from scaled semiconductor production for microchips. Over time, crystalline Silicon (c-Si) photovoltaic cells have seen a remarkable efficiency increase from 6% to a current record of 26.1%. Advances in semiconductor production, driven by the demand for increased computing power, have contributed to this enhancement. Currently, Silicon-based PV cells, with over 80% of the world's installed capacity and a 90% market share. Complex architectures based on heterojunctions have already surpassed c-Si homojunction efficiency records, potentially shaping the future of photovoltaics with streamlined technologies and reduced production costs [72-74].

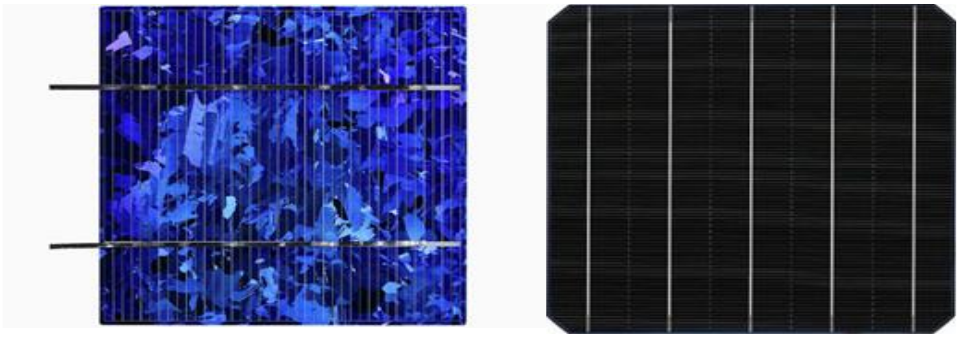

Figure 2. 12: (a) Polycristalline solar cell, (b) : monocristalline solar cell [75].

2.5.2.2 Second generation

Second-generation solar cells, particularly thin-film variants using materials like amorphous silicon or II-VI compounds (GaAs, CdTe, CuInSe2, TiO2), offer cost-effective production in contrast to their first-generation counterparts. This cost advantage stems from reduced semiconductor material consumption and the omission of the "wafer" transformation process. Despite being flexible and adaptable, these cells exhibit lower efficiency than mono or polycrystalline cells. Moreover, the flexibility and versatility of these second-generation cells make them suitable for diverse environments, operating effectively with low light levels and are less sensitive to high temperatures compared to mono or polycrystalline cells [72-74].

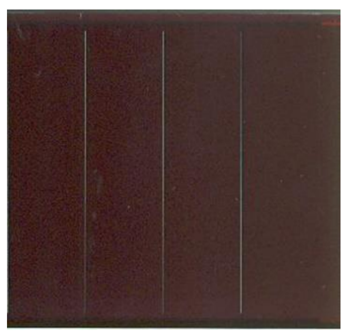

Figure 2. 13: Amorphous solar cell [76].

2.5.2.3 Third generation

Ongoing research in the photovoltaic industry focuses on developing third-generation solar cells with efficiencies surpassing 20%. This generation utilizes diverse materials beyond silicon, including tandem, perovskite, dye-sensitized, organic, and other innovative technologies. Although predominantly at the experimental stage due to high production costs, these cells aim to achieve both high efficiency and low cost. These range from cost-effective low-efficiency systems (dye-sensitized, organic solar cells) to expensive high-efficiency systems (III-V multi junction cells), addressing applications from building integration to space applications [72-74].

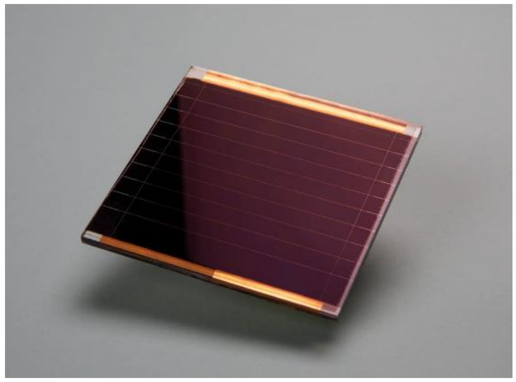

Figure 2. 14: Perovskite solar cell [77].

2.5.3 Electrical characteristics of PV cell

A photovoltaic cell is characterized by a current-voltage (I-V) and power-voltage (P-V) curve as shown in Figure 2.15, these characteristics representing the behavior of the PV cell under specific weather conditions (irradiation level and ambient temperature) [78,79].

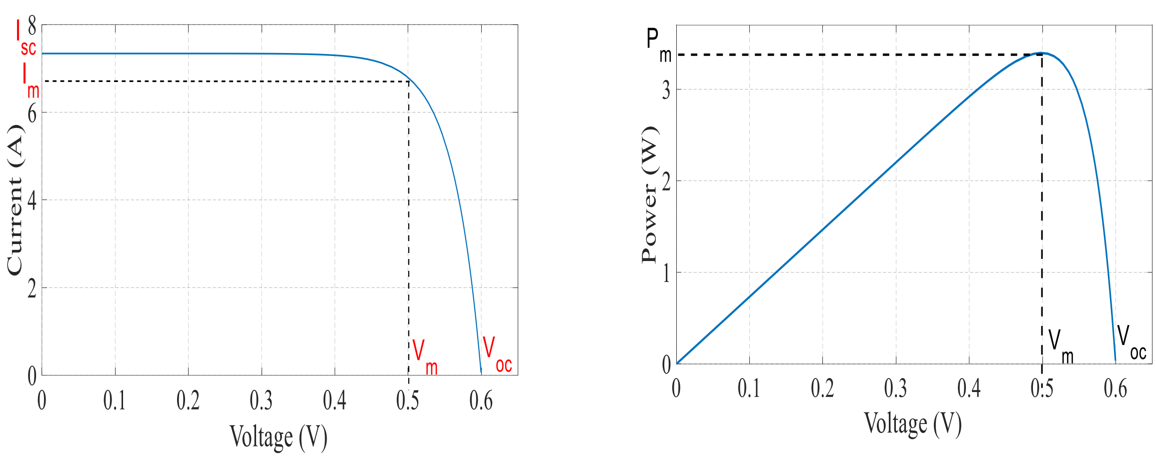

(a) (b)

Figure 2. 15: (a) (I-V) characteristics of solar cell, (b) (P-V) characteristics of solar cell.

- Short circuit current: represents the current flowing through the photovoltaic cell when it is short-circuited, the voltage at its terminals being zero. In this case, the power supplied by the cell ($P_m = V_m * I_m$) is zero [78].

- Open circuit voltage: This is the voltage across the cell when it is in an open circuit, it means: when the positive and negative poles are electrically isolated from any other electrical circuit (the current flowing through it is then zero). In this case, the power supplied by the cell ($P_m = V_m * I_m$) is zero [78,79].

- Maximum Power point: it represents a crucial operating point at which the solar cell generates the highest possible electrical power output under a given set of conditions, such as sunlight intensity and temperature [79].

- Efficiency: We can define the efficiency of a photovoltaic cell as the quotient of the maximum power which can be determined by characteristic graph (I-V) and the incident power equal to the product of the illuminance G and the total surface S area of the solar cells [79].

$$\eta = \frac{P_{\max}}{P_{inc}} \tag{2.1}$$

with

$$P_{inc} = G \times S \tag{2.2}$$

- Fill Factor: It is used to judge the quality of a photovoltaic cell. It is defined as the ratio of maximum power to the power at short-circuit current and open-circuit voltage. The form factor will therefore be unity. The form factor of a good photovoltaic cell should be between 0.75 and 0.85 [78,79].

$$FF = \frac{V_m I_m}{V_{oc} I_{sc}} \tag{2.3}$$

2.5.4 Photovoltaic generator

Due to the fact that a typical PV cell produces less than 4 W at 0.5 V, the cells must be connected in series-parallel configuration. Thus, we use the module configuration followed by the so-called photovoltaic generator (GPV) arrangement in order to provide appropriate high power. The latter is composed of a number of PV cells connected electrically in series and parallel to supply the required current and voltage, respectively. The architecture of a PV module involves the interconnection of PV cells in both series and parallel configurations, complemented by protective devices. Connecting solar cells in series elevates the module's voltage, while parallel connections increase the current. This strategic combination optimizes the performance of the PV module, which serves as the fundamental unit for large-scale PV power generation. Commercially available modules typically incorporate 36 or 72 cells. The combination of several modules in series/parallel forms a PV array or generator. This makes it possible to increase the amount of power generated, depending on the area of application [80].

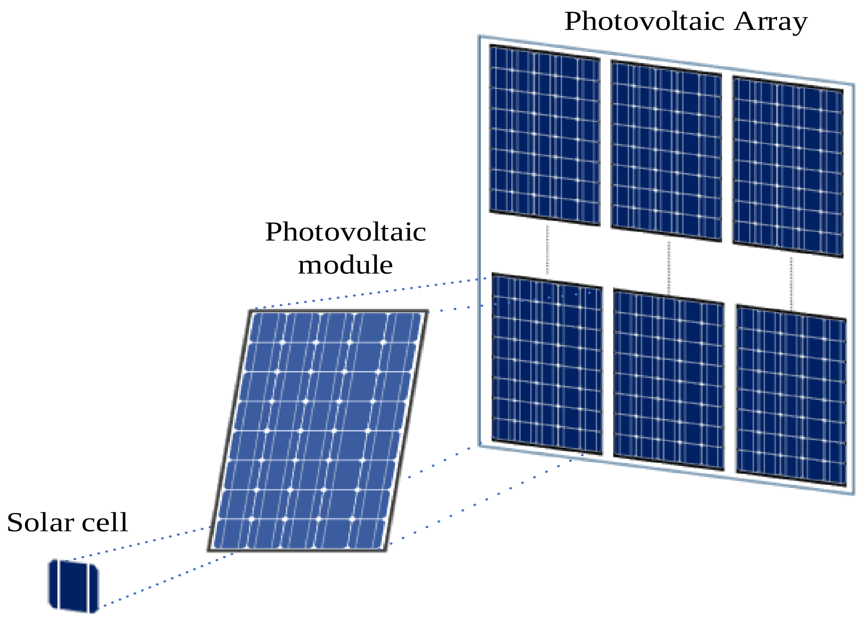

Figure 2. 16: PV generator [80].

2.5.4.1 Photovoltaic Module design

In a typical PV module design, individual solar cells are often connected in series to achieve the desired voltage output. However, this series connection makes the module susceptible to shading effects, which can lead to reduced performance, hotspots, and potential long-term damage. To address these concerns, protection diodes are commonly integrated into PV module designs [81].

- Bypass diodes, placed in antiparallel to the solar cells or specific cell substrings, serve as crucial safeguards. Their role is to provide alternative current paths in instances where shading occurs, ensuring continuous current flow and preventing hotspots. The bypass diode provides an alternate path for the. This ensures that the unaffected cells can still contribute to the overall power output of the solar panel, optimizing energy production even in partially shaded conditions [81,82].

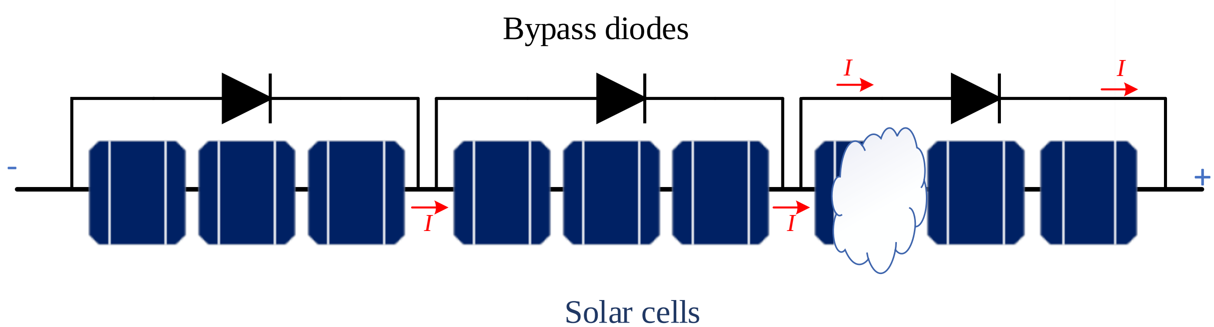

Figure 2. 17: Function of bypass diodes [82].

- Blocking diodes, also known as anti-reverse play a crucial role in the connection of solar cells within PV modules. Their utility lies in preventing reverse current flow. Blocking diodes are positioned in parallel with individual solar cells or groups of cells within a PV module. Their primary purpose is to prevent reverse current flow during periods of low light or darkness. Without blocking diodes, the electricity generated by the illuminated cells could flow backward into the shaded cells, leading to inefficiencies and potential damage [81,83].

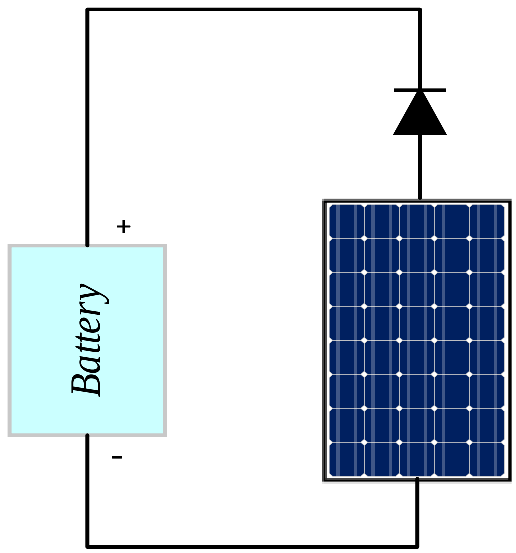

Figure 2. 18: Function of blocking diode [83].

2.5.4.2 Electrical characteristics of PV module:

The operating curve of a base module is a curve derived from the operating curve of an elementary cell by changing the echelle along the abscises axis. When you connect a number (N_s) of solar cells in series, aiming to increase the system's voltage. In contrast, to enhance the current, you connect N_p solar cells in parallel. The combination of these series and parallel connections results in what's termed a "Solar Photovoltaic Array". The Figures below illustrate the (I-V) characteristics for series/parallel connection of solar cells [84,85]. In the following Figures the electrical characteristics of the PV module.

- The Short circuit current of the PV module:

$$I_{sc(module)} = N_p \times I_{sc(solarcell)} \tag{2.4}$$

- The Open circuit voltage of the PV module:

$$V_{oc(module)} = N_s \times V_{oc(solarcell)} \tag{2.5}$$

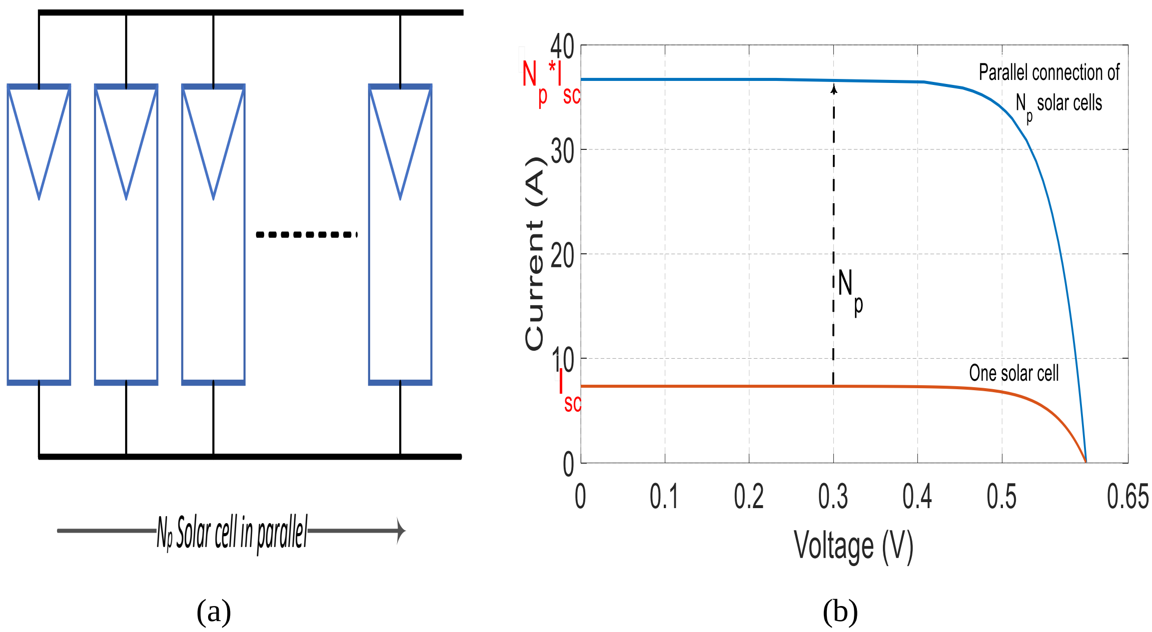

Figure 2. 19: (a): connection of solar cells in parallel, (b): (I-V) characteristics for parallel connection of solar cells.

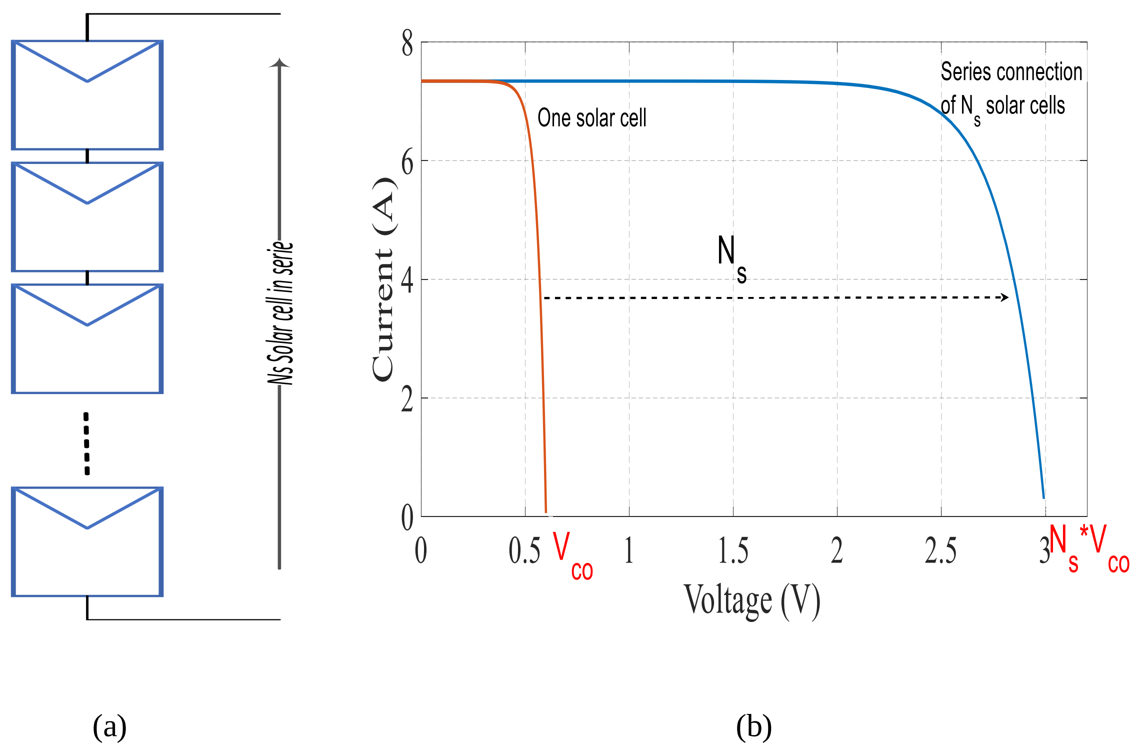

Figure 2. 20: (a): connection of solar cells in series, (b) : (I-V) characteristics for series connection of solar cells.

2.5.5 Influence of Temperature and Irradiation

The dynamic relationship between temperature and irradiation significantly shapes the fundamental characteristics of a solar cell, dictating its overall functionality across diverse environmental conditions.

Figure 2. 21 shows, respectively, the (I-V) and (P-V) characteristics of the simulated PV panel under a temperature of 25°C and an irradiation level varying from 200 W/m^2 to 1000 W/m^2 with a step of 200 W/m^2. From these results, we can see that the open-circuit voltage varies very slightly with variations in insolation. On the other hand, the short-circuit current I_{sc} varies greatly with variations in insolation. Furthermore, an increase in G leads to an increase in the power generated.

Figure 2. 22 illustrates, respectively, the (I-V) and (P-V) characteristics of the simulated PV panel under a constant insolation G = 1000 W/m^2 and a temperature ranging from 10°C to 75°C with a step of 25°C. From these curves, we can see that the influence of temperature is negligible on the value of I_{sc}. Nevertheless, the voltage V_{co} decreases significantly with increasing temperature. Increasing temperature leads to a decrease in generated power.

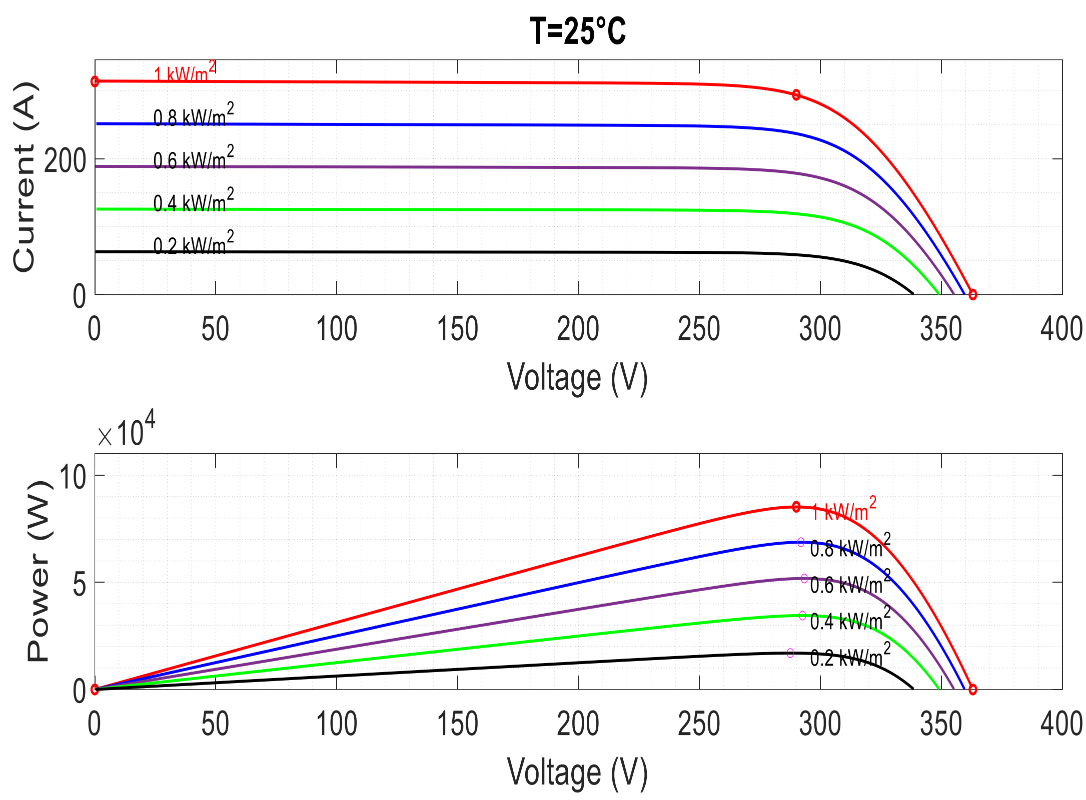

Figure 2. 21: Influence of irradiation on (I-V) and (P-V) characterstics.

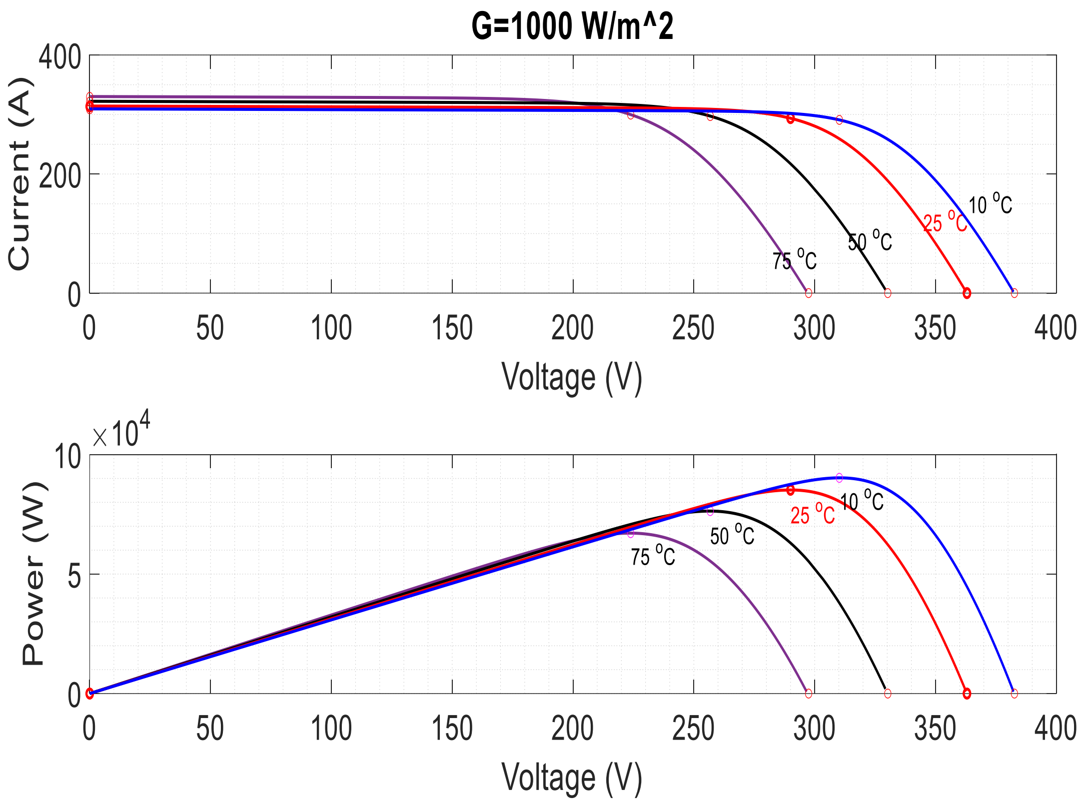

Figure 2. 22: Influence of temperature on (I-V) and (P-V) characterstics.

2.6 Photovoltaic systems

By harnessing the sun's energy to produce clean, renewable electricity, photovoltaic systems represent a significant advance in energy generation. They offer a sustainable response to the world's growing demand for electricity by converting sunlight directly into electricity. This technology, which has evolved over the decades, is now an essential component of the energy landscape, playing a crucial role in the transition to cleaner, more sustainable energy.

2.6.1 Configuration of PV system

The photovoltaic conversion chain consists of a series of interconnected components that collectively enable the conversion of solar energy into electrical energy. This chain begins with the primary component, the PV generator, which consists of PV modules, these modules absorb sunlight and convert it into direct current (DC) electricity through the PV effect. In addition to the PV generator, secondary components are integral to the PV system. These components include the power adaption stage and the energy storage system. The power adaption stage comprises various electronic components such as inverters, transformers, and controllers, which ensure the compatibility and efficient transfer of power between the PV generator and the electrical load or the grid. The energy storage system, when incorporated, typically involves rechargeable batteries that store excess energy generated by the PV system. These batteries allow for energy utilization during periods of low sunlight or high demand. The storage system requires careful selection and management to optimize efficiency and longevity [86,87].

2.6.1.1 Power Interface in PV system

The simplest and most economical configuration for PV systems is to supply DC loads directly, without a matching stage, via a non-return diode. However, it has significant limitations in terms of power optimization. Direct connection relies on the intersection of the current-voltage characteristics of the solar panel and the load, which can result in efficiency losses, especially when illumination conditions fluctuate [84].

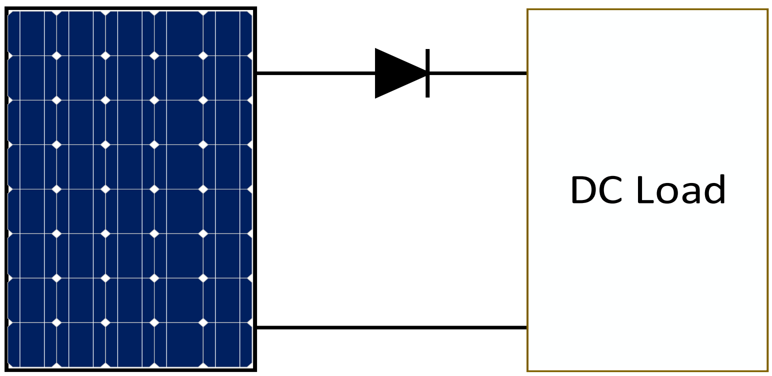

Figure 2. 23: Direct connection of PV module and DC load.

To overcome these challenges and maximize energy efficiency, other PV systems incorporate a more sophisticated approach with a power electronics interface. This interface plays a crucial role in improving performance, this transition to more advanced power electronics offers increased control, thus enhancing the optimal use of the generated solar energy. By highlighting the crucial importance of power electronics, these systems overcome the limitations of direct coupling, ensuring a more sophisticated power management and better adaptation to fluctuations in environmental conditions [88].

In general Power converters, essential components in electrical systems, are broadly categorized based on their functionality categorizes them according to their specific roles and tasks in managing electrical energy into four main types: DC-DC, DC-AC (inverters), AC-DC (rectifiers) and AC-AC converters as it is presented in Figure 2. 24.

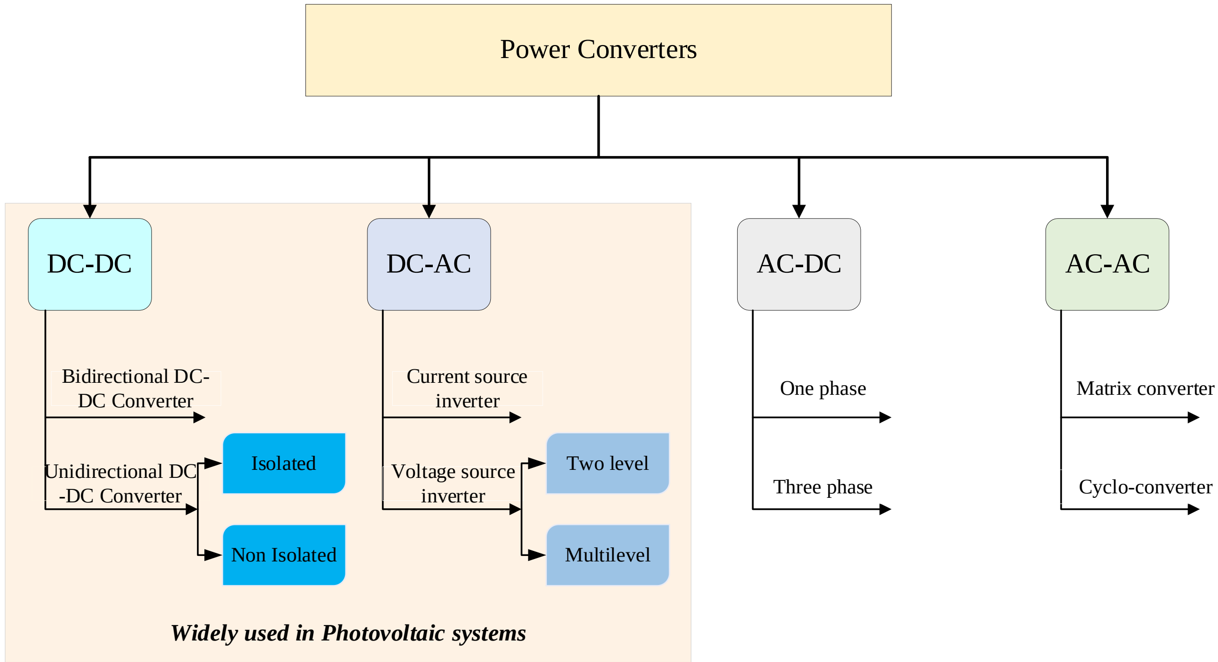

Figure 2. 24: Power converters classification [89].

In the context of PV systems, where the primary source of energy is solar-generated DC power, the focus is particularly directed towards DC-DC converters and inverters. DC-DC converters are integral in optimizing the performance of PV systems by adjusting the voltage levels of DC power. This adjustment is vital for efficient energy transfer between various components within the system, such as solar panels and energy storage devices like batteries. DC-DC converters enable the system to adapt to varying sunlight conditions, ensuring maximum energy harvest and system efficiency. Inverters, another critical component in PV systems, serve the purpose of converting the DC power produced by solar panels into AC power. This transformation is necessary for the integration of PV systems with the external electrical grid, as grid-connected applications operate on AC power. Inverters play a central role in facilitating the seamless transfer of solar energy to the grid or for local consumption, thus enabling the utilization of solar power in conventional electrical systems [89].

2.6.1.1.1 Single-Stage PV System

- DC Load Configuration: In a DC load configuration within a single-stage PV system, the essential components consist of solar panels generating DC power and a dedicated DC-DC converter. The primary operation involves the DC-DC converter optimizing and adjusting the DC power generated by the solar panels. This configuration is specifically designed for applications where a seamless power supply for devices or systems operating on direct current is required. By employing the DC-DC converter in this setup, the system ensures efficient adaptation and utilization of the DC power output from the solar panels to meet the precise needs of DC loads [89,90].

- AC Load Configuration: In the AC load configuration of a single-stage PV system, the key components include solar panels generating DC power and a single inverter. The seamless operation involves the singular inverter performing the crucial task of converting the DC power harnessed from solar panels into alternating current, finely tuned for compatibility with AC loads. This configuration proves particularly advantageous for applications where the load demands alternating current, catering to the diverse needs of household appliances and other systems reliant on AC power [89,90].

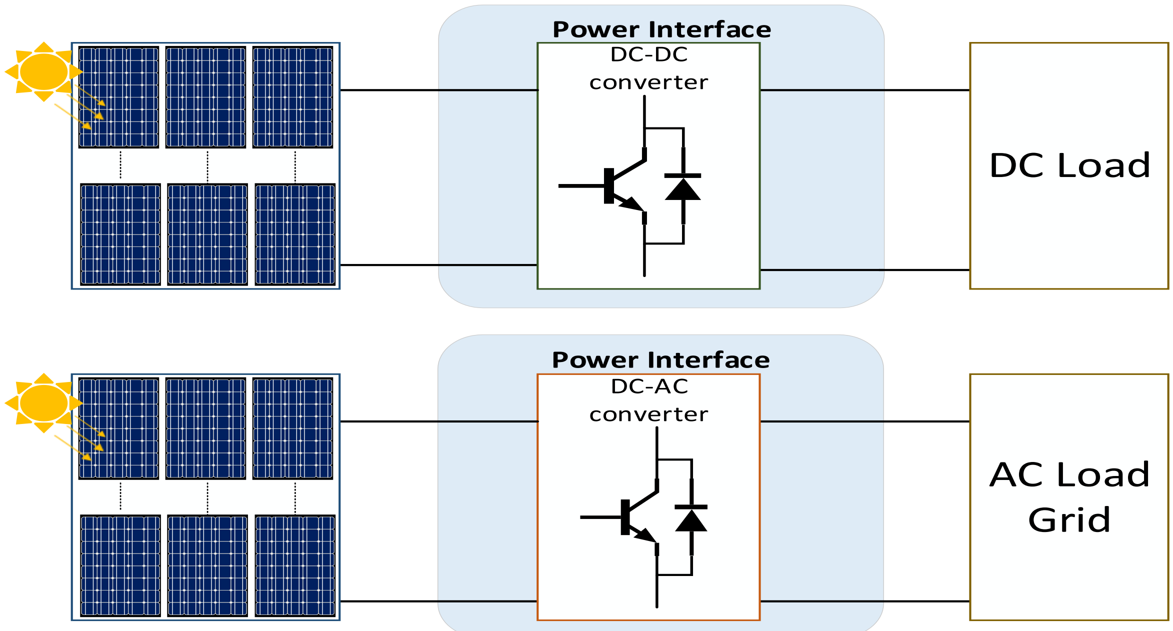

Figure 2. 25: Power Interface in single stage PV system.

2.6.1.1.2 Double-Stage PV System

In the field of double-stage PV systems, the core components include solar panels as the primary energy source, accompanied by a two-step setup involving a DC-DC converter in the initial stage and an inverter in the subsequent stage. The DC-DC converter plays a crucial role in refining the voltage characteristics of the electricity generated by the solar panels, laying a customized foundation for the subsequent stage led by the inverter. The inverter transforms the optimized DC power into alternating current, suitable for typical household use [89,90].

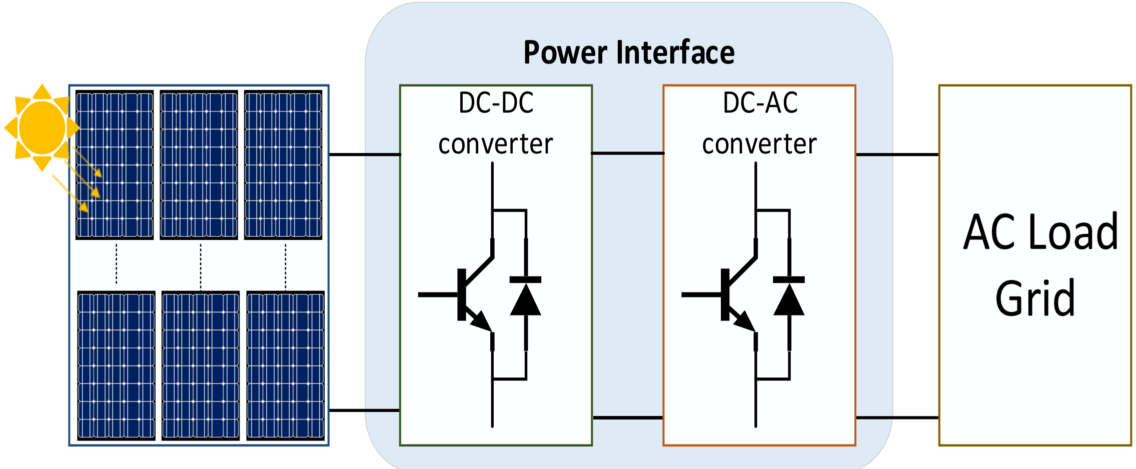

Figure 2. 26: Double stage PV system.

2.6.1.2 Energy storage systems

The growing significance of solar and wind energies is evident, driven by the imperative to reduce greenhouse gas emissions. As the world transitions toward a low-carbon economy, the intermittent nature of renewable resources, particularly solar and wind, poses a challenge to maintaining a reliable and steady energy supply. Energy storage systems (ESSs) emerge as crucial players in this scenario, serving to store excess energy during periods of low demand and releasing it when demand peaks. This not only addresses the intermittency of renewables but also aligns with the global shift towards a renewable-centric energy system. The need for energy storage is further emphasized by the desire for transportation alternatives with reduced CO_2 emissions. Various storage technologies, including electrochemical, mechanical, electrical, and hybrid systems, are explored for their suitability in harnessing energy from renewable sources. The future role of ESSs is pivotal in achieving a more flexible and resilient electricity grid, offering backup capacity, peak load shaving, and overall system stability. Key large-scale energy storage solutions, such as compressed air storage, pumped hydro storage, molten salt thermal storage, and flow batteries, contribute to enhancing the overall flexibility of the energy system. As the energy landscape evolves, ESSs are anticipated to play a critical role in optimizing the integration of non-dispatchable and variable renewable energy sources, contributing to the partial decentralization of the energy system. Table 2. 3 represents comparative analysis of several energy storage methods [91-95].

ESS type	*Example*	*Advantages*	*Disadvantages*	*Efficiency*
Electrochemical	Lithium-ion battery	High energy density High efficiency low self-discharge rate.	Expensive to manufacture. possible safety issues.	85-90
	Lead acid battery	Low cost mature technology, reliable.	Relatively low energy density, heavy, limited cycle life.	70-90
	Nickel cadmium (NiCd) battery	Good cycle life, reliable performs well in extreme temperatures.	Contains toxic cadmium, lower energy density compared to newer technologies like lithium-ion.	60-65
Mechanical	Flywheel	High power density rapid response time long cycle life no chemical degradation issues	High initial cost, limited energy storage capacity, some energy loss due to friction.	93-95
	Pumped hydro	High efficiency large-scale storage capacity long cycle life, and proven technology.	requires large suitable topography, high cost.	75-85
	Compressed air	Potentially large-scale storage, relatively low cost.	site-specific requirements.	70-89
Electrical	Super capacitor	High power density. rapid charge and discharge. long cycle life	Lower energy density higher cost limited energy storage capacity.	90-95
	Superconducting magnetic	high efficiency potentially large energy storage capacity.	high initial cost, Requires cryogenic temperatures	95-98

Thermal	Sensible heat	Simple technology Cost-effective thermal energy storage. Environmentally friendly.	Lower energy density compared to latent heat storage.	50-90
	Latent heat	High energy density. Efficient use of phase change.	Limited to specific temperature ranges. Challenges in material selection.	75-90
Chemical	Hydrogen fuel cell	Zero emissions at the point of use High energy density infrastructure development issues.	Hydrogen production challenges Relatively low overall efficiency.	25-58

Table 2. 3: Classification of energy storage systems.

2.6.2 Classification of PV system

In general, there are three types of photovoltaic system: grid-connected, stand-alone and hybrid systems. The last two are independent of the public electricity distribution service, and are often found in areas that are far from the electricity grid.

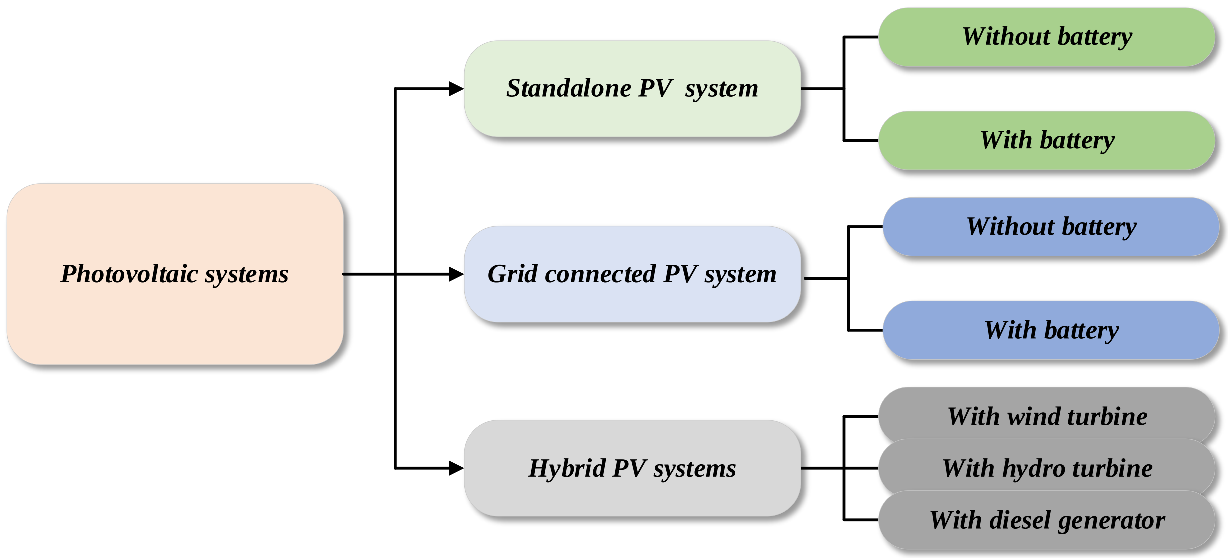

Figure 2. 27: Classification of PV system.

2.6.2.1 Stand-alone photovoltaic system

Stand-alone photovoltaic systems are characterized by their ability to generate electrical energy independently, without requiring a connection to an external electrical grid. They are specially designed to power isolated sites where access to a conventional electrical grid is impractical or not feasible [96,97].

Autonomous photovoltaic systems can be divided into two fundamental configurations. The first type consists of systems that operate without energy storage. These systems directly power loads during sunlight hours and stop functioning in the absence of sunlight. The second type of autonomous photovoltaic system incorporates energy storage devices, usually in the form of batteries. These systems operate by charging the batteries during sunlight hours and drawing from these batteries to power loads during periods without sufficient sunlight [96,97].

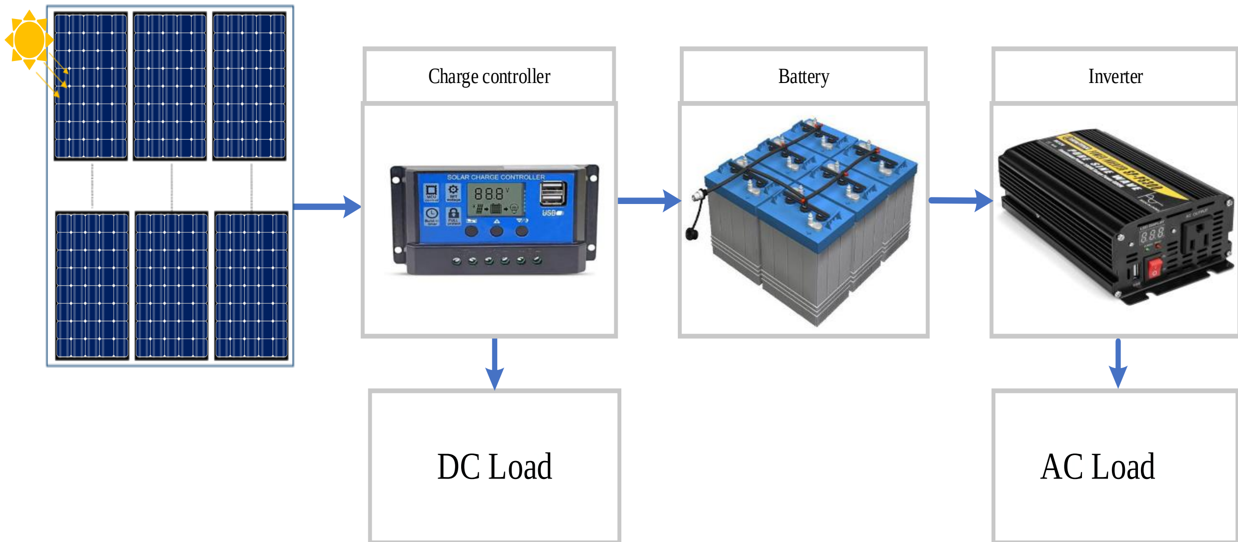

Figure 2. 28: Configuration of standalone PV system.

2.6.2.2 Grid connected photovoltaic system

Grid-connected PV systems are designed to be able to inject the extracted PV power into the public grid. These systems contain numerous power conversion stages that extract power from the PV array and feed it into the public grid. In these systems, the inverter is the key element that converts direct current into alternating current [97].

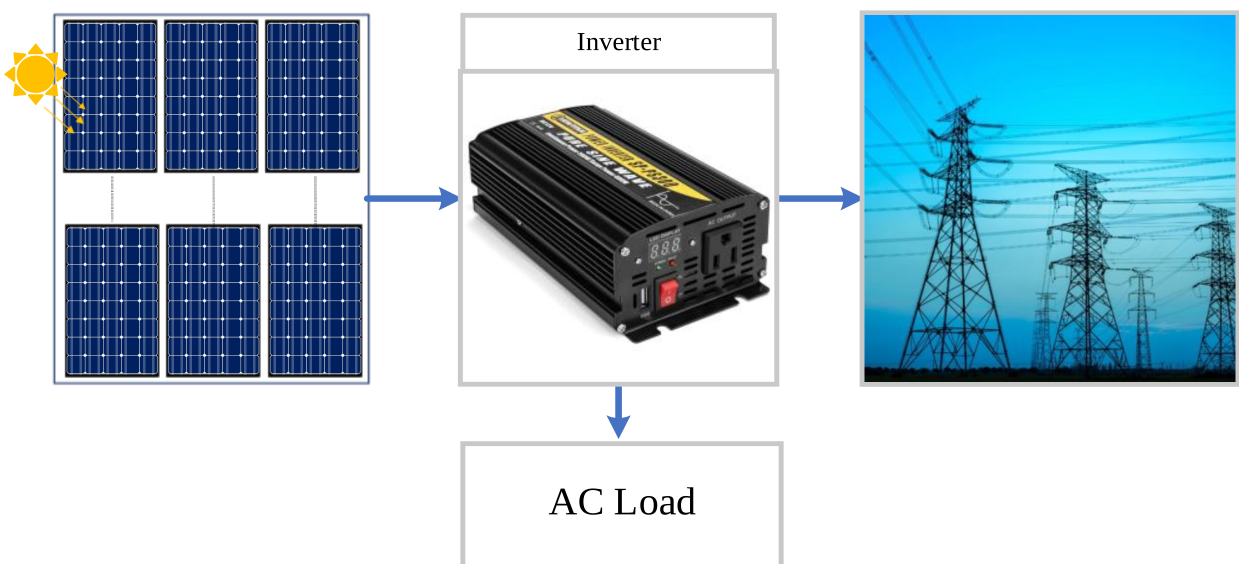

Figure 2. 29: Configuration of Grid connected PV system.

2.6.2.3 Hybrid photovoltaic system

Hybrid systems in the context of solar PV refer to combining solar energy with other sources such as Diesel Generators, Wind Turbines, or Biomass. These systems typically incorporate a battery bank to store solar energy for periods of insufficient sunshine. In cases of prolonged poor weather, an alternative source like a diesel generator is activated to ensure continuous power production. PV-hybrid systems blend PV modules with another power source, usually a diesel generator, to meet base load demand, calling on the alternate supply only when necessary. This approach maintains low operation and maintenance costs while ensuring a reliable power supply. Hybrid systems are also practical for situations with occasional demand peaks significantly higher than base load demand, offering a compromise between efficiency and peak demand requirements [96,97].

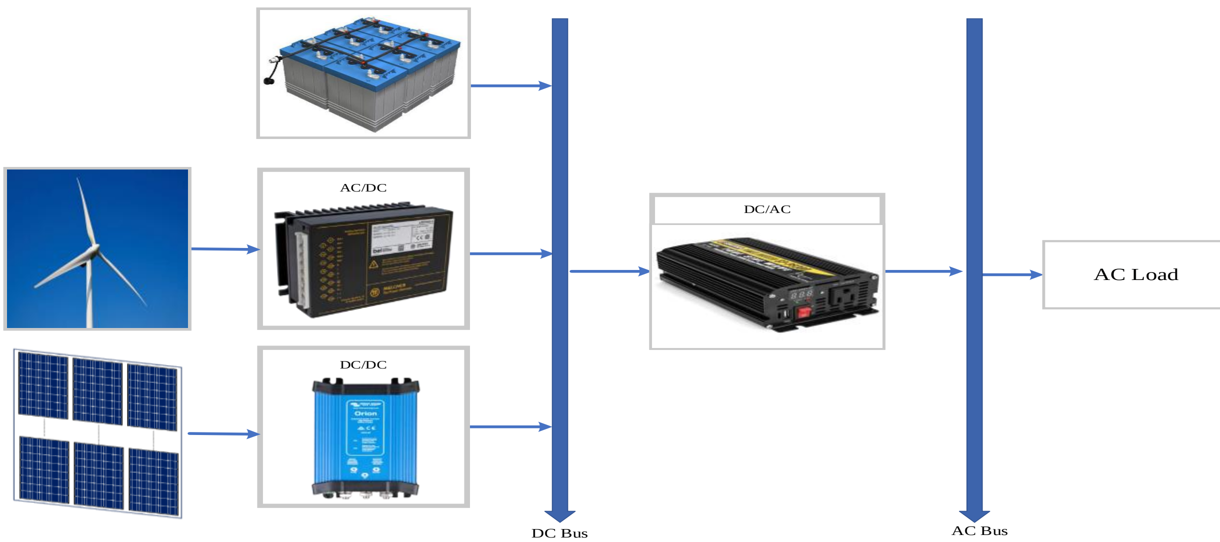

Figure 2. 30: Configuration of Hybrid PV system.

2.7 Advantages and Inconvenient of solar energy

2.7.1 Advantages

- Photovoltaic installations are characterized by high reliability and low maintenance requirements.

- Given the widespread availability of sunlight, photovoltaic energy proves to be viable in diverse settings, ranging from secluded mountain villages to the bustling urban landscapes of large cities.

- The assembly of photovoltaic installations is straightforward, and they are adaptable to the needs of each project, with systems scalable from milliwatt to megawatt applications. Photovoltaic energy can be installed anywhere, even in urban areas.

- It represents a completely silent source of electrical energy, distinguishing it from, for example, wind installations.

- Photovoltaic energy is an inexhaustible and clean source that produces no greenhouse gases.

2.7.2 Inconvenient

- The technologically advanced manufacturing of photovoltaic panels involves substantial research and development investments, reflected in the high initial cost of installations.

- The dependency on sunlight introduces an element of unpredictability and necessitates considering the intermittent nature of solar energy when evaluating its overall efficiency and reliability.

- Panel efficiencies, while improving, still hover around 20%, limiting suitability for high energy needs.

- Autonomous installations require expensive batteries, and the variability of electricity production based on sunlight poses challenges.

- The limited lifespan of photovoltaic installations, around 20 to 30 years, with an annual efficiency loss of about 1%.

2.8 Conclusion

In summary, this chapter provides a brief overview of the current state of global electricity production, focusing on renewable sources. Subsequently, we introduced the solar potential in Algeria and emphasized the significance of the ambitious renewable energy program in meeting a portion of the national electricity demand. The bibliographical research conducted provides a comprehensive overview of the direct generation of electricity from solar irradiation. We began with a thorough understanding of the PV effect, followed by insights into the design and safeguarding of PV Generators. The chapter delves into diverse architectures and topologies of PV systems, offering a holistic perspective on the intricate facets of harnessing solar energy for electricity production. These fundamental insights pave the way for a deeper exploration of advanced topics and practical applications in the upcoming chapters.

Chapter 3

Modeling and Control of grid connected PV system

3.1 Introduction

The integration of grid-connected PV systems is of crucial importance in today's energy landscape. These systems offer a sustainable and efficient solution for electricity generation, contributing to the transition to RE sources. Connecting PV installations to the grid extends the reach of their impact, enabling a wider distribution of the solar energy produced. A PV system's modeling is crucial for the performance optimization, as it is with any physical systems. To ensure that solar systems operate as efficiently as possible, electrical modeling and characterization of PV panels is required. This can lower installation costs greatly and boost the effectiveness of PV generators. In this chapter, a study of control structures specific to grid-connected generation systems was carried out. Fundamental concepts related to classical control strategies for power converter management were also presented. The dynamic behavior of the generation systems studied was evaluated by simulation using MATLAB/Simulink software. Simulation results are presented to validate the effectiveness of the control schemes and evaluate the dynamic performance of the systems examined.

3.2 Description of grid connected PV system

Grid-connected PV systems represent a significant advancement in renewable energy technology, integrating solar power into the electrical grid. These systems utilize essential components working together to generate and distribute electricity efficiently. The PV array, composed of solar panels, captures sunlight and converts it into DC electricity. Inverters play a crucial role in transforming DC power into AC suitable for grid connection, while control systems optimize overall performance [90].

The integration of solar power into distribution systems poses various challenges that necessitate careful analysis and mitigation to safeguard the grid and maintain power quality. Key issues arising from high solar penetration include voltage-related concerns, harmonics, and islanding detection. These critical aspects must align with standards set by international committees or regional regulatory bodies, categorizing these standards into general specifications, safety protocols, and power quality requisites. Key international standards include IEEE 1547, IEC 61727, and IEEE Std 929 being widely adopted. For voltage-related concerns, the IEC standard (IEC 61000-2-2 or IEC 61000-2-4) is widely used in European countries, ensuring that the voltage in a Low Voltage system does not deviate more than 7-10% of the nominal voltage to prevent equipment damage. Voltage stability, a subset of these issues, is addressed according to IEEE standards, with IEEE 1547 focusing on the interconnection of distributed energy resources. Harmonics in the system, observed in voltage and current signals, must stay within permissible levels defined by standards such as IEEE Std. 519. Additionally, IEEE Std. 929 provides guidelines. International standards like IEEE 1547 detail the requirements for the interconnection of distributed energy resources, while IEEE 519 provides guidelines for harmonic distortion limits in power systems [98,99]. The classification of grid-interfaced connected PV systems is based on the number of conversion stages, generally grouped into two distinct categories: one stage and two stages. This classification reflects the predominant power electronics topologies for photovoltaic systems. Single-stage and two-stage systems define how energy is converted and processed. These categories play a fundamental role in the design of PV systems, influencing their respective performance, benefits, and applications. Exploring these different topologies contributes to an in-depth understanding of the energy conversion mechanisms in grid-connected systems, an essential aspect of our study into the efficiency and optimization of PV systems.

3.3 Model of grid connected PV system

Figure 3.1 illustrates the configuration of the two stages photovoltaic system connected to the electrical distribution network. This structure is composed of the following elements:

- A photovoltaic field producing the supplied power.
- A boost converter and its control.
- A DC bus for energy storage and filtering.
- A three-phase voltage inverter and its control for interconnection with the grid.

Together, these elements form a cohesive structure for efficient solar energy utilization and seamless integration with the grid, contributing to the advancement of RE applications. The basic working principles involve converting sunlight into electrical power using the PV effect. Solar panels within the PV array generate DC electricity, which is connected to a DC-DC converter that ensures tracking of the optimal operating point, and then the whole system is connected to the electrical network through a voltage inverter controlled by a strategy that synchronizes the photovoltaic source with the grid. The DC bus decouples each of the two converters, and its purpose is to act as a filter and an energy storage element. In addition to providing galvanic isolation [100].

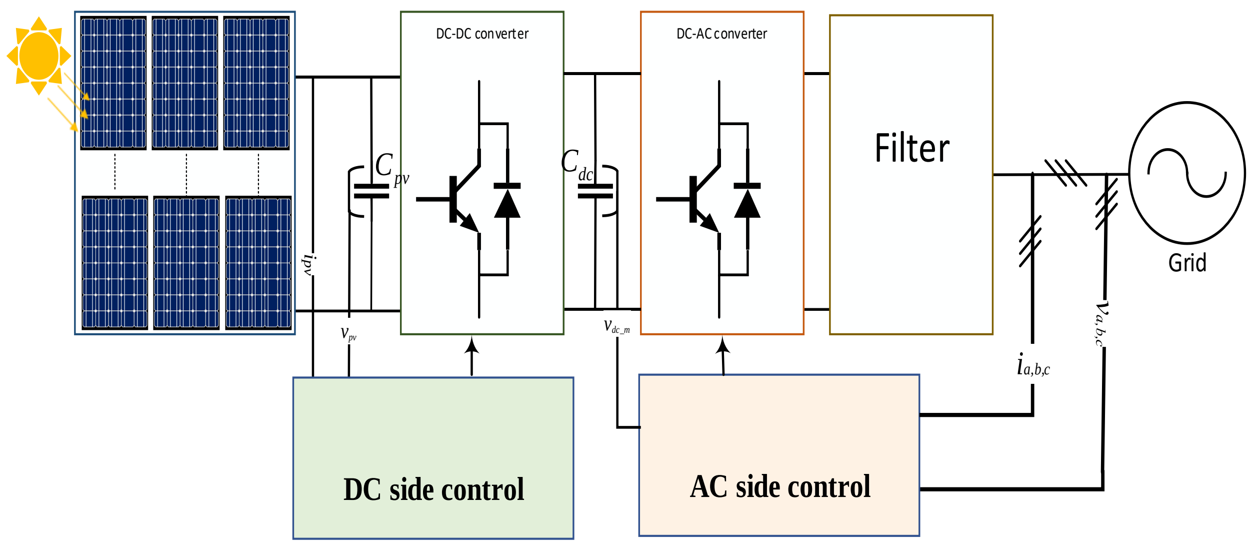

Figure 3. 1: Scheme of grid connected PV system.

3.3.1 Electrical model of a PV cell.

The literature provides a variety of models to represent a PV cell. The single diode model is the one that is most frequently used. Due to its accuracy and simplicity, this model is commonly used for applications including grid connection stability studies, performance study of MPPTs, sizing of PV systems, and analysis of PV plant performance. The equivalent diagram of the PV cell's single diode model is shown in Figure 3. 2. According to this model, the PV cell behaves like current generator whose is equivalent to a current source connected in parallel with a diode. This diagram introduces two resistors. The voltage loss is modeled by the series resistance R_s, while the leakage current is modeled by the parallel resistance R_{sh} [101,-102].

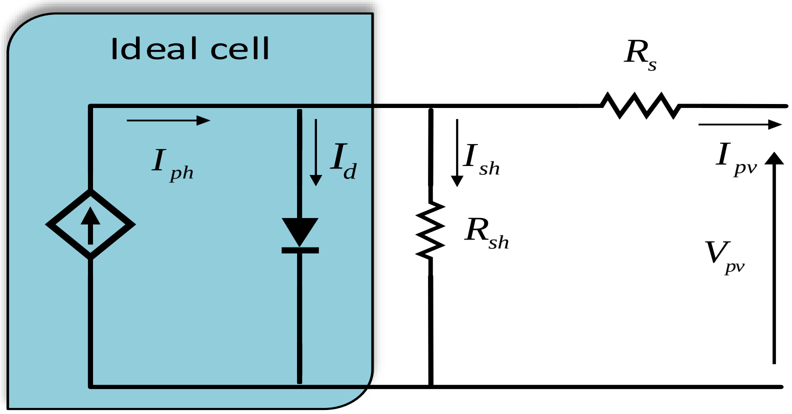

Figure 3. 2: Solar cell equivalent circuit [101].

The mathematical description of the one-diode model is given by the equation [101,102]:

$$I_{pv} = I_{ph} - I_d - I_{sh} \tag{3.1}$$

$$I_{pv} = I_{ph} - I_0 \left(\exp^{\frac{q(I_{pv} \times R_s + V_{pv})}{akT}} \right) - \frac{I_{pv} \times R_s + V_{pv}}{R_{sh}} \tag{3.2}$$

Where:

I_{pv} : The photon current generated by the PV cell.

I_d : The reverse saturation current of the diode.

I_{sh} : The leakage current through R_{sh}.

q: The charge of an electron $(1.6 * 10^{-19} C)$.

V_{pv} : The cell output voltage.

a : The diode ideality constant (varies from 1 to 2).

k : Boltzmann's constant $(1.38*10^{-23} J/K)$.

T : The cell temperature.

I_{ph} : The photon current generated by a PV cell is directly related to the irradiance G absorbed by the cell, (T_n = 25°C and G_n = 1000 W/m^2). It is given by the following equation:

$$I_{pv} = (I_{pv-n} + K_i \Delta T)\frac{G}{G_n} \tag{3.3}$$

Where:

$\Delta T = T - T_n$ generated by the cell under standard test conditions (STC) for PV panels (irradiation level G = 1000 W/m^2, Air Masse coefficient: 1.5, cell temperature T = 25°C).

At standard test conditions, the current I_{pv-n} is practically equal to the short-circuit current I_{cc-n}, however, it can be estimated according to the following expression [8-10]:

$$I_{pv-n} = \frac{R_p + R_s}{R_p} I_{cc-n} \tag{3.4}$$

The diode saturation current varies with temperature as follows [101,102]:

$$I_0 = \frac{I_{cc-n} + K_i \Delta T}{\exp(\frac{V_{co} + K_v \Delta T}{aV_t}) - 1} \tag{3.5}$$

Where:

K_v : The open-circuit temperature coefficient.

V_{co} : The open circuit voltage.

V_t : The thermodynamic potential ($V_t = akT/q$).

3.3.2 Input Capacitor dimensioning

A PV system's input capacitors can have a variety of uses. They are typically used to smooth and stabilize the input voltage from the solar panels. Depending on the weather and light intensity, solar panels can produce a variable voltage, which can lead to changes in the system's input voltage. Voltage fluctuations can be reduced by utilizing a capacitor. As a result, the input voltage to the electrical components of the PV system is kept more consistently, increasing system performance and dependability. The input capacitance can be calculated with the relation below [103-104]:

$$C_{pv} = \frac{D}{8\gamma V_{pv} {F_{sw}}^2 L} \tag{3.6}$$

From Equation (3.6), it is concluded that the input capacitor is mainly dependent upon the inductor L, switching frequency F_{sw}, D duty cycle and γV_{pv} the maximum power point voltage ripple factor.

3.3.3 Power electronics Modeling

The field of power electronics plays a crucial role in enhancing the performance of PV systems by efficiently converting, controlling, and managing the electrical energy generated by solar panels. This technology is instrumental in maximizing efficiency, optimizing energy production, and ensuring effective energy management. The evolution of power electronics, marked by the invention and development of components, has significantly advanced the capabilities of power conversion in PV systems. These components have paved the way for the creation of various static converters, which are integral to the functioning of PV systems connected to the grid [105].

Two primary types of static converters employed in PV systems are DC-DC converters and inverters. DC-DC converters are devices that control the average DC voltage by varying the duty cycle of the input waveform, making them essential for regulating the output of solar panels. Inverters, on the other hand, play a key role in converting DC power generated by solar panels into AC power suitable for grid connection. They enable seamless integration with the grid, facilitating the efficient distribution and utilization of solar-generated electricity [105].

3.3.3.1 DC-DC converters

The current landscape of DC-DC converters offers a choice between isolated and non-isolated configurations to regulate input voltage based on specific application requirements. Isolated converters characterized by galvanic isolation between input and output providing a separate ground and insulating the two sides and various topologies like Flyback, Forward, Push-Pull, Half-Bridge, and Full-Bridge. Despite addressing issues like leakage inductance and core saturation, isolated converters are challenged by factors such as thermal effects, high voltage spikes, and increased size and cost. In contrast, non-isolated converters including Buck, Boost, Buck-Boost, and Cuk converters present lack galvanic isolation, directly linking input variations to the output. These converters, simpler and more cost-effective with fewer components. The choice between isolated and non-isolated converter categories hinges on specific application needs. The significance of DC-DC converters spans various domains, dating back to their proposal in the 1920s. These converters play a pivotal role in power electronics, industrial applications, computer hardware circuits, and especially in renewable energy generation. The power quality of renewable energy systems relies heavily on the stable operation and control techniques of DC-DC converters [106].

3.3.3.1.1 Boost converter

A boost chopper, or parallel chopper, is a switching power supply that converts a DC voltage into another DC voltage of greater value, this converter makes it possible to adjust the voltage across the GPV in order to extract the maximum available power. The power circuit of a boost chopper is shown in Figure 3. 3. It is essentially made up of an inductor L at its input, a switch controlled on opening and closing, a diode and a capacitor C at its output. The switch is controlled by a Pulse Width Modulation (PWM) signal of fixed frequency F_{sw} and variable duty cycle D [20].

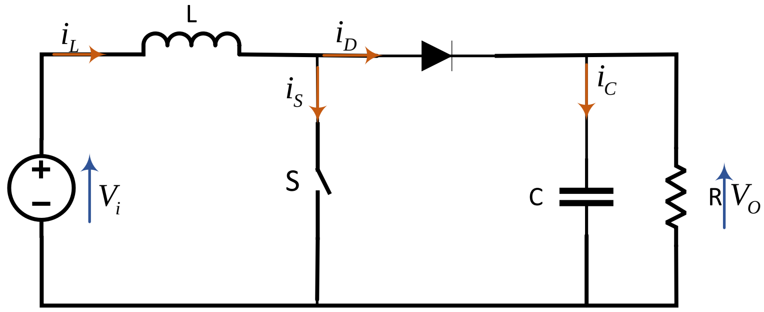

Figure 3. 3: Boost converter circuit [107].

The analysis is based on the following assumptions:

- ✓ The system operates under steady-state conditions.
- ✓ The switching occurs periodically with a period T, where the switch is closed for a duration DT and open for (1-D)T.
- ✓ The inductor current remains continuous, consistently positive.
- ✓ All components are assumed to be ideal. These assumptions apply throughout the analysis.

The mathematical representation of the step-up chopper involves the formulation of differential equations that capture its behavior in both operational modes. The control mechanism for the transistor S employs PWM, where the duration of each pulse is determined by the T period, influencing the converter's switching time. The PWM signal regulates the opening and closing cycles of the power switch, and the associated duty cycle, denoted as D (where D belongs to the interval [0,1]) [107], where:

$$D = \frac{T_{on}}{T_{on} + T_{off}} \quad \text{and} \quad T = T_{on} + T_{off} \tag{3.7}$$

The control signal for the switch, utilizing PWM technique, is derived from comparing the duty cycle D with the output from a triangular or sawtooth generator. The frequency of this generator is predetermined by the converter's operation, as illustrated in the following Figure 3. 4.

The generation of control pulses operates in the following manner:

- ✓ When D is greater than A_t, P is set to 1, indicating that the switch S is in the closed state.
- ✓ When D is less than A_t, P is set to 0, signifying that the switch S is in the open state.

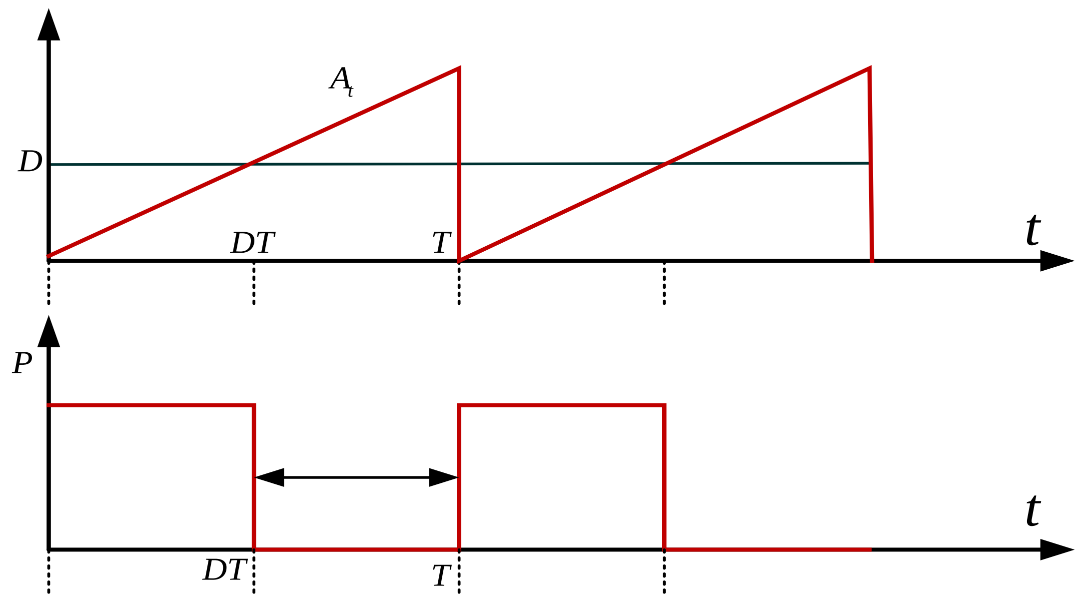

Figure 3. 4: Generation of the pulse of the of DC-DC converter.

During the converter operation, the transistor will be switched at a constant frequency F_s with a closing time T_{on} = *DT* and an opening time T_{off} = *(1-D) Ts*.

The operating principle of a boost converter is divided into two distinct phases depending on the state of the switch:

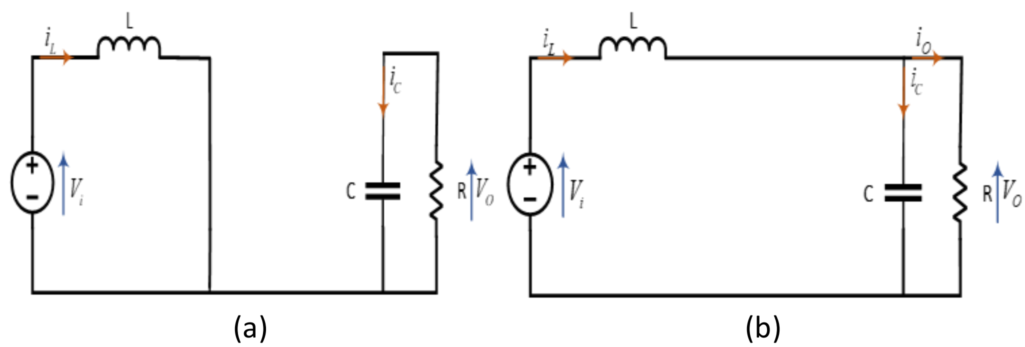

Figure 3. 5: Equivalent scheme of boost converter: (a) when S is closed, (b) when S is opened.

- Switch is closed

When the switch is closed, the current in the inductor will increase, and energy in the form of magnetic energy is stored. The diode is reverse biased [107].

$$\begin{cases} \dfrac{di_L}{dt} = \dfrac{V_i}{L} \\ \dfrac{dV_C}{dt} = \dfrac{1}{C}(\dfrac{V_O}{R}) \end{cases} \tag{3.8}$$

- Switch is opened

When the switch is opened, so the diode becomes forward-biased. The energy accumulated in the inductor will therefore be transferred to the capacitor [20,21].

$$\begin{cases} \dfrac{di_L}{dt} = \dfrac{1}{L}(V_i - V_O) \\ \dfrac{dV_O}{dt} = \dfrac{1}{C}(i_L - \dfrac{V_O}{R}) \end{cases} \tag{3.9}$$

The waveform of the inductor current is shown in Figure 3. 6:

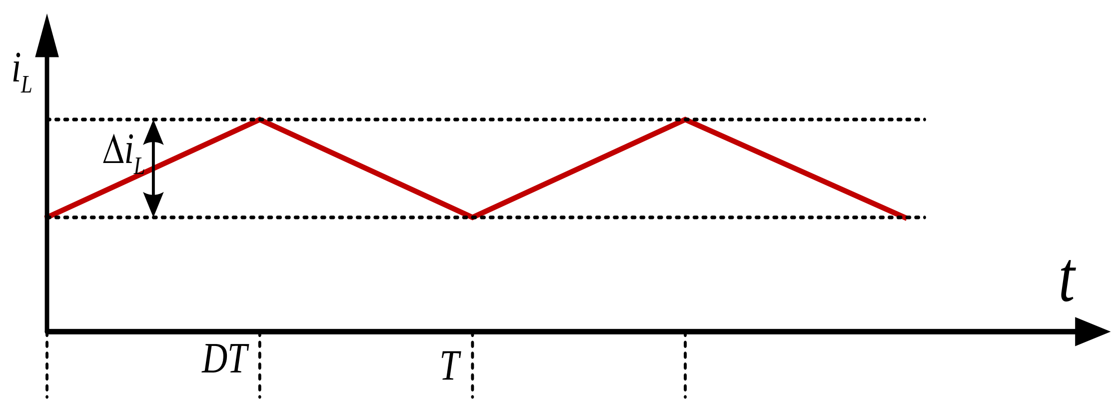

Figure 3. 6: The inductor current waveform of boost converter.

The inductor current experiences a constant rate of change, resulting in a linear increase during the time when the switch is closed, as depicted in Figure 3. 6. The calculation of Δi_L when S is closed.

$$\frac{\Delta i_L}{\Delta t} = \frac{\Delta i_L}{DT} = \frac{V_i}{L} \tag{3.10}$$

$$(\Delta i_L)_{closed} = \frac{V_i DT}{L} \tag{3.11}$$

The change in inductor current during the switch's open duration is calculated in equations (3.12) and (3.13):

$$\frac{\Delta i_L}{\Delta t} = \frac{\Delta i_L}{(1-D)T} = \frac{V_i - V_o}{L} \tag{3.12}$$

$$(\Delta i_L)_{opened} = \frac{(V_i - V_o)(1-D)T}{L} \tag{3.13}$$

The change in inductor current must be zero during the one switching cycle is calculated in the following equations.

$$(\Delta i_L)_{closed} + (\Delta i_L)_{opened} = 0 \tag{3.14}$$

When we replace (3.11) and (3.13) in (3.14), we obtain the following equation:

$$\frac{V_i DT}{L} + \frac{(V_i - V_o)(1-D)T}{L} = 0 \tag{3.15}$$

$$V_o = \frac{V_i}{1-D} \tag{3.16}$$

- Sizing the inductor parameter of boost converter

The estimation of boost converter inductors becomes crucial in electronic design. Typically, inductor values are provided within a specified range in datasheets, but when this data is unavailable, engineers resort to estimating the inductor directly. This estimation process involves key parameters such as the desired output voltage, switching frequency, duty cycle, inductor current ripple. Accurate inductor estimation is essential for maintaining the stability and efficiency of the converter, ensuring that it operates within desired performance [107].

$$L = \frac{V_i(V_o - V_i)}{\Delta i_L F_{sw} V_o}$$

Where:

Δi_L: Estimated inductor ripple current.

F_{sw} : Switching frequency.

V_o: Desired output voltage.

V_i: Typical input voltage.

3.3.3.1.2 Three phase inverters

The DC-AC converter (inverter) is the second type of matching step. They provide an AC load and guarantee the proper operation of PV systems. An inverter, a part of power electronics, converts DC energy into AC energy. Electronic switches like IGBTs (Insulated-Gate Bipolar Transistors), power transistors, or thyristors are frequently used in the construction of inverters. Inverters are versatile, classified based on the number of outputs and input types. Classification is further refined based on the number of output phases, input types (Voltage Source Inverter or Current Source Inverter). Single-phase VSIs suit low-power applications, while three-phase VSIs are recommended for medium and high-power scenarios. Our thesis focuses on a high-power application, leading us to consider a three-phase VSI inverter. The fundamental structure of a two-level voltage inverter is illustrated in Figure 3. 7. It comprises bridge arms. Each bridge arm, consists of two switches with bidirectional current flow and unidirectional voltage capability, that are fully controllable on opening and closing. The switching cell is made up of a power transistor, of the IGBT or MOSFET type which is placed in antiparallel with diodes to ensure bidirectional current flow [108,109].

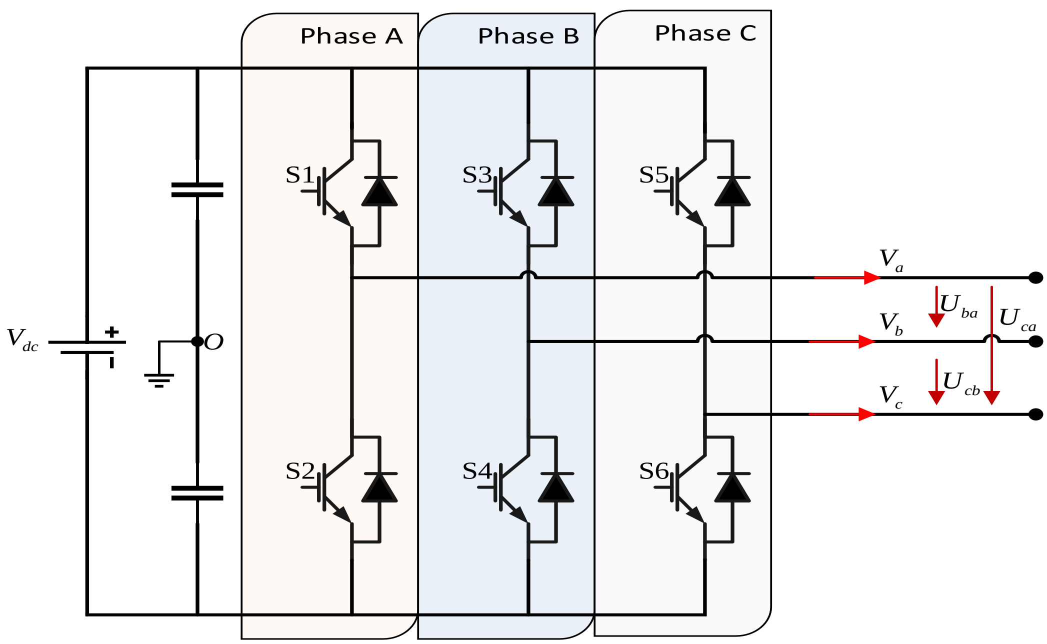

Figure 3. 7: Schematic circuit of three phase inverter [108].

In order to avoid short-circuiting the input source, the switches of each inverter arm must be controlled in a complementary manner. The switching states of the switches S_x (with $x=1,...,6$) can be represented by the control commands (S_a, S_b, S_c) defined as follows:

$$S_y = \begin{cases} 1 \quad if \quad S_i \quad is\,closed \quad and \quad S_{i+1} \quad is\,opened \\ \\ 0 \quad if \quad S_i \quad is\,opened \quad and \quad S_{i+1} \quad is\,closed \end{cases} \quad i = 1,3,5 \quad and \quad y = a,b,c \tag{3.17}$$

The switching function S_y (y=a,b,c) therefore takes the value of 1 when the upper switch of the y arm is closed. It is equal to 0 when the lower switch of phase y is closed.

There are two possible states for each inverter arm:

State P: While the bottom switch is open, the top switch is closed. Therefore, V_{dc} is the output voltage with respect to the source neutral.

State N: The top switch is open, while the bottom switch is closed. The output voltage relative to the source neutral is therefore equal to 0V.

Since each arm can have two states, the whole inverter has $2^3 = 8$ states: PPP, PPN, PNN, PNP, NNN, NNP, NPP and NPN. They are identified by indicating the states of the three arms of the inverter (P state or N state). For example, the PNN state indicates that the first arm is in the P state, the second is in the N state and the third is in the N state [110].

- Inverter output voltages

The three-phase output voltages with respect to the DC source reference (o) can be expressed by:

$$\begin{pmatrix} V_{ao} \\ V_{bo} \\ V_{co} \end{pmatrix} = V_{dc} \begin{pmatrix} S_a \\ S_b \\ S_c \end{pmatrix} \tag{3.18}$$

V_{dc} being the DC supply voltage to the inverter.

The phase-phase voltages are given by:

$$\begin{pmatrix} V_{ab} \\ V_{bc} \\ V_{ac} \end{pmatrix} = \begin{pmatrix} V_{ao} - V_{bo} \\ V_{bo} - V_{co} \\ V_{ao} - V_{co} \end{pmatrix} \tag{3.19}$$

Also, we can express phase-phase voltages with the DC link voltage and the control commands:

$$\begin{bmatrix} V_{ab} \\ V_{bc} \\ V_{ca} \end{bmatrix} = V_{dc} \begin{bmatrix} 1 & -1 & 0 \\ 0 & 1 & -1 \\ -1 & 0 & 1 \end{bmatrix} \begin{bmatrix} S_a \\ S_b \\ S_c \end{bmatrix} \tag{3.20}$$

Assuming that the three-phase load is balanced, the three-phase output voltages can be deduced with respect to the neutral point of the three-phase load:

$$\begin{bmatrix} V_a \\ V_b \\ V_c \end{bmatrix} = \frac{V_{dc}}{3} \begin{bmatrix} 2 & -1 & -1 \\ -1 & 2 & -1 \\ -1 & -1 & 2 \end{bmatrix} \begin{bmatrix} S_a \\ S_b \\ S_c \end{bmatrix} \tag{3.21}$$

- Modulation technique

To attain the desired waveform, amplitude, and frequency in the output voltage, control signals responsible for switching transistors can be generated using the carrier-based PWM technique. This method defines the ON and OFF states of each switch by comparing one or more control voltages, denoted as A_r (modulating signal), with a triangular carrier signal represented as A_t. For implementing PWM, a high-frequency triangular carrier wave is compared to a sinusoidal reference signal with the desired frequency. The points where these two waves intersect determine when the modulated pulse should switch.

The PWM scheme, illustrated in Figure 3. 8, uses A_t to represent the peak value of the triangular carrier wave and A_r for the peak value of the reference or modulating signal. The Figure 3. 8 displays triangular waves at 1000Hz and modulation signals at 50Hz. In the inverter switches S1 and S2 are controlled based on a comparison between the control signal and the triangular wave, mixed in a comparator, is depicted in Figure 3. 9. When the magnitude of the sinusoidal wave exceeds that of the triangular wave, the comparator outputs a high signal; otherwise, it outputs a low signal. This process enables precise control over pulse width modulation for effective inverter operation [111].

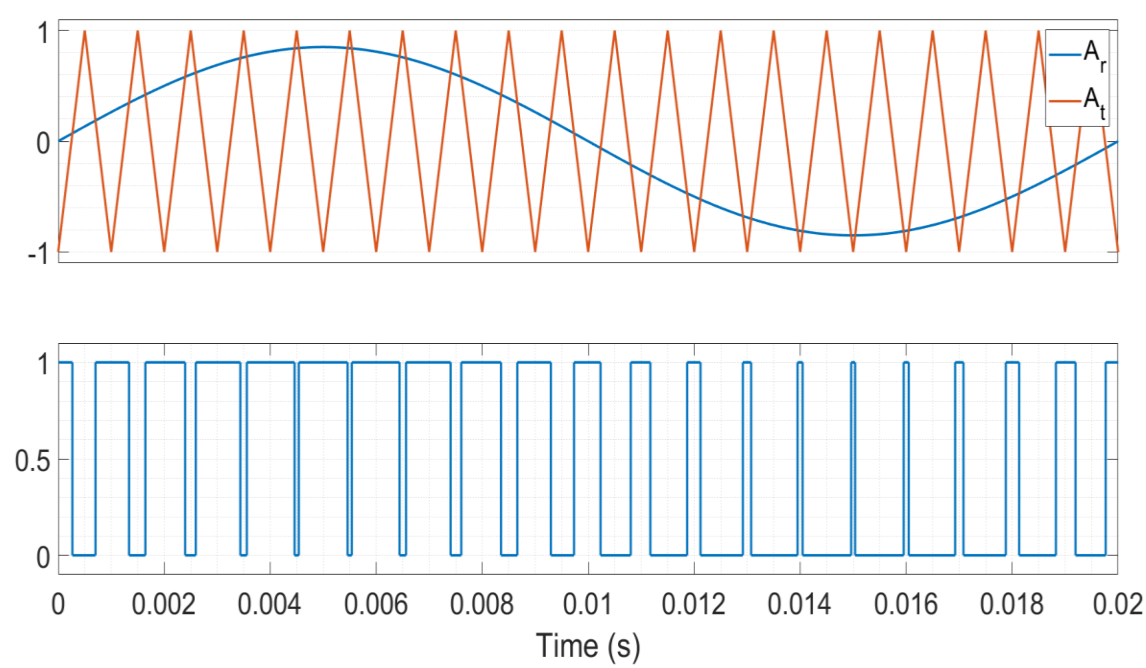

Figure 3. 8: PWM: Sinusoidal and triangular signals comparison.

The modulation index, denoted as m_a, is a crucial parameter in this process. It is determined by the ratio of the peak value of the control signal (A_r) to the peak value of the carrier signal (A_t), as expressed in equation (3.22). The modulation index plays a significant role because it dictates the pulse width of the signal, influencing the duration for which the switches are in the ON state [111].

$$m_a = \frac{A_r}{A_t} \tag{3.22}$$

We also introduce the concept of the frequency modulation index, which is the ratio between the switching frequency and the frequency of the control signal.

$$m_f = \frac{f_t}{f_r} \tag{3.23}$$

Furthermore, Figure 3. 9 illustrates a PWM modulator, providing a visual representation of how the control signals and carrier signal interact in this modulation process.

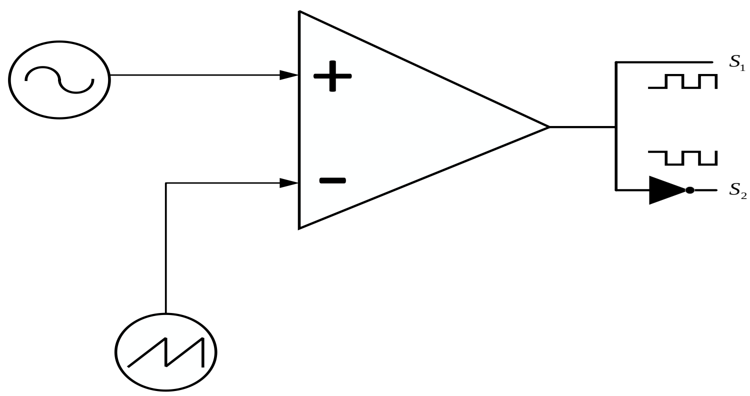

Figure 3. 9: PWM modulator [111].

3.3.4 DC link voltage and capacitor sizing

The DC link capacitor in a PV system plays a multifaceted role, serving as a crucial component with several vital functions. Primarily, it acts as a protective element during grid connection, managing the ripple effect and ensuring stability in the Maximum Power Point Tracking (MPPT) system. It serves as an energy storage unit, regulating the voltage between the source and load, supplying power during source reductions, and storing excess energy during periods of generator surplus. In the context of a grid-integrated PV system, especially with a VSI, the DC-link capacitor becomes indispensable, absorbing voltage ripple and maintaining a constant DC voltage source to counteract issues related to PV module nonlinearity. Additionally, the capacitor compensates for switching losses, acting as an electrostatic energy storage device for transient faults, and recharges through anti-parallel diodes after such events. Furthermore, when a VSI is employed to address power quality issues by generating controlled harmonics in the output current, the DC capacitor becomes pivotal in managing pulsating power, particularly under unbalanced loading conditions, with a large capacitor enforcing strict deviation limits at the VSI's DC-bus [112]. The value of the DC link capacitor can be calculated by using the equation provided in:

$$C_{dc} = \frac{P_{pv}}{2\omega V_{dc} \Delta V_{dc}} \tag{3.24}$$

Where:

P_{PV}: is the nominal power of PV modules.

ω: is the rotational frequency of the generated sine wave.

V_{dc}: is the mean voltage across the capacitor.

ΔV_{dc} : is the amplitude of voltage ripple.

The compatibility of the AC output involves calculating an appropriate DC link voltage. This voltage is pivotal for supplying energy to the inverter responsible for converting DC to AC. The calculation process requires defining the desired AC output characteristics, considering inverter specifications [113], the reference DC link voltage is defined in equation:

$$V_{dc} = \frac{2\sqrt{2}}{m_a \sqrt{3}} V_{LL} \tag{3.25}$$

Where:

V_{LL}: a line-to-line grid voltage.

m_a: the modulation index.

3.4 Control of grid connected PV system

The GPV harnesses incident solar irradiation to generate electricity, optimizing its performance at a unique operating point in specific climatic conditions. An integral MPPT algorithm ensures a continuous extraction of maximum energy. Currently, the integration of PV sources into the public grid is flourishing. In this application, PV panels connect to the grid through power converters, a boost converter and a three-phase inverter linked to the grid through a filter. The Perturb and Observe (P&O) algorithm in the boost converter tracks the optimal operating point of the Generation of Photovoltaic system. Additionally, inverter control involves a DC link voltage and *dq* current regulatory scheme, along with a PWM modulator. Precise control is imperative for the inverter to execute various tasks, including stabilizing the DC bus voltage, control active and reactive power flow, and delivering a sinusoidal current with low harmonic to the electrical grid [113].

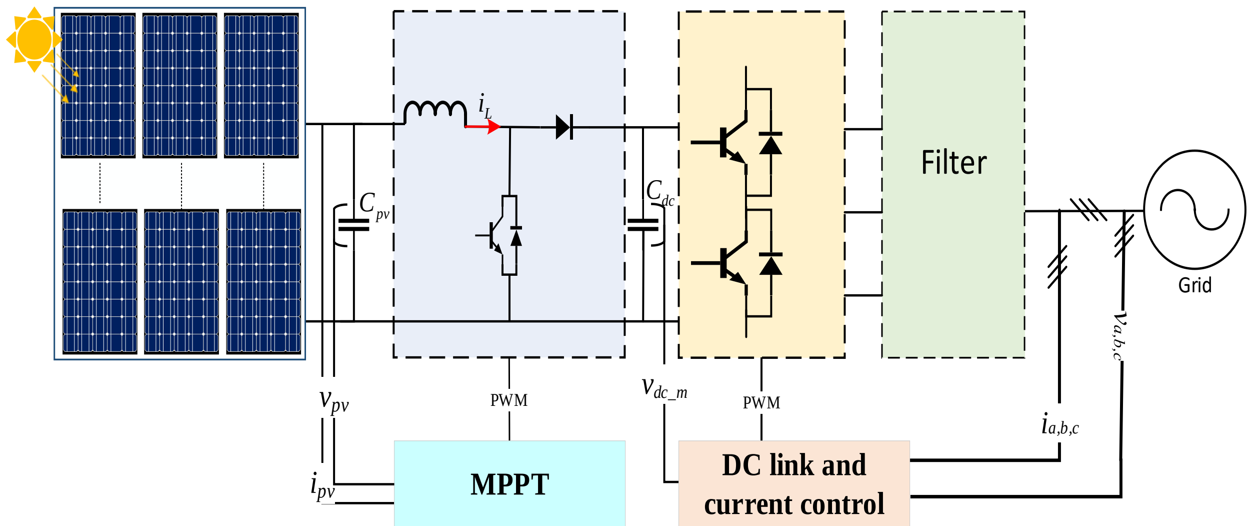

Figure 3. 10: Grid connected PV system control schematic.

3.4.1 Control of the boost converter

In recent years, maximizing the energy output of PV systems, crucial for solar renewable energy, has driven extensive research into MPPT techniques. The primary goal of MPPT is to ensure that solar panels operate at their MPP, optimizing the match between the generator and load for maximum power transfer. A variety of approaches to MPPT, spanning conventional, Intelligent, Optimization and hybrid techniques, have been developed. These methods manipulate input variables such as solar irradiance, PV panel power, temperature, voltage, and current. Conventional techniques, including constant voltage, incremental conductance, open-circuit voltage, short-circuit current, hill climbing, perturb and observe, improved perturb and observe, and others, are straightforward to implement. However, they may exhibit rapid oscillations around the MPP and struggle with partial shading conditions. Intelligent PV MPPT like fuzzy logic control, artificial neural network, sliding mode control, Fibonacci series-based MPPT, and Gauss-Newton approach are designed for dynamic weather conditions. They offer high tracking accuracy and speed but may involve complex control circuits and extensive data processing for training. Optimization PV MPPT: Methods such as cuckoo search-based, Particle Swarm Optimization, gray wolf optimization, ant-colony optimization, and artificial bee colony are known for searching the true MPP in dynamic environments. PSO is a faster tracking algorithm, and these techniques are relatively easy to implement using low-cost microcontrollers. Hybrid PV MPPT: Hybrid techniques combine classical, intelligent, or optimization-based MPPTs. Examples include FPSO, ANFIS, GWO-P&O, PSO-P&O, and HC-ANFIS. These hybrids operate in two stages: estimating the MPP using classical methods and fine-tuning it with advanced methodologies. They aim to overcome the limitations of individual approaches [114,115].

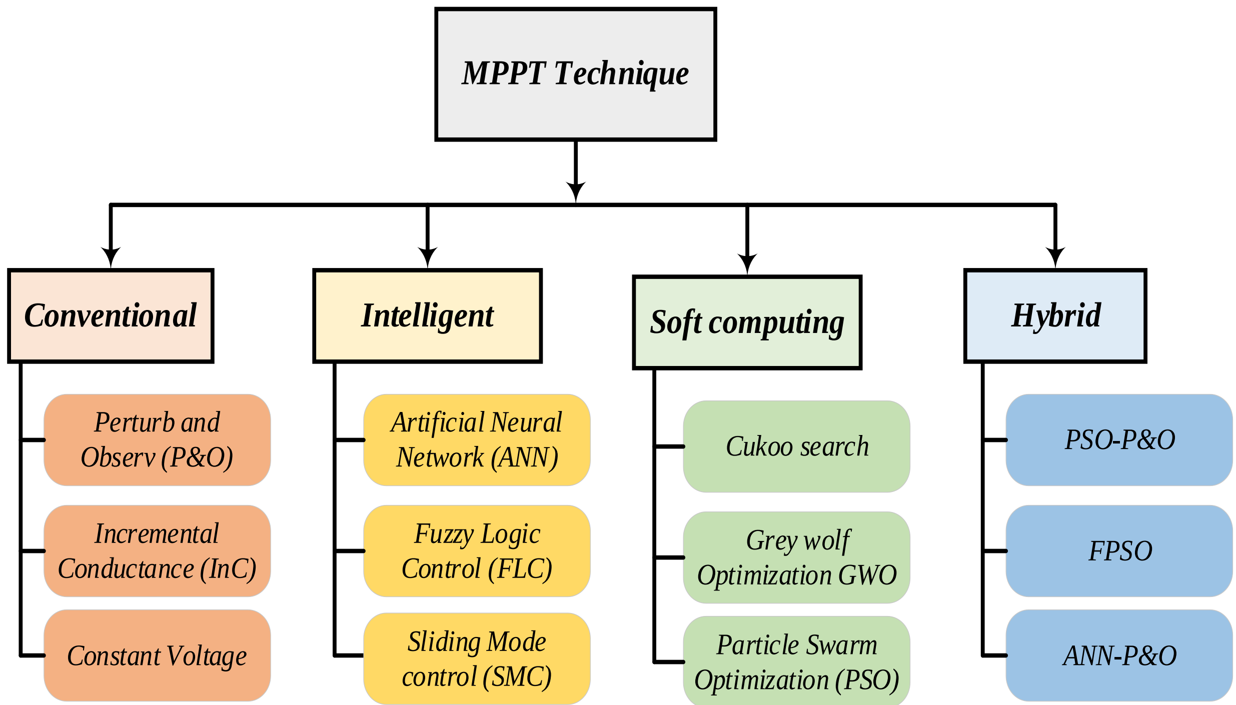

Figure 3. 11: Classification of MPPT technique [114].

Figure 3. 12 shows the schematic diagram of a DC-DC MPPT converter, which consists of an electronic device controlled through its duty cycle in such a way as to minimize the error between the operating power and the maximum reference power, which varies according to the weather conditions.

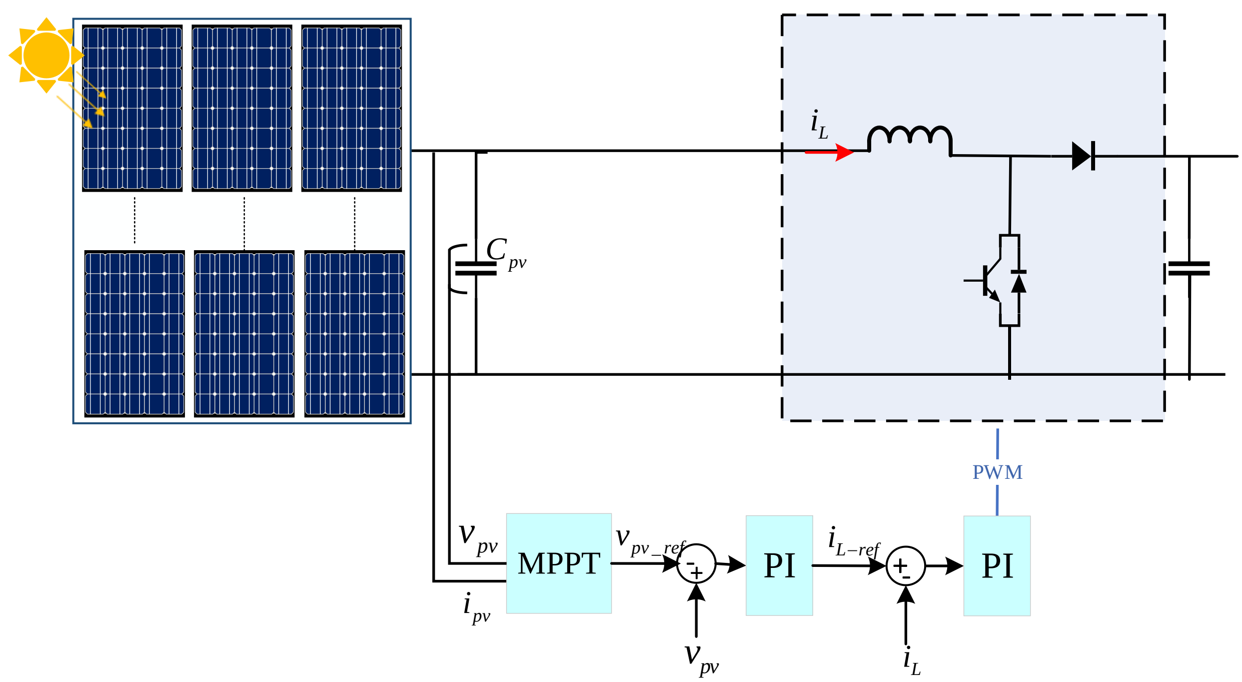

Figure 3. 12:Control of boost converter with MPPT method.

3.4.1.1 Peturb and Observe method

P&O method stands out as a widely utilized MPPT algorithm in the context of boost DC-DC converters for PV systems. Known for its simplicity and ease of implementation, the P&O algorithm operates by perturbing the operating voltage of the PV generator and observing the resultant change in power.

The P&O method operates by continuously perturbing the output voltage of the PV generator and observing the resulting changes in power to track the MPP. The algorithm incrementally adjusts the operating voltage, either increasing or decreasing it based on the observed power variation during each iteration. If the power increases ($\Delta P > 0$), it signifies that the system is moving towards the optimal state. In response, the algorithm continues perturbing in the same direction, either increasing the voltage if ΔV is positive or decreasing it if $\Delta V > 0$. Conversely, if the change in power is negative ($\Delta P < 0$), indicating a deviation from the optimum, corrective action is required. The algorithm responds by reversing the direction of adjustments: increasing the voltage if ΔV is negative or decreasing it if $\Delta V > 0$. This dynamic adjustment process continues iteratively, with the algorithm persistently perturbing the system and observing the resulting changes in power. The ultimate goal is to converge towards the MPP for efficient PV system operation. The principle of the P&O algorithm is illustrated in Figure 3. 13 [84,116].

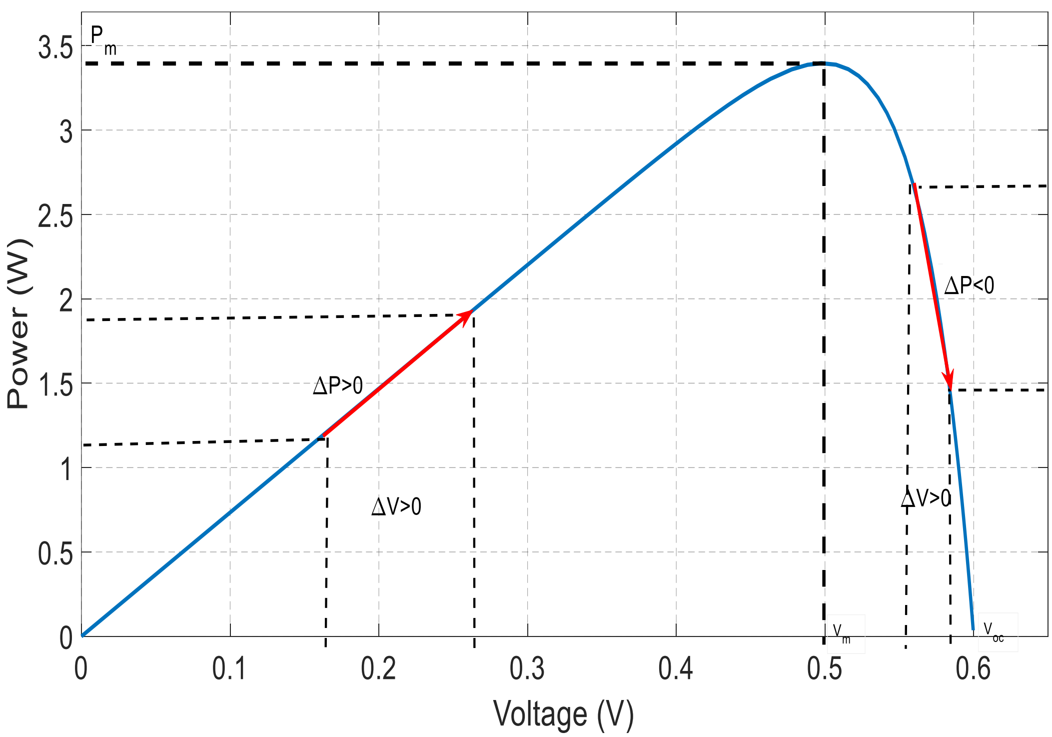

Figure 3. 13: Characteristic of operation of P&O.

The flowchart in Figure 3. 14 illustrates the P&O algorithm's control process in a PV system with a Boost converter as an adaptation stage.

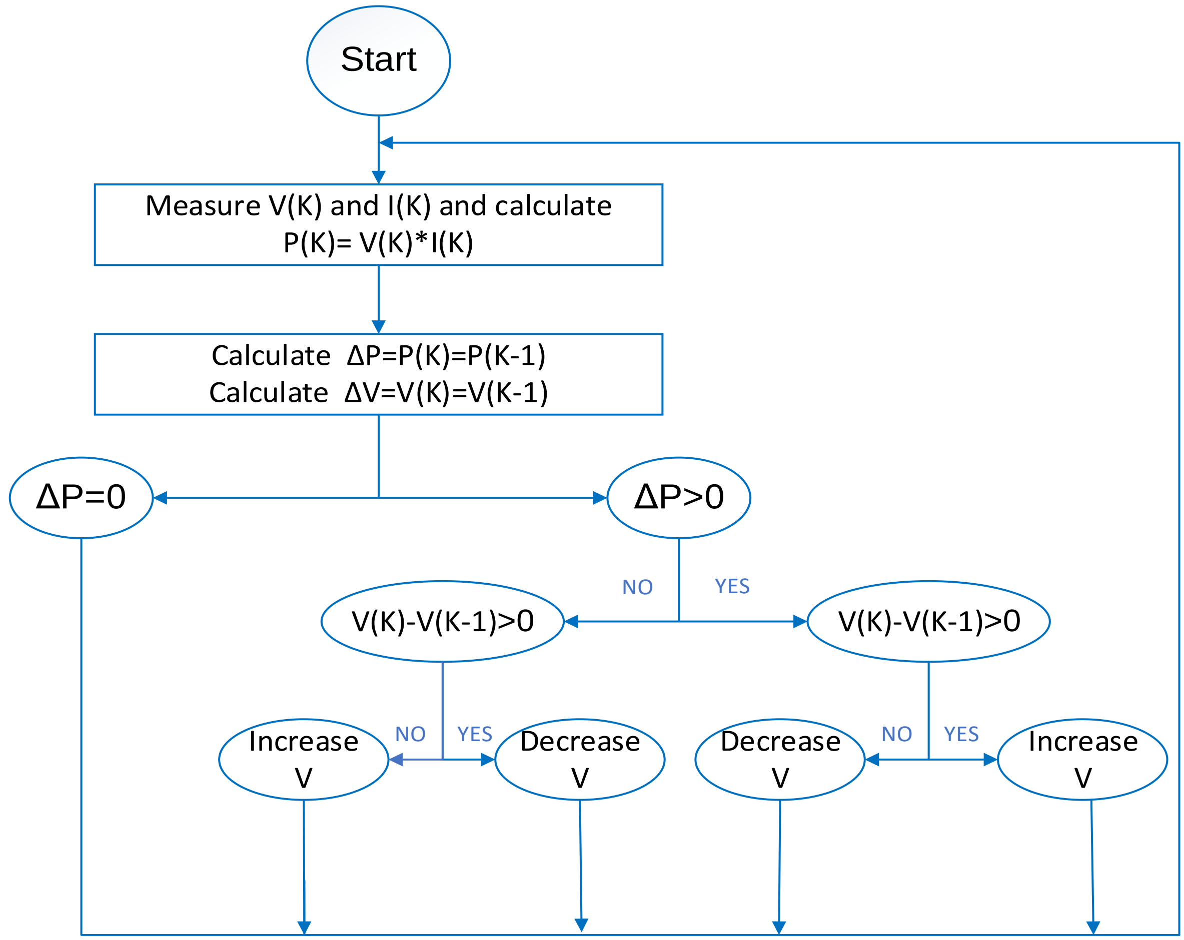

Figure 3. 14: Flowchart of P&O.

P&O algorithm, commonly used for MPPT in solar systems, presents several drawbacks. Notably, it faces a challenging balance; smaller perturbation values lead to slower responses, while larger values induce steady-state oscillations. Furthermore, the algorithm's perturbation value is system-dependent, lacking generality. P&O methods can face challenges under rapidly changing atmospheric conditions, causing divergence from MPP and reduced efficiency. At steady state, the operating point oscillates around the MPP, resulting in energy waste [116].

3.4.2 Power control of grid connected three-phase inverter

In designing grid-connected Photovoltaic inverter, it's crucial to consistently monitor and control the power transferred to the grid. The system employs two key control loops: one for external voltage and another for internal current. The DC link voltage control loop manages the power output from PV modules to the grid and ensures a balanced power flow, while the current control loop regulates the injected current into the grid to align with the grid voltage for a unity power factor. In some cases, control strategies utilize both an outer power loop and an inner current loop. Looking ahead, these strategies are categorized based on the reference frame they employ. Each category possesses distinct properties that impact its performance characteristics. The commonly employed control methods for three-phase inverters connected to the grid are mentioned below [117,118]:

- *dq reference frame:* The *dq* reference frame, a cornerstone in grid-tied inverter control,

revolves around transforming current and voltage into synchronized components. I_d and I_q represent the direct and quadrature components, simplifying control tasks. This framework excels in power quality management, employing proportional-integral (PI) controllers for their satisfactory behavior in regulating dc variables. The control structure aims to synchronize the controlled current with the grid voltage, demanding careful extraction of phase angles through methods like filtering or phase-locked loop (PLL) techniques. The dq control structure often integrates cross-coupling terms and voltage feedforward to enhance the performance of PI controllers [117,118].

- *Alpha-beta reference frame:* The αβ reference frame serves as a bridge between the

synchronized and stationary components. Converting current and voltage into stationary components (I_α and I_β), it operates in both three-phase and occasional one-phase systems. This frame facilitates control variable transformation into sinusoidal quantities, offering flexibility in adapting to diverse system configurations. Controllers like proportional resonant (PR) find a natural fit in the αβ framework, boasting high gain around resonance frequencies and effectively eliminating steady-state errors. This approach provides an alternative strategy in the vast landscape of grid-tied inverter control, catering to scenarios where synchronization and swift dynamics are paramount [36,37].

- *abc reference frame:* In the abc reference frame, applied directly to three-phase systems,

This is a coordinate system used to analyze and control three-phase electrical systems, the abc reference frame doesn't require any transformation of the electrical quantities. This means that the phase currents and voltages are directly represented in this frame without any conversion. The non-linear controllers are used in this system, because they deliver a quick dynamic response [117,118].

3.4.2.1 Voltage Oriented Control (VOC)

The grid-connected inverter employs various control strategies, and one notable approach is voltage-oriented control (VOC), illustrated in Figure 3.15. This method is grounded in the transformation between the *abc* stationary reference frame and the *dq* synchronous frame. The control algorithm operates in the grid-voltage synchronous reference frame, wherein all variables assume DC components during steady-state conditions, simplifying the inverter's design and control. The grid connection process involves synchronization through a PLL, generating a reference angle crucial for transforming grid voltage and current from abc to dq axes reference frames. This transformation is pivotal for effective inverter control within the dq model [113,118].

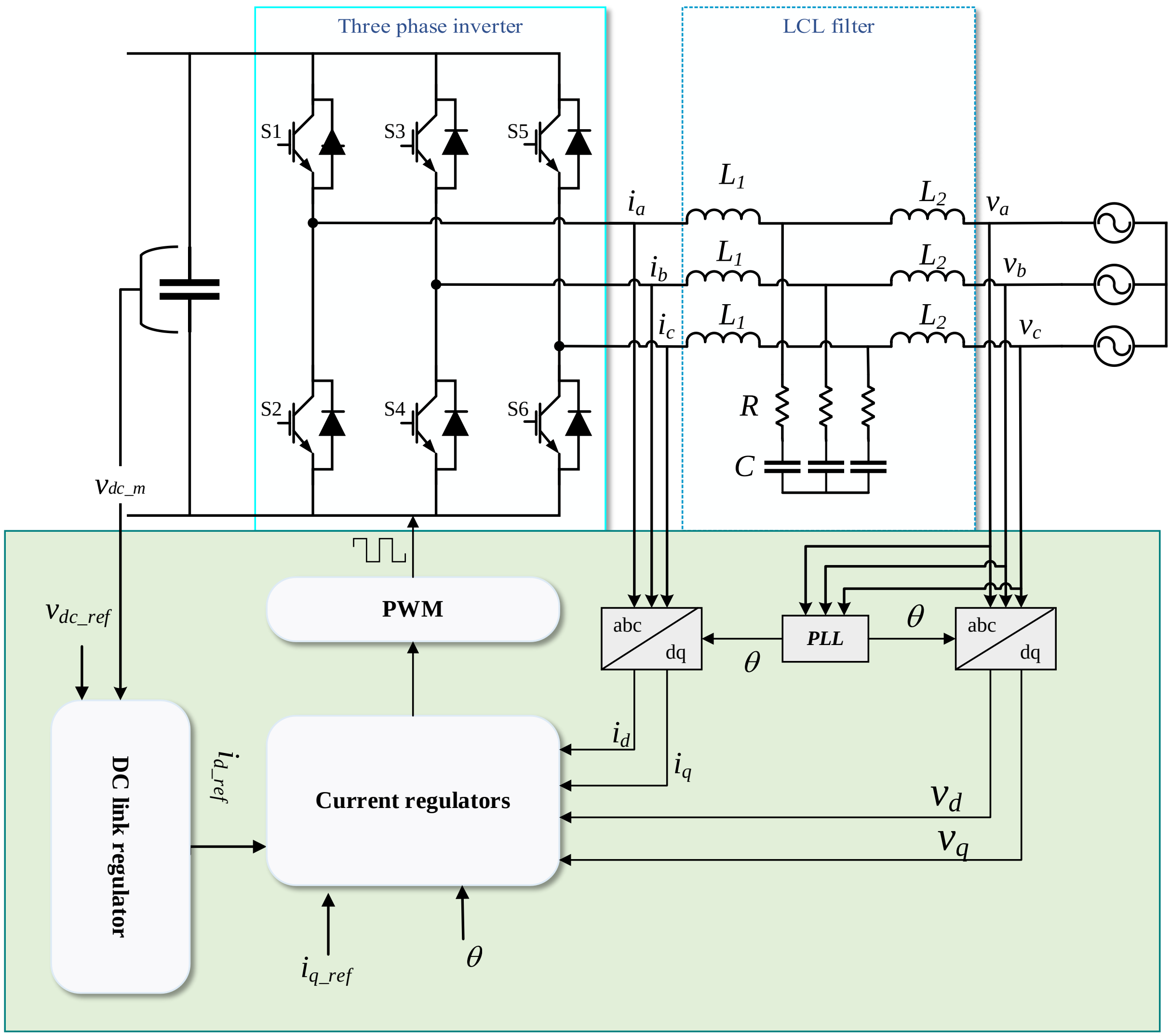

Figure 3. 15: Grid connected inverter with VOC method.

3.4.2.1.1 Decoupling of the current loop

The control scheme for a grid-connected inverter is designed, with a primary focus on decoupled active and reactive power control. This approach is implemented in the synchronous reference frame (dq control) through the use of the *abc-dq* transformation. This transformation serves a crucial role by converting grid currents and voltages into a rotating reference system, effectively decoupling AC current into distinct active (i_d) and reactive (i_q) power components [113].

The equations for the three-phase balanced grid can be represented by:

$$\begin{cases} v_a = V\cos(\omega t) \\ v_b = V\cos(\omega t - \frac{2\pi}{3}) \\ v_c = V\cos(\omega t + \frac{2\pi}{3}) \end{cases} \tag{3.26}$$

The conversion of AC variable quantities from a natural frame to a DC quantity in a two-phase rotating reference frame facilitates straightforward filtering and control. This process, often referred to as dq transformation, involves equations (3.28)–(3.30):

$$\begin{cases} i_a = I_m\sin(\omega t) \\ i_b = I_m\sin(\omega t - \frac{2\pi}{3}) \\ i_c = I_m\sin(\omega t + \frac{2\pi}{3}) \end{cases} \tag{3.27}$$

$$\begin{bmatrix} v_d \\ v_q \\ v_0 \end{bmatrix} = \left[M\right]\begin{bmatrix} v_a \\ v_b \\ v_c \end{bmatrix} \tag{3.28}$$

$$\begin{bmatrix} i_d \\ i_q \\ i_0 \end{bmatrix} = \left[M\right]\begin{bmatrix} i_a \\ i_b \\ i_c \end{bmatrix} \tag{3.29}$$

$$\left[M\right] = \sqrt{\frac{2}{3}}\begin{bmatrix} \cos(\theta) & \cos(\theta - \frac{2\pi}{3}) & \cos(\theta + \frac{2\pi}{3}) \\ \sin(\theta) & \sin(\theta - \frac{2\pi}{3}) & \sin(\theta + \frac{2\pi}{3}) \end{bmatrix} \tag{3.29}$$

The direct axis current i_d directly controls the active power exchanged with the grid P, in the same way, the quadrature axis current i_q, directly controls the reactive power Q exchanged with the grid. The advantage is that the control of these two components i_d and i_q is that they provide an effective means for controlling active and reactive power on the grid side. The active and reactive power of the grid are given by:

$$\begin{cases} P = \frac{3}{2}(v_d i_d + v_q i_q) = \frac{3}{2} v_d i_d \\ Q = \frac{3}{2}(v_q i_d - v_d i_q) = -\frac{3}{2} v_d i_d \end{cases} \quad (v_q = 0) \tag{3.30}$$

The active i_d current is given by:

$$i_d = \frac{2P}{3v_d} \tag{3.31}$$

Similarly, the reactive power is dominated only by the quadrature component of the current i_q . The reference for this current is kept zero to ensure power feeding at unity power factor.

$$i_q = -\frac{2Q}{3v_d} \tag{3.32}$$

In the control scheme of a grid-connected inverter, effective regulation of active power flow to the grid is achieved by enforcing the trajectory of $i_{d\text{-}ref}$. This power control loop is followed by a current control system. In this system, both i_d and i_q are subject to independent PI controllers, tracking reference values $i_{d\text{-}ref}$ and $i_{q\text{-}ref}$. The output of these controllers, combined with cross-coupling terms and voltage feed-forward, produces voltage references $v_{ref,d\text{-}pwm}$ and $v_{ref,q\text{-}pwm}$. The final step involves the application of the inverse transformation dq-abc of the voltage references in turn, drive the PWM, generating corresponding commands for the switches of the grid-connected inverter [113,118], as shown in Figure 3.16:

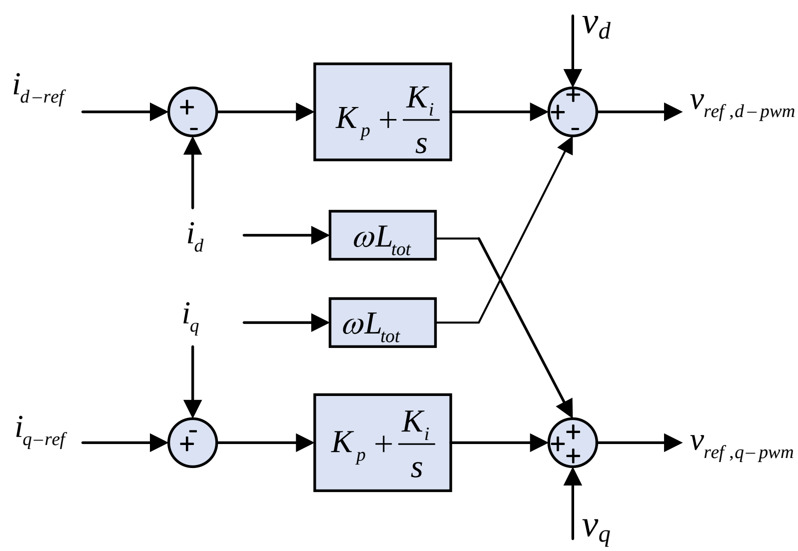

Figure 3. 16: PI decoupled control.

$$\begin{cases} v_{ref,d-pwm} = v_d - \omega L_{tot} i_q + (K_p + \frac{K_i}{s})(i_{d-ref} - i_d) \\ v_{ref,q-pwm} = v_q + \omega L_{tot} i_d + (K_p + \frac{K_i}{s})(i_{q-ref} - i_q) \end{cases} \tag{3.33}$$

Where:

v_{dq} are the dq-axis components corresponding to the grid phase voltage, ($v_{refd\text{-}pwm}$,$v_{refq\text{-}pwm}$) inverter output phase voltage and ω indicates the grid nominal angular frequency.

3.4.2.1.2 DC link voltage controller

The DC voltage V_{dc} across the DC bus must be kept constant. Fluctuations in this voltage must be low so as not to exceed the voltage limit of the semiconductors making up the switches, and so as not to degrade the performance of the inverter. In order to regulate the DC voltage, a regulator is essential. The DC link controller plays a crucial role in governing the voltage stability across the DC link of the inverter. At the core of this control mechanism is the PI controller, a fundamental tool for regulating and maintaining the desired DC link voltage. Let $V_{dc\text{-}ref}$ be the reference DC link voltage and V_{dc_m} the measured DC link, the reference current for active power control is set by the DC link voltage.

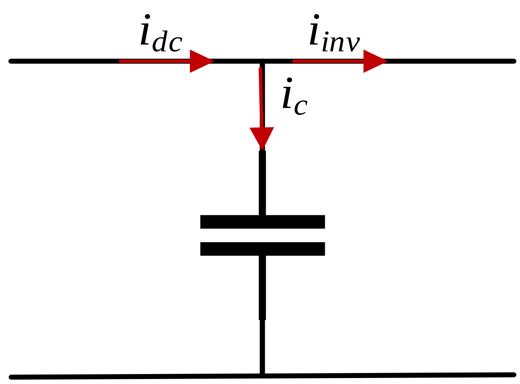

Figure 3. 17: DC link capacitor scheme.

$$\frac{d}{dt}V_{dc} = \frac{1}{C_{dc}} i_c = \frac{1}{C_{dc}}(i_{dc} - i_{inv}) \tag{3.34}$$

3.4.2.1.3 Phase Locked Loop

The synchronization of injected current into the utility network with the grid voltage is imperative to meet industry standards. These algorithms output of the grid voltage vector's phase, facilitating synchronization of control variables, such as grid currents, using various transformations like abc, dq. Various algorithms, the PLL technique is currently the leading method for determining the phase angle of grid voltages. Implemented within the dq synchronous reference frame, this approach involves an abc to dq coordinate transformation. The synchronization is achieved by setting the reference V_d to zero, with a typical PI regulator controlling this variable and outputting the grid frequency [118].

3.5 Simulation results

To verify the validity of the proposed PV system, a photovoltaic array connected to a utility grid, a perturb and observe MPPT controlled boost chopper, a three-phase PWM-controlled two level inverter were used to evaluate the behavior of the studied system. The grid connected PV system is developed and simulated in the MATLAB/Simulink environment. In order to verify the effectiveness of the control scheme studied, a simulation test for a variable irradiation level is carried out.

The parameters of the chosen photovoltaic generator in Annex B, and its current-voltage and power-voltage curves are illustrated in Figures below. Annex B displays the parameters of the grid connected PV system. The temperature is maintained at 25 °C. The variation in solar irradiance applied to the MPPT algorithms is shown in Figure 3.18 and 3.19. The dynamic responses for the current, voltage, and power outputs of the PV generator for different simulated algorithm are depicted in Figures 3.18 and 3.19.

In the simulation study of the MPPT algorithms, the system's response to irradiation variations was thoroughly examined using two distinct irradiation profiles. The first scenario involved an irradiation profile characterized by abrupt changes, simulating sudden shifts in solar intensity. This profile aimed to evaluate the robustness and dynamic response of the MPPT algorithms under challenging and rapidly changing environmental conditions. The simulation results, as illustrated in Figures 3.18, showcase the system's ability to swiftly adapt to abrupt variations in irradiation. The responses of the current, voltage, and power outputs of the PV generator are analyzed, providing valuable insights into the algorithms' performance during scenarios of immediate and drastic irradiation shifts.

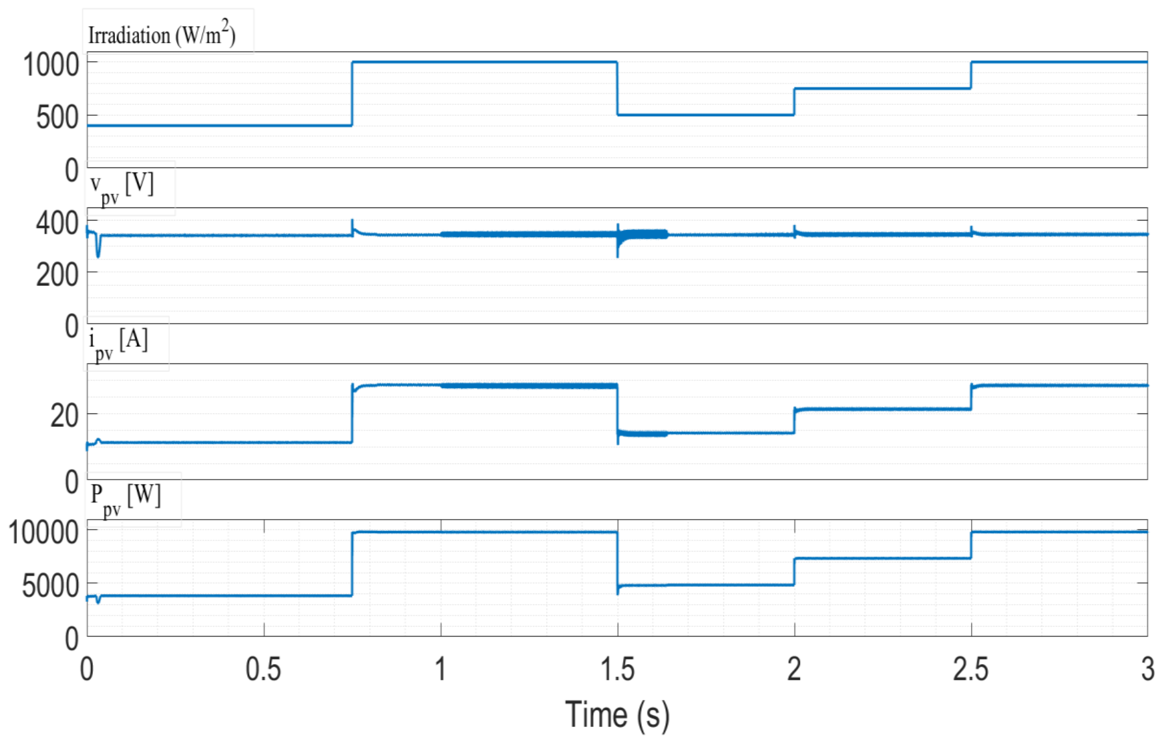

Figure 3. 18: Simulation results of electrical characteristics under abrupt irradiation changes.

In contrast to the abrupt irradiation changes, the second simulation scenario employed an irradiation profile with a gradual ramp evolution. This profile aimed to imitate a smoother and more gradual transition in solar intensity, simulating realistic environmental changes. The simulation results, depicted in Figure 3.19, provide the MPPT algorithms respond to a more gradual evolution of irradiation. This scenario is particularly relevant in practical applications where solar intensity changes occur gradually, such as during sunrise or sunset. The analysis of current, voltage, and power outputs reveals the algorithm’s ability to optimize power generation even in scenarios with less abrupt irradiation variations, demonstrating the versatility and adaptability of the MPPT control strategy.

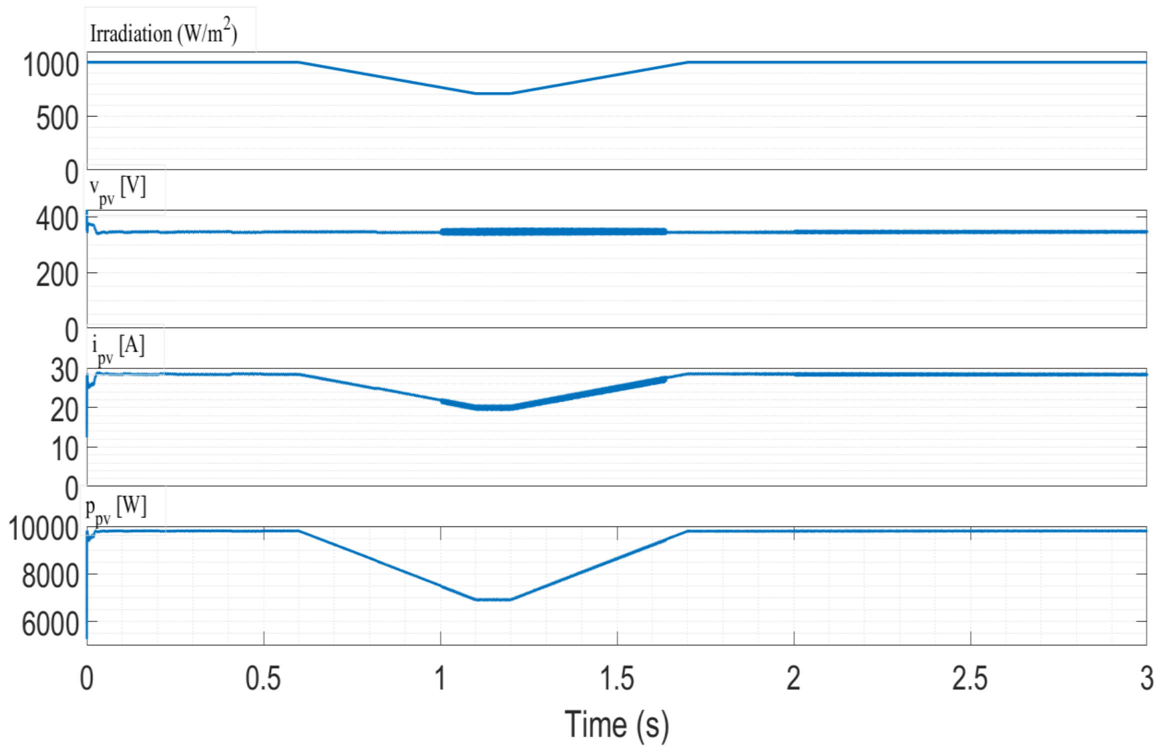

Figure 3. 19: Simulation results of PV parameters under solar irradiance profile.

All the obtained results indicate that the Boost converter and MPPT control fulfill effectively the role. The converter provides, under optimal conditions. The MPPT control ensures the transfer of the maximum power delivered by the PV array to the grid.

The results obtained after varying climatic conditions demonstrate that the PV current (i_{Pv}) and power (p_{pv}) are highly sensitive to irradiance: as irradiance increases to 1000 W/m², i_{Pv} increases and power also increases. However, the voltage v_{pv} hardly varies with irradiance changes.

The MPPT algorithm employed in the study demonstrates remarkable performance under various irradiation profiles. Its efficiency is evident in its ability to promptly and accurately track the MPP of the PV system. Regardless of the irradiation profile, whether characterized by abrupt changes or a more gradual evolution, the MPPT algorithm consistently exhibits a robust response. It efficiently adjusts the duty cycle to optimize power output, ensuring that the PV system operates at its maximum efficiency. The algorithm's adaptability is particularly noteworthy, as it seamlessly navigates through fluctuations in solar irradiance, promptly aligning the operating point with the MPP. Additionally, during transient periods, the algorithm showcases a quick response, achieving a stable operating condition.

The Figures presented below illustrate simulation results incorporating AC side control in a grid-connected PV system. Specifically, these results highlight the impact of DC link control on active and reactive current regulation. These simulations provide valuable insights into the system's behavior, emphasizing the effectiveness of AC side control in managing both active and reactive power components within the grid-connected PV system.

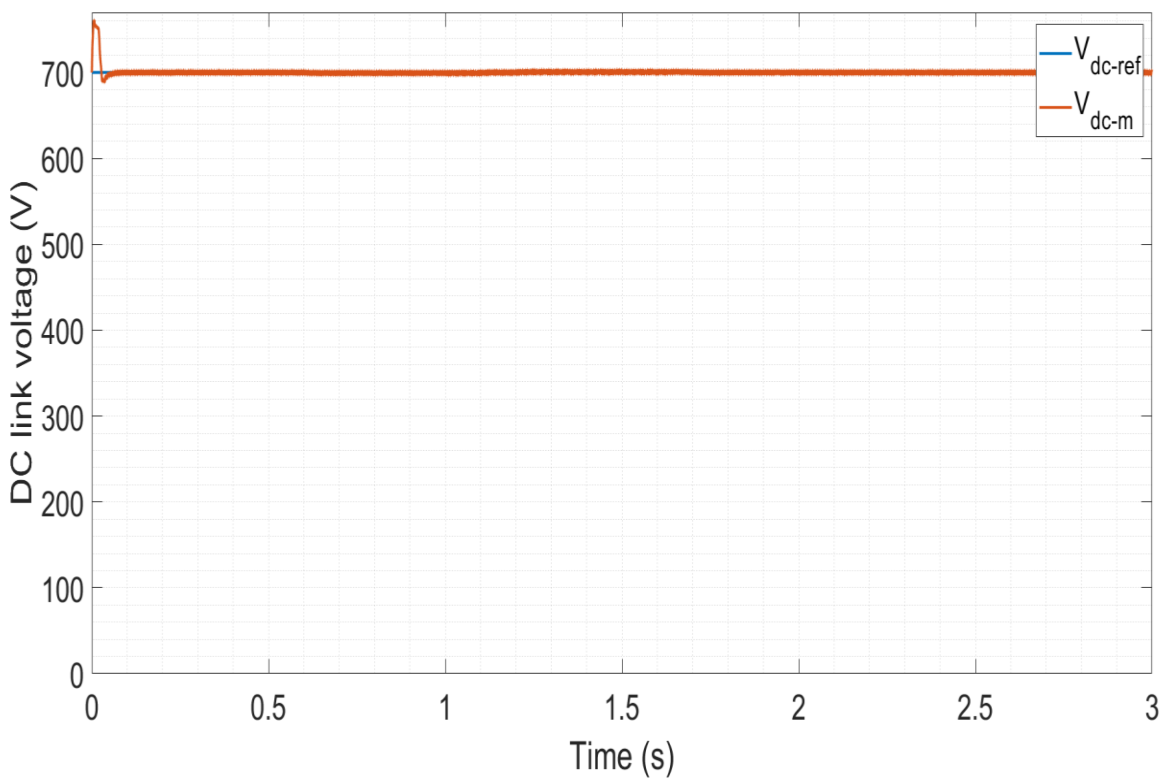

Figure 3. 20: DC link voltage and its reference.

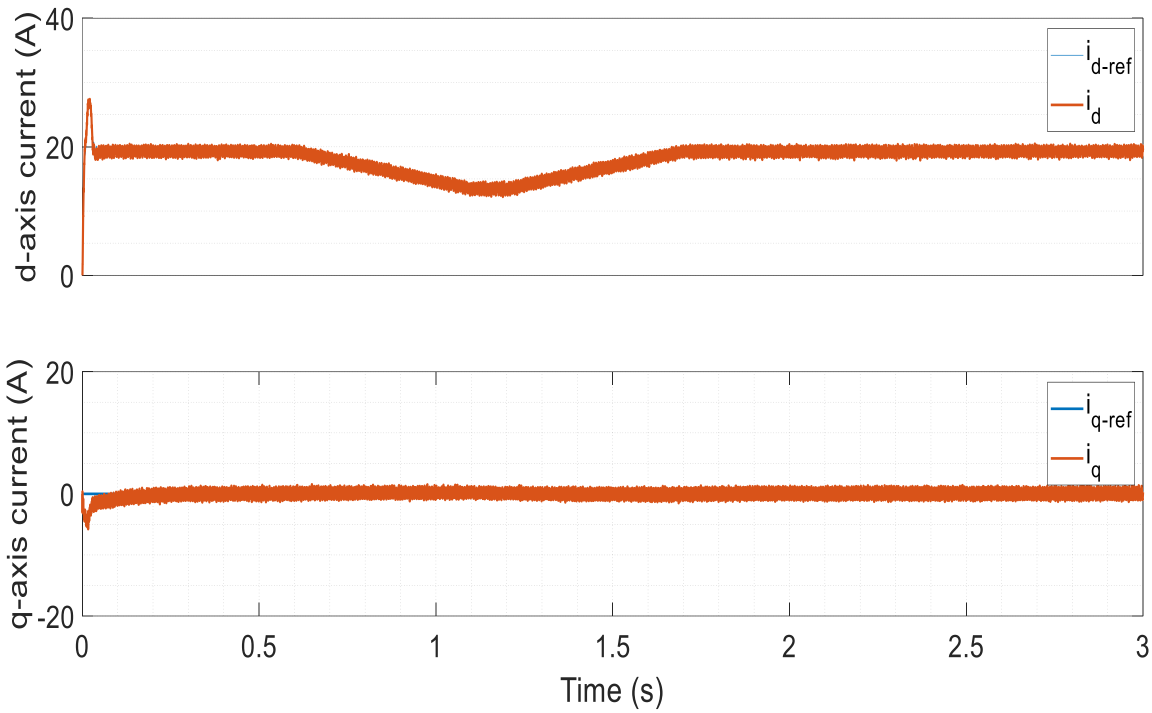

Figure 3. 21: Active and reactive currents and their references.

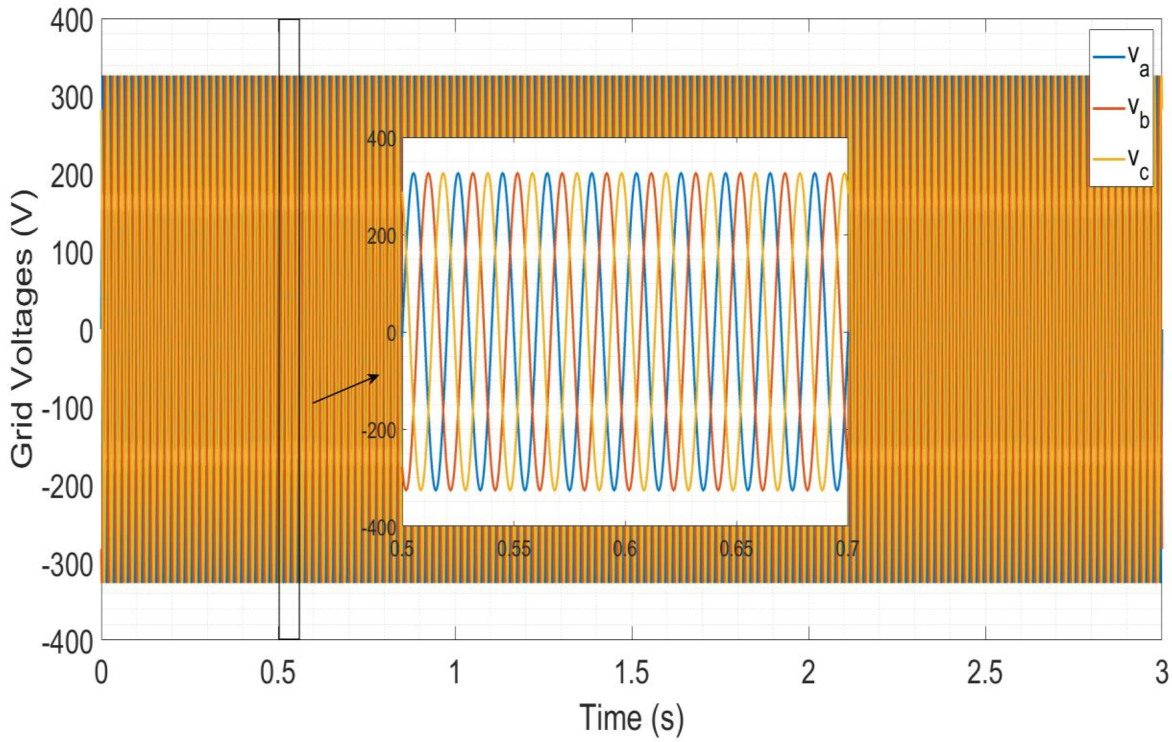

Figure 3. 22: Grid voltage.

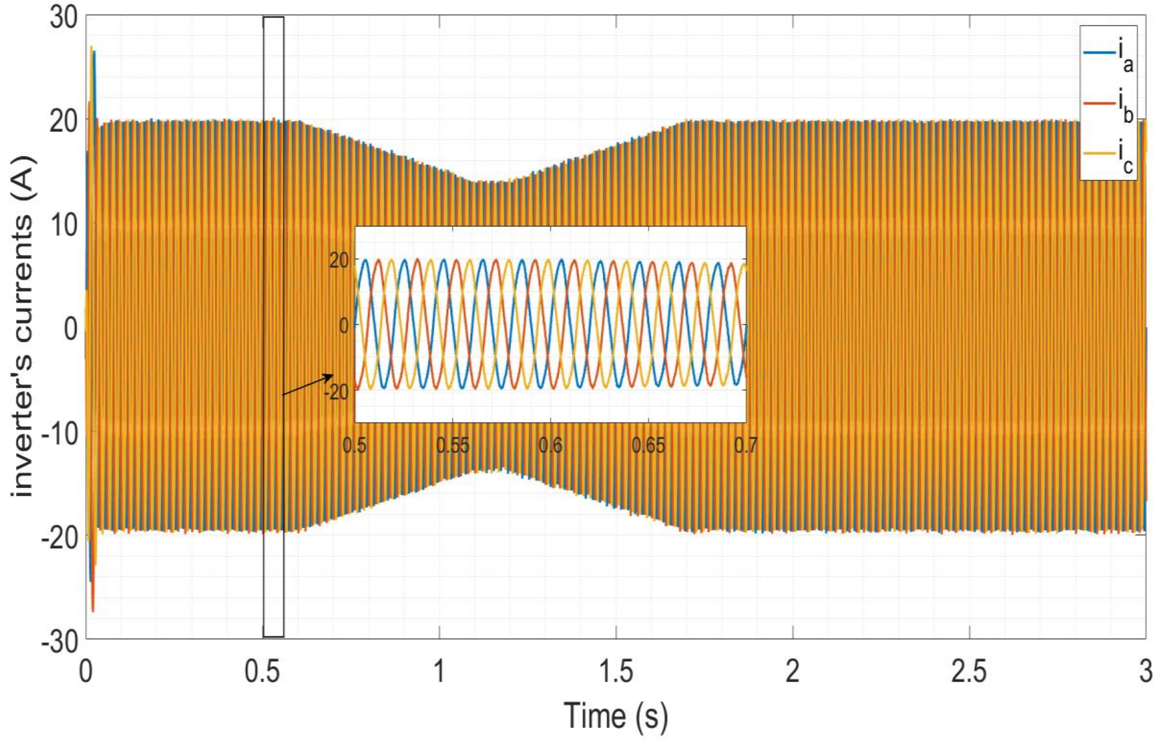

Figure 3. 23: Injected current into the grid.

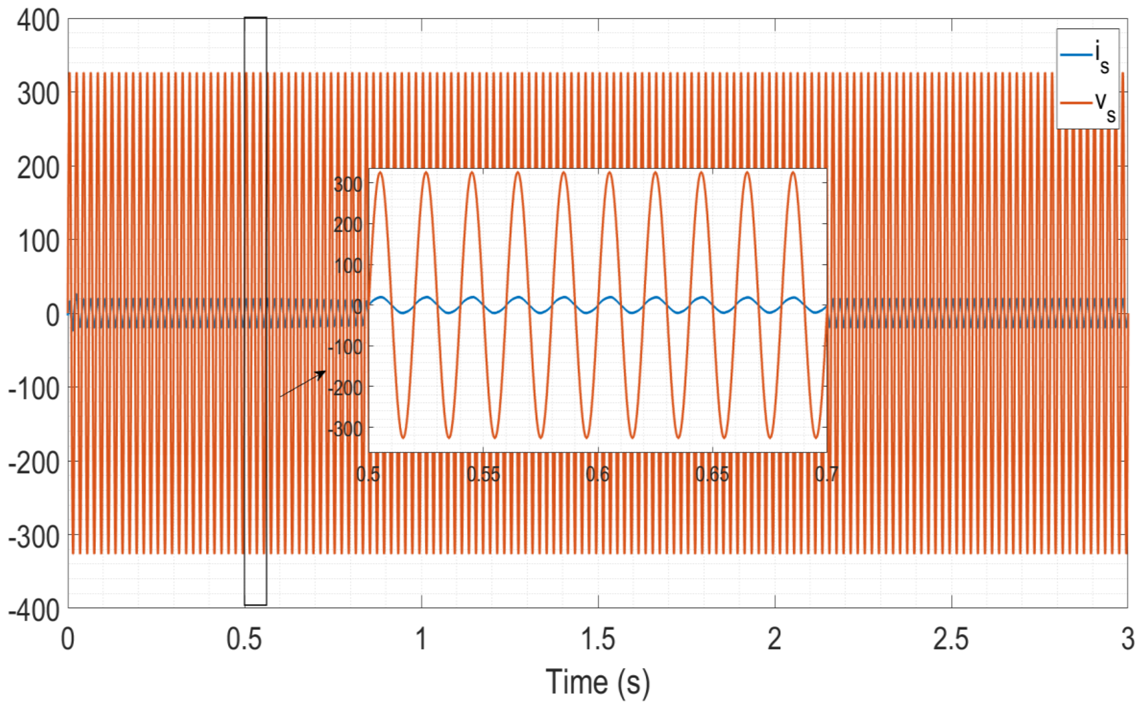

Figure 3. 24: Evolution of grid voltage and injected current.

In the curves presented in Figure 3.20, it is evident that the DC link voltage regulator continues to prove its effectiveness in maintaining a constant voltage at the DC bus terminals. The voltage undergoes a transient regime lasting less than 0.05s before returning to its reference with virtually low static error. Simulation results show satisfactory static performance and improved transient response. As shown in Figure 3.21 the VOC scheme ensures correct regulation of active and reactive current while minimizing their static errors. Operation at unity power factor is ensured by keeping the reactive power constantly zero (i_{q_ref}=0). On the other hand, the active current generated by the GPV is totally injected into the electrical network. As shown in Figure 3.21, this demonstrates the effectiveness of the PI controllers.

Figure 3.24 shows the results of simulations of the evolution of the grid voltage and current in phase obtained with VOC control. It can be seen that the amplitude of the currents injected into the grid is proportional to the illuminance, sinusoidal and in phase with the line voltage, which means that the power factor is very close to unity.

3.6 Conclusion

In conclusion, this chapter has delved into the modeling and control of grid-connected PV systems, focusing on the method within the MPPT technique and the implementation of VOC. Specifically, P&O method has proven its efficacy in dynamically adjusting the operating point to maximize power output. Simultaneously, the VOC strategy has demonstrated its instrumental role in regulating both active and reactive power, ensuring a seamless integration of the PV inverter with the grid.

Simulation results validate the success of these strategies, emphasizing the enhanced energy harvesting capabilities of the MPPT algorithm and the grid power injection stability achieved through VOC. The careful selection of component sizes, from power converters to filters, strikes a crucial balance between efficiency and effectiveness. These meticulously chosen parameters ensure the reliability of the system, providing a robust foundation for seamlessly integrating RE into the grid. As we move forward, these findings contribute not only to the advancement of grid-connected PV systems but also align with broader objectives of enhancing RE integration, contributing to grid stability, and addressing environmental concerns.

Chapter 4

Diagnosis of DC-DC converter in grid connected PV system

Diagnosis of DC-DC converter in grid connected PV system

4.1 Introduction

In the domain of RE, PV systems have emerged as a cornerstone, offering sustainable and efficient power generation solutions. Central to the operation of these systems are power converters, which facilitate the conversion of DC power generated by solar panels into usable AC power for various applications. These converters, including DC-DC converters and three-phase inverters, are essential components that ensure the integration of solar energy into electrical grids, standalone systems, or hybrid configurations. Despite the remarkable advancements in PV technology, the reliability and performance of PV systems are susceptible to the occurrence of faults. These faults, ranging from minor deviations to catastrophic failures, can disrupt system operation and compromise energy output. Among the components vulnerable to faults, power converters stand out due to their intricate nature and the critical role they play in energy conversion and regulation.

One of the most prevalent and concerning types of faults in power converters, particularly in DC-DC converters, is related to semiconductor components. Semiconductor switches, such as IGBTs, are integral to the operation of DC-DC converters, governing the flow of electrical current and voltage regulation. However, these switches are subject to various stress factors, including thermal cycling and material degradation, which can lead to the development of faults such as open-circuit or short-circuit conditions. A failure in power semiconductors can lead to serious system malfunctions. Any undetected and uncorrected fault can quickly damage the entire power system. Therefore, when a fault occurs in one of the converters in the system, it is imperative to implement an efficient and rapid method of fault detection and compensation to prevent the fault from spreading to other system components and to ensure uninterrupted service continuity. In this chapter, we will delve into the fault diagnosis in DC-DC converters, with a particular focus on semiconductor faults. Through a comprehensive exploration of fault mechanisms and diagnostic methodologies, we aim to provide insights into effective fault detection strategies for enhancing the reliability and performance of PV systems. By gaining a deeper understanding of semiconductor fault diagnosis.

4.2 Classification of faults in PV system

Ensuring optimal power generation is imperative for sustainable energy production. However, the functionality of PV system can be compromised by various factors, both temporary and permanent. temporary factors, such as cloud cover, dust or snow accumulation, or partial shading, can intermittently obstruct solar irradiance, resulting in temporary reductions in output power. Conversely, permanent faults such as electrical disconnections, wiring degradation, or component aging can lead to prolonged decreases in power output. It is essential to comprehensively understand the spectrum of faults that can afflict PV systems to maintain their reliability and operational longevity.

Diagnosis of DC-DC converter in grid connected PV system

Figure 4. 1 illustrates the categorization of the prevalent types of faults in PV systems, as depicted in Figure 4. 1, categorizes faults based on physical, environmental, and electrical faults. Within the electrical faults category, further classification includes array faults, DC side faults, and AC side faults. The PV system typically comprises two stages: the boost and inverter stage, where DC power from the PV array is boosted and converted to AC, and the DC and AC stage, representing the overall system configuration with distinct DC and AC components. Array faults involve issues within the PV array itself, while DC side faults pertain to components like DC-DC converter and MPPT failure, and AC side faults relate to inverters, etc…. This classification framework aids in identifying and addressing specific types of faults for efficient fault management and system reliability in grid-connected PV installations [119].

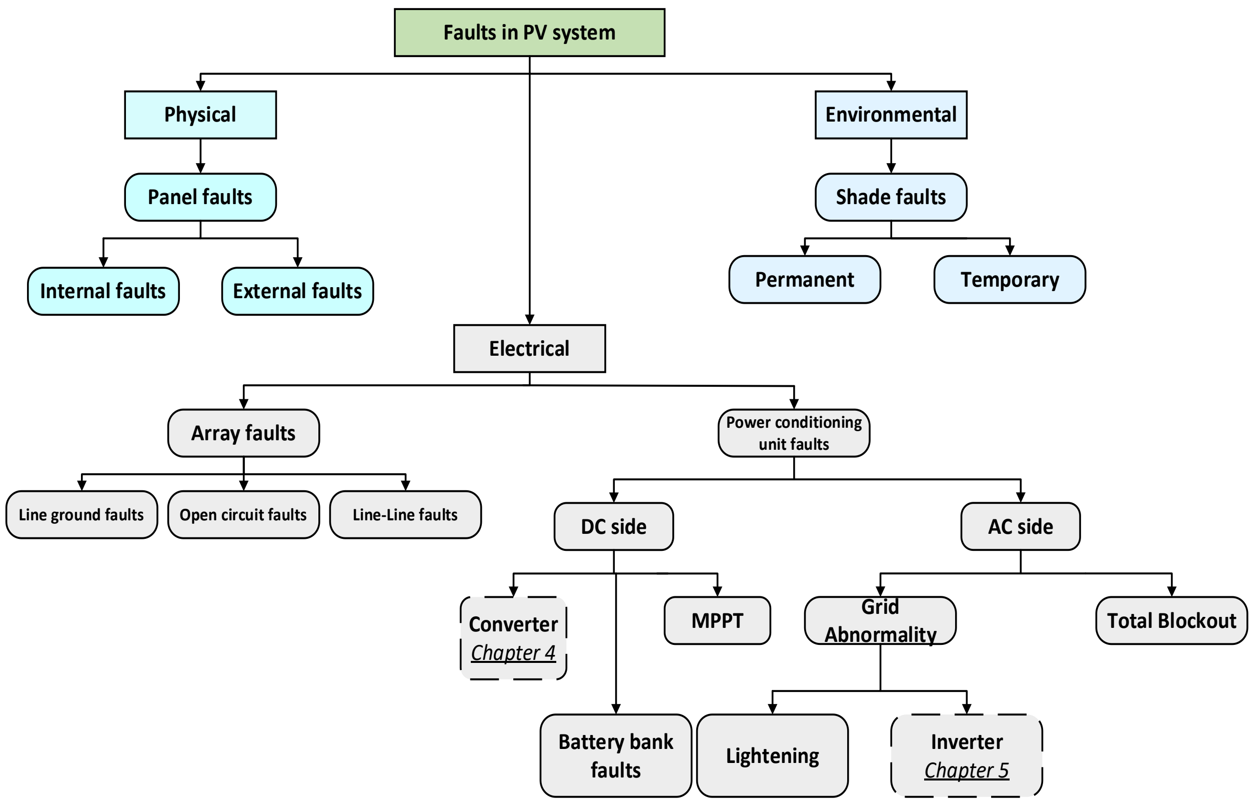

Figure 4. 1: Classification of faults in PV System.

The primary focus of this thesis is to explore the faults surrounding in power converters within PV systems. By understanding the causes, behaviors, and solutions related to these faults, the aim is to improve the reliability and efficiency of PV systems. Through thorough investigation and innovative approaches, this research aims to contribute to robust fault detection and diagnosis methods, thereby promoting the widespread and sustainable adoption of solar energy worldwide. In the complex domain of power electronics, faults can arise from several of factors, ranging from component degradation to external environmental influences. These faults pose significant challenges to the reliable operation of electronic systems, necessitating a deep understanding of their root causes. In power electronics, various stress factors can lead to component degradation and eventual system failure. Thermal stresses, influenced by temperature fluctuations, can induce material fatigue and solder joint failures. Electrical stresses, such as voltage spikes and overcurrent events, can exceed component ratings, causing insulation breakdown and semiconductor failures. Mechanical stresses from vibration or wear can weaken structural integrity over time. Understanding these stress factors is crucial for identifying failure modes and implementing effective mitigation strategies. Through comprehensive examination of failure distributions, insights into reliability performance can be gained [4]. Figures 4. 2. and 4. 3 illustrate the distribution of failures among different components, aiding in prioritizing improvement efforts.

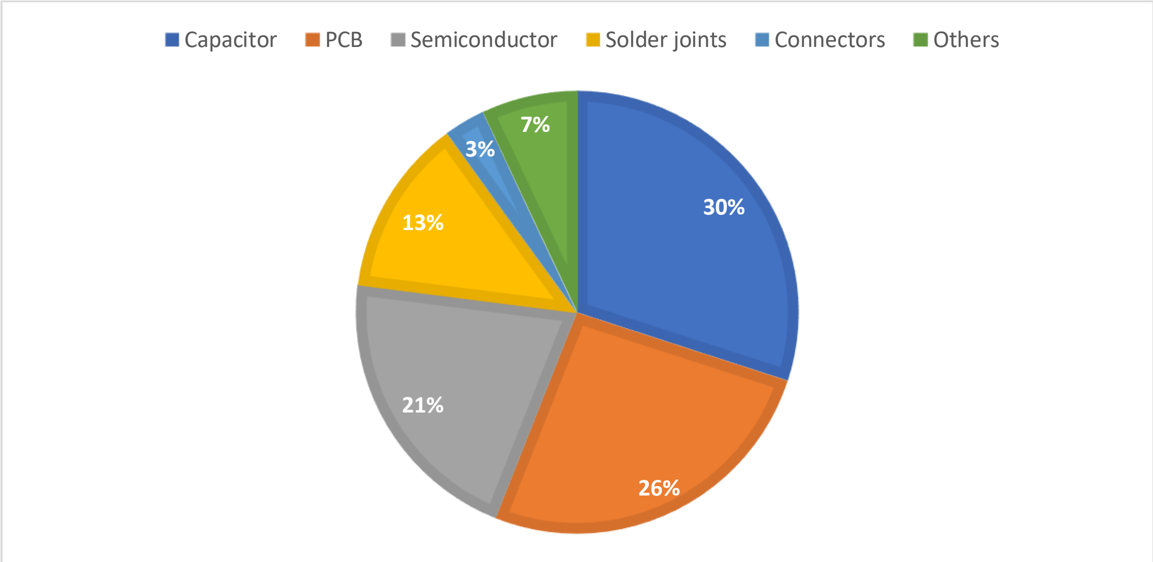

Figure 4. 2: Classification of faults in Power converters.

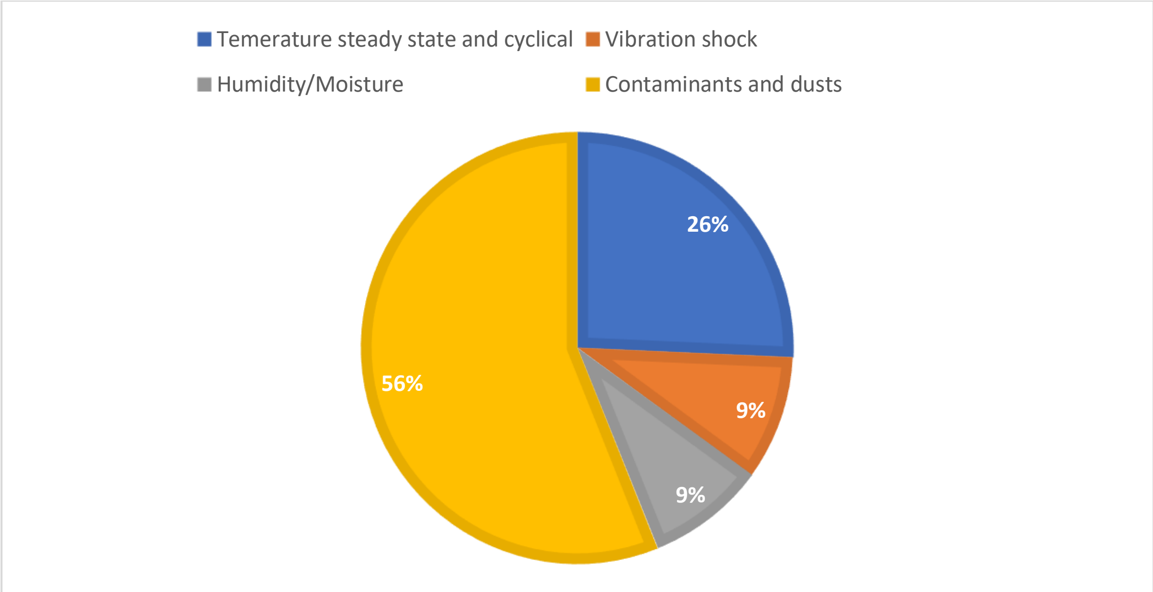

Figure 4. 3: Source of stress distribution.

Capacitors and semiconductors are often identified as vulnerable components, susceptible to degradation and overstress conditions. Temperature, a significant factor, accelerates degradation mechanisms, emphasizing the importance of proper thermal management.

4.3 Classification of faults in DC-DC converters

In PV systems, non-isolated DC-DC power converters play a pivotal role. Maintaining uninterrupted service, reliability, and optimal performance in these systems is paramount. Among the critical components, aluminum electrolytic capacitors and semiconductor switches are particularly vulnerable to faults. Research indicates that more than half of reported malfunctions and breakdowns stem from capacitor failures, with switch faults accounting for around 30% [120].

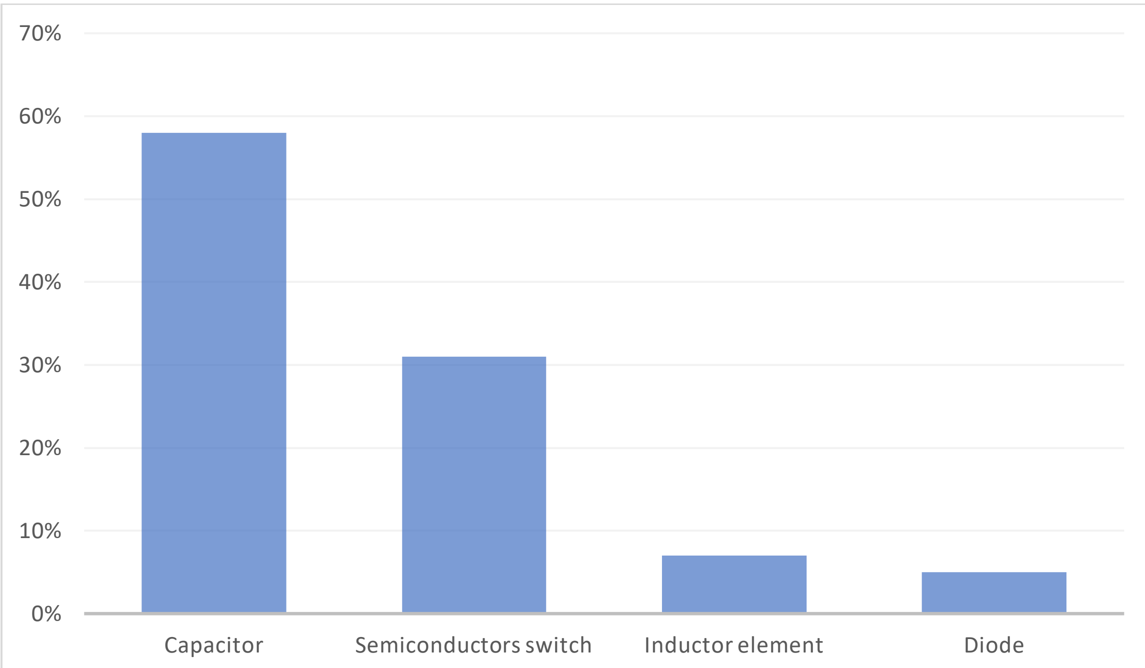

Figure 4. 4: Classification of faults in DC-DC converters.

This chapter focuses on the detection and diagnosis of faults, with a particular emphasis on switch faults, which play a significant role in the operation of DC-DC converters within PV systems. We will delve into the intricacies of switch faults and explore methods to identify and mitigate them effectively.

4.3.1 Classification of faults in power switches

IGBT catastrophic failures can manifest in different ways, primarily as open-circuit failures or short-circuit failures [121,122].

4.3.1.1 Open-Circuit Failure

Open-circuit failure occurs when the IGBT fails to conduct current due to a break in the circuit path. In this scenario, the converter can still operate, although with reduced efficiency and output quality. Open-circuit failures are typically less severe compared to short-circuit failures.

In the context of IGBT open-circuit failures, two critical components warrant examination: bond wires and gate drivers. Bond wires, essential for connecting various parts within the IGBT, may suffer from lift-off or rupture due to mechanical stress. Similarly, gate drivers, responsible for controlling the IGBT's operation, are susceptible to various failures that can impact the device's performance.

4.3.1.2 Short-Circuit Failure

Short-circuit failures are highly detrimental to converters as they can lead to rapid and extensive damage. The uncontrolled short-circuit current can potentially destroy the failed IGBT and other components within the circuit. This type of failure poses a significant risk of catastrophic damage to the converter and associated systems. The several failure mechanisms in power switch, particularly focusing on high voltage breakdown, latch-up, second breakdown, and energy shocks during short circuits.

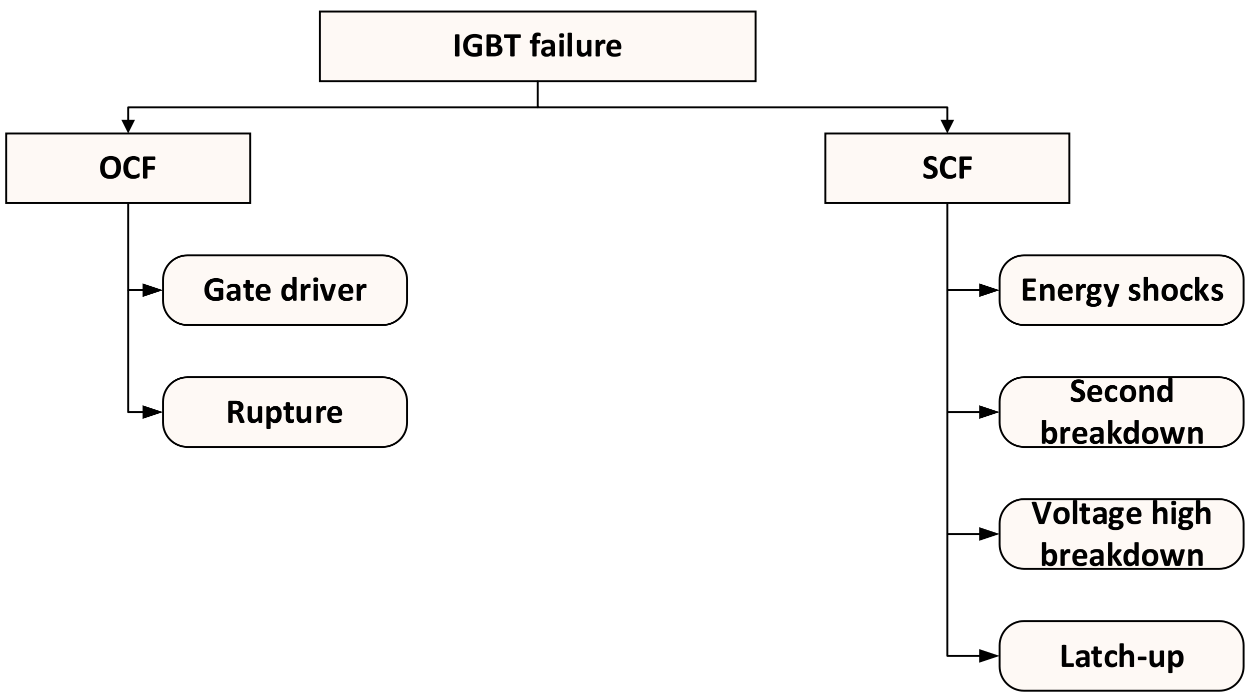

Figure 4. 5: Classification of catastrophic failures in IGBT.

4.4 Impact of faults of open circuit faults in DC-DC converter in grid connected PV system

In this thesis, our focus will primarily be on investigating the impact of OCF rather than SCF in DC-DC converters within grid-connected PV systems. OCF, while not as immediately destructive as SCF, can still have significant implications for the overall performance and reliability of the system. By studying the effects of OCF, we aim to gain a comprehensive understanding of how these faults can disrupt the operation of DC-DC converters in PV systems and potentially affect the grid-connected operation. Through simulation tests, we will examine the behavior of the system under OCF fault scenario, ultimately contributing to the development of effective fault detection and mitigation strategies in grid-connected PV applications.

When there's an OCF in the switch of a boost converter in a PV system, it will affect the operation of the entire system.

Cases	Voltage	Current	Power
OCF	Increase	Decrease	Decrease
SCF	Decrease	Increase	Decrease

Table 4. 1: OCF and SCF effects on the PV module electrical characteristics.

- Effect on PV Module

Voltage: The voltage across the PV module will increase significantly. Without the boost converter regulating the voltage, the PV module will operate at its maximum voltage point (V_{oc}).
Current: The current through the PV module will decrease. With the open circuit fault, there's no path for current flow, so the current will drop to zero.

Power: The power output of the PV module will decrease to zero. Since power is the product of voltage and current (P = V× I), and both voltage and current decrease to zero or near-zero levels, the power output will also drop to negligible levels.

- Effect on Inverter Connected to the Grid

Inverter behavior: The inverter will likely detect the absence of power from the PV module due to the open circuit fault. In the event of an open circuit fault in the boost converter switch, the inverter current would typically decrease significantly or drop to zero.

In simulating a grid-connected PV system to assess the impacts of faults, particularly OCF in the switch of the boost converter, a simulation results approach is essential to capture the system's dynamic behavior accurately. These results enable us to observe how OCF faults in the boost converter affect the overall performance of the PV system.

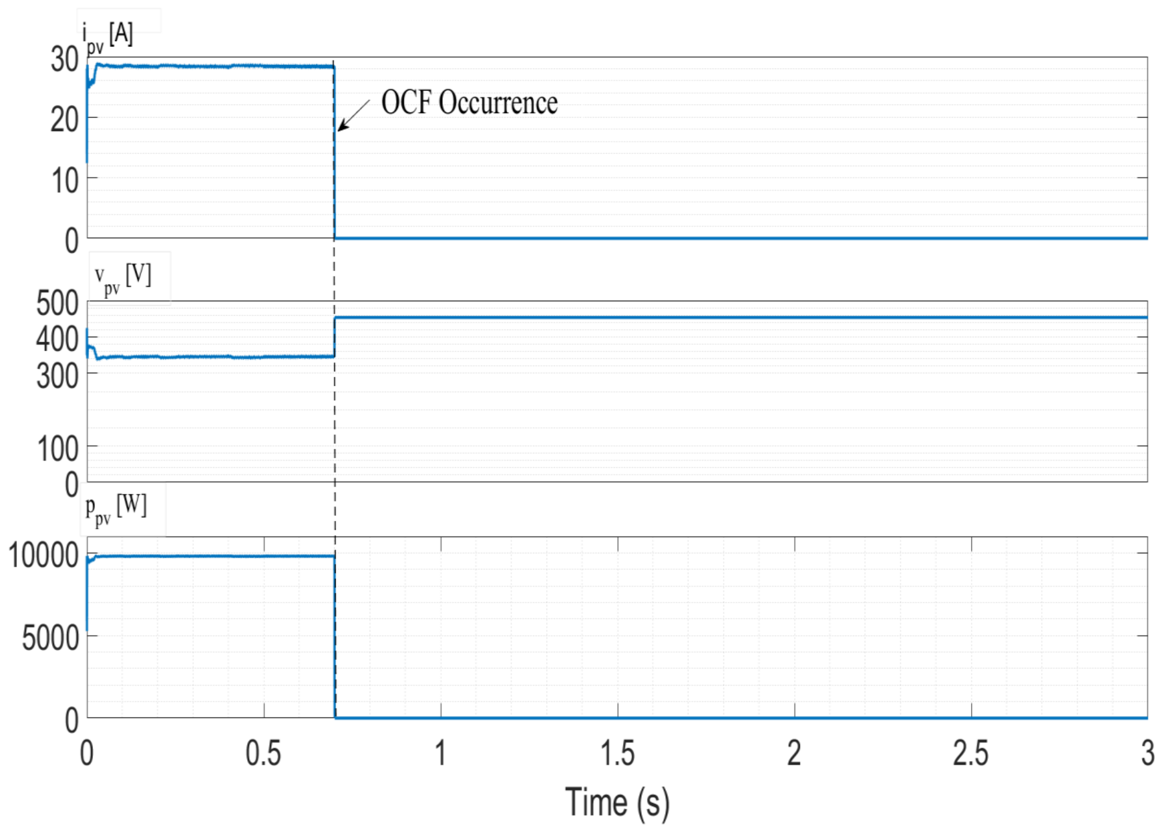

Figure 4. 6: Impact of OCF occurrence in boost converter on the PV module electrical characteristics.

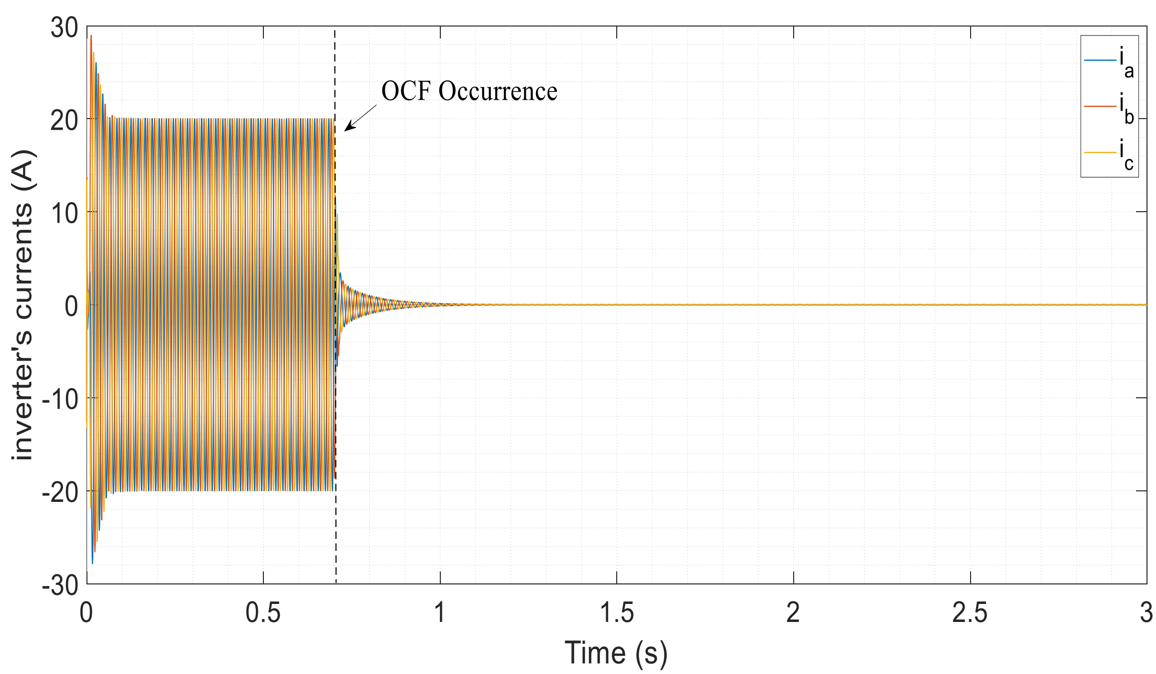

Figure 4. 7: Impact of OCF occurrence in boost converter on the inverter's currents.

4.5 State of art of diagnosis methods in DC-DC converter

The state of the art in diagnosis methods for DC-DC converters is essential for ensuring the reliability and performance of various electronic systems. These converters play a crucial role in regulating voltage levels, making them fundamental components in PV system. Effective diagnosis methods are necessary for detecting OCFs particularly, thereby minimizing downtime and preventing potential damage.

This overview explores the latest advancements in diagnosis techniques, highlighting their significance in maintaining the stability and functionality of DC-DC converters. Numerous studies have investigated fault diagnosis in DC-DC converters. Regarding diagnosis approaches, these studies generally categorize methods into two main types: Model-based, Signal -based methods.

Model-based algorithms require modeling the behavior of the converter using knowledge of the converter topology, its parameters, and input signals. The converter states have been modeled using sliding mode observer in [123], [124] and through state estimator in [125]. Once modeled, the estimated states of the system are compared to the measured converter response and the residue is processed to extract information of the OC faults. The model-based algorithms like Kalman filter [126], self-tuned Kalman filter [127], observer featuring adaptive estimation of parameter [128] or adaptive gradient descent algorithm were developed to estimate the converter parameters. These could also be potentially used to carry out fault diagnosis of converter. The above-mentioned model-based fault diagnosis approaches require accurate models and significant computational effort to improve the robustness of the diagnosis.

On the other hand, signal processing-based approaches are computationally less intensive and use commonly available variables for diagnosis purpose. The variables could be an analyzed in time-domain or frequency-domain to extract the fault signature of the converter. In [129], a method based on statistical moments of the converter voltages and currents is proposed to detect OC faults in DC-DC converters. Other variables such as inductor current slope [130]–[131], diode voltage [132], inductor voltage [133], voltage of specially designed Rogowski coil sensor for capturing inductor current derivative [134], transformer primary winding voltage [135] were also suggested for different topologies of converter. The frequency- based approach suggested in [136] analyzes the switching frequency based harmonic component for fault detection and localization using fast Fourier transform (FFT).

Ref	Diagnosis method	Type of converter	Type of fault	Diagnosis speed	Cost
130	Inductor current slope sign	Non isolated DC-DC converter	OC-SC	Relatively fast	Medium
133	Inductor voltage	DC-DC converter	OC,SC	Relatively fast	High
137	PV variables (I,V,P)	DC-DC converter in PV system	OC,SC	Relatively fast	Low
132	Diode voltage	Non isolated DC-DC converter	OC,SC	Relatively fast	Low
138	Reference current error	Interleaved DC-DC converter	OC	fast	Low
134	Rogowski coil voltage	Non isolated DC-DC converter	OC,SC	fast	Low
135	Magnetic component voltage	Buck converter	OC,SC	fast	Low
139	Input current derivative	Non isolated DC-DC converter	OC	Relatively fast	Low
136	Frequency components of input current	Interleaved converter	OC	fast	Low
123	Sliding mode observer	modular multilevel DC–DC converters	OC	100ms	Low

Table 4. 2: Diagnosis method for diagnosis DC-DC converter.

4.6 Proposed fault detection method of boost converter

Before detailing the proposed diagnostic method for identifying OCFs in DC-DC boost converters integrated with PV panels, it's crucial to set the context of our study. In our case, we focus on the boost converter's role within the PV system, where it facilitates voltage regulation to optimize power conversion efficiency. However, the switch components within the boost converter are susceptible to faults, particularly OCFs, which can significantly affect system performance. Our investigation aims to develop a precise diagnostic technique tailored for detecting OCFs in boost converters within PV systems, thereby enhancing fault tolerance and system reliability.

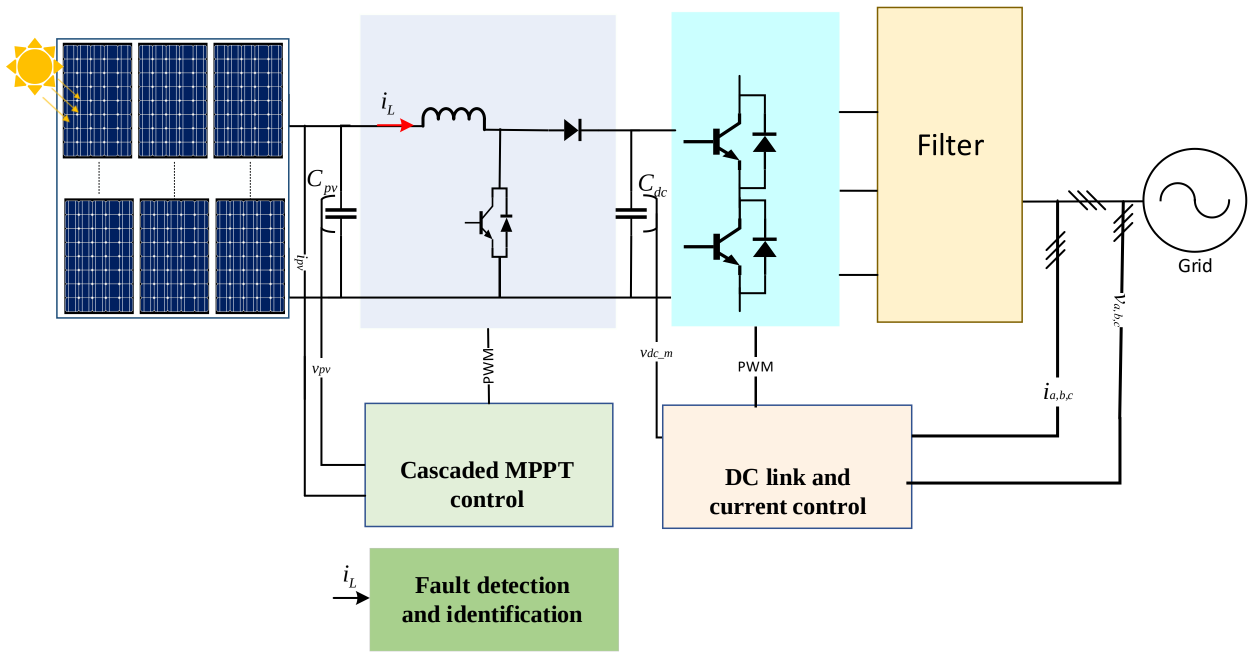

Figure 4. 8: Fault detection and identification of OCF of boost converter in grid connected PV system.

Our diagnostic strategies for boost converters in PV systems incorporates two distinct approaches, both centered around the analysis of a crucial parameter: the inductor current. These methods leverage the intricate behavior of inductor currents to enhance fault detection capabilities and ensure system reliability. By utilizing two distinctive diagnosis approaches that share a common foundation in inductor current analysis, we aim to comprehensively address OCF and improve the overall performance and safety of boost converters in photovoltaic applications.

4.6.1 Primary Algorithm

To diagnose an open switch fault in a boost converter in a closed loop control, the process involves several steps. The reference current error e, a fundamental parameter in closed-loop current controllers, represents the difference between the reference input current i_{L_ref} and the measured inductor current i_L. During healthy operation case i_L adeptly tracks i_{L_ref}, resulting in a small value of *e* that is typically neglected.

$$e = i_{L\_ref} - i_L \tag{4.1}$$

However, this equilibrium is disrupted by sudden system perturbations such as open fault occurrence. For instance, in the occurrence of an open-circuit fault in a converter switch, i_L experiences an abrupt decrease, deviating from i_{L_ref} and causing an increase in *e*. This sudden increase in *e* will indicate the occurrence of the fault. To highlight the different variations in *e*, it involves differentiating the actual error value from its previous value, which enable us to detect any minor deviations or significant changes in the error signal that may indicate fault conditions, in a boost converter. By comparing the current error value with its immediate past value, we can identify sudden peaks that exceed predefined thresholds, signifying potential fault occurrences. This differentiation process is crucial for enhancing the sensitivity and reliability of our fault detection system. A threshold is established specifically targeting peak increases in the error signal *e*. This threshold is carefully set to detect fault-induced peaks that surpass minimum 2 times the previous error value, a criterion chosen for its sensitivity to significant deviations indicative of an OCF. When such a peak is detected, an increase detection block is activated to further detect and confirm the fault condition, to preserve the detected peak value for subsequent analysis or action, a sample and hold block is implemented capturing and storing the peak error value accurately.

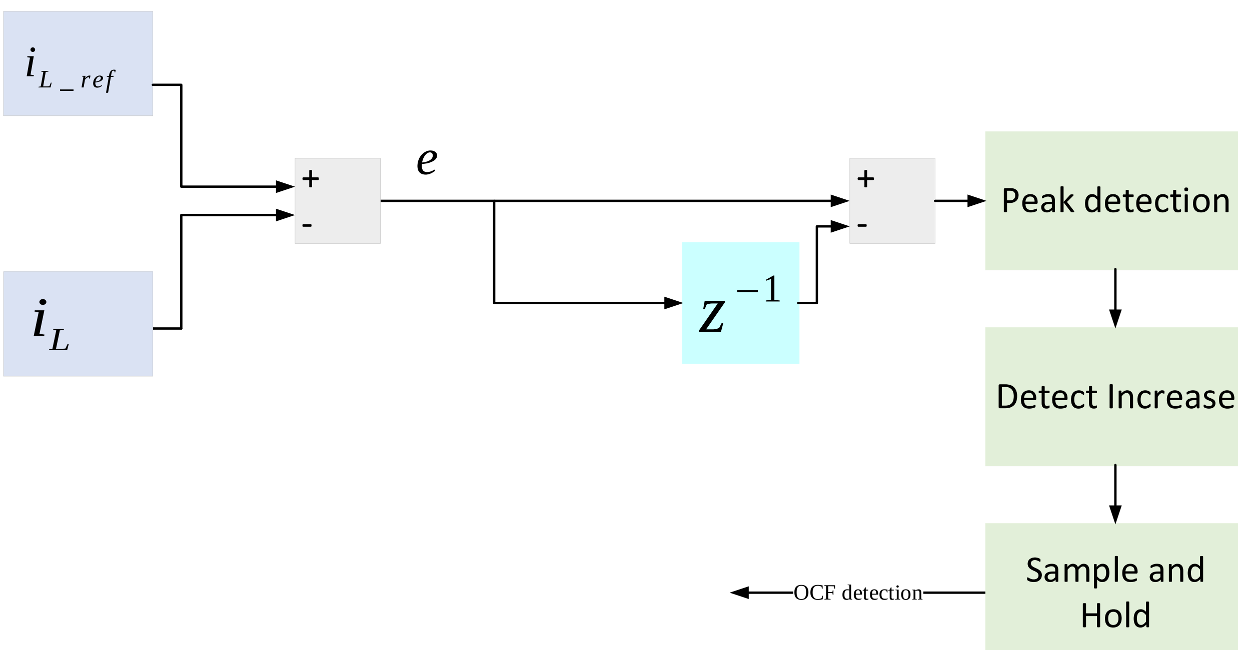

Figure 4. 9: Primary fault detection.

We conduct thorough testing to evaluate the response time of the diagnosis method for detecting OCF in the boost converter. This testing will involve simulated fault scenarios, including variations in environmental conditions, to assess how quickly and accurately the method can detect and respond to fault events. Additionally, validation tests will be conducted to ensure that the detected faults are robust and do not cause noise or transient disturbances in the system.

4.6.2 Secondary Algorithm

In a DC-DC converter, the inductor current plays a crucial role in energy transfer and regulation. Analyzing the inductor currents at the rising and falling edges of the gate command signal provides valuable insights into the converter's operation and can help diagnose OCF effectively. During normal operation, the inductor current exhibits a characteristic behavior: it increases during the rising edge of the gate command signal and decreases during the falling edge. This behavior is attributed to the positive slope of the current as energy is stored in the inductor during the rising edge and released during the falling edge.

Mathematically, the inductor current (i_L) can be represented as a function of time (t). During the rising edge of the gate command signal, the inductor current increases according to the following equation:

$$\frac{di_{L-inc}}{dt} > 0 \tag{4.2}$$

Conversely, during the falling edge of the gate command signal, the inductor current decreases as energy is discharged from the inductor, leading to a negative slope.

$$\frac{di_{L-dec}}{dt} < 0 \tag{4.3}$$

Under normal operating conditions, the inductor current sampled during the rising edge ($I_{L\text{-inc}}$) is expected to be higher than the current sampled during the falling edge ($I_{L\text{-dec}}$). This is consistent with the positive slope of the current during the rising edge and the negative slope during the falling edge. However, in the presence of OCF, this relationship may be reversed. By comparing the sampled currents at the rising and falling edges of the gate command signal and applying a diagnostic condition, OCF can be identified. This method offers the advantage of directly assessing the current behavior of the converter, providing insights into potential faults related to current variations.

$$i_{L-inc} \geq i_{L-dec} \quad \textit{Healthy Operation} \tag{4.4}$$

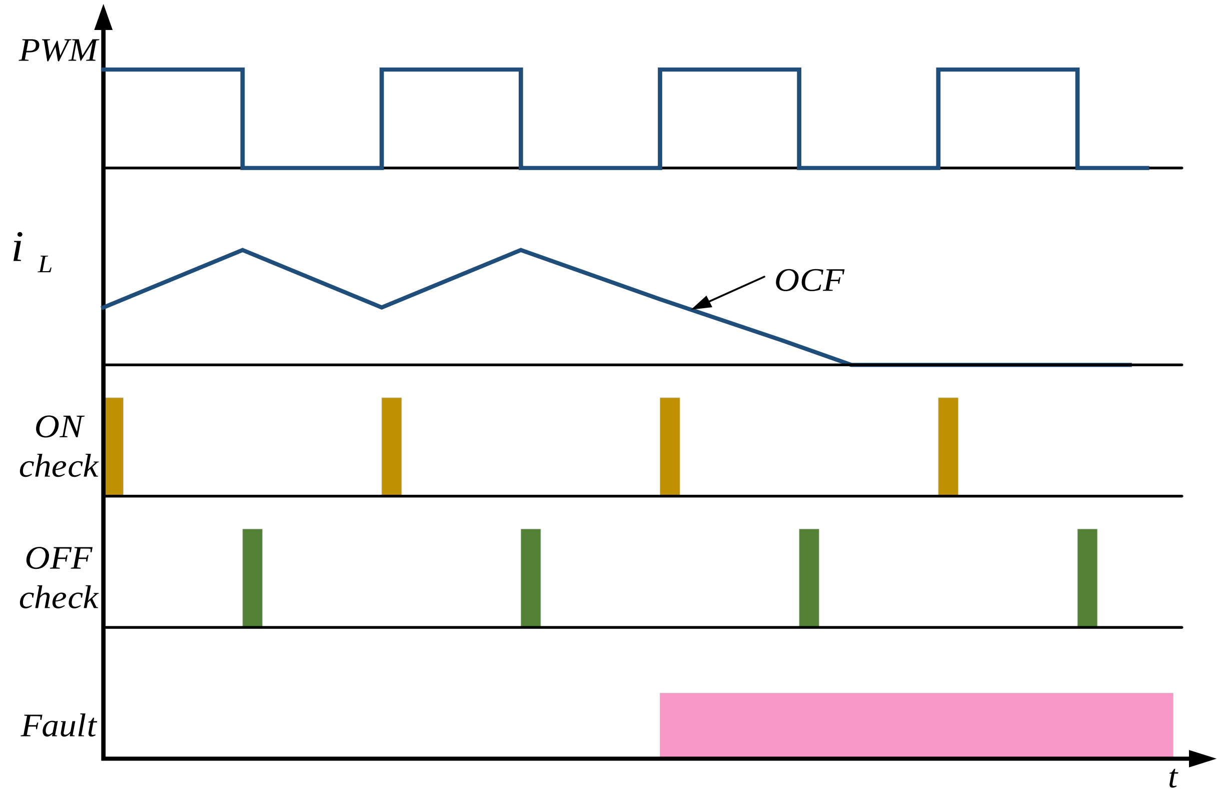

Figure 4. 10: Secondary fault detection principle.

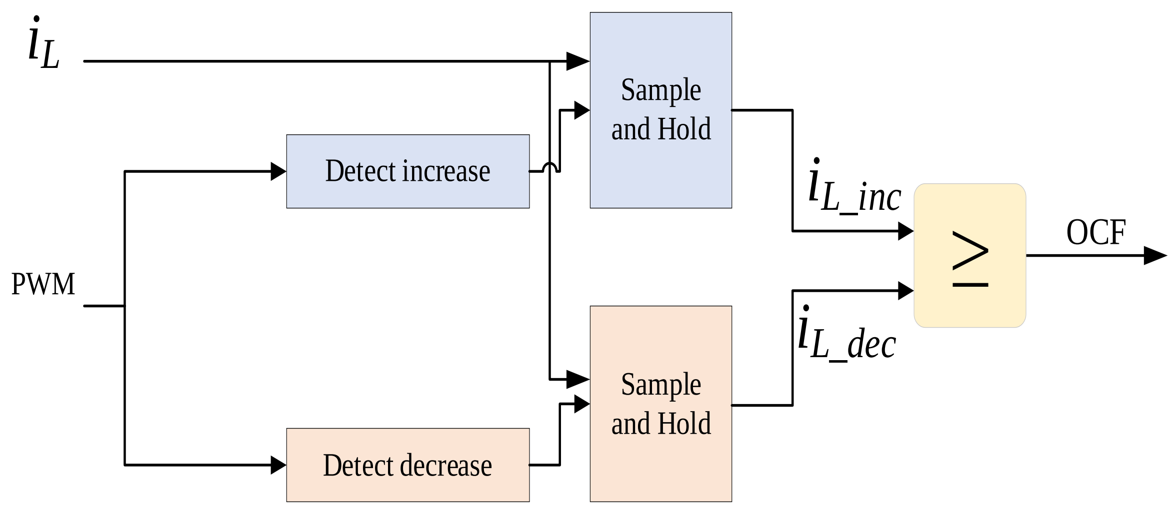

Figure 4. 11: Secondary fault detection method.

4.7 Fault reconfiguration of DC-DC boost converter

Fault-tolerant control strategies become paramount in ensuring the continuous and reliable operation of PV systems in the presence of faults. Specifically, in the case of OCFs in boost converters, fault-tolerant approaches are essential for promptly detecting, isolating, and then reconfigure the control strategy to maintain system functionality or at least ensure degraded performance until the system can be safely shut down for maintenance or repair.

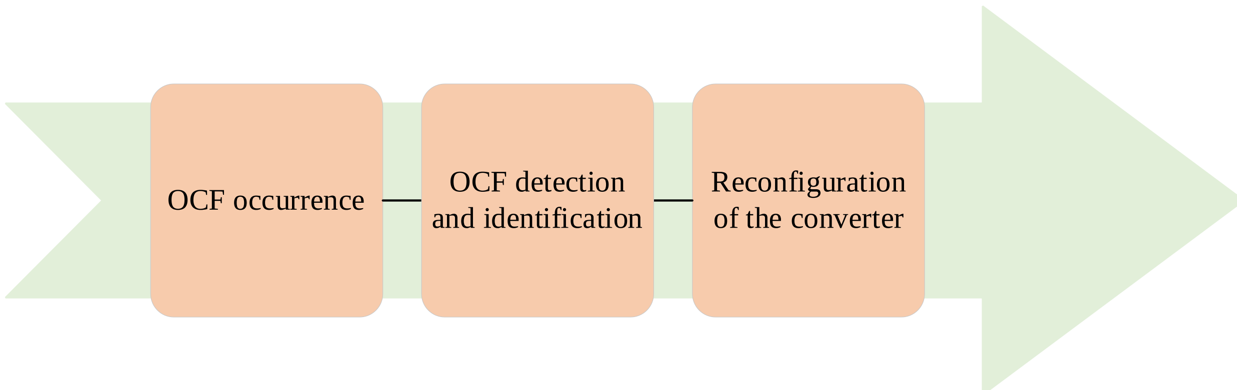

Figure 4. 12: Sequences of a system reconfiguration strategy after the occurrence of a fault.

By implementing fault-tolerant mechanisms such as redundant switches and reconfiguration strategies, PV systems can effectively mitigate the impact of OCFs, ensuring uninterrupted power generation and maximizing overall system efficiency. Thus, the importance of fault-tolerant control in addressing OCFs in boost converters within PV systems cannot be overstated, as it directly contributes to system reliability, resilience, and long-term sustainability. This part highlights the trade-off involved in implementing fault-tolerant designs, as they often add complexity and cost to the system, which can introduce new failure points. However, despite these challenges, fault-tolerant designs are crucial for applications where system reliability is paramount.

To ensure the continued operation of the system in the event of OCFs occurring in the boost converter switch, it becomes imperative to develop remedial measures. At this stage, two primary procedures are identified: isolation and reconfiguration of the PV system to address the faulty switch. The Fault Tolerant (FT) strategy, as outlined in this part, is depicted in Figure 4.13. This strategy aims to maintain system functionality despite the occurrence of faults.

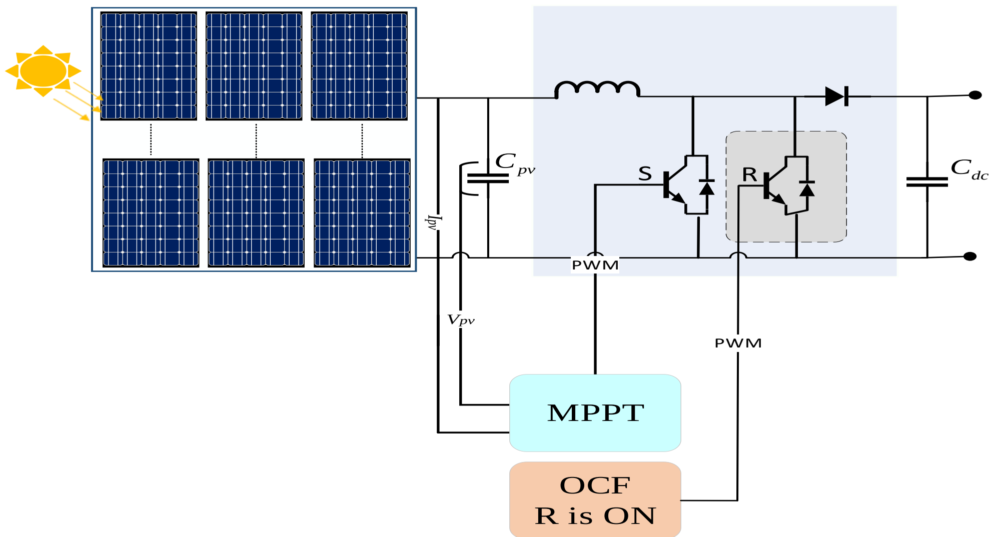

Figure 4. 13: Fault tolerant DC/DC boost converter topology.

In the event of an OCF occurrence in a PV system, a fault-tolerant mechanism is activated. Initially, the fault is detected, followed by the identification of the faulty component, typically the S switch. Upon detection, the redundant component, often denoted as the R switch, is activated to replace the faulty switch. This activation triggers a switching mechanism, physically disconnecting the faulty switch and connecting the redundant switch in its place.

4.8 Simulation results

In this section, the efficacy of the devised method for detecting OCF in power switches integrated within the DC/DC converter for PV system will be validated. This validation process will involve conducting numerical simulations utilizing MATLAB. We will use MATLAB to design simulations that replicate the system's behavior under fault scenarios. This will enable us to conduct a comprehensive evaluation of the effectiveness and reliability of our proposed detection method. Leveraging MATLAB's computational capabilities, we aim to assess the robustness of our detection technique in identifying and addressing OCF within the power switch in boost converter in grid connected PV system at different climatic conditions.

4.8.1 Primary FD algorithm results

Firstly, an OCF is induced in the power switch in the converter, to simulate an OCF is to disable the transistor entirely. This can be done by setting its control signal (gate voltage for a switch) to zero, effectively preventing current flow through the transistor.

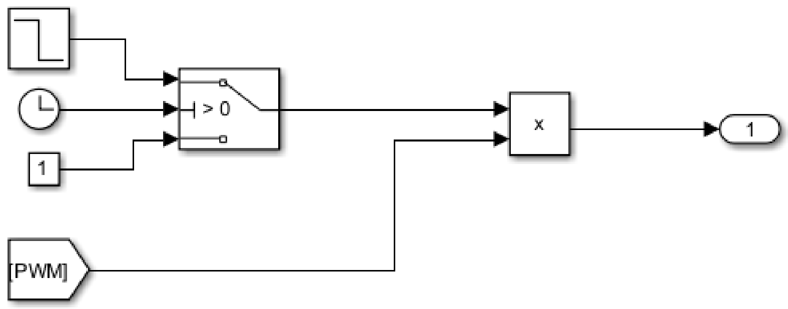

Figure 4. 14: Block of OCF.

The results of the simulation, as depicted in Figure 4.15, offer valuable insights into the efficacy of the fault detection algorithm, notably primary fault detection algorithm. At the precise moment t=0.8s, a switch fault occurrence of the open-circuit type is induced by setting the control command to "0." Prior to this fault event, the system exhibited correct functionality. Subsequently, the fault detection algorithm 1 effectively identified the fault after one switching cycle, showcasing its ability to swiftly and accurately detect faults.

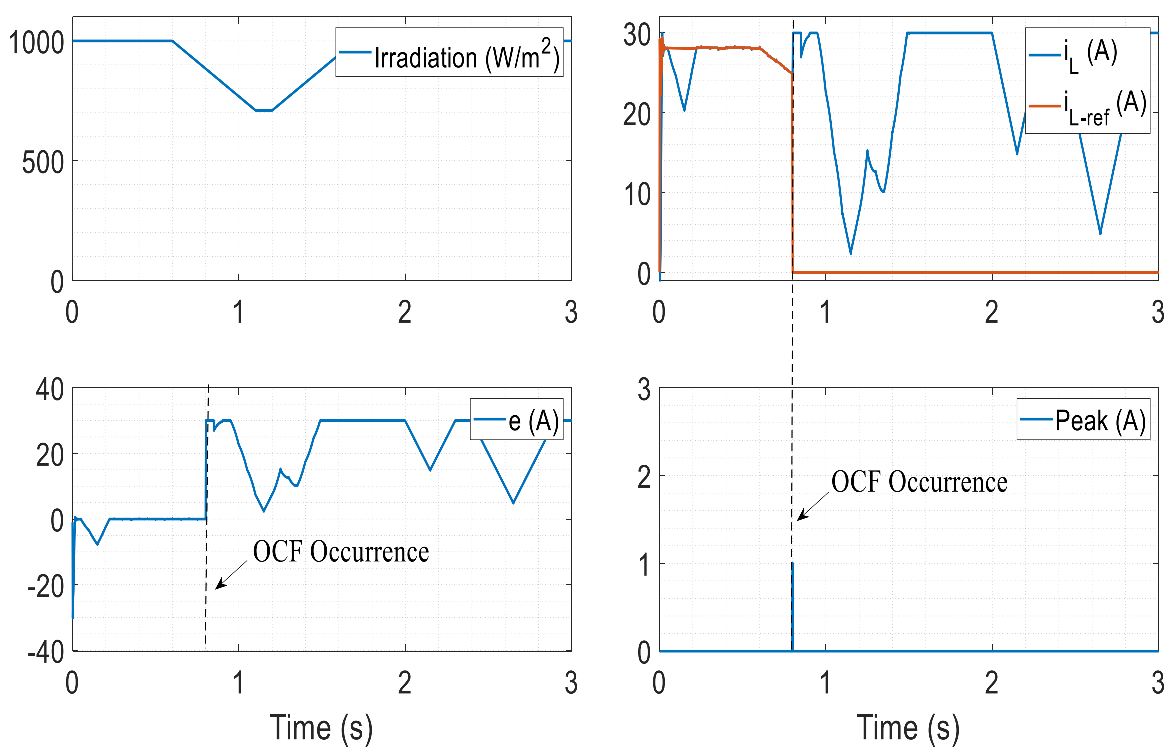

Figure 4. 15: OCF fault detection with primary algorithm.

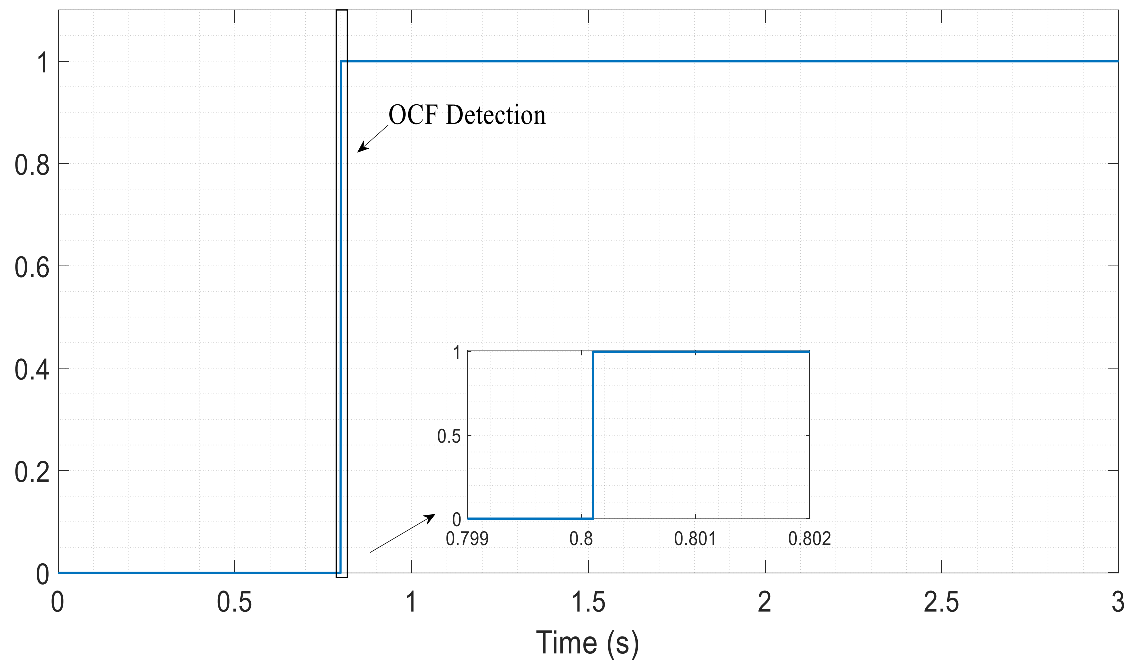

Figure 4. 16: OCF fault detection.

Upon simulating the diagnostic method and analyzing the results, we have observed significant deviation regarding fault detection in the boost converter system. The differentiation of the measured inductor current and the reference current induce a significant change in the error value from its previous value has proven to be an effective technique for detecting peaks and deviations in the error signal. Through this differentiation process, we can identify sudden changes in the error signal. The fault flag obtained in Figure 4.16 demonstrates the robustness of the fault detection method. The results from these simulations revealed that our fault detection mechanism effectively distinguished genuine OCF occurrences from false flags and able to detect OCF within one switching period.

4.8.2 Secondary FD algorithm results

The simulation results presented in Figure 4.17 present the efficacy of the fault detection approach in the context of a boost converter operating under CCM. OCF is introduced into the system at 0.8s while the control parameter is active. This fault event leads to a cessation in the increase of current, followed by a gradual decrease until it reaches null, as presented in Figure 4.17. Remarkably, this decrease stabilize after one switching cycle.

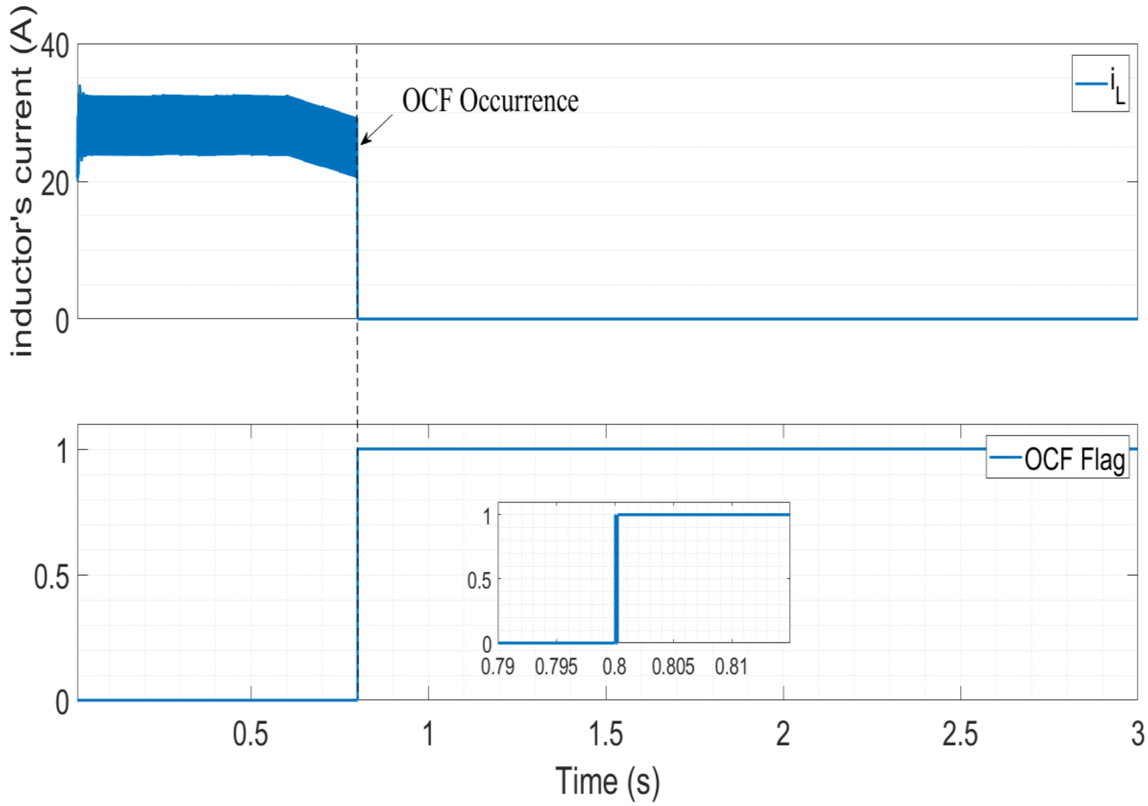

Figure 4. 17: OCF fault detection with Secondary algorithm.

4.8.3 Fault tolerant results

This part describes a simulation result at validating and evaluating the effectiveness of a FT topology in handling switch OCF. The system comprises switches controlled by signals "PWM" with u_s governing the main switch and u_R controlling the redundant switch. Subsequently, upon detecting a fault, the system proceeds to fault isolation, where the specific faulty switch is identified. The next phase is crucial may necessitate distinct isolation techniques and reconfiguration strategies. The reconfiguration process is implemented to replace the faulty component with a redundant switch, thereby restoring normal operation.

According to the results from Figure 4. 18 to 4. 20, electrical quantities exhibit disturbances at the moment of the OCF occurrence, which are completely mitigated by the reconfiguration system. We can observe in Figure 4.19 that the detection time is very short, thus enabling prompt fault isolation and reconfiguration of the converter with the redundant switch. Moreover, this quick reconfiguration time less than 0.0002s plays a vital role in maintaining system stability and functionality, minimizing downtime, and ensuring uninterrupted operation, particularly in critical applications where continuous performance is paramount.

Despite the occurrence of faults, the simulation results demonstrate that the system continues to operate normally following fault detection and reconfiguration. This resilience underscores the effectiveness of the FT topology in ensuring uninterrupted system performance even in the face of switch faults.

Figure 4.18 depicts the control of the redundant switch R. We observe that once the fault occurs at the boost converter, it quickly assumes the control command of the faulty switch.

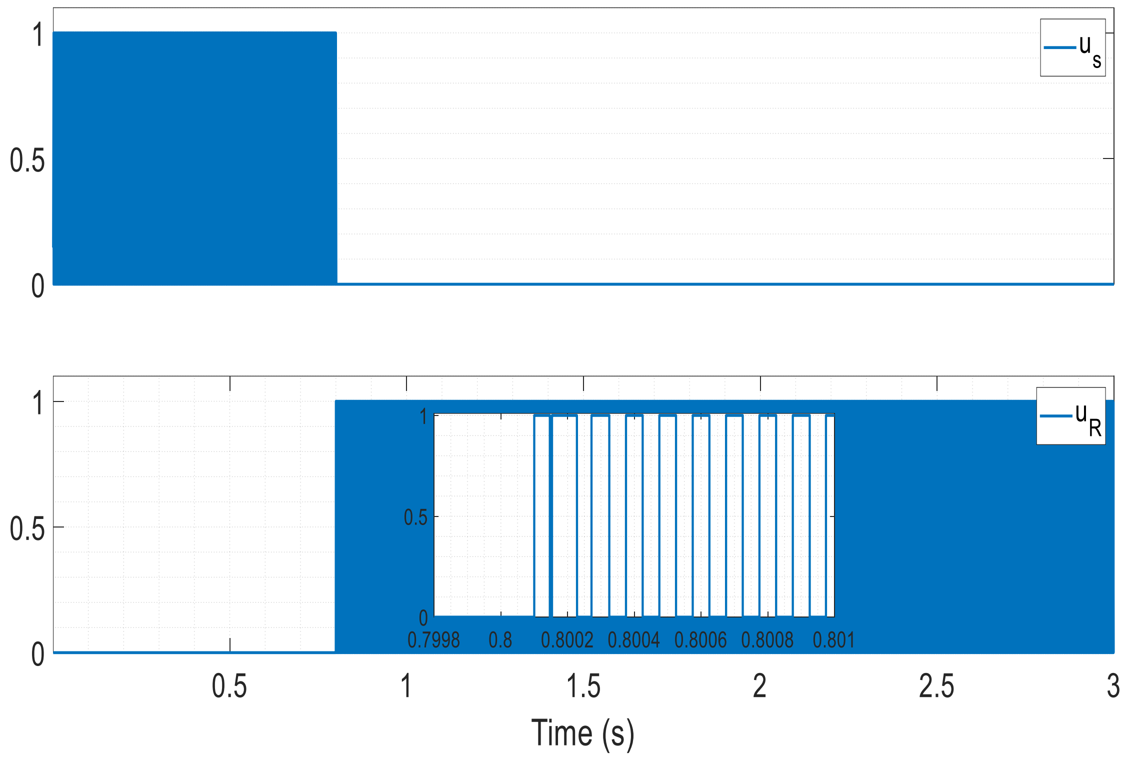

Figure 4. 18: The control signals of the faulty and redundant switch.

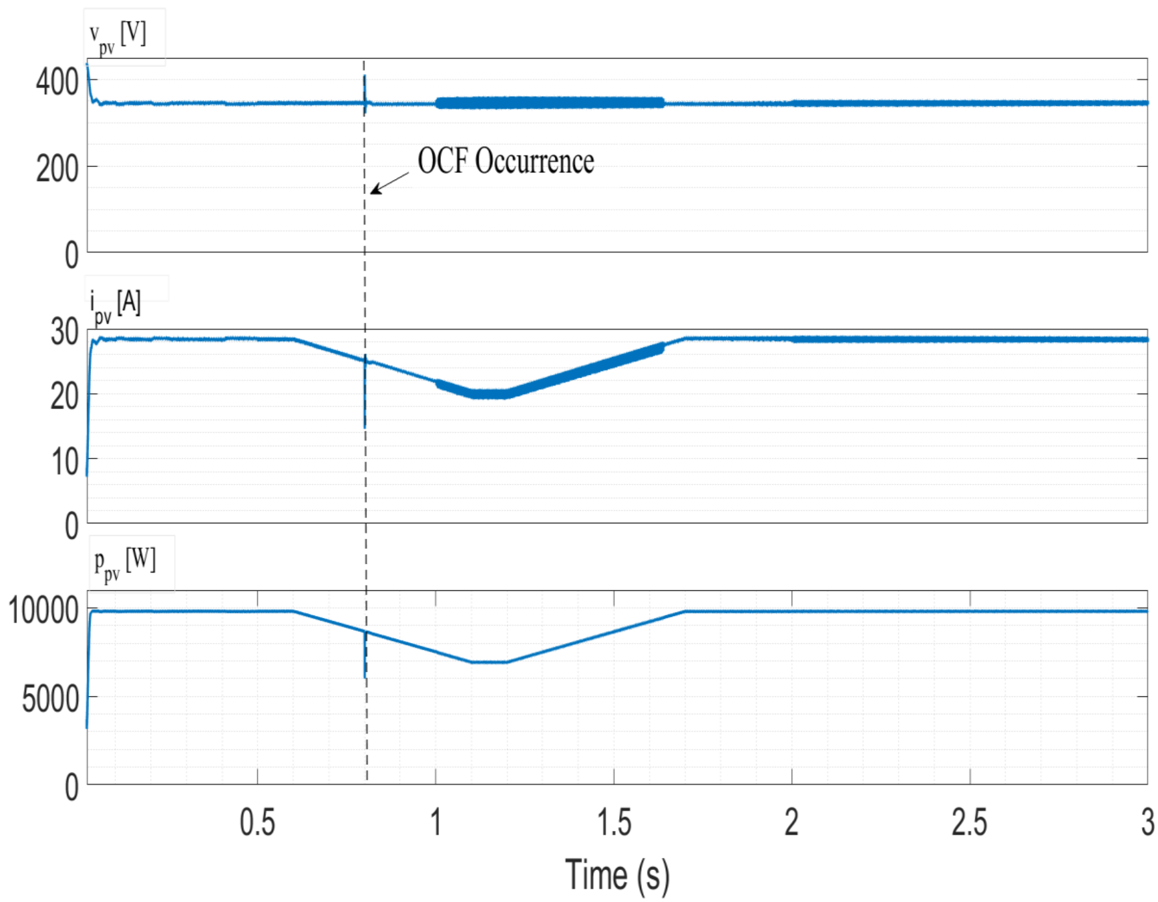

Figure 4. 19: Electrical characteristics of PV module under OCF reconfiguration.

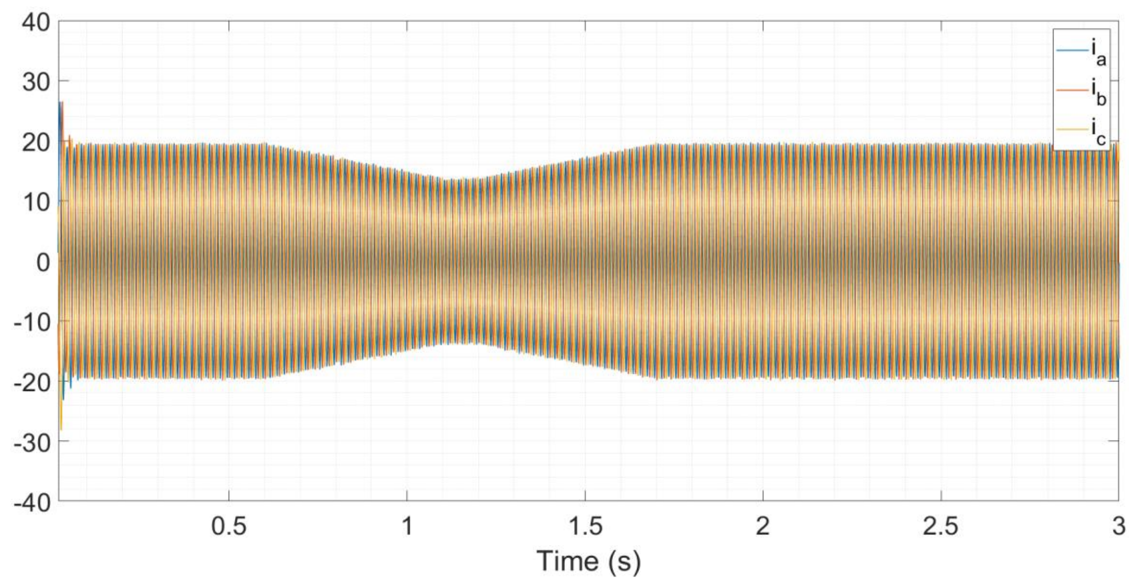

Figure 4. 20: Three phase currents while OCF occurrence and reconfiguration.

4.9 Conclusion

This chapter has delved into a comprehensive examination of fault diagnosis and fault-tolerant control methods within the boost converter of PV systems, with a primary focus on enhancing the reliability and functionality of renewable energy systems. Through a thorough analysis, two distinct algorithms have been developed and evaluated for detecting OCF within the boost converter. Algorithm 1, dedicated to analyze the reference error of inductor current, demonstrates a systematic approach in identifying deviations from the expected value of the error, thereby contributing significantly to fault detection efficacy. Conversely, Algorithm 2 monitors inductor currents, known for their sensitivity to fault-induced changes, providing a complementary perspective for fault detection. The proposed methodologies, integrating the strengths of both algorithms, presents a promising approach for enhancing fault detection and system reliability. Moreover, the integration of fault-tolerant control strategies, including redundant switches, ensures continuous system operation even in the presence of faults. The efficacy of these methodologies has been substantiated through rigorous simulation studies. Ultimately, this research contributes valuable insights into optimizing renewable energy systems, paving the way for enhanced reliability and efficiency in the field of renewable energy technology.

Chapter 5

Diagnosis of inverter in grid connected PV system

Diagnosis of inverter in grid connected PV system

5.1 Introduction

In grid-connected PV systems, the inverter plays a pivotal role in converting DC power generated by the solar panels into AC power for grid integration. However, faults in the power switches of the inverter pose significant challenges to system reliability and performance. Semiconductor power switches, integral to the inverter's operation, are particularly susceptible to faults, with OCFs and SCFs being primary concerns. OCFs, while not catastrophic, can degrade system efficiency by allowing the converter to continue operating with reduced performance. On the other hand, SCFs can lead to system shutdown, causing irreparable damage and necessitating costly repairs. These faults not only compromise system operation but also pose safety risks and can escalate into more severe issues if left undetected.

To address these challenges, research has been directed towards developing fault detection and diagnosis, thereby safeguarding system integrity and optimizing performance. In this chapter, we delve into the diagnosis of inverter faults within grid-connected PV systems, focusing particularly on OCFs. OCFs present significant challenges to system reliability and performance, potentially leading to efficiency degradation. To address these issues, we propose solutions aimed at both diagnosing OCFs and mitigating their consequences. Our study aims to develop robust fault detection methodologies specifically for OCFs in grid-connected PV system inverters. By using diagnostic variables and predefined thresholds, we seek to achieve timely and accurate detection of OCFs, thus enabling prompt intervention to prevent further damage and ensure system stability. Through our research, we seek to reinforce the importance of fault diagnosis and identification while highlighting the crucial role of thresholds in enabling effective fault detection and mitigation strategies. Our proposed approach involves implementing current limitation strategies aimed at swiftly reacting to fault conditions, thereby preventing overcurrent situations that could otherwise result in irreparable damage to system components. By limiting the flow of current during fault events, we aim to mitigate the impact of OCFs and safeguard the overall reliability of the PV system.

5.2 Impact of three phase inverter faults

The analysis of maintenance in PV systems provides valuable insights into the challenges and costs associated with system reliability. One significant finding is that PV inverters contributing to 37% of unscheduled maintenance events. Moreover, the Figure 5.1 shows that power inverter failures are responsible for a substantial portion, specifically 59%, of the total unplanned maintenance expenditure. This indicates that addressing issues related to power inverters, such as failures or malfunctions, constitutes a significant financial burden in PV system maintenance. Therefore, implementing proactive maintenance strategies for power inverters can help mitigate such unplanned costs and improve cost-effectiveness in the long term.

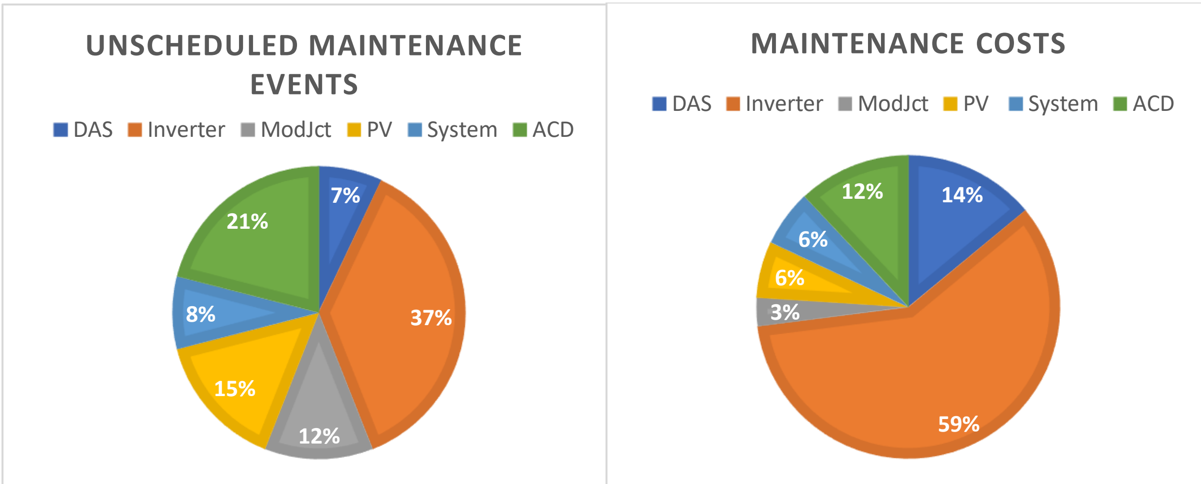

Figure 5. 1: Failures in commercial PV power plant (DAS: Data Acquisition System, ACD: ac disconnects, ModJct: Module Junction Box)

A thorough examination of the survey reveals indicates that semiconductor power devices found within power converters emerge as the most vulnerable elements, attributing to 31% of all converter failures. This highlights the pivotal importance of semiconductor reliability in the broader context of system performance and maintenance. Fault in power switches can be mainly classified into two main categories: Open or Short circuit faults. When these faults occur, they can significantly degrade the performance of VSIs. Therefore, it's essential to diagnose and address such faults promptly.

Extensive research in this field has focused on developing methods for diagnosing short-circuit and/or open-circuit faults in VSIs. SCFs are a major concern in electrical systems because they can happen suddenly and cause serious damage. These faults occur when there's a direct connection between points with different electrical levels, leading to a sudden increase in current flow. This abrupt occurrence of SCFs often results in a quick rise in current or voltage, which can be easily noticed by standard protective devices like fuses or relays. However, even though we can detect them, SCFs present significant challenges that require immediate action to avoid severe consequences. That's why special hardware circuits are carefully designed to quickly identify and address SCFs, minimizing further harm and ensuring system safety. In contrast to short-circuit faults, OCFs pose a different set of challenges in VSIs, although they don't immediately threaten system destruction. Various methods have been proposed to quickly identify and detect OCFs as they can significantly impact system reliability and performance. OCFs, which occur when there's a break in the electrical circuit, can lead to efficiency loss and, in severe cases, system shutdown if not addressed promptly.

Our research aims to thoroughly understand OCFs within the context of inverters, with the goal The detection and diagnosis of OCFs in VSIs hold significant importance in ensuring the reliability and safety of electrical system. Identifying and addressing OCFs promptly is crucial to prevent potential system shutdowns, minimize downtime, and avoid costly equipment damage.

By implementing effective fault detection and diagnosis strategies for OCFs, we can proactively safeguard the integrity and optimal functioning of grid-connected PV systems, contributing to the overall reliability and longevity of the system.

In the event of an OCF in the switch, specifically indicated by an open gate connection, distinct characteristics in line currents become apparent, since the faulty transistor cannot conduct any current, the line current can only be positive or negative, depending on which transistor is damaged. This leads to currents as shown in Figure 5.2. It is important to remark that all line currents contain a direct component, whereas currents in healthy condition do not. The occurrence of an OCF in the IGBT in the inverter leads to a loss of current reversibility within the IGBT. This issue becomes apparent in inverter mode through the absence of one phase current cycle, resulting in a unipolar and non-sinusoidal waveform. Consequently, if the upper IGBT of the inverter remains open it will loss of the positive half wave of the inverter phase current. Regarding the fault in the lower switch, it can lead to a loss of negative half-wave current. When the lower switch experiences an OCF, it disrupts the flow of current during the negative half-cycle of the AC output waveform. In the case of both switches in the same arm being open in the inverter, the corresponding phase current is zero throughout the operating period.

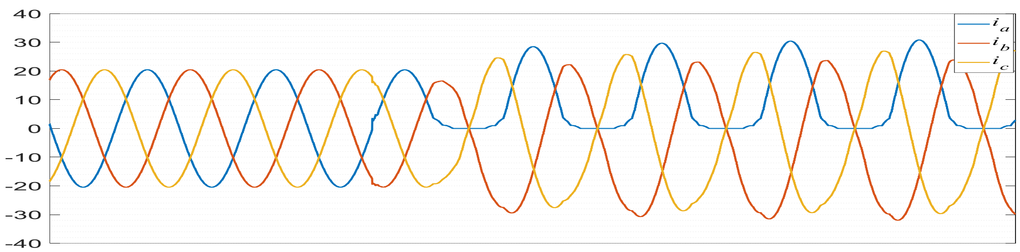

(a)

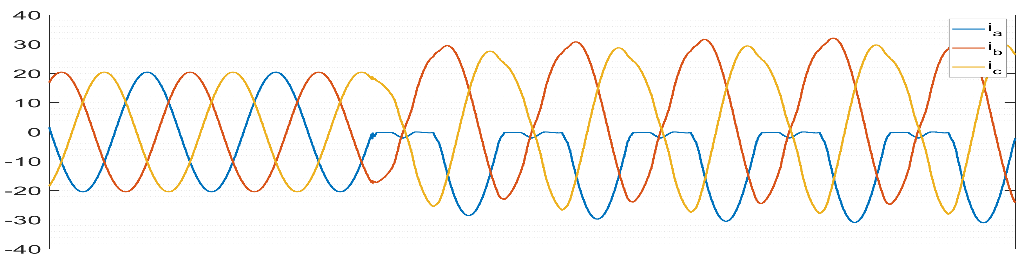

(b)

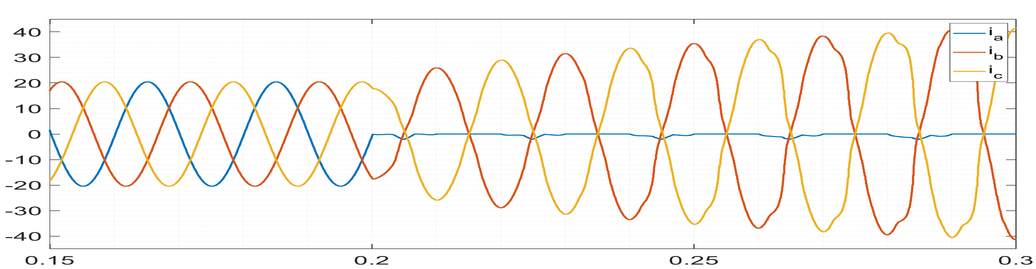

(c)

Figure 5. 2: Three phase currents under (a): upper switch OCF, (b): lower switch OCF, (c) Open phase.

An OCF in a grid-connected inverter can have significant implications for the performance and operation of a PV system. In a grid-connected PV system, the inverter plays a crucial role in converting the DC power generated by the PV array into AC power that can be fed into the electrical grid. When an open circuit fault occurs in single switch of the inverter, it essentially disrupts the connection between the PV array and the inverter. Simulating an OCF in an inverter in a grid-connected PV system can indeed lead to oscillations in voltage and current in the PV modules as well as the DC link voltage which is presented in Figure 5. 3:

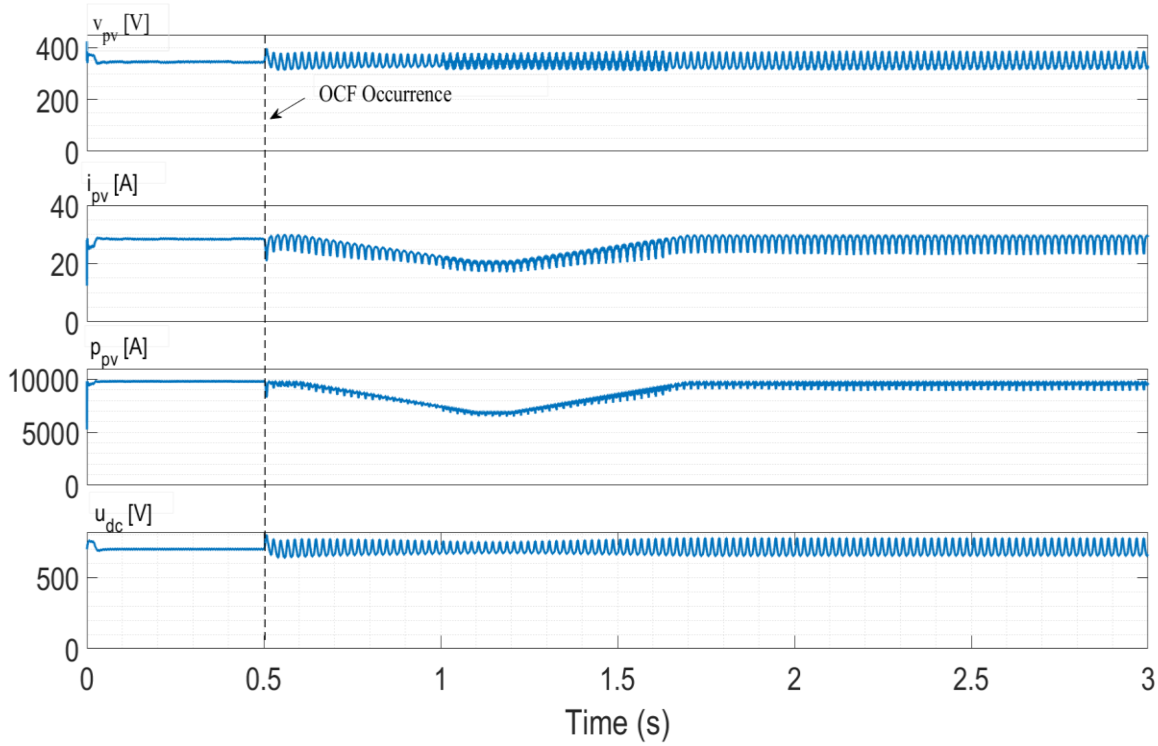

Figure 5. 3: Electrical characteristics of PV modules and DC link voltage in case of OCF in the inverter.

5.3 State of art of fault diagnosis method of inverters

Fault diagnosis in three-phase inverters is crucial for ensuring the reliable operation of power inverters. There are various methodologies for fault diagnosis, broadly categorized into model-based and signal-based approaches.

Model-based and signal-based methodologies can be categorized further into voltage-based or current-based algorithms. Within model-based fault diagnosis techniques, observers are essential for open-circuit fault detection. This process typically involves generating residuals, where some contributions focus on estimating motor or grid currents [4–9], while others concentrate on estimating converter output voltages [10–18].

In current-based algorithms, a residual is produced by comparing measured current with observed current. Various observer types have been proposed for this purpose, including state estimators [140], Luenberger observers [141], proportional integral PI observers [142], sliding mode observers [143], and Kalman filters [144]. In voltage-based approaches, to avoid the need for additional sensors, the residual is derived from comparing the estimated voltage with the reference voltage obtained from feedback control. State estimators are commonly employed for this purpose [145], although PI and model reference adaptive system observers have also been suggested in [146] and [147], respectively. While model-based algorithms offer robustness and fast fault detection, they come with notable drawbacks. They are computationally intensive, requiring meticulous tuning efforts for observer parameter design, and they necessitate prior knowledge of machine parameters.

Signal-based fault diagnosis methods in the context of three-phase inverters can be broadly classified into two primary categories: current-based and voltage-based methods, the main advantage of this approach is that it is free from system's model knowledge. Current-based diagnostic methods constitute a significant area of research, employing various techniques These methods usually detect OC faults directly via three-phase currents, i_q/i_d, i_α/i_β or bus currents.

Current-based methods harness existing current sensors within the system to analyze distorted currents, providing a direct means of fault detection. These methods encompass a range of techniques, including current vector analysis in Park coordinates [148], analysis of the DC component of load currents [149], current reference errors [150] , space trajectory analysis [151] and root mean square analysis [152]. Normalization appears as a solution for load currents changing and made the diagnosis method suitable for standardizing signals across various operating conditions. Despite their efficacy in leveraging readily available data, current-based methods face limitations in forming a unified diagnostic architecture across different converter topologies. In voltage-based methods with extra measurement circuits, voltage-based fault diagnosis methods for three-phase inverters rely on the analysis of various voltage signals as highlighted in literature including pole to pole voltages proposed in [153], phase voltages [154], and turn on gate voltages [155]. Compared with the current-based method, these methods possess fast diagnosis speed. But extra measurement circuits are required, which increases the system's cost and complexity.

In recent years, there has been a notable shift towards frequency domain signal processing approaches in fault diagnosis, particularly in the context of open-circuit fault detection in VSIs. These approaches leverage techniques such as FFT to extract fault signatures from measured signals, as demonstrated in references [156]. For instance, authors in [157] used empirical mode decomposition, SVM, and PCA to achieve better diagnostic performance for three-level inverters. An improved version of EMD called complete ensemble EMD with adaptive noise is presented in [158] to identify the instantaneous frequency of the IGBT open-circuit fault. Authors in [159] exploited the local mean decomposition algorithm and correlation coefficients to diagnose the open-circuit fault of PWM inverters. In parallel, AI techniques have emerged as powerful tools for fault classification and diagnosis in VSIs. Neural networks and fuzzy logic, in particular, have been successfully applied as fault classifiers in open-circuit VSI fault detection, as demonstrated in references [160,161]. For instance in [161] the authors combine using the average

values of positive and the negative parts of the normalized output currents with fuzzy logic approaches to identify faulty power switches, enabling the detection and localization of both single and multiple faults. Also in [160] an ANN and the extraction of features corresponding to the open circuit fault of the IGBT switch. This approach is based on the Clarke transformation of the three-phase currents of the inverter output as well as the calculation of the average value of these currents to determine the exact angle of the open circuit fault. However, despite their effectiveness, AI-based methods often come with computational demands that increase detection time and complexity, posing challenges for real-time implementation. Nonetheless, the integration of AI techniques into fault diagnosis frameworks showcases the potential of intelligent algorithms to enhance fault detection capabilities in VSIs, offering sophisticated solutions for reliable and efficient fault diagnosis in power electronic systems.

5.4 Diagnosis of three phase inverter

Our system, constituting the process under surveillance, is depicted in a simplified diagram shown in Figure 5.4. It consists of a control block, and a three-phase static converter. This converter comprises a three-armed inverter, with each arm composed of two transistors (S_i, S_{i+1}) in parallel with freewheeling diodes (D), forming controllable switching cells for opening and closing.

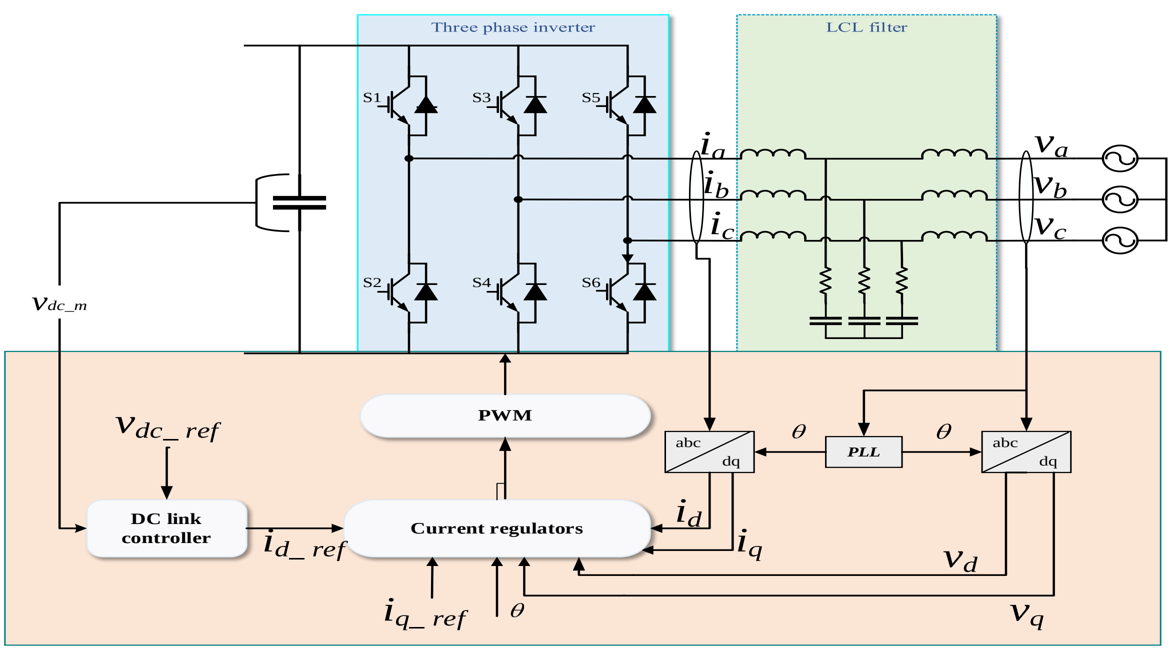

Figure 5. 4: Grid connected three phase inverter.

5.4.1 Description of the diagnosis method

This section presents a diagnosis approach for single and multiple OCFs in a three-phase inverter based on symmetrical and DC components. The magnitude ratio of the negative sequence to the positive sequence of phase currents is created as a fault detection measure to assess the asymmetry and distinguish the open fault types. Then, single faults are located using the DC components of the phase currents.

5.4.1.1 Diagnosis variables

In a three-phase inverter, open circuit faults can lead to imbalances in the system. By utilizing Symmetrical components analysis allows for the detection of the unbalanced conditions caused by the fault which becomes easier to identify the presence of an open circuit fault. By examining the magnitudes of the symmetrical components, it becomes possible to determine the affected phase or location of the fault.

Positive, negative and zero sequence refer to the symmetrical components of a three-phase system.

- ✓ Positive sequence: The positive sequence is a symmetrical component of a three-phase system in which the three phases have the same order of rotation. The voltages and currents of the three phases are in phase with each other and have equal amplitudes. This sequence represents normal, balanced operation of the three-phase system. It is used as a reference for assessing imbalances and variations from the nominal state.

- ✓ Negative sequence: The negative sequence is also a symmetrical component of a three-phase system, but in this case the phases have a reverse order of rotation. As a result, phase voltages and currents have equal amplitudes, but are 120° degrees out of phase with each other, in the opposite direction to the positive sequence.

- ✓ Zero sequence: It represents three equal phasors with zero-degree phase displacement.

The symmetrical components extraction is shown in Figure 5. 5.

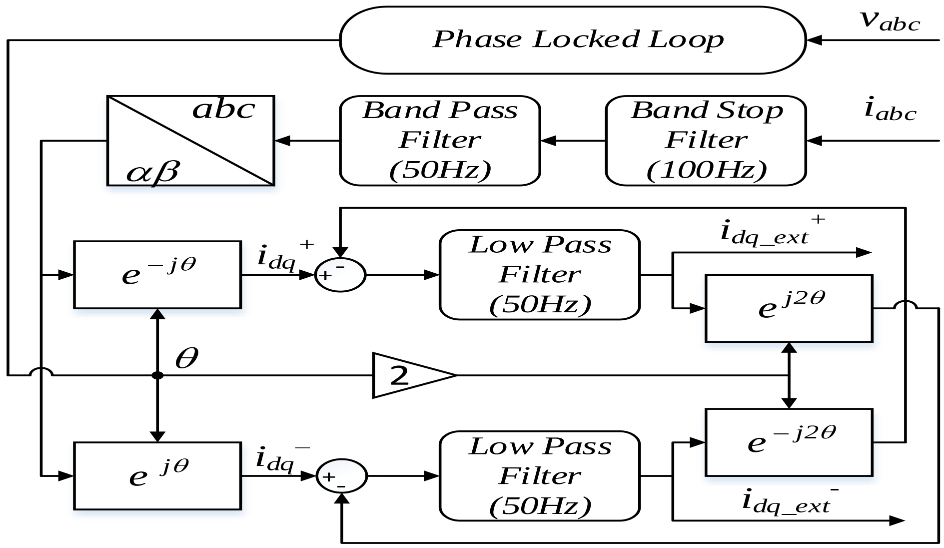

Figure 5. 5: Block diagram of the symmetrical components extraction.

From the extraction of the symmetrical components above. The amplitude and the angle of positive and negative sequence respectively can be expressed in the equations below:

$$m_p = \sqrt{(i_{d\_ext}^{+})^2 + (i_{q\_ext}^{+})^2} \tag{5.1}$$

$$m_n = \sqrt{(i_{d\_ext}^{-})^2 + (i_{q\_ext}^{-})^2} \tag{5.2}$$

$$\varphi_p = \tan^{-1}(i_{q\_ext}^{+} / i_{d\_ext}^{+}) \tag{5.3}$$

$$\varphi_n = \tan^{-1}(i_{q\_ext}^{-} / i_{d\_ext}^{-}) \tag{5.4}$$

5.4.1.2 Fault detection of OCF

The proposed approach for OCF detection focuses on using current measurements for fault detection in three phase inverter system, employing symmetrical components, which allow for the extraction of diagnostic variables. Symmetrical components are crucial tool in detecting faults. During normal operation, the negative sequence component typically maintains a small amplitude, while the positive sequence remains relatively constant. However, in the event of an OCF, the negative sequence amplitude experiences a significant increase, serving as a crucial diagnostic indicator [162].

To further enhance fault detection, a diagnostic variable denoted as "R" is introduced, representing the ratio between the negative sequence amplitude (m_n) and the positive sequence amplitude (m_p). Mathematically, R is expressed as the following equation:

$$R = m_n / m_p \tag{5.5}$$

This variable R serves as a key metric in assessing the balance of the system and detecting deviations indicative of faults. Threshold-based fault detection is employed, where R is compared to a predefined threshold value (denoted as th_1). Under normal conditions, R remains close to zero, indicating a balanced system. However, when IGBT open-circuit faults occur, R deviates from zero due to imbalanced phase currents. If R surpasses the threshold value th_1, set at 0.15 in this case, it signifies the presence of an OCF within the inverter system. This approach enables rapid and reliable fault detection, ensuring the integrity and performance of the inverter system [162].

$$\begin{cases} No\,fault & R < th_1 \\ Fault & R \geq th_1 \end{cases} \tag{5.6}$$

The fault diagnosis technique proposed in Figure 5.6, for grid-connected inverters involves two main steps. Initially, it focuses on detecting open-circuit faults within the switches by analyzing the sensed phase currents. Subsequently, the method proceeds to localize faulty IGBTs, identifying both leg open-circuit and single IGBT faults through symmetrical components analysis.

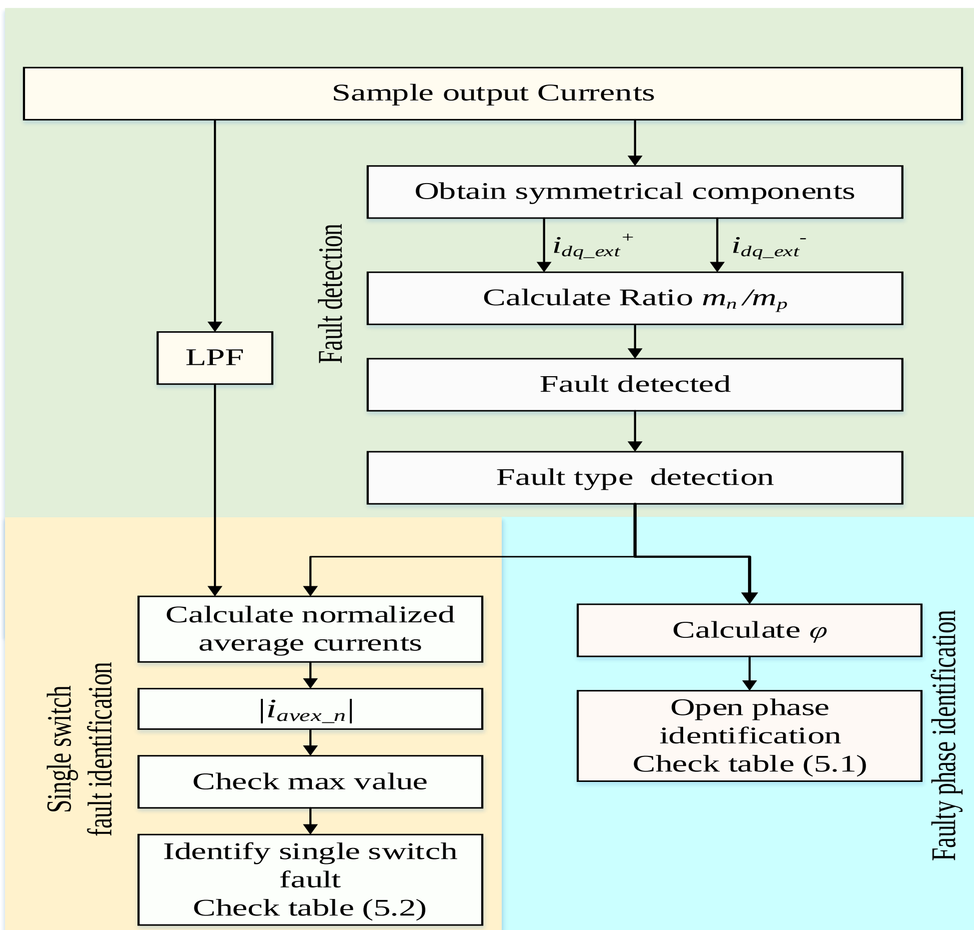

Figure 5. 6: Principle fault detection and diagnosis.

5.4.1.2.1 Localization of Faulty IGBTs

The study examines two groups of failures based on their location and the number of defective devices:

- ✓ Single OCFs
- ✓ Multiple OCFs in one leg.

The multiple scenarios of open circuit faults can be accurately determined according to the ratio of the negative to the positive amplitude, by selecting two different threshold values th_1 and th_2. If the ratio exceeds th_1 and have a stable value under th_2 it will indicate single switch fault, otherwise when the ratio exceeds the second threshold th_2 it will simply indicate presence of open phase in the three-phase inverter.

- Open phase faulty

An open-phase fault refers to the disconnection of one of the phases from the inverter circuit. This occurrence disrupts the balance in the three-phase system, leading to distinct fault characteristics. In the event of an open-phase fault, the negative component, becomes significantly elevated compared to a single switch fault. The heightened negative component is a result of the imbalanced phase currents induced by the open-phase condition. This distinguishing feature allows for the effective differentiation between an open-phase fault and a single switch fault.

The Open phase scenarios can be accurately determined according to the ratio of the negative to the positive amplitude, by selecting two different threshold values th_1 and th_2. If the ratio exceeds the second higher threshold th_2, a clear indication of the presence of an open phase in the three-phase inverter is established, Indeed the identification of precise faulty phase is further refined through an analysis of the sum of the positive and negative angle, where different value of the sum refers to precise open phase, which is calculated in (5.7).

$$\varphi = \varphi_p + \varphi_n \tag{5.7}$$

Faulty Phase	Ratio m_n/m_p	Sum of angle	Open Phase Flag		
			P_A	P_B	P_C
Phase A	>0.7=th_2	±180°	1	0	0
Phase B		60°	0	1	0
Phase C		-60°	0	0	1

Table 5. 1: Open phase detection and localization.

- Single switch fault identification

The fault identification method for a single switch in the grid-connected inverter follows a systematic two-step process. Conversely to open phase fault in this scenario where the ratio falls between the lower threshold th_1 and the higher threshold th_2, the methodology signals the potential occurrence of a single fault. This dual-threshold strategy provides a distinct range within which the system recognizes the single fault. However, it is difficult to distinguish in the case of single fault whether the fault is in the upper arm or lower arm of the phase with the ratio and the angle only. Thus, the normalized DC component is also used as diagnosis variable in the proposed method, for accurately identifying the precise location of faults within the system. Equation (5.8) describes the calculation process for the DC component. This component is pivotal in understanding the overall behavior of the system, particularly during fault conditions.

$$\langle i_x \rangle = \frac{1}{T}\int_{t-T}^{t} i_x(\tau)\,d\tau \tag{5.8}$$

Normalization is crucial for ensuring the diagnostic approach remains adaptable across diverse operating conditions, which may vary in terms of power values. Equation (5.9) provides a detailed procedure for calculating this diagnostic variable, accomplished by dividing the DC component by the magnitude of the current Park's vector. Through normalization of the DC component, the fault diagnosis method can effectively accommodate fluctuations in operating conditions, thereby improving the accuracy of fault identification and localization.

$$i_{avex,n} = \left. \langle i_x \rangle \middle/ \left| \sqrt{(i_{d\_ref})^2 + (i_{q\_ref})^2} \right| \right. \tag{5.9}$$

The use of low-pass filters (LPF) is essential to mitigate the impact of high-frequency noise in the phase currents. In this implementation, the LPF is characterized as second-order filter with a designated cutoff frequency of 70 Hz. The diagnosis variables of the three-phase inverter under single switch fault operations are summarized in Table 5.2.

Faulty Switch	Ratio of m_n/m_p	Absolute normalized DC components	Normalized DC components	Single fault flag		
				F_A	F_B	F_C
S1	$\in [th_1, th_2]$	Max= $\lvert i_{aveA,n}\rvert$	<-0.05	1	0	0
S2			>0.05	-1	0	0
S3		Max= $\lvert i_{aveB,n}\rvert$	<-0.05	0	1	0
S4			>0.05	0	-1	0
S5		Max= $\lvert i_{aveC,n}\rvert$	<-0.05	0	0	1
S6			>0.05	0	0	-1

Table 5. 2: Open single fault identification and localization.

$$F_x = \begin{cases} 1 & \Leftarrow i_{avex,n} < -0.05 \\ -1 & \Leftarrow i_{avex,n} > 0.05 \end{cases} \tag{5.10}$$

The block diagram summarizes the proposed diagnostic algorithm in Figure 5.7.

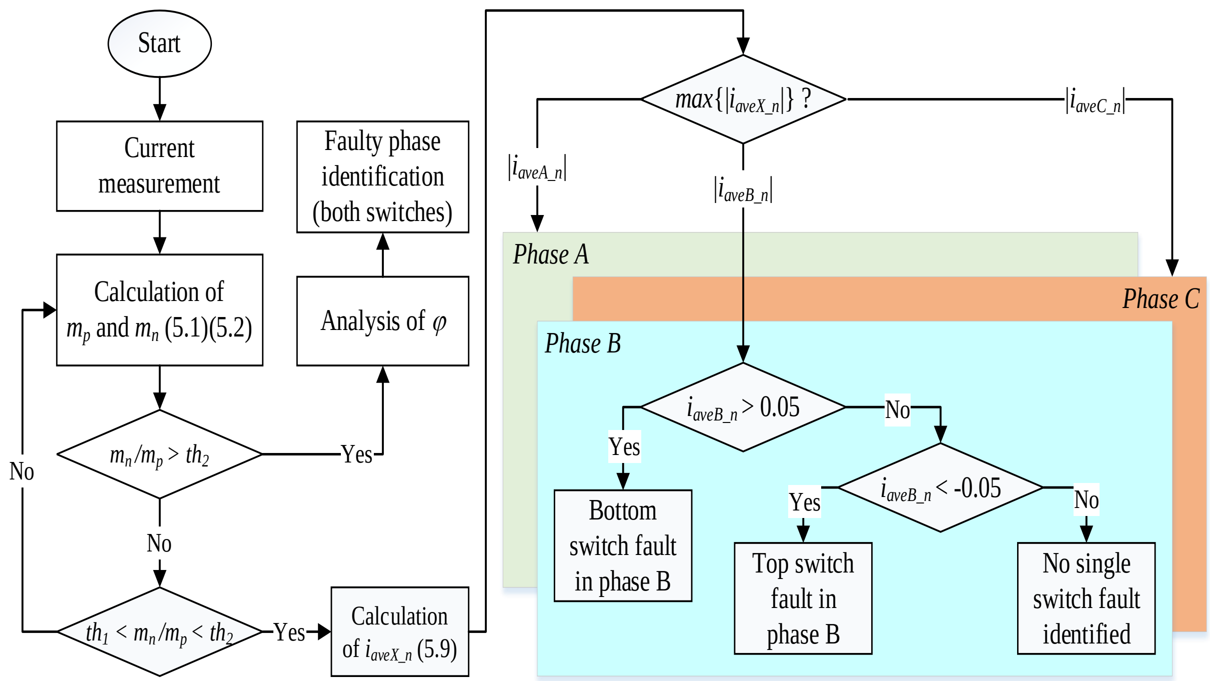

Figure 5. 7: Flowchart of the diagnosis approach algorithm.

Throughout this fault diagnosis process, multiple thresholds are employed to differentiate between open-phase and switch faults, ensuring accurate fault detection. By integrating symmetrical components analysis with normalized average currents, the fault diagnosis method systematically identifies and locates faulty components within the inverter. This systematic and effective approach is essential for maintaining system reliability, as it enables timely identification and resolution of faults, thereby minimizing downtime and ensuring continued operation.

5.4.3 Simulation of grid connected inverter with the diagnosis of OCF

In order to develop the fault diagnosis method for OCF in grid connected inverter, it is very important to study its behavior in degraded mode and to highlight the points of difference from the healthy mode. To verify the performance of the diagnosis approach, simulation tests are carried out in MATLAB/Simulink. The grid connected inverter model and two-loop control are implemented. We present the simulation results obtained in the case of healthy operation of the grid connected inverter under varying irradiation conditions.

5.4.3.1 *Case of single switch fault*

The effectiveness of the approach developed for the detection of power switches included into the three- phase inverter for the grid connected application is validated in this part. As a result, a single open-circuit fault was generated in simulation by setting the power switch S_1 signal control to 0. The simulation results obtained are shown in Figure 5.8.

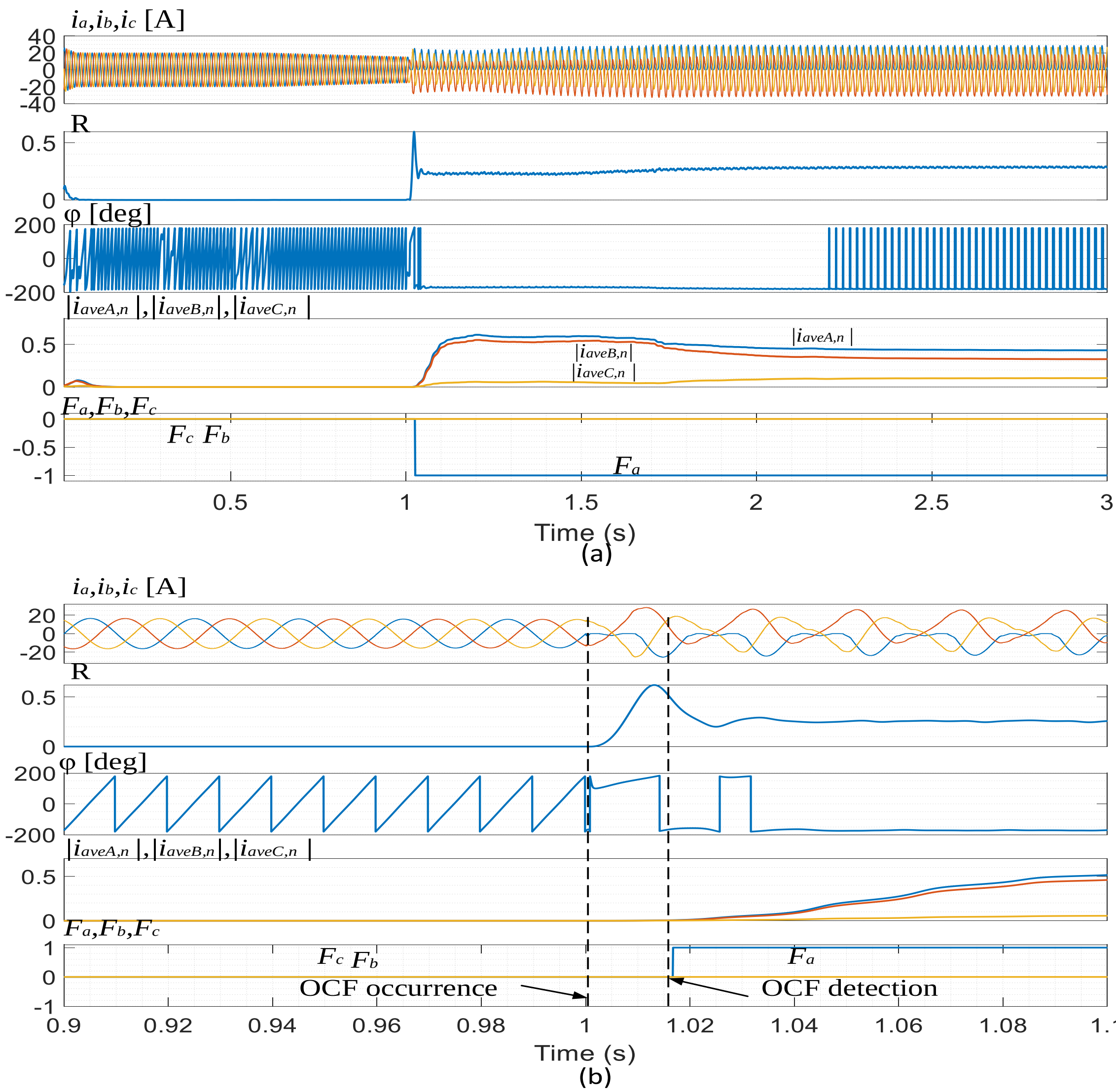

Figure 5. 8: (a): OCF S_1 identification, (b): Zoom of OCF S_1 identification.

Figure 5.8 show the measured currents and the diagnosis variables when a simple IGBT opening fault occurs. The fault is applied to S_1 at time t=1s. Under fault mode operating, the impact of a fault on the measured currents results in the loss of the positive current wave of the faulty phase i_a. Based on the proposed diagnosis method the difference between the healthy state and the faulty operation lies into the increase of the ratio of symmetrical components, which is in the range of [th_1, th_2], based on the proposed algorithm. This simply indicate the presence of single switch fault. After the single switch fault identification, it can be seen in Figure 5.8 the fault in S_1 is accurately localized because the $\left|i_{aveA,n}\right|$ takes the maximum value and the currents' average value $i_{aveA,n}$ takes negative values. the faulty switch S_1 is correctly located within 17.5 ms.

When an open-circuit fault in IGBT S_2 is applied at the instant t = 1 s, the negative half-cycle of the current i_a is eliminated. Consequently, the diagnostic variable R increases immediately to converge approximately to near 0.32, exceeding the threshold th_1. As a result, the detection of single switch fault. Regarding the normalized currents average values that are used as identification for single switch fault. Following the identification of a single switch fault, the fault in transistor T_2 is precisely localized, as depicted in Figure 5.9. This localization is confirmed by the polarity of DC component. The faulty switch T_2 is accurately identified within a timeframe less than 20 milliseconds.

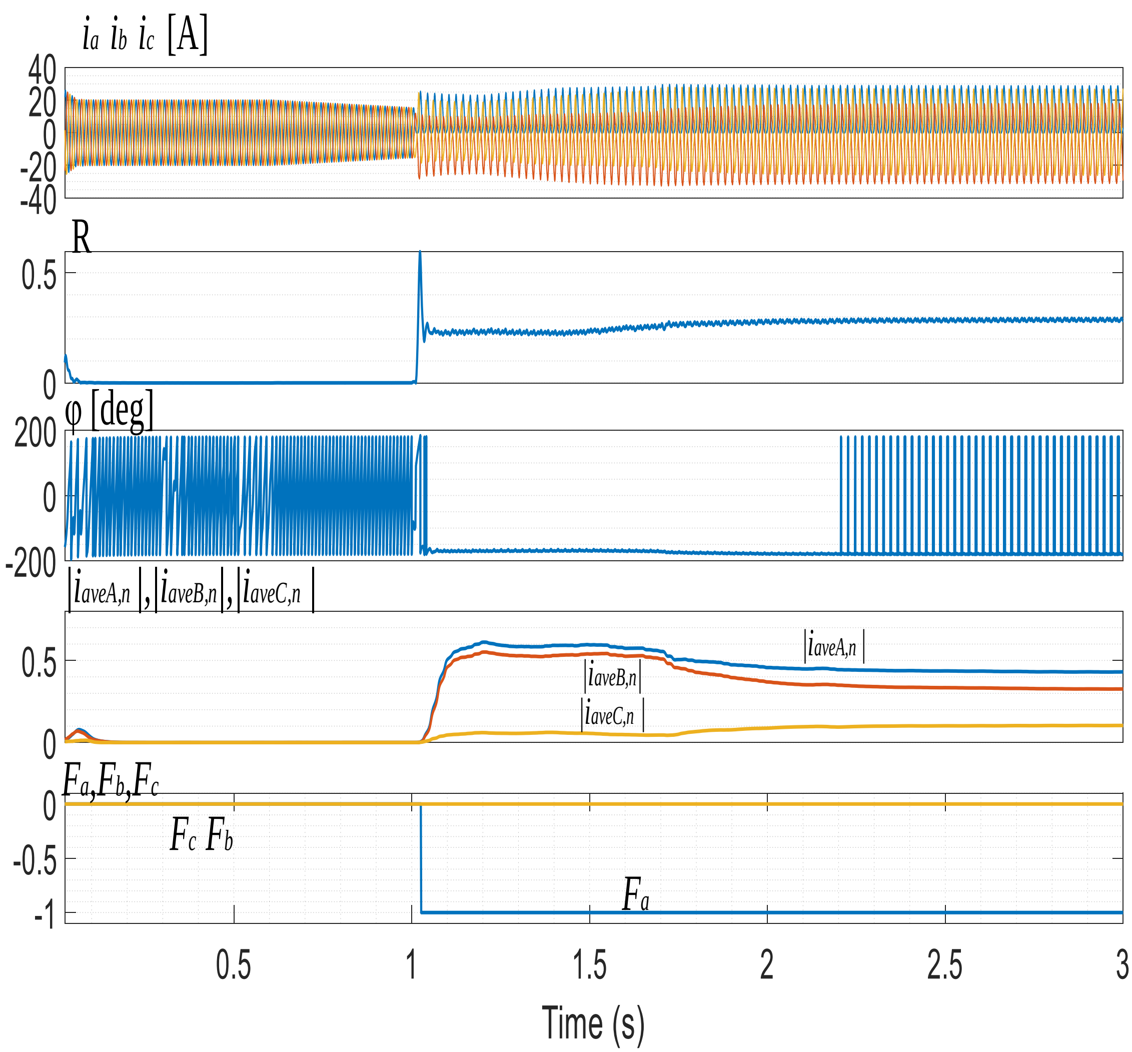

Figure 5. 9: OCF S_2 identification.

5.4.3.2 Case of open phase fault

The first leg of the inverter experiences an open-phase failure at time t = 0.5s when S_3 and S_4 are open circuited. Figure 5.10 show the simulation results of the three phase currents and the diagnostic variables.

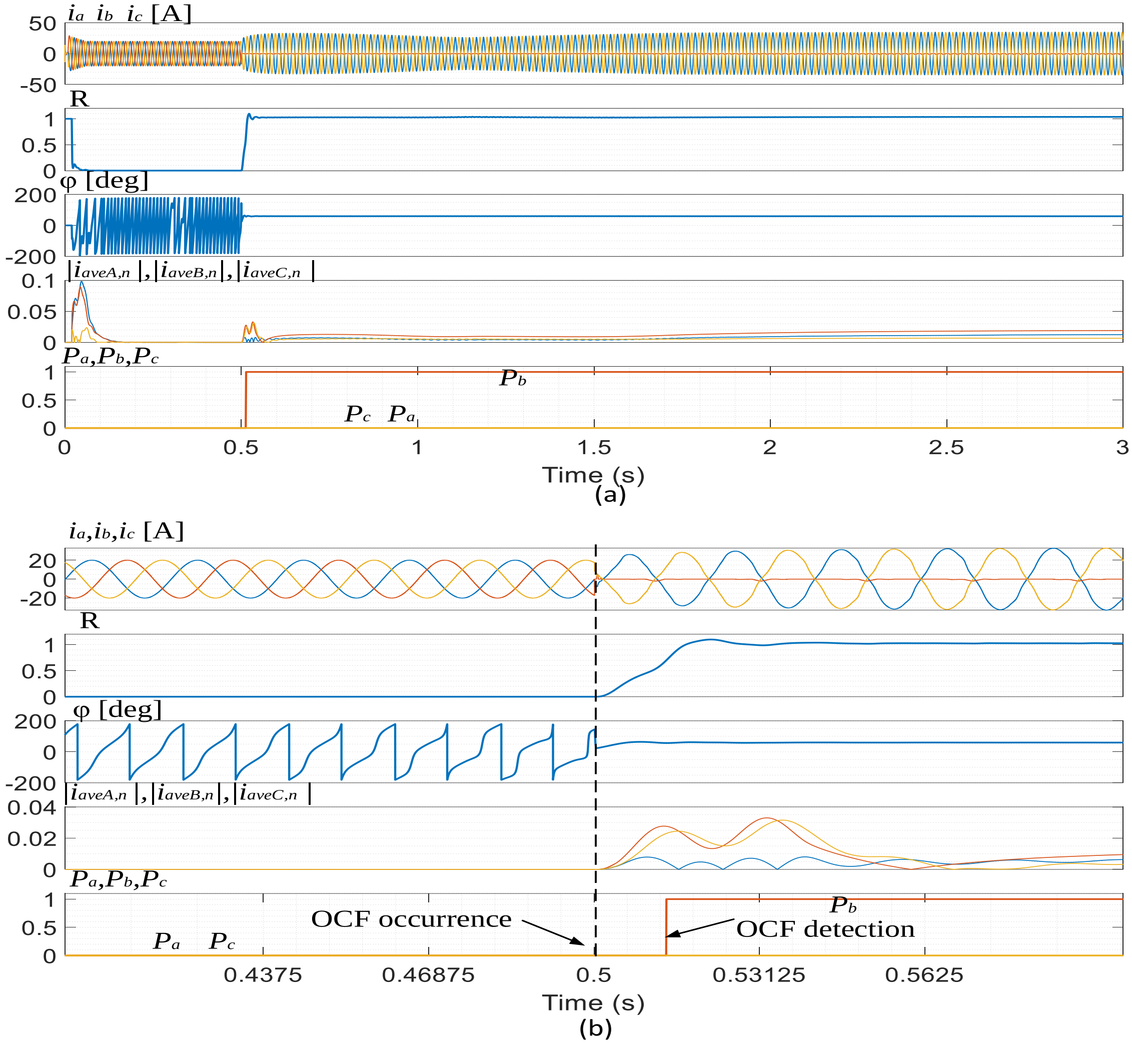

Figure 5. 10: (a): Open phase B identification, (b): Zoom of Open phase B identification.

Figure 5.10 represent the simulation results of fault diagnosis in the occurrence of simultaneous open-circuit faults on the leg b's upper switch S_3 and lower switch S_4. As a result, the current i_b is equal to zero and the currents waveforms distortion increases. Consequently, the ratio R rises above th_2 to detect the open phase. The analysis of φ is required to locate the exactly faulty phase. As it shown in Figure 5.10 the value of φ is 60°, based on Table 5.1. It clarifies presence of open phase in leg B. When the associated fault diagnosis flag leg B changes from 0 to 1. 12.5 ms after the open phase occurs, which corresponds approximately to a half of the current fundamental period, the open-phase fault has been identified.

The simulation results reveal a crucial approach to identifying the precise location of open phases within the grid-connected inverter. The fault has introduced in both phase arms A (S_1 and S_2) and C (S_5 and S_6) occurred at 1s, through the initial detection phase, the ratio of positive to negative components increase above the value of th_2, effectively selecting the presence of an open phase.

However, upon progressing to the identification step, where the specific faulty phase must be determined, the simulation presents distinct challenges. With multiple simulated instances of open phases across different phases, the analysis confronts the need to differentiate between these scenarios accurately. This phase identification process relies heavily on analyzing the values of associated angles. The simulation demonstrates the results of the approach aimed at achieving precise fault localization within the inverter system. Through rigorous analysis and interpretation of simulation results. In our simulation study on OCFs in grid-connected inverters, we observe distinct angular values for fault identification. A faulty phase A consistently shows an angle of 180 degrees, while an open phase C registers at -60 degrees. These findings highlight the precision of fault localization techniques, advancing our understanding of inverter reliability and performance optimization.

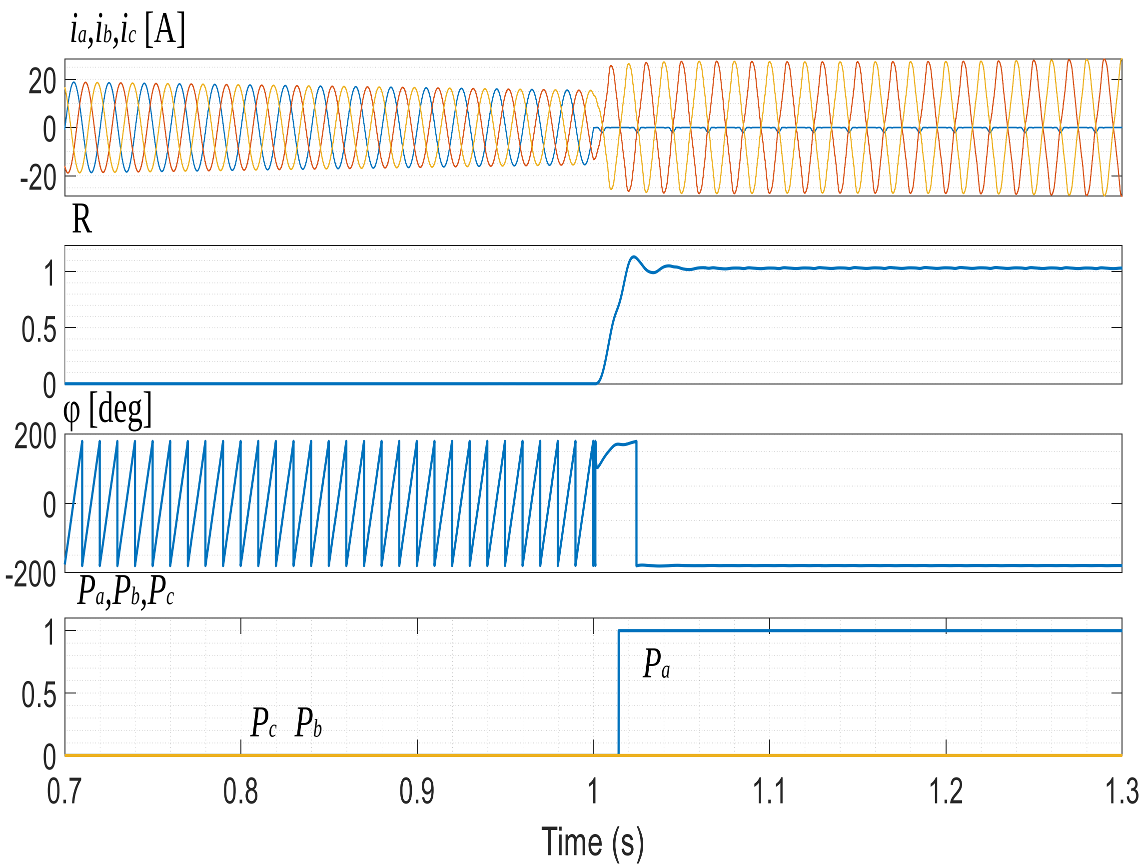

Figure 5. 11: Open phase A identification.

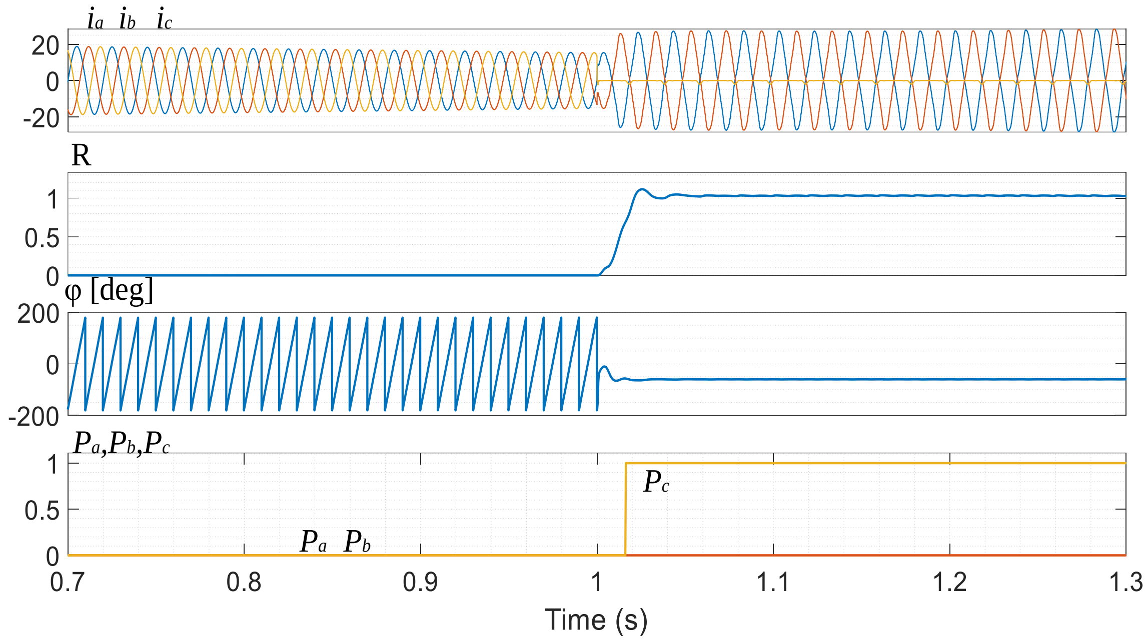

Figure 5. 12: Open phase C identification.

To further investigate the effectiveness of the proposed approach against current variations and exactly low currents. The test with low current 10% of the rated current is performed to evaluate the robustness of the proposed diagnosis method. Figure 5.13 presents the simulation waveforms of the three phase currents and the diagnostic variables under open phase operation with low current. Similar to the previous test an open fault occurs in S_1 and S_2 (open phase A). It is noticeable that the fault detection method also guarantees the desired robustness. While the localization variables reach R the threshold value th_2, and prevent the generation of any false alarm. The whole diagnosis process takes 10ms, which is equivalent to 50% of the phase-current fundamental period.

In open phase operation with low current, Figure 5.13 shows the simulated waveforms for the three phase currents and the diagnostic variables for an open fault (open phase A) occurs at t=1s which is similar to the previous test.

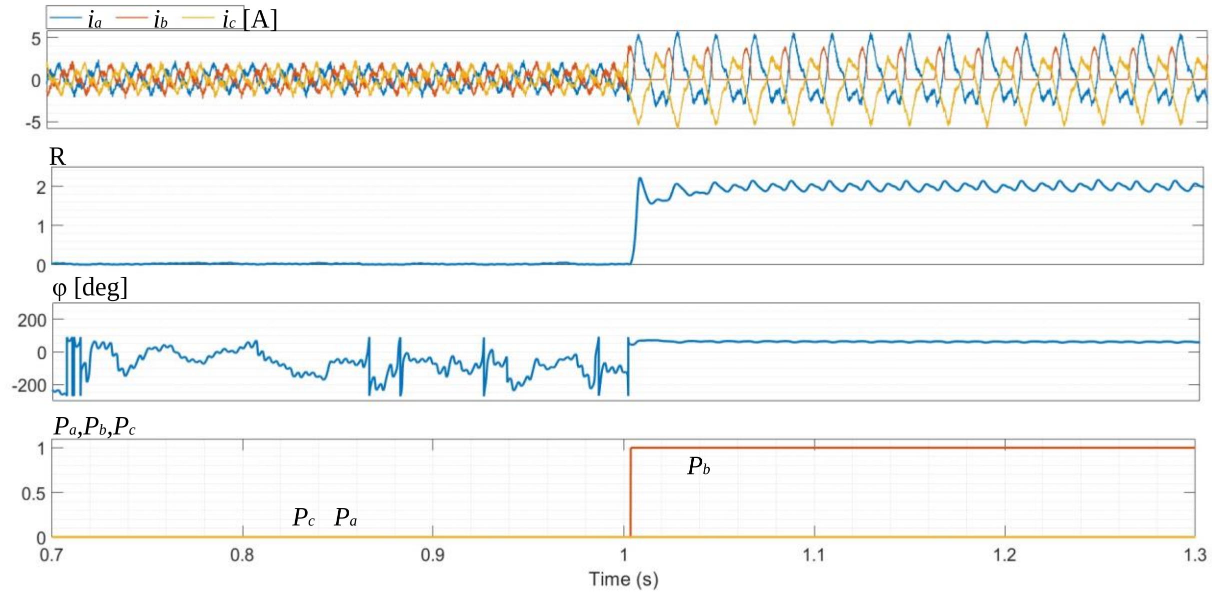

Figure 5. 13: Open phase B identification in low current scenario.

5.4.3.3 Application of OCF diagnosis approach on experimental data

In our investigation of grid-connected inverter operation in case of faults, our initial focus was on examining simulation results to understand how these inverters operate under OCF scenario. These simulations provided valuable understanding into the expected behavior of the inverters within theoretical models. However, it's crucial to verify the reliability of these simulations and confirm their relevance in experimental data. This necessitates evaluating their performance using experimental data.

The transition from simulation to experimental data marks the commencement of offline diagnosis, a crucial method for examining the performance of grid-connected inverters. Offline diagnosis involves systematically comparing simulation results with the experimental results. The comparison between our simulation results and experimental data serves important purpose, it confirms the accuracy of the simulation results by confirming their alignment. The offline diagnosis method in our study serves two main purposes. Firstly, it confirms the accuracy of our simulation results through time detection, also the selection of the predefined thresholds. Secondly, by testing the diagnosis approach of OCF under various current values.

The experimental setup comprised an external DC source with a voltage stabilization set at 200 V, a three-phase two-level power inverter equipped with an inner loop for current vector components, an inductive filter of 1.1 mH, and a three-phase grid with a voltage of 3x133 $V_{L-L(RMS)}$.

At t = 0.17s, an open-circuit fault was induced in switch S1. This fault caused the disappearance of the positive half-cycle of current i_a and a rapid increase in the diagnostic variable R to approximately 0.25, exceeding the threshold th_1. This feature confirmed the presence of a single switch fault. Subsequently, a detailed analysis of the normalized DC component accurately identified the single open-circuit fault in IGBT S1 at t = 0.185s, resulting in an immediate transition of the identification flag F_a to 1 within 18 ms of the fault occurrence.

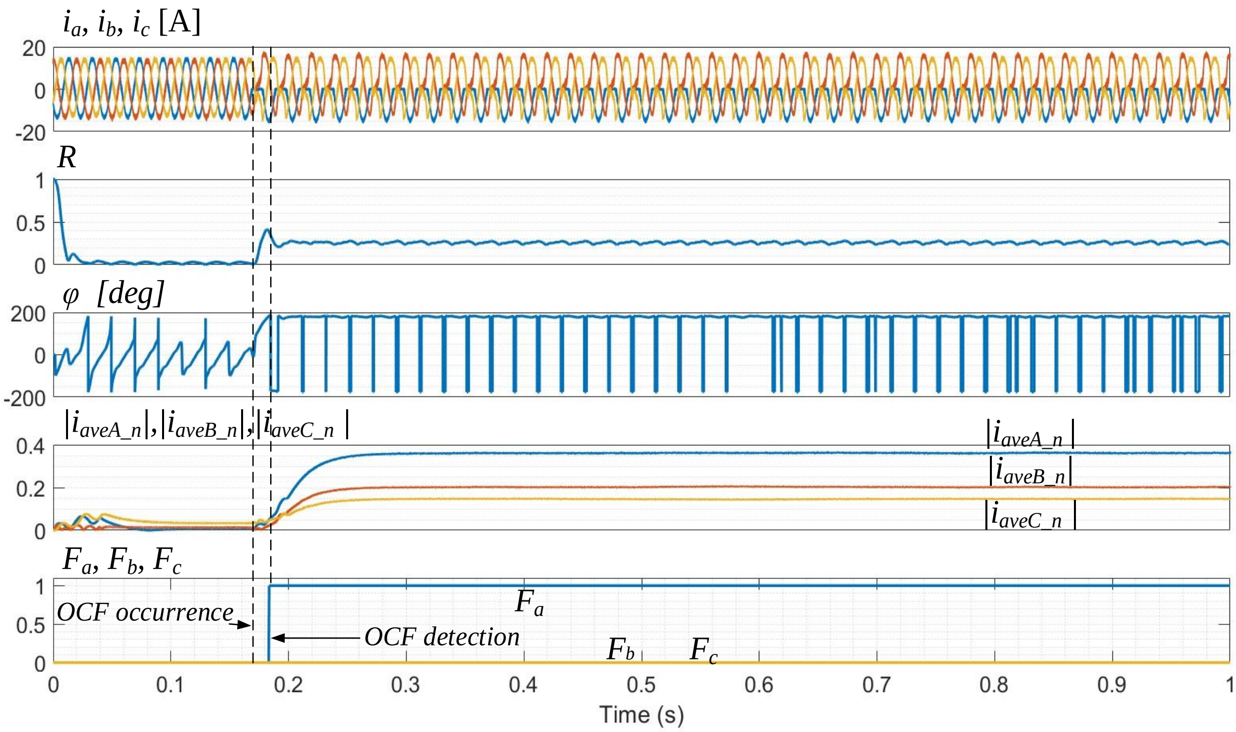

Figure 5. 14: Identification of OCF of S_1 switch.

Figure 5.15 illustrates the experimental data related to the open phase fault in phase A. Before the fault occurred, the fault detection variables uniformly converged toward zero. Following the occurrence of open-circuit faults in S1 and S2 at 0.4s, the three-phase currents exhibited distortion, with the current in phase A approaching zero. The detection variable R experienced an increase, surpassing the threshold th_2. Additionally, the angle value corresponded to 180 degrees, indicating a fault in phase A. Consequently, only the fault flag P_a transitioned from 0 to 1, signifying the detection of the faulty phase A.

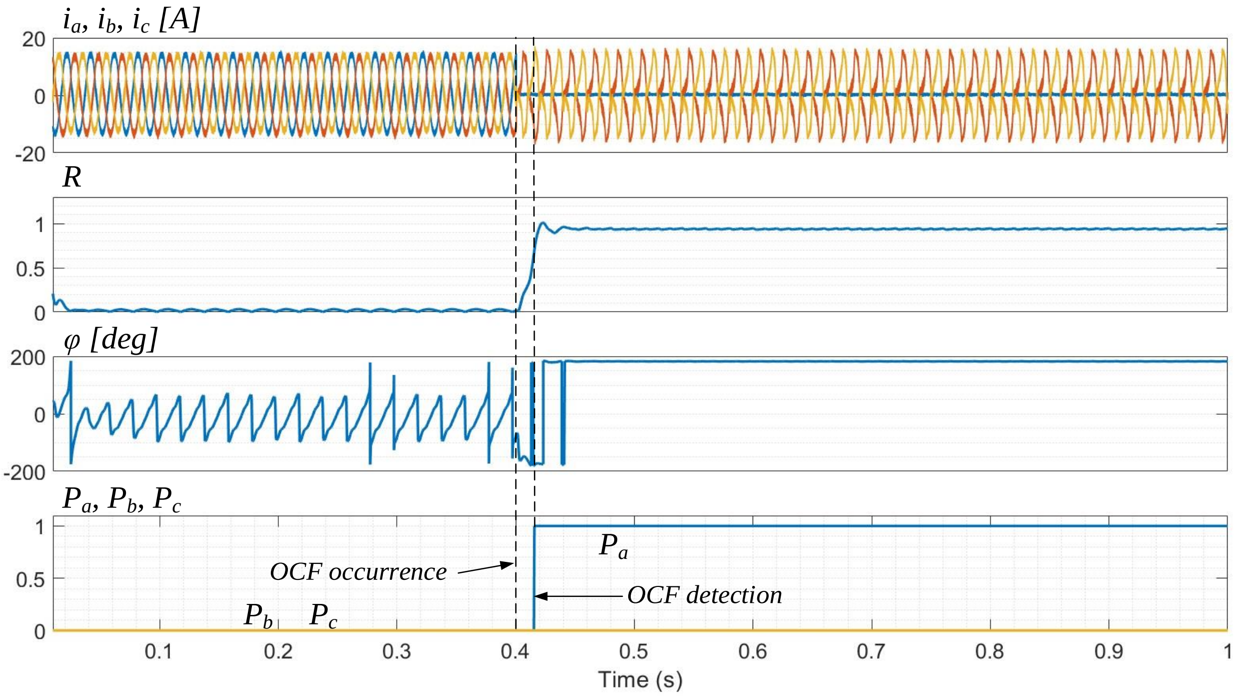

Figure 5. 15: Identification of open phase fault in the phase A.

Furthermore, the study involves examining an open phase fault in case of low current value (2A) that occurs at 0.42s specifically in both switches (S1 and S2) phase A of the system. In this situation, we observe significant changes in the diagnostic variables, which clearly indicate the presence of the faulty phase. These alterations serve as clear indicators of the fault and aid for the identification of open phase.

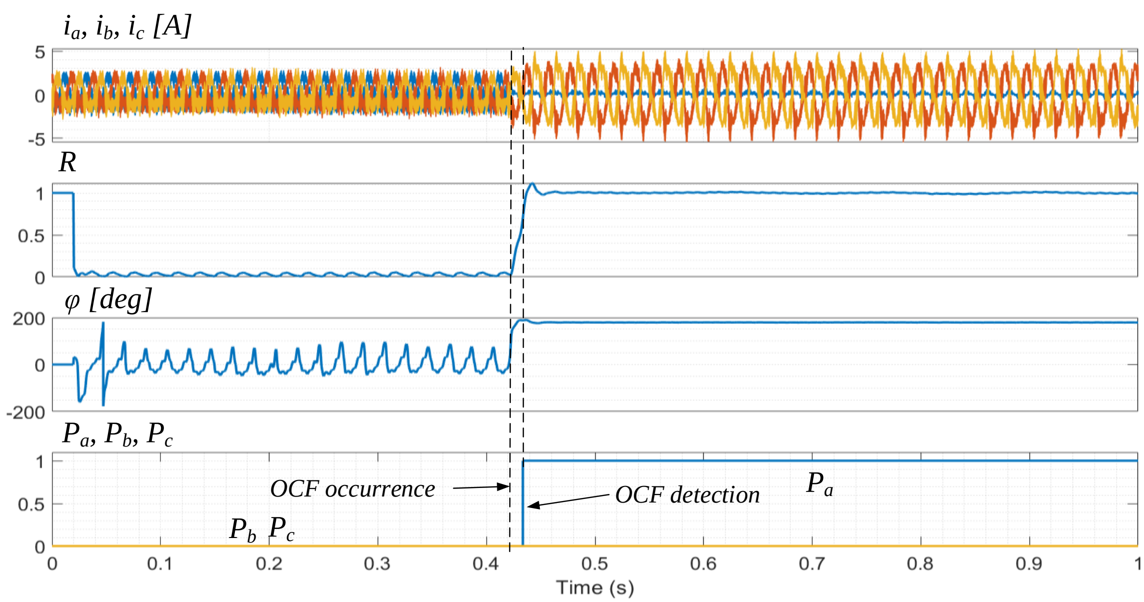

Figure 5. 16: Identification of open phase fault in the phase A (low current).

In Figure 5.17, a single bottom switch fault and an open phase fault, is depicted. For the single bottom switch fault (IGBT S2), the fault initiates at t = 0.462 seconds, resulting in immediate consequences including the loss of the negative half wave, a notable increase in the diagnostic variable R to 0.3, and an elevation in the normalized DC component for phases A and B. Notably, phase A experiences a more significant rise compared to phase C, which remains negligible. The system swiftly identifies this fault within 14 milliseconds, showcasing its efficiency in fault detection and response.

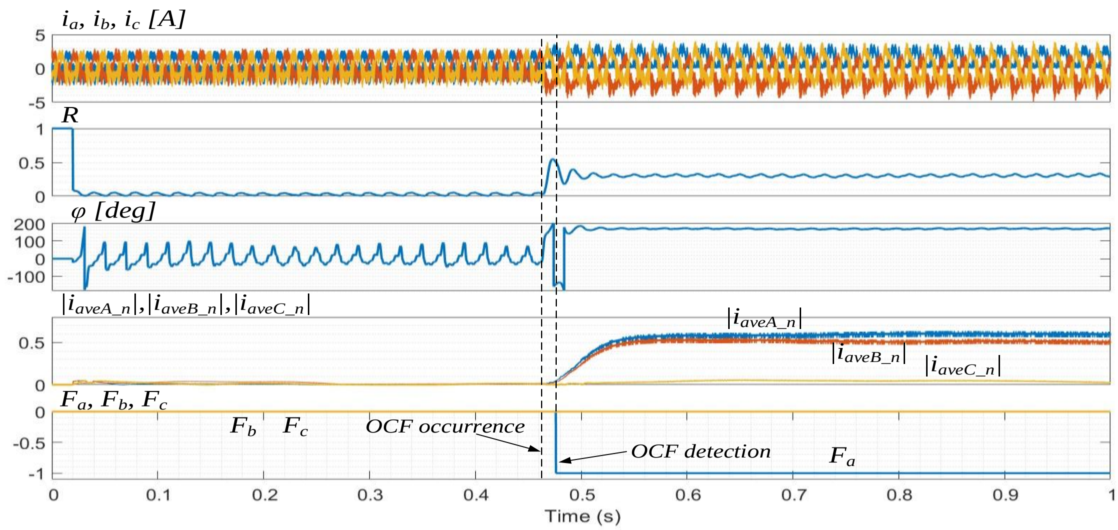

Figure 5. 17: Identification of S_2 OCF (low current).

Importantly, the experimental results closely align with the results obtained from simulations. This consistency between the experimental and simulated data provides strong evidence supporting the robustness and reliability of our diagnostic methodology. It demonstrates that our approach is capable of accurately detecting faults across different current levels and under varying operating conditions. This validation reinforces the effectiveness of our diagnostic technique and its potential for practical applications.

5.5 Fault Tolerant Control

In the field of PV systems, maintaining stability and safety is of importance. One of the critical challenges faced by grid-connected PV systems is the occurrence of faults particularly an open circuit fault in the inverter which was presented in this chapter. This fault can lead to various undesirable consequences, including overcurrent and DC link overvoltage, which can pose significant risks to the system's integrity and operation. The occurrence of an open circuit in a solar power system can lead to significant consequences, including overcurrent and DC link overvoltage issues. These issues pose considerable risks to the system's operational functionality and long-term reliability. The necessity of incorporating protective measures such as overcurrent limitation and DC link overvoltage protection mechanisms in response to an open circuit fault in the inverter is paramount to mitigating these risks and ensuring the integrity and performance of the system's components. Specifically, during an OCF case, there is a heightened risk of overcurrent that exceeds the rated capacity of critical components. Therefore, the implementation of overcurrent limitation mechanisms is indispensable to prevent component damage by maintaining the current within safe parameters, thereby avoiding potential overstressing and overheating concerns.

Figure 5.18 represents a two-stage grid-connected PV system equipped with comprehensive protection control to ensure safe and efficient operation under various conditions. In addition to its primary function of converting solar energy into electricity, the system incorporates limitation of overcurrent and DC link overvoltage control.

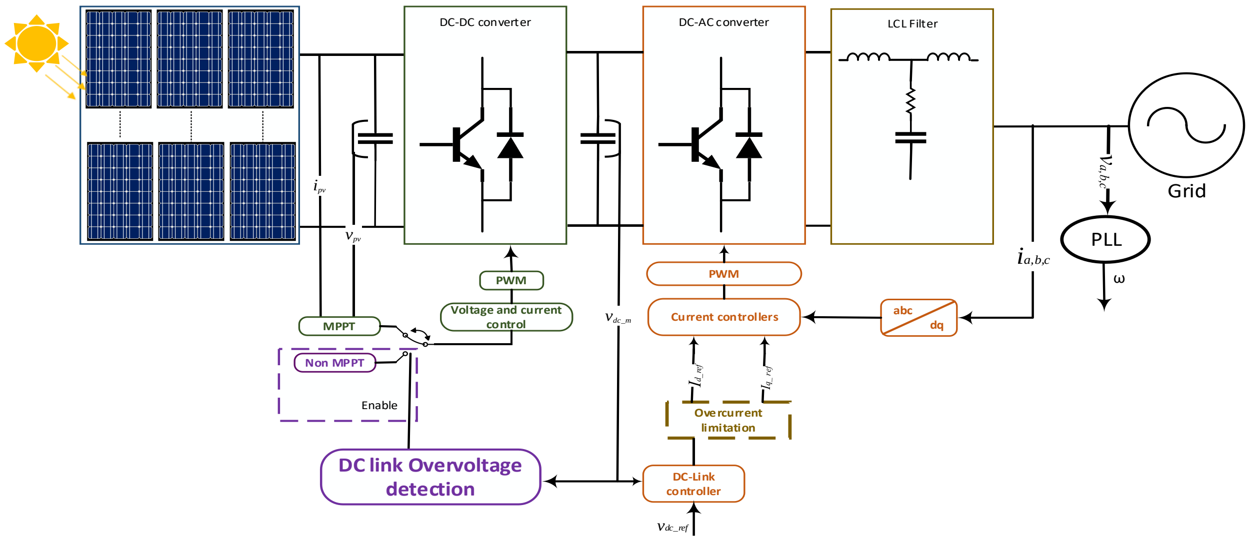

Figure 5. 18: Grid-connected photovoltaic system with current and overvoltage limiting.

5.5.1 DC Link Overvoltage Limitation

An OCF in the inverter can also result in an imbalance in the power flow within the system. This imbalance can lead to an increase of voltage in the DC link, exceeding the allowable voltage limits and potentially damaging the DC link capacitors and other components. To address this issue, it is essential to incorporate DC link overvoltage protection mechanisms. These mechanisms monitor the voltage level across the DC link and activate protective measures, to prevent the voltage from exceeding safe thresholds. Thus, DC link overvoltage protection the integrity and reliability of the PV system. During an OCF in the inverter, if no action is taken in the control of the DC-DC converter, the power from the PV modules is not reduced and therefore, the DC-link voltage keeps rising and may exceed the maximum limit. A specific control action has to be taken to reduce the power generated by the PV modules.

For this purpose, the PV system is controlled to inject less power into the grid during the OCF in the inverter compared with the prefault case, while avoiding overvoltage in the DC-link. In normal operation, the MPPT function is performed by the DC-DC converter, whereas the DC-link voltage is regulated by the inverter. However, under an OCF, some modifications should be implemented in order to keep the grid connected PV system connected to the grid. The proposed method tries to match the power generated by the PV modules with the power injected into the grid while trying to keep the DC-link voltage constant. In the proposed method, the target of the DC-DC converter is no longer achieving MPP operation but regulating the power generated by the PV to match the maximum active power that can be injected into the grid.

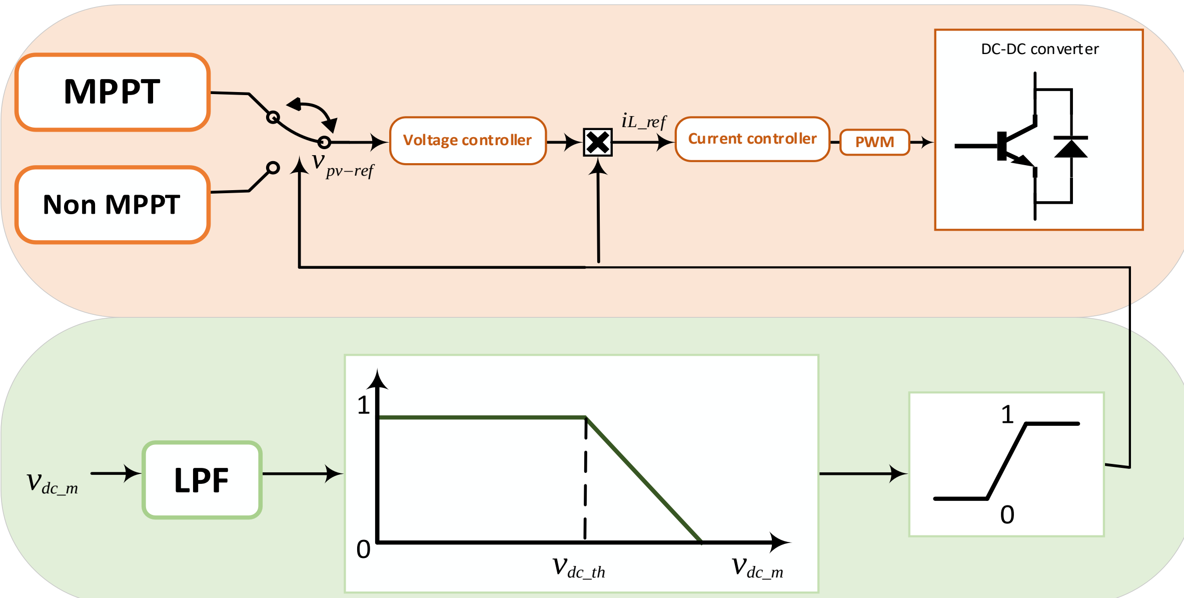

Figure 5. 19: Overvoltage limitation approach in grid connected PV system.

The operational flowchart is shown in Figure 5.19. Initially the DC-link voltage is measured and compared with the allowed DC link voltage. If it exceeds the allowed value, the “control without MPPT” mode is enabled; otherwise, the MPPT control is enabled. The “control Non MPPT” controller is enabled. The implemented overvoltage limitation approach using a threshold and saturation function. When an overvoltage condition is detected, this function limits the voltage level to prevent excessive power production from the photovoltaic panel especially in case of a fault. This limitation is achieved by adjusting the control of the associated DC-DC converter, thereby reducing the power output from the panel and maintaining a safe operation of the system. Through this approach, it is able to mitigate the risks associated with overvoltage and effectively protect the components of the photovoltaic system from potential damage.

5.5.2 Overcurrent limitation

In the presented Figure 5.20, an overcurrent limitation approach is implemented to address the overcurrent problem. The maximum root-mean-square (RMS) current is carefully monitored to ensure it remains within a predefined interval. This interval serves as a safety threshold to prevent the current from surpassing an acceptable limit. When an overcurrent is detected, a dedicated function with saturation block is employed. This function constrains the output to a range between 0 and 1. The resulting value is then multiplied by the *dq* reference current components, effectively scaling them down to mitigate the overcurrent condition. By implementing this approach, the photovoltaic system effectively controls and limits the current during fault conditions, ensuring that it remains within a safe operating range. This helps prevent equipment damage and maintains system stability.

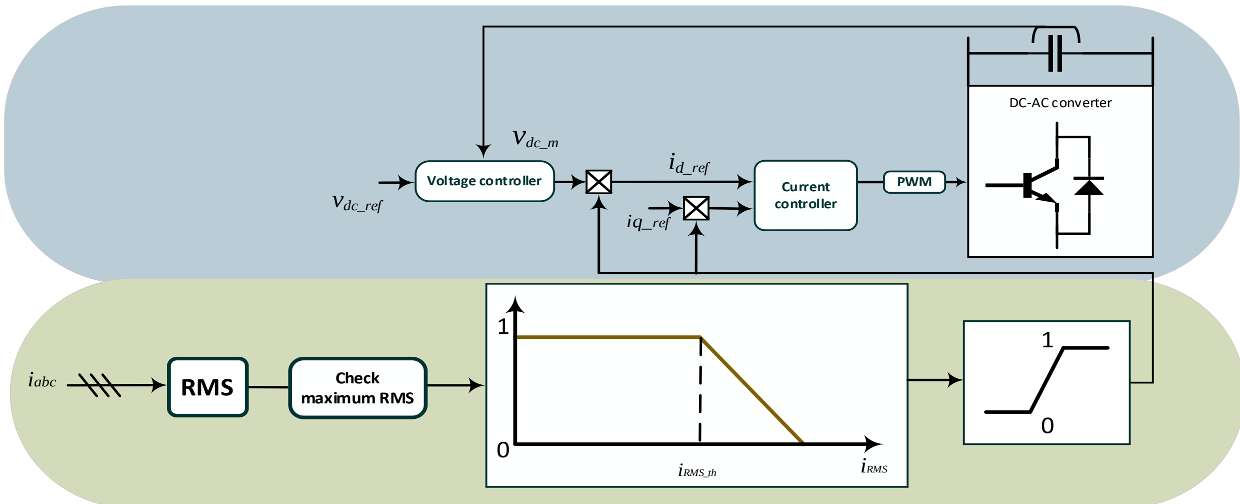

Figure 5. 20: Overcurrent limitation approach in grid connected PV system.

A simulation test is developed in MATLAB/Simulink to verify the proposed strategy, it's essential to test the effectiveness of overvoltage and overcurrent limitations, especially during open phase fault condition. To conduct this simulation, we will continue with the same system “grid connected PV system model”. Next, we will introduce an open phase fault scenario in the inverter. During this fault, the inverter's behavior can lead to an excessive in DC link voltage and excessive current flow. To test the overvoltage limitation, we monitor the DC link voltage and ensure it doesn't exceed the predefined maximum allowed voltage. The overvoltage protection mechanism activates if the DC link voltage surpasses this limit, preventing damage to the system components. Simultaneously, we monitor the three-phase current RMS’s value to check for overcurrent conditions. The overcurrent protection system triggers if the current exceeds the specified threshold.

By analyzing simulation results, we can evaluate the overvoltage and overcurrent limitations respond to fault conditions and ensure the grid-connected PV system. This simulation helps validate the system's protective measures. An open phase A was occurred at time 0.4s.

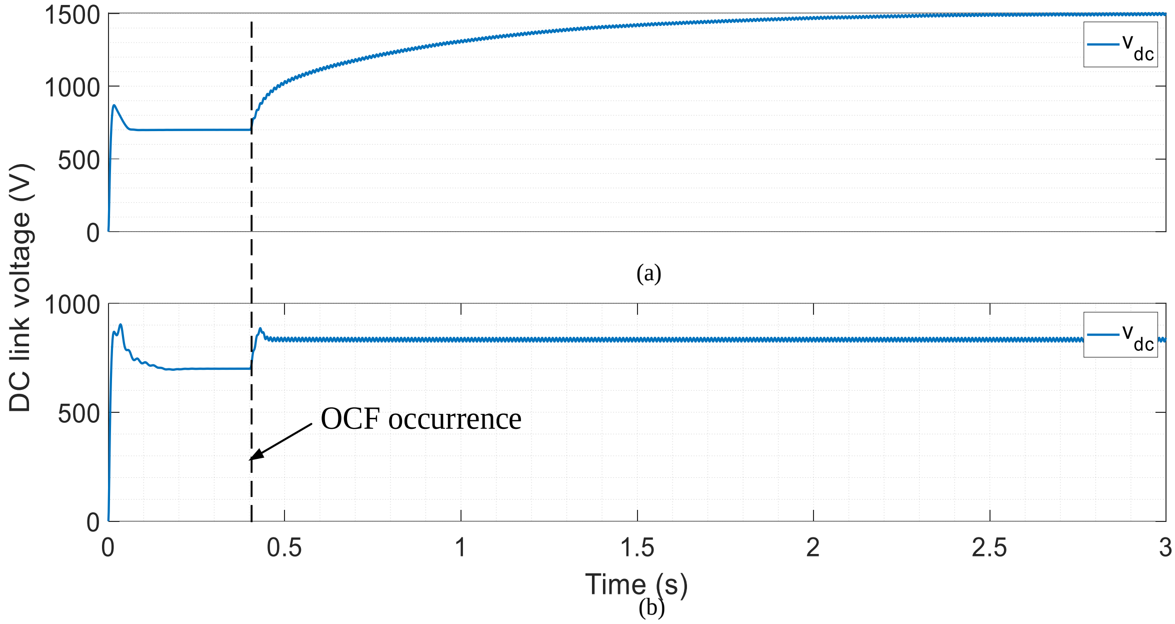

Figure 5. 21: DC link voltage under case of open phase, (a): without DC link overvoltage , (b) with DC link limitation.

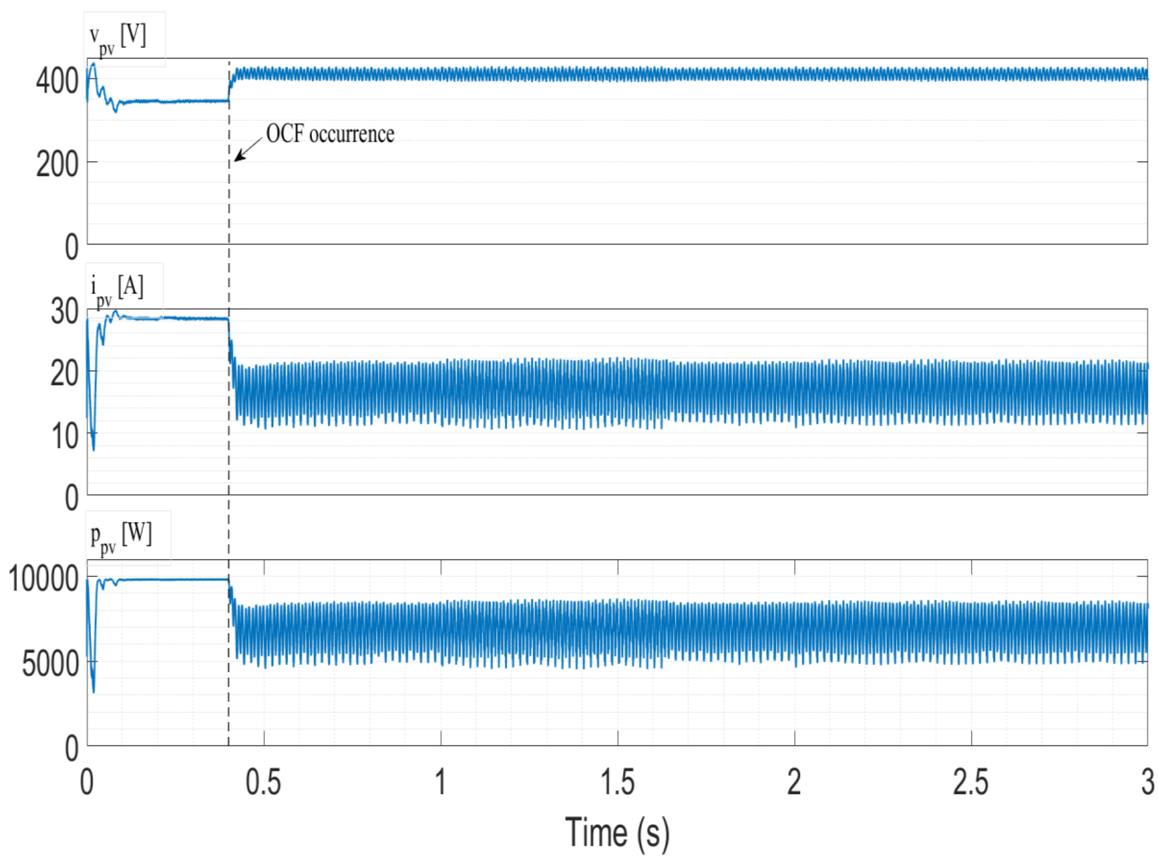

Figure 5. 22: PV Electrical characteristics under DC link limitation.

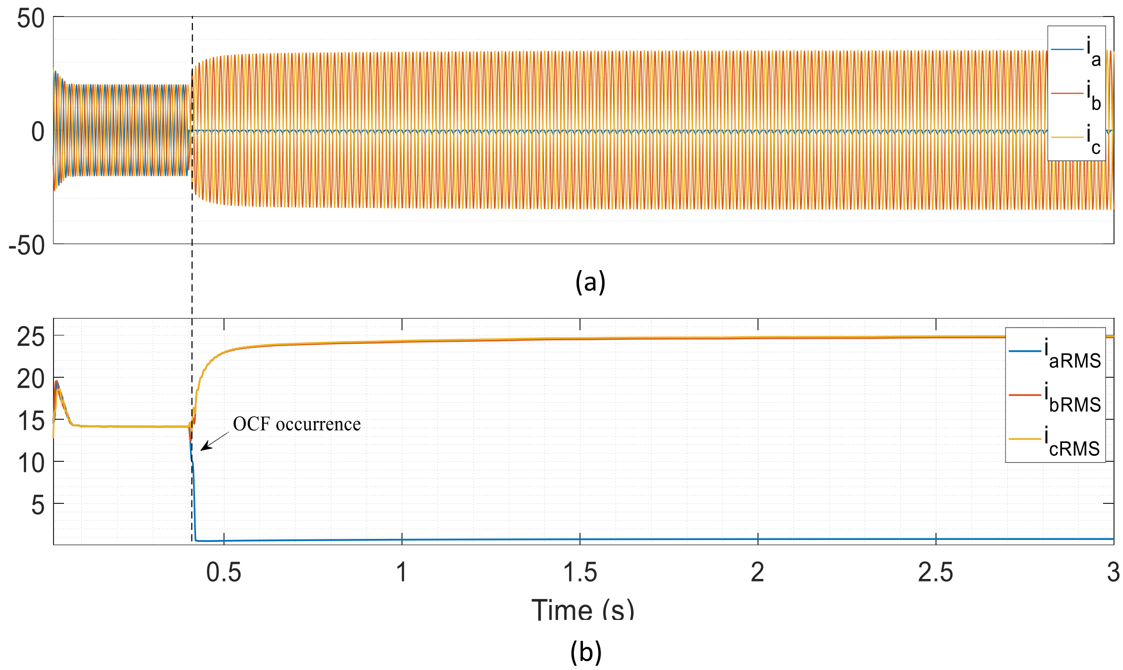

Figure 5. 23: Three phase inverter currents under case of open phase without currents limitation, (a) : three phase currents , (b) RMS value of currents.

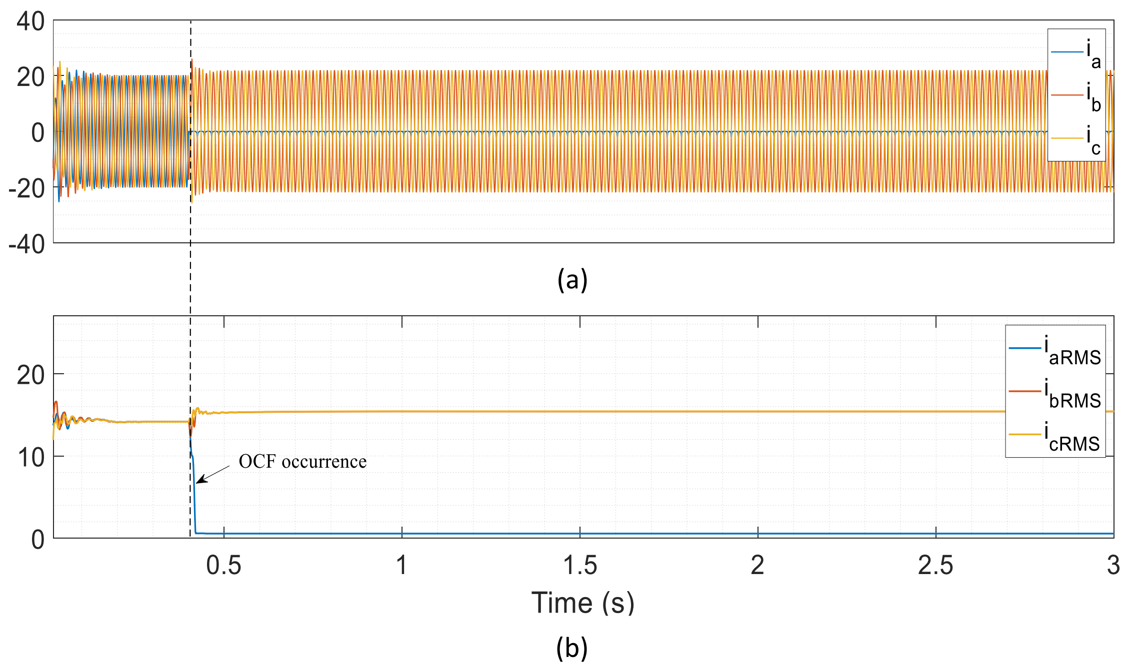

Figure 5. 24: Three phase inverter currents under case of open phase with currents limitation, (a) : three phase currents , (b) RMS value of currents.

In the scenario of an open phase A fault in the inverter within a PV system connected to the grid, the control scheme plays a crucial role in managing the system's response to the fault. Initially, when the fault occurs in phase A, it leads to an increase in the DC link voltage and results in overcurrent within the three-phase inverter. To address this, the control system takes several measures. Firstly, it reduces the active power, thereby decreasing the power extracted from the PV array by switching from MPPT mode to non-MPPT mode.

The simulation results illustrate the performance and effectiveness of the proposed strategy in managing a PV system during an open phase fault in the inverter scenario. The normal operation of the system, as depicted in Figures 5.21 and 5.24, shows stable DC-link voltage and injected currents. However, during the fault of open phase A which was introduced at time 0.4s, the system's response is analyzed. The DC-link voltage increases initially at the fault instant, reaching 880V which represents the allowed DC link voltage, but swiftly recovers to its stabilized value of 830 V within a short duration, demonstrating efficient voltage stabilization. As a consequence of the reduced PV power due to the switch to non-MPPT mode.

The injected currents during the fault are controlled to remain limited to a certain value for the other phase B and C, with phase B and C currents RMS values are limited to 18A while phase A decreases is null. For the limitation of the injected currents are initially decreased. The control scheme ensures proper control of phase B current, limiting it to the rated RMS value of 15A. The simulation results validate the efficiency and efficacy of the proposed strategies of limitation in effectively managing currents, stabilizing voltages, limiting power, and ensuring system stability during faults in the inverter.

5.6 Conclusion

In this chapter, we presented the impact of OCF of an IGBT in a classic two-level voltage inverter on the behavior of grid connected PV system. The analyses and simulation results conducted and presented in this chapter have shown that the classical configuration of power converters used in PV system does not ensure service continuity in the presence of a possible fault in one of the power switches. Subsequently, we synthesized literature on fault detection methods, initially opting for a method to detect faulty switches in a voltage inverter. Our proposed method for fault diagnosis in three-phase systems leverages the analysis of current signals. Initially, we acquire the three-phase current signals. We proceed to extract their positive and negative components. This involves the calculation of positive and negative magnitudes. Next, we compare the extracted positive and negative magnitudes of the current signals against a predefined threshold. This threshold serves as a reference value, beyond which the magnitude of the component is considered indicative of a fault occurrence. Furthermore, in addition to analyzing the magnitude of the components, we also examine their angles. Moreover, we incorporate an assessment of the DC component of the current signals into our fault diagnosis process. The DC component represents the average value of the current signals and can provide valuable information about the overall system behavior. By analyzing the DC component with the positive and negative components, to the precise detection of single switch faults

General Conclusion

General Conclusion

The exploration of diagnosis and surveillance techniques for power converters in PV systems offers a significant contribution to the broader field of renewable energy research. By addressing the challenges associated with fault detection and monitoring in power converters, this thesis has supported the reliability and efficiency of solar energy systems, thus advancing the overarching goals of RE adoption. These efforts play a crucial role in the transition towards a more sustainable energy future. By developing effective diagnosis and surveillance methods, we contribute to the continued growth and viability of solar power as a RE source. In this thesis, we have delved into the critical field of surveillance and diagnosis of power converters in PV systems including the DC-DC converter and the inverters. Our thesis aimed to address the pressing need for effective monitoring and fault detection mechanisms to enhance the reliability and performance of PV installations.

Methodology and Contribution

Our research has employed distinct methodologies to address fault diagnosis in both inverter and DC-DC converter systems, aiming to enhance the reliability and performance of RE systems.

For inverter fault diagnosis, our proposed method capitalizes on the analysis of three-phase current signals as primary inputs. By using these signals, we extract both positive and negative components and subject them to evaluation against predefined thresholds to detect fault occurrences accurately. Moreover, by considering the angle of these components in conjunction with an examination of the DC component, our approach enables precise fault localization of open phase faults and single open switch faults. Through rigorous validation via different tests, our methodology has exhibited remarkable accuracy and effectiveness across diverse operational conditions, thus affirming its reliability as a diagnostic method for inverter faults.

In order to prevent the overcurrent and DC link overvoltage problems, an efficient DC link voltage and current limitation methods is proposed. The rated power of the system must be updated once an exceeding in (current and DC link voltage) is detected. Thus, the PV power output must be reduced below the MPP when the DC link voltage exceeds a certain value. A non-maximum power point tracking (non-MPPT) operation mode is applied for the DC-DC converter. The mode is enabled under open switch faults when the system cannot handle the maximum PV power. Also, an effective overcurrent limitation algorithm can detect the excessive current caused by the open switch fault. This algorithm can promptly limit the currents values to prevent further escalation of the fault and safeguard the system. The current limitation has been achieved through adjusting the current references of the inverter.

Similarly, in the case of DC-DC converter fault diagnosis, we have presented two different algorithms based on the analysis of inductor current. Utilizing these algorithms, we aim to detect and localize OCF within DC-DC converter systems efficiently. Through diverse simulation tests, our methodologies have demonstrated robust performance and efficacy, underscoring their potential to enhance fault diagnosis capabilities in DC-DC converter systems.

General Conclusion

Perspectives and Future Directions

The extensive research conducted in this thesis has uncovered promising avenues for future investigation within the field of diagnosing and implementing new methods capable of detecting simple or multiple faults, notably those related to power component failure. These future research directions aim to address key challenges and opportunities in the field of diagnosis and exploration of new applications and topologies.

Exploration of New Applications and Topologies

- Investigate the integration of grid-connected PV systems with other renewable energy sources such as wind systems or hybrid systems.
- Investigate emerging converter topologies such as multilevel converters, Z-source inverters for PV applications.
- Evaluate the performance, efficiency, and reliability of these topologies under varying operating conditions and grid configurations.

Futures works in diagnosis field

- Investigate and develop advanced diagnostic algorithms tailored to grid-connected PV inverters, with a focus on multilevel inverters.
- Explore the integration of machine learning, artificial intelligence, and real-time monitoring techniques for fault detection and diagnosis.
- Address specific fault scenarios such as DC capacitor faults and other components to enhance system resilience.
- Investigate fault diagnosis and fault tolerance methods for diverse DC-DC converter topologies tailored for renewable energy applications.
- In addition to power converter faults, investigating machine-related faults in PV systems, such as those occurring in the photovoltaic modules or the PV array itself, can provide a view of system reliability and performance. Comparing and contrasting the diagnostic approaches for inverter faults and machine faults will help identify synergies and opportunities for integrated fault detection and diagnosis strategies, ultimately enhancing the overall resilience of PV systems.
- Given the critical role of DC capacitors in ensuring smooth operation and stability of grid-connected PV inverters, examining fault diagnosis techniques specifically targeting DC capacitor faults is essential. By analyzing the root causes, fault manifestations, and diagnostic challenges associated with DC capacitor failures, you can develop effective diagnostic algorithms and monitoring strategies to detect and mitigate capacitor-related faults pro
- actively, thereby preventing potential system downtime and safety hazards.

Appendix

Appendix A

Boost converter regulator
Control of Vpv voltage

The equation of the C_{PV} capacitor is:

$$C_{pv}\frac{dV_{pv}}{dt}=i_{pv}-i_L$$

By applying a Laplace transformation, we obtain the transfer function:

$$G_1(p)=\frac{V_{pv}(p)}{i_L(p)}=-\frac{1}{C_{pv}p}$$

With a PI corrector $C_1(p)=K_{p1}+\frac{K_{i1}}{p}$ the transfer function of the closed loop is written as:

$$F_1(p)=\frac{C_1(p)G_1(p)}{1+C_1(p)G_1(p)}$$

Comparing the denominator of F_1(p) with the normalized form of $p^2+2\xi_1\omega_1 p+\omega_1^2$, we obtain:

$$\begin{cases}K_{p1}=2\xi_1 C_{pv}\omega_1\\ K_{i1}=C_{pv}\omega_1^2\end{cases}$$

Control of inductor current

The equation of the boost converter:

$$L\frac{di_L}{dt}=V_{pv}-V_{DC}(1-D)$$

By applying a Laplace transformation, we obtain the transfer function:

$$G(p)=\frac{i_L(p)}{D(p)}=\frac{V_{DC}}{Lp}$$

With a PI corrector $C(p)=K_p+\frac{K_i}{p}$ the transfer function of the closed loop is written as:

$$F(p)=\frac{C(p)G(p)}{1+C(p)G(p)}$$

Comparing the denominator of F(p) with the normalized form of $p^2+2\xi\omega p+\omega^2$, we obtain:

$$\begin{cases} K_p = \dfrac{2\xi L\omega}{V_{DC}} \\ K_i = \dfrac{L\omega^2}{V_{DC}} \end{cases}$$

Control of currents in grid connected inverter

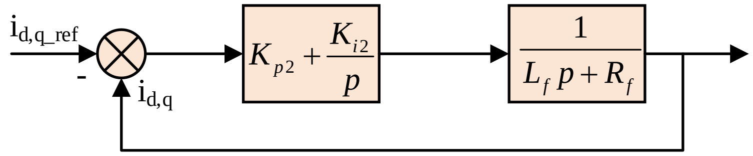

The transfer function of inverter is : $G_2(p) = \dfrac{1}{L_f p + R_f}$

With a PI corrector $C_2(p) = K_{p2} + \dfrac{K_{i2}}{p}$ the transfer function of the closed loop is written as:

$$F_2(p) = \frac{C_2(p)G_2(p)}{1 + C_2(p)G_2(p)}$$

Comparing the denominator of $F_2(p)$ with the normalized form of $p^2 + 2\xi_2\omega_2 p + \omega_2^{\,2}$, we obtain:

$$\begin{cases} K_{p2} = 2\xi_2 L_f \omega_2 - R_f \\ K_{i2} = L_f \omega_2^{\,2} \end{cases}$$

Control of DC link voltage

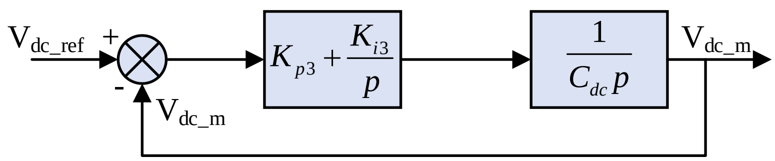

The transfer function of the DC link capacitor is $G_3(p) = \dfrac{1}{C_{dc} p}$:

With a PI corrector $C_3(p) = K_{p3} + \dfrac{K_{i3}}{p}$ the transfer function of the closed loop is written as:

$$F_3(p) = \frac{C_3(p)G_3(p)}{1 + C_3(p)G_3(p)}$$

Comparing the denominator of $F_2(p)$ with the normalized form of $p^2 + 2\xi_3\omega_3 p + \omega_3^{\,2}$, we obtain:

$$\begin{cases} K_{p3} = 2\xi_3 C_{dc} \omega_3 \\ K_{i3} = C_{dc} \omega_3^{\,2} \end{cases}$$

Appendix B

Photovoltaic module	**Values**
Open circuit voltage V_{oc} (V)	453.6
Short circuit current I_{sc}(A)	30.6
Voltage at MPP V_{mpp}(V)	351.54
Current at MPP I_{mpp}(A)	27.9
Power at MPP (W)	9807.966

Parameters	Value
V_{dc} (V)	700
DC bus capacitor C_{in} (F)	500e-6
LCL filter parameters	
L_{1f} (H)	1.3e-3
L_{2f} (H)	1.3e-3
C_f (F)	10e-6
R_f (Ω)	1
Outer control parameter	
K_p	0.2
K_i	20
Inner control parameter	
K_p	10
K_i	100
Switching frequency F_{sw} (Hz)	10000
Sampling time T_s (s)	1e-4
Grid parameters	
Voltage (RMS)	230
Grid frequency (Hz)	50

Bibliography

Bibliography

[1]: GE. Halkos and E.C. Gkampoura, "Reviewing Usage, Potentials, and Limitations of Renewable Energy Sources", *Energies*, vol. 13, no. 11, pp. 2906, 2020. https://doi.org/10.3390/en13112906.

[2]: IRENA, Renewable Energy Statistics 2022, The International Renewable Energy Agency, Abu Dhabi,2022.

[3]: Snapshot of Global PV Markets 2023. International energy agency photovoltaic power systems programme IEA pvps Task 1 Strategic PV Analysis and Outreach Report IEA-PVPS T1-44:2023 April 2023.

[4]: G.K. Kumar and D. Elangovan, "Review on fault-diagnosis and fault-tolerance for DC–DC converters", *IET Power Electronics*, vol. 13, pp. 1-13, 2020. https://doi.org/10.1049/iet-pel.2019.0672.

[5]: Gianluca Fadda, Supervision and diagnosis of industrial systems, PhD Disseration, Universita degli Studi Di Cagliari, 2017.

[6]: Gilles Rostaing, Diagnostic de défaut dans les entrainements électriques, PhD Disseration, Institut National Polytechnique de Grenoble - INPG, 1997.

[7]: Imane Idrissi, Contribution au Diagnotic des Défauts de la Machine Asynchrone Doublement Alimentée de l'Eolienne à Vitesse Variable, PhD dissertation ,Université Sidi Mohamed ben Abdellah, 2019.

[8]: Moufida Handis, Modélisation des défaillances et leur diagnostic par les méthodes de reconnaissance des formes floue, PhD dissertation, Université de badji mokhtar-Annaba, 2013.

[9]: Djeddi abldeghani, Diagnostic des systemes non linéaire à base d'observateurs, PhD Disseration, Université de badji mokhtar-Annaba, 2017.

[10]: Abdelhakim Khatab, Contribution à l'optimisation des stratégies de maintenance des systèmes, PhD dissertation , Université de Lorraine; École doctorale IAEM, 2019.

[11] : Chakour Chouaib, Diagnostic et surveillance des procédés industriels et de leur environnement sur la base de l'analyse de données. PhD Disseration. Université de badji mokhtar-Annaba, 2016.

[12] : Soufi Youcef, Modelisation et diagnostic d'une association convertisseur machine electrique. PhD Disseration. Université de badji mokhtar-Annaba.2012.

[13] : Matthieu Lucke. Industrial fault detection and diagnosis using alarms and process measurements. PhD Disseration. Imperial College London, 2019.

[14] : Michel Batteux. Diagnosticabilité et diagnostic de systèmes technologiques pilotés Développement d'une chaîne de conception outillée d'un système de diagnostic appliquée aux systèmes technologiques pilotés, PhD Disseration, Université Paris Sud - Paris XI, 2011.

[15] : Ayan Mahamoud, Observation et diagnostic de processus industriels à modèle non linéaire : application aux machines électriques, PhD Disseration, Ecole Centrale de Nantes (ECN), 2010.

[16] : Mickael Rodrigues, Diagnostic et Commande Active Tolérante aux Défauts appliqués aux Systèmes décrits par des Multi-Modèles Linéaires, PhD Disseration, Université Henri Poincaré - Nancy I, 2005.

[17] : Dhouha Kharrat, Commande tolérante aux défauts des systèmes non linéaires : application à la dynamique du véhicule, PhD Disseration, Université de Picardie Jules Verne, 2019.

[18] : J. Jin and Y. Xiang, "Fault-tolerant control systems: A comparative study between active and passive approaches", *Annual Reviews in control*, vol. 36, no. 1, pp. 60-72, 2012.

[19] : A. Abbaspour, S. Mokhtari and A. Sargolzaei, "A Survey on Active Fault-Tolerant Control Systems", *Electronics*, vol. 9, no. 9, pp. :1513, 2020. https://doi.org/10.3390/electronics9091513.

[20] : A. Amin and K.M. Hasan, "A review of Fault Tolerant Control Systems: Advancements and applications", *Measurement*, vol. 143, pp. 58–68, 2019. doi:10.1016/j.measurement.2019.04.083.

[21] : ABID Muhammad. Fault detection in nonlinear systems: An observer-based approach, PhD dissertation, 2010.

[22] : Y.G. Park, S.K. Fan, C.Y. Hsu. "A Review on Fault Detection and Process Diagnostics in Industrial Processes", *Processes*, vol. 8, no. 9, pp.1123, 2020. https://doi.org/10.3390/pr8091123.

[23] : K. Zhong, M. Han and B. Han, "Data-driven based fault prognosis for industrial systems: a concise overview," *IEEE/CAA Journal of Automatica Sinica*, vol. 7, no. 2, pp. 330-345, March 2020, doi: 10.1109/JAS.2019.1911804.

[24] : A. Rajeevan, F.Khan Faisal *et al,* "An analysis of process fault diagnosis methods from safety perspectives", *Computers & Chemical Engineering*, vol. 145, pp. 107197, 2021.

[25]: I.Matetić, I.Štajduhar, I.Wolf, and S. Ljubic, "A Review of Data-Driven Approaches and Techniques for Fault Detection and Diagnosis in HVAC Systems", *Sensors*, vol. 23, no. 1, pp. 1, 2023. https://doi.org/10.3390/s23010001.

[26]: F. Hodavand, I.J. Ramaji, and N. Sadeghi, "Digital Twin for Fault Detection and Diagnosis of Building Operations: A Systematic Review", *Buildings*, vol. 13, no. 6, pp. 1426, 2023, https://doi.org/10.3390/buildings13061426.

[27]: Y. Wilhelm, P. Reimann, W. Gauchel and B. Mitschang, "Overview on hybrid approaches to fault detection and diagnosis: Combining data-driven, physics-based and knowledge-based models",*Procedia CIRP*, vol. 99, pp. 278-283, 2021, https://doi.org/10.1016/j.procir.2021.03.041.

[28]: L. H. Chiang, E. L. Russell and R. D. Braatz. Fault Detection and Diagnosis in Industrial Systems, *John wiley and sons*, 2001.

[29]: I. Fagarasan and S. S. Iliescu, "Parity equations for fault detection and isolation," *2008 IEEE International Conference on Automation, Quality and Testing, Robotics*, Cluj-Napoca, Romania, 2008, pp. 99-103, doi: 10.1109/AQTR.2008.4588715.

[30]: R.Isermann, Fault-Diagnosis Systems An Introduction from Fault Detection to Fault Tolerance, Springer Science and Business Media, 2006.

[31]: A. D. Pouliezos and G. S. Stavrakakis, Real Time Fault Monitoring of Industrial Processes, 1994.

[32]: S. Joe Qin, Data-driven Fault Detection and Diagnosis for Complex Industrial Processes, IFAC Proceedings Volume 42, Issue 8,2009, Pages 1115-1125, https://doi.org/10.3182/20090630-4-ES-2003.00184.

[33]: R.R. Kumar, M. Andriollo, G. Cirrincione, M. Cirrincione and A.A. Tortella, "Comprehensive Review of Conventional and Intelligence-Based Approaches for the Fault Diagnosis and Condition Monitoring of Induction Motors", *Energies*, vol. 15, no. 23, pp. 8938, 2022. https://doi.org/10.3390/en15238938.

[34]: A.A.A.Mohd Amiruddin, H. Zabiri, S. A.A. Taqvi, and L. D. Tufa, "Neural network applications in fault diagnosis and detection: an overview of implementations in engineering-related systems", *Neural Comput. Appl*, vol. 32, no. 2, pp. 447–472, 2020. https://doi.org/10.1007/s00521-018-3911-5.

[35]: A. Samanta, S. Chowdhuri, S.S. Williamson, "Machine Learning-Based Data-Driven Fault Detection/Diagnosis of Lithium-Ion Battery: A Critical Review", *Electronics*, vol. 10, no. 11, pp. 1309, 2021, https://doi.org/10.3390/electronics10111309.

[36]: M.C. Kim, J.H. Lee, D.H.Wang and I.S. Lee, "Induction Motor Fault Diagnosis Using Support Vector Machine, Neural Networks, and Boosting Methods", *Sensors*, vol. 23, no. 5, pp. 2585, 2023, https://doi.org/10.3390/s23052585.

[37]: S. Mahadevan and S. L. Shah, "Fault detection and diagnosis in process data using one-class support vector machines", *Journal of process control*, vol. 19, no.10, pp. 1627-1639, 2009.

[38]: S. Yin, X. Gao, H.R. Karimi and X. Zhu, "Study on Support Vector Machine-Based Fault Detection in Tennessee Eastman Process", *Abstract and Applied Analysis*, vol. 2014, 8 pages, 2014. https://doi.org/10.1155/2014/836895.

[39]: R. Muzzammel and A.A. Raza, "Support Vector Machine Learning-Based Protection Technique for MT-HVDC Systems", *Energies*, vol. 13, no. 24, pp. 6668, 2020, https://doi.org/10.3390/en13246668

[40]: A. Hosameldin, A. K. Nandi, Condition Monitoring with Vibration Signals: Compressive Sampling and Learning Algorithms for Rotating Machines, *Wiley-IEEE Press*, 2019.

[41]: W. Zhang, D. Yang and H. Wang, "Data-Driven Methods for Predictive Maintenance of Industrial Equipment: A Survey," *in IEEE Systems Journal*, vol. 13, no. 3, pp. 2213-2227, Sept. 2019, doi: 10.1109/JSYST.2019.2905565.

[42]: J. Long, X. Wang, W. Zhou, J. Zhang, D. Dai and G. Zhu, "A Comprehensive Review of Signal Processing and Machine Learning Technologies for UHF PD Detection and Diagnosis (I): Preprocessing and Localization Approaches," *in IEEE Access*, vol. 9, pp. 69876-69904, 2021, doi: 10.1109/ACCESS.2021.3077483.

[43]: M. Benbouzid, Signal processing for fault detection and diagnosis in electric machines and systems. *Institution of Engineering & Technology*, 2021.

[44]: S. Li, Y. Xin, X. Li, J. Wang and K. Xu, "A Review on the Signal Processing Methods of Rotating Machinery Fault Diagnosis," *2019 IEEE 8th Joint International Information Technology and Artificial Intelligence Conference (ITAIC)*, Chongqing, China, 2019, pp. 1559-1565, doi: 10.1109/ITAIC.2019.8785572.

[45]: Chen Jing Jian Hou, "SVM and PCA based fault classification approaches for complicated industrial process", *Neurocomputing*, 2015. DOI: 10.1016/j.neucom.2015.03.082.

[46]: S. Yin, X. D. Steven, A. Naik, P. Deng and A. Haghani, "On PCA-based fault diagnosis techniques," *2010 Conference on Control and Fault-Tolerant Systems (SysTol)*, Nice, France, 2010, pp. 179-184, doi: 10.1109/SYSTOL.2010.5676031.

[47]: G. Demidova, A. Rassõlkin, T. Vaimann, A. Kallaste, J. Zakis and A. Suzdalenko, "An Overview of Fuzzy Logic Approaches for Fault Diagnosis in Energy Conversion Devices," *2021 28th International Workshop on Electric Drives: Improving Reliability of Electric Drives (IWED)*, Moscow, Russia, 2021, pp. 1-7, doi: 10.1109/IWED52055.2021.9376389.

[48]: Imad Eddine KAID. Détection et localisation des défauts a base de la logique floue appliquée à un système hybride d'énergie renouvelable. PhD dissertation. Universite de Djelfa, 2018.

[49]: M. Geetha and N. Sivaraman, "Integrating Fuzzy based fault diagnosis with constrained model predictive control for industrial applications", *Journal of Electrical Engineering & Technology* , vol. 12, no. 2, pp. 886-889, 2017.

[50]: S. R. T. Kumara, S. Joshi, R. L. Kashyap, C. L. Moodie, " Expert systems in industrial engineering", *International Journal of Production Research*, vol. 24, no. 5, pp. 1107-1125, 1986, DOI: 10.1080/00207548608919791.

[51]: M.Silvano, "Diagnostic expert systems: a method for engineering knowledge used in sequential diagnosis", *Expert systems*, vol. 17, no. 4, pp. 199-211, 2000.

[52]: A. M. Tanjin, S. Imtiaz, and F. Khan, "Process system fault detection and diagnosis using a hybrid technique", *Chemical Engineering Science*, vol. 189, pp. 191-211, 2018.

[53]: M. M.Raihan, and Syed A. Imtiaz, "A hybrid method for process fault detection and diagnosis", *IFAC Proceedings*, vol. 46, no. 32, pp. 827-832, 2013.

[54]: M.G. Hemeida, A. M. Hemeida, T. Senjyu, and D. Osheba, "Renewable Energy Resources Technologies and Life Cycle Assessment: Review", *Energies*, vol. 15, no. 24, pp. 9417, 2022, https://doi.org/10.3390/en15249417.

[55]: S. Adams, C. Nsiah, "Reducing carbon dioxide emissions; Does renewable energy matter? ", *Science of the total environment*, vol. 693, pp. 133288.

[56]: J. Jia, J. Lei, C. Chen, X. Song and Y. Zhong, "Contribution of Renewable Energy Consumption to CO_2 Emission Mitigation: A Comparative Analysis from a Global Geographic Perspective", *Sustainability*, vol. 13, no. 7, pp. 3853, 2021, https://doi.org/10.3390/su13073853.

[57]: T. E. K. Zidane et al., "Grid-Connected Solar PV Power Plants Optimization: A Review," *in IEEE Access*, vol. 11, pp. 79588-79608, 2023, doi: 10.1109/ACCESS.2023.3299815.

[58]: D. Gielen, F. Boshell, D. Saygin et al, "The role of renewable energy in the global energy transformation", *Energy strategy reviews*, vol. 24, pp. 38-50, 2019.

[59]: M. Bouznit, M.d.P. Pablo-Romero, A. Sánchez-Braza, "Measures to Promote Renewable Energy for Electricity Generation in Algeria. Sustainability", vol. 12, no. 4, pp. 1468, 2020, https://doi.org/10.3390/su12041468

[60]: Y. Zahraoui, M.R.B. Khan, I. AlHamrouni, S. Mekhilef, M. Ahmed M, "Current Status, Scenario, and Prospective of Renewable Energy in Algeria: A Review", *Energies*, vol. 14, no. 9, pp. 2354, 2021, https://doi.org/10.3390/en14092354.

[61]: https://www.energy.gov.dz/?rubrique=energies-nouvelles-renouvelables-et-maitrise-de-lrenergie. (Consulted on 12/01/2024)

[62]: https://fr.m.wikipedia.org/wiki/Fichier:AFRICA_Location_Algeria.png. (Consulted on 12/01/2024)

[63]: S.B. Djelloul Saiah, A. Boudghene Stambouli, "Prospective analysis for a long-term optimal energy mix planning in Algeria: Towards high electricity generation security in 2062, Renewable and Sustainable Energy Reviews", vol. 73, pp. 26-43, 2017, https://doi.org/10.1016/j.rser.2017.01.023.

[64]: https://en.m.wikipedia.org/wiki/File:SolarGIS-Solar-map-Algeria-en.png. (Consulted on 12/01/2024)

[65]: Said DIAF. Intégration des systèmes à sources renouvelables d'énergie pour la production décentralisée d'électricité en site isolé. PhD dissertation, Ecole Nationale Supérieure Polytechnique, 2009.

[66]: J. J.C.S. Santos, J. C.E. Palacio, A.M.M. Reyes, M. Carvalho, A. J.R. Freire, M. A. Barone, "Chapter 12 - Concentrating Solar Power", *Advances in Renewable Energies and Power Technologies*, vol.1, pp. 373-402, 2018, ISBN 9780128129593, https://doi.org/10.1016/B978-0-12-812959-3.00012-5.

[67]: P. E. Tomaszewski, J.Czochralski, "father of the Czochralski method", *Journal of Crystal Growth*, vol. 236, no. 1–3, pp. 1-4, 2002, https://doi.org/10.1016/S0022-0248(01)02195-9.

[68]: Abdelkader Mekemeche, Modélisation à deux dimensions des propriétés physiques de cellules solaires au silicium à base de substrat de type n. Étude de quelques cas particuliers de cellules innovantes, PhD dessertation, Université de Abd El hamid Ibn Badis, Mostaganem, 2017.

[69]: L. Fraas, L. Partain, "Solar cells and their applications", John Wiley & Sons, 2010.

[70]: O.K. Simya, P. Radhakrishnan Nair and M. Ashok Anuradha, "Nanomaterials for Solar Energy Generation", *In Handbook of Nanomaterials for Industrial Applications*, Chapter 41, pp. 931-950, Elsevier, 2018.

[71]: N. Groß, J. Pfafferott, K. K. Orehounig, M. Simas, "High Efficiency Plants and Building Integrated Renewable Energy Systems" *Handbook of Energy Efficiency in Buildings*, pp. 441-595, 2019, DOI: 10.1016/b978-0-12-812817-6.00040-1.

[72]: R.A. Marques Lameirinhas, J.P.N Torres, J.P. Melo Cunha, "A Photovoltaic Technology Review: History, Fundamentals and Applications", *Energies*, vol. 15, no. 5, pp. 1823, 2022, https://doi.org/10.3390/en15051823.

[73]: J. Pastuszak and P. Węgierek, "Photovoltaic cell generations and current research directions for their development", *Materials*, vol. 15, no. 16, pp. 5542, 2022.

[74]: J. Dhilipan, N. Vijayalakshmi, D.B. Shanmugam, et al, "Performance and efficiency of different types of solar cell material–A review", *Materials Today: Proceedings*, vol. 66, pp. 1295-1302, 2022.

[75]: https://www.solarquotes.com.au/panels/photovoltaic/monocrystalline-vs-polycrystalline/. (Consulted on 17/02/2024)

[76]: https://www.wsl-solar.com/a-si-solar-cell.html. (Consulted on 17/02/2024)

[77]:https://www.pv-magazine-india.com/2021/04/08/unist-epfl-claim-25-6-efficiency-world-record-for-perovskite-solar-cell/. (Consulted on 17/02/2024)

[78]: A.Athil, M. Ansari, et al, "Photovoltaic solar cells: a review. Applied System Innovation", vol. 5, no. 4, pp. 67, 2022.

[79]: T. Dittrich, "Materials Concepts for Solar Cells: Second Edition (567 Pages), Basic Characteristics and Characterization of Solar Cells", 2018.

[80]: https://pveducation.com/solar-concepts/solar-cells-modules-arrays/ (Consulted on 17/02/2024)

[81]: C. Chellaswamy and R. Ramesh, "Parameter extraction of solar cell models based on adaptive differential evolution algorithm", *Renewable energy*, vol. 97, p. 823-837, 2016.

[82]: Gao, Lijun, et al, "Parallel-connected solar PV system to address partial and rapidly fluctuating shadow conditions." *IEEE Transactions on industrial Electronics*, vol. 56, no. 5, pp. 1548-1556, 2009.

[83]: H. Islam, S. Mekhilef, V.B.M. Shah, T.K. Soon, M. Seyedmahmousian, B. Horan, A. Stojcevski, "Performance Evaluation of Maximum Power Point Tracking Approaches and Photovoltaic Systems", *Energies*, vol. 11, no. 2, pp. 365, 2018, https://doi.org/10.3390/en11020365.

[84]: Yacine Triki. Contribution à l'optimisation des systèmes hybrides de production d'énergies renouvelables. PhD dissertation. Université de Haute Alsace- Mulhouse; Université Mouloud Mammeri (Tizi-Ouzou, Algérie), 2020.

[85]: Cuong Hung Tran. Améliorations d'une chaîne de conversion de l'énergie solaire en électricité autonome en vue d'application dans les pays en voie de développement. PhD dissertation. Université de Reims Champagne-Ardenne, 2019.

[86] : L. Hernández-Callejo, S. Gallardo-Saavedra, and V. Alonso-Gómez. "A review of photovoltaic systems: Design, operation and maintenance ", *Solar Energy*, vol. 188, pp.426-440, 2019, https://doi.org/10.1016/j.solener.2019.06.017.

[87] : V.R. Vakacharla, K. Gnana, P. Xuewei, B.L. Narasimaharaju, *et all*. "State-of-the-art power electronics systems for solar-to-grid integration". *Solar Energy*, vol. 210, pp. 128-148, 2020.

[88]: H. Abu-Rub, M. Malinowski and K. Al-Haddad, K, Power Electronics for Renewable Energy Systems, Transportation and Industrial Applications. *Wiley-IEEE Press*, 2014.

[89]: P.K. Maroti, S. Padmanaban, M.S. Bhaskar, V.K. Ramachandaramurthy, and F. Blaabjerg. " The State-of-The-Art of Power Electronics Converters Configurations in Electric Vehicle Technologies", *Power Electronic Devices and Components*, vol. 1, pp. 100001, 2021.

[90]: N. Chettibi. Contribution à la Commande Intelligente d'un Système Photovoltaïque Hybride. PhD dissertation. University of Djijel, 2017.

[91] : C.K. Das, O. Bass, G. Kothapalli, et all. "Overview of energy storage systems in distribution networks: Placement, sizing, operation, and power quality", *Renewable and Sustainable Energy Reviews* , vol. 91, pp. 1205-1230, 2018.

[92] : S.O. Amrouche, D. Rekioua,S. Bacha. " Overview of energy storage in renewable energy systems", *International journal of hydrogen energy*, vol. 41, no 45, pp. 20914-20927, 2016.

[93] : J. Mitali, S. Dhinakaran, A.A. Mohamad. "Energy storage systems: a review ", *Energy Storage and Saving*, vol. 1, no. 3, pp.166-216, 2022.

[94] : S. Koohi-Fayegh, M.A. Rosen. "A review of energy storage types, applications and recent developments", *Journal of Energy Storage*, vol. 27, pp. 101047, 2020.

[95] : D. Rekioua, Djamila. "Energy Storage Systems for Photovoltaic and Wind Systems: A Review", *Energies*, vol. 16, no. 9, pp. 3893, 2023, https://doi.org/10.3390/en16093893

[96]: LOUKRIZ, Abdelouadoud. Contribution au Développement de Techniques de Recherche de la Topologie Optimale d'un Générateur Photovoltaïque. PhD dissertation. University of Biskra, 2022.

[97]: A. Belkaid. Conception et implémentation d'une commande MPPT de haute performance pour une chaine de conversion photovoltaïque autonome. PhD dissertation. Ferhat abbas University. 2018.

[98] : Y.K. Wu, J. H. Lin and H. J. Lin, "Standards and Guidelines for Grid-Connected Photovoltaic Generation Systems: A Review and Comparison," *IEEE Transactions on Industry Applications*, vol. 53, no. 4, pp. 3205-3216, July-Aug. 2017, doi: 10.1109/TIA.2017.2680409.

[99] : O. Manasseh, and R. Bass. "Trends and challenges of grid-connected photovoltaic systems–A review." *Renewable and Sustainable Energy Reviews*, vol. 58, pp. 1082-1094, 2016.

[100]: M.H. Hariri, M.K. Mat Desa, S. Masri, M.A.A. Mohd Zainuri. "Grid-Connected PV Generation System—Components and Challenges: A Review", *Energies,* vol. 13, no. 17, pp. 4279, 2020, https://doi.org/10.3390/en13174279.

[101]: S. Adak and H. Cangi, "Development software program for finding photovoltaic cell open-circuit voltage and fill factor based on the photovoltaic cell one-diode equivalent circuit model", *Electrical Engineering*, vol. 106, pp. 1251-1264, 2024. https://doi.org/10.1007/s00202-023-02082-0.

[102]: A. Zekry, A. Shaker and M. Salem, "Solar Cells and Arrays: Principles, Analysis, and Design", *Advances in Renewable Energies and power technologies*, vol. 1, pp. 3-56, 2018.

[103]: M. Nasiri, S. Chandra, M. Taherkhani and S. J. McCormack, "Impact of Input Capacitors in Boost Converters on Stability and Maximum Power Point Tracking in PV systems," *2021 IEEE 48th Photovoltaic Specialists Conference (PVSC)*, Fort Lauderdale, FL, USA, 2021, pp. 1004-1008, doi: 10.1109/PVSC43889.2021.9518903.

[104]: S. Obukhov, A. Ibrahim, A. A. Zaki Diab, A. S. Al-Sumaiti and R. Aboelsaud, "Optimal Performance of Dynamic Particle Swarm Optimization Based Maximum Power Trackers for Stand-Alone PV System Under Partial Shading Conditions," *IEEE Access*, vol. 8, pp. 20770-20785, 2020, doi: 10.1109/ACCESS.2020.2966430.

[105]: V.R. Vakacharla, K.G. Gnana, P. Xuewei, B. Narasimaharaju, M. Bhukya et al, " State-of-the-art power electronics systems for solar-to-grid integration", *Solar Energy*, vol. 210, pp. 128-148, 2020.

[106]: I. Jagadeesh, V. Indragandhi, " Comparative Study of DC-DC Converters for Solar PV with Microgrid Applications", *Energies*, vol. 15, no. 20, pp. 7569, 2022, https://doi.org/10.3390/en15207569.

[107]: D. W. Hart, Power Electronics, 1st Edition, 2010.

[108]: Castellini, Gabriele, Design, Simulation and Prototyping of a 20kW Three-Phase Inverter for heavy-duty applications, PhD dissertation, Politecnico di Torino, 2019.

[109]: Abdellatif Mahammedi. Contribution to the control of a Power Converter with Improved Topologies Associated with a Photovoltaic Generator Based on Advanced Techniques. PhD Dessertation. Ziane Achour University of Djelfa, 2020.

[110]: Alexandre Battiston. Modélisation, commande, stabilité et mise en oeuvre des onduleurs à source impédante : application aux systèmes embarqués, PhD Dessertation, Université of Lorraine, 2014.

[111]: Sang. H. Kim, Chapter 7 - Pulse width modulation inverters, *In book: Electric Motor Control*, 2017, http://dx.doi.org/10.1016/B978-0-12-812138-2.00007-6.

[112]: M.A. Memon, G.M. Bhutto, E.A. Buriro, " Sizing of dc-link capacitor for a grid connected solar photovoltaic inverter" , *Indian Journal of Science and Technology*, vol. 13, no. 22, pp. 2272-2281, 2020, https://doi.org/ 10.17485/IJST/v13i22.406

[113]: A. Turksoy, Y. Hames, A. Teke, M. Barghi Latran, " A novel adaptive switching method to reduce DC-Link capacitor ripple in PV based grid-connected inverter ", *Solar Energy*, vol. 173, pp. 702-714, 2018.
[114]: M. Kumar, K. P. Panda, J. C. Rosas-Caro, A. Valderrabano-Gonzalez and G. Panda, "Comprehensive Review of Conventional and Emerging Maximum Power Point Tracking Algorithms for Uniformly and Partially Shaded Solar Photovoltaic Systems," *IEEE Access*, vol. 11, pp. 31778-31812, 2023, doi: 10.1109/ACCESS.2023.3262502.
[115]: R.B. Bollipo, S. Mikkili, and P. K. Bonthagorla, "Hybrid, optimal, intelligent and classical PV MPPT techniques: A review", *CSEE Journal of Power and Energy Systems*, vol. 7, no. 1, pp. 9-33, 2020.
[116]: T. Esram and P. L. Chapman, "Comparison of Photovoltaic Array Maximum Power Point Tracking Techniques," *IEEE Transactions on Energy Conversion*, vol. 22, no. 2, pp. 439-449, 2007, doi: 10.1109/TEC.2006.874230.
[117]: S. Tahir, J. Wang, M.H. Baloch and G.S. Kaloi, " Digital Control Techniques Based on Voltage Source Inverters in Renewable Energy Applications: A Review ", *Electronics*, vol. 7, no. 2, pp. 18, 2018, https://doi.org/10.3390/electronics7020018
[118]: H. Athari, M. Niroomand, and M. Ataei, "Review and Classification of Control Systems in Grid-tied Inverters," *Renewable and Sustainable Energy Reviews*, vol. 72, pp. 1167-1176, 2017.
[119]: Ehsan Jamshidpour, Maryam Shahbazi, Shahrokh Saadate, Philippe Poure, Eskandar Gholipour. FPGA based fault detection and fault tolerance operation in DC-DC converters. *SPEEDAM 2014, International Symposium on Power Electronics, Electrical Drives, Automation and Motion*, Jun 2014, Ischia, Italy. pp.37-42.
[120]: E. Jamshidpour, M. Shahbazi, S. Saadate, P. Poure and E. Gholipour, "FPGA based fault detection and fault tolerance operation in DC-DC converters," *2014 International Symposium on Power Electronics, Electrical Drives, Automation and Motion*, Ischia, Italy, 2014, pp. 37-42, doi: 10.1109/SPEEDAM.2014.6872062.
[121]: R. Wu, F. Blaabjerg, H. Wang, M. Liserre and F. Iannuzzo, "Catastrophic failure and fault-tolerant design of IGBT power electronic converters - an overview," *IECON 2013 - 39th Annual Conference of the IEEE Industrial Electronics Society*, Vienna, Austria, 2013, pp. 507-513, doi: 10.1109/IECON.2013.6699187.
[122]: H. Wang, D. Zhou and F. Blaabjerg, "A reliability-oriented design method for power electronic converters," *2013 Twenty-Eighth Annual IEEE Applied Power Electronics Conference and Exposition (APEC)*, Long Beach, CA, USA, 2013, pp. 2921-2928, doi: 10.1109/APEC.2013.6520713.
[123]: S. Shao, P. W. Wheeler, J. C. Clare, and A. J. Watson, "Fault detection for modular multilevel converters based on sliding mode observer", *IEEE Trans. Power Electron*, vol.28, no. 11, pp. 4867-4872, 2013
[124]: S. Shao, A. Watson, J. Clare, and P. Wheeler, " Robustness analysis and experimental validation of a fault detection and isolation method for the modular multilevel converter", *IEEE Trans. Power Electron*, vol. 31, no. 5, p. 3794-3805, May 2016.

[125]: J. Poon, P. Jain, I. C. Konstantakopoulos, C. Spanos, S. K. Panda, and S. R. Sanders, "Model-based fault detection and identification for switching power converters", *IEEE Trans. Power Electron*, vol. 32, no. 2, pp. 1419-1430, 2017.
[126]: A. Izadian and P. Khayyer, "Application of Kalman filters in model-based fault diagnosis of a DC-DC boost converter," *IECON 2010 - 36th Annual Conference on IEEE Industrial Electronics Society*, Glendale, AZ, USA, 2010, pp. 369-372, doi: 10.1109/IECON.2010.5674998.
[127]: M. Ahmeid, M. Armstrong, S. Gadoue, M. Algreer, and P. Missailidis, " Real-time parameter estimation of DC-DC converters using a self-tuned kalman filter ", *IEEE Trans. Power Electron*, vol. 32, no. 7, pp. 5666- 5674, 2017.
[128]: Z. Cen and P. Stewart, "Condition Parameter Estimation for Photovoltaic Buck Converters Based on Adaptive Model Observers," *IEEE Transactions on Reliability*, vol. 66, no. 1, pp. 148-160, March 2017, doi: 10.1109/TR.2016.2618320.
[129]: R. Jayabalan and B. Fahimi, "Monitoring and Fault Diagnosis of Multiconverter Systems in Hybrid Electric Vehicles," *IEEE Transactions on Vehicular Technology*, vol. 55, no. 5, pp. 1475-1484, Sept. 2006, doi: 10.1109/TVT.2006.878716.
[130]: E. Jamshidpour, P. Poure, E. Gholipour and S. Saadate, "Single-Switch DC–DC Converter With Fault-Tolerant Capability Under Open- and Short-Circuit Switch Failures," *IEEE Transactions on Power Electronics*, vol. 30, no. 5, pp. 2703-2712, May 2015, doi: 10.1109/TPEL.2014.2342878.
[131]: E. Jamshidpour, P. Poure and S. Saadate, "Photovoltaic Systems Reliability Improvement by Real-Time FPGA-Based Switch Failure Diagnosis and Fault-Tolerant DC–DC Converter," *IEEE Transactions on Industrial Electronics*, vol. 62, no. 11, pp. 7247-7255, Nov. 2015, doi: 10.1109/TIE.2015.2421880.
[132]: H. Givi, E. Farjah and T. Ghanbari, "Switch and Diode Fault Diagnosis in Non isolated DC–DC Converters Using Diode Voltage Signature," *IEEE Transactions on Industrial Electronics*, vol. 65, no. 2, pp. 1606-1615, Feb. 2018, doi: 10.1109/TIE.2017.2733486.
[133]: H. K. Cho, S. S. Kwak, and S. H. Lee, "Fault diagnosis algorithm based on switching function for boost converters, " *Int. J. Electron* , vol. 102, no. 7, pp. 1229-1243, 2015.
[134]: E. Farjah, H. Givi, and T. Ghanbari, "Application of an efficient rogowski coil sensor for switch fault diagnosis and capacitor ESR monitoring in non isolated single-switch DC-DC converters, " *IEEE Trans. Power Electron*, vol. 32, no. 2, pp. 1442-1456, 2017.
[135]: E. Ribeiro, A. J. M. Cardoso and C. Boccaletti, "Fault analysis of dual active bridge converters," *IECON 2012 - 38th Annual Conference on IEEE Industrial Electronics Society*, Montreal, QC, Canada, 2012, pp. 398-403, doi: 10.1109/IECON.2012.6388787.
[136]: M. W. Ahmad, N. B. Y. Gorla, H. Malik and S. K. Panda, "A Fault Diagnosis and Postfault Reconfiguration Scheme for Interleaved Boost Converter in PV-Based System," *IEEE Transactions on Power Electronics*, vol. 36, no. 4, pp. 3769-3780, 2021, doi: 10.1109/TPEL.2020.3018540.
[137]: M.A. Zdiri, M. Ben Ammar, B. Bouzidi, A. Rabhi and A. Hsan Hadj , "An Advanced Switch Failure Diagnosis Method and Fault Tolerant Strategy in Photovoltaic Boost Converter ", *Electric Power Components and Systems*, vol. 48, no. 18, pp. 1932-1944, 2020, DOI: 10.1080/15325008.2021.1909182

[138]: F. Bento and A. J. Marques Cardoso, "Fault diagnosis in DC-DC converters using a time-domain analysis of the reference current error," *IECON 2017 - 43rd Annual Conference of the IEEE Industrial Electronics Society*, Beijing, China, 2017, pp. 5060-5065, doi: 10.1109/IECON.2017.8216874.

[139]: E. Ribeiro, A. J. M. Cardoso and C. Boccaletti, "Open-Circuit Fault Diagnosis in Interleaved DC–DC Converters," in *IEEE Transactions on Power Electronics*, vol. 29, no. 6, pp. 3091-3102, 2014, doi: 10.1109/TPEL.2013.2272381.

[140]: C. Sui, C et al, " The post-fault current model of voltage source converter and its application in fault diagnosis", *IEEE Trans. Power Electron*, vol. 36, no. 2, pp. 1209–1214, 2021.

[141]: I. Jlassi et al, " A Robust observer-based method for IGBTs and current sensors fault diagnosis in voltage-source inverters of PMSM drives " , *IEEE Trans. Ind. Appl,* vol. 53, no. 3,pp. 2894–2905, 2017.

[142]: D.R. Espinoza-Trejo et al, " Robust fault diagnosis scheme for open-circuit faults in voltage source inverters feeding induction motors by using non linear proportional-integral observers" , *IET Power Electron*, vol. 5, no. 7, pp. 1204- 1216, 2012.

[143]: R. Maamouri et al, " Mixed model-based and signal-based approach for open-switches fault diagnostic in sensorless speed vector controlled induction motor drive using sliding mode observer" , *IET Power Electron*, vol. 12, no. 5, pp. 1149–1159, 2019.

[144]: F. Naseri et al, " Real-time open-switch fault diagnosis in automotive permanent magnet synchronous motor drives based on Kalman filter", *IET Power Electron*, vol. 13, no. 12, pp. 2450–2460, 2020.

[145]: K. Hu et al, " Fault diagnosis and tolerance with low torque ripple for open-switch fault of IM drives", *IEEE Trans. Transportation Elec*, vol. 7, no. 1, pp. 133–146, 2021.

[146]: M. Wang,Y. Xu,Y,J. Zou, " Sliding mode control with open switch fault diagnosis and sensorless estimation based on PI observer for PMSM drive connected with an LC filter", *IET Power Electron*, vol. 13, no. 11, pp. 2334–2341, 2020.

[147]: S. M. Jung, J. S. Park, H. W. Kim, K. Y. Cho and M. J. Youn, "An MRAS-Based Diagnosis of Open-Circuit Fault in PWM Voltage-Source Inverters for PM Synchronous Motor Drive Systems," *IEEE Transactions on Power Electronics*, vol. 28, no. 5, pp. 2514-2526, 2013, doi: 10.1109/TPEL.2012.2212916.

[148]: J.O. Estima, N.M.A, Freire, A.J.M. Cardoso, " Recent advances in fault diagnosis by Park's vector approach", *2013 IEEE Workshop on Electrical Machines Design, Control and Diagnosis (WEMDCD)*, Paris, France, 2013, pp. 279-288, doi: 10.1109/WEMDCD.2013.6525187.

[149]: I. Jlassi and A.J.M. Cardoso, " A single method for multiple IGBTs, current and speed-sensor faults diagnosis in regenerative PMSM drives", *IEEE J. Emerging Selected Topics Power Electron*, vol. 8, no. 3, pp. 2583–2599, 2020.

[150]: J. Zhang, J. Zhao, D. Zhou, and C. Huang, " High-performance fault diagnosis in PWM voltage-source inverters for vector-controlled induction motor drives, " *IEEE Trans. Power Electron*, vol. 29, no. 11, pp. 6087–6099, 2014.

[151]: K. Li, S. Cheng, T. Yu, X. Wu, C. Xiang, and A. Bilal, " An on line multiple open-circuit fault diagnostic technique for railway vehicle air-conditioning inverters, " *IEEE Trans. Veh. Technol*, vol. 69, no. 7, pp. 7026–7039, 2020.
[152]: J. O. Estima and A. J. M. Cardoso, "A new approach for real-time multiple open-circuit fault diagnosis in voltage-source inverters, " *IEEE Trans. Ind. Appl*., vol. 47, no. 6, pp. 2487–2494, 2011.
[153]: Z. Li, H. Ma, Z. Bai, Y. Wang and B. Wang, "Fast Transistor Open-Circuit Faults Diagnosis in Grid-Tied Three-Phase VSIs Based on Average Bridge Arm Pole-to-Pole Voltages and Error-Adaptive Thresholds," *IEEE Transactions on Power Electronics*, vol. 33, no. 9, pp. 8040-8051, 2018, doi: 10.1109/TPEL.2017.2773130.
[154]: Z. Li et al., " Open-transistor faults diagnosis in voltage-source inverter based on phase voltages with sliding-window counting method, " *Proc. 42nd Annu. Conf. IEEE Ind. Electron. Soc*., vol. 2, pp. 435–440, 2003.
[155]: M. A. Rodrıguez-Blanco et al., "Fault detection for IGBT using adaptive thresholds during the turn-on transient, " *IEEE Trans. Ind. Electron*, vol. 62, no. 3, pp. 1975–1983, 2015.
[156]: B.D.E. Cherif, A. Bendiabdellah, "Detection of Two-Level Inverter Open-Circuit Fault Using a Combined DWT-NN Approach", *Journal of Control Science and Engineering*, vol. 2018, 11 pages, 2018. https://doi.org/10.1155/2018/1976836
[157]: M. Beibei, S. Yanxia, W. Dinghui, and Z. Zhipu, " Three level inverter fault diagnosis using EMD and support vector machine approach, " *Proc. 12th IEEE Conf. Ind. Electron. Appl. (ICIEA)*, Jun. 2017, pp. 18–20, doi: 10.1109/ICIEA.2017.8283093.
[158]: B. Cherif, A. Bendiabdellah, and M. Tabbakh, "Diagnosis of an inverter IGBT open-circuit fault by Hilbert-Huang transform application", *Traitement Signal*, vol. 36, no. 2, pp. 127–132, 2019, doi: 10.18280/ts.360201.
[159]: X. Zhang, " Fault diagnosis for PWM inverter based on LMD", *Proc. 4th Int. Conf. Mech., Control Comput. Eng. (ICMCCE)*, Oct. 2019, pp. 167–171, doi: 10.1109/ICMCCE48743.2019.00047.
[160]: A. Mimouni, S. Laribi S, M. Sebaa, T. Allaoui, A.A. Bengharbi , " Fault diagnosis of power converters in a grid connected photovoltaic system using artificial neural networks" , *Electrical Engineering & Electromechanics*, 2023, no. 1, pp. 25-30. doi: https://doi.org/10.20998/2074-272X.2023.1.04
[161]: A. Mimouni, S. Laribi S, M. Sebaa, T. Allaoui, A.A. Bengharbi, " Identification of Open-Circuit Faults in T-Type Inverters Using Fuzzy Logic Approach", *Advances in Electrical and Electronic Engineering*, vol. 21, no. 4, pp. 282- 294, 2023. DOI: 10.15598/aeee.v21i4.5218.
[162]: A. Mimouni, S. Laribi, H. Bizhani and G. Iwanski, "Switch Fault Diagnosis of Grid-Connected Inverter Using Symmetrical Components," in *IEEE Journal of Emerging and Selected Topics in Power Electronics*, vol. 12, no. 5, pp. 5258-5272, Oct. 2024, doi: 10.1109/JESTPE.2024.3428397.

Promotion of Thesis Research

Publications

1. A. Mimouni, S. Laribi S, M. Sebaa, T. Allaoui, A.A. Bengharbi , " Fault diagnosis of power converters in a grid connected photovoltaic system using artificial neural networks" , *Electrical Engineering & Electromechanics*, 2023, no. 1, pp. 25-30. doi: https://doi.org/10.20998/2074-272X.2023.1.04
2. A. Mimouni, S. Laribi S, M. Sebaa, T. Allaoui, A.A. Bengharbi, " Identification of Open-Circuit Faults in T-Type Inverters Using Fuzzy Logic Approach", *Advances in Electrical and Electronic Engineering*, vol. 21, no. 4, pp. 282- 294, 2023. DOI: 10.15598/aeee.v21i4.5218.
3. A. Mimouni, S. Laribi, H. Bizhani and G. Iwanski, "Switch Fault Diagnosis of Grid-Connected Inverter Using Symmetrical Components," in *IEEE Journal of Emerging and Selected Topics in Power Electronics*, vol. 12, no. 5, pp. 5258-5272, Oct. 2024, doi: 10.1109/JESTPE.2024.3428397.

Communications

1. A.Mimouni, S. Laribi and M.Sebaa. 'Fault diagnosis of three phase inverter in photovoltaic systems '. the 2nd International Conference on Electronics and Electrical Engineering (IC3E'2020), University of Bouira, Algeria, November 2020. http://ic3e.univ-bouira.dz/
2. A.Mimouni, S. Laribi, M.Sebaa, T.Allaoui. 'Fault tolerant control of three phase inverter in grid connected photovoltaic system'. International Hazar Scientific Researches Conferences II, BAKU, AZERBAIJAN, KHAZAR UNIVERSITY , April 2021.
3. A.Mimouni, S. Laribi, M.Sebaa, T.Allaoui, A.A. Bengharbi.'Comparison of different dc-dc converters in photovoltaic system'.6th international congress innovative scientific approaches held on December 19-20, 2021/ Samsun, Turkey.
4. A.Mimouni, S. Laribi, M.Sebaa, T.Allaoui, A.A. Bengharbi. Open circuit fault diagnosis of power converters in photovoltaic system. 1st international conference on modern electrical engineering and technology. (CIETM'22) held at the University of Soukahras, Algeria, February 18-19, 2022.
5. A.Mimouni, S. Laribi, M.Sebaa, T.Allaoui, A.A. Bengharbi. Open circuit fault diagnosis of NPC inverter in grid connected photovoltaic system. 19th IEEE International Multi-Conference on Systems, Signals& Devices SSD, Algeria, During May 06th -10th , 2022.
6. A. Mimouni. S. Laribi. M.Sebaa. T. Allaoui. A.A Bengharbi. Diagnosis Method of an Open circuit fault for a T-Type inverter in PV System. "IArcSAS" 2nd International Architectural Sciences and Applications Symposium held on September 09-11, 2022 / Baku Engineering University Baku, Azerbaijan.
7. A. Mimouni. S. Laribi. M.Sebaa. T. Allaoui. A.A Bengharbi. "Open Switch Fault Diagnosis Method of inverter in Photovoltaic system using Phase Currents. The first national conference in Materials Science and Engineering (NCMSE'1_2022) on November 27-28, 2022.